



FACULTY OF PHARMACEUTICAL SCIENCES

Ghent University

Faculty of Pharmaceutical Sciences

**INVESTIGATION OF THE TABLETING PROCESS
IN CONTINUOUS PRODUCTION: INFLUENCE OF FEEDING
AND EXTENDED DWELL TIME DURING COMPRESSION
ON DEPENDENT PROCESS VARIABLES AND TABLET PROPERTIES**

Elisabeth PEETERS

Industrial Pharmacist

Thesis submitted to obtain the degree of Doctor in Pharmaceutical Sciences

2014

Scientific Promoters: **Prof. dr. J. P. Remon, Prof. dr. C. Vervaet**

Laboratory of Pharmaceutical Technology, Ghent University

The author and the promoters give the authorization to consult and to copy part of this thesis for personal use only. Any other use is limited by the Laws of Copyright, especially concerning the obligation to refer to the source whenever results are cited from this thesis.

Ghent, September 8th, 2014

The Promoters

The Author

Prof. dr. J.P. Remon

Prof. dr. C. Vervaet

Elisabeth Peeters

DANKWOORD

De afgelopen jaren die ik op het Laboratorium van Farmaceutische Technologie aan de Universiteit Gent heb doorgebracht waren ongetwijfeld een boeiende en leerrijke ervaring. Bij het voltooien van dit werk is het officieel tijd om alle mensen te bedanken die een belangrijke bijdrage aan dit proefschrift hebben geleverd. Geen dankwoord zonder thesis, geen thesis zonder jullie...

Een eerste woord van dank gaat uit naar mijn promotoren, *Prof. Dr. Jean Paul Remon* en *Prof. Dr. Chris Vervaet*. Bedankt om mij de kans te bieden te doctoreren binnen uw onderzoeksgroep. Uw ervaring, begeleiding en steun hebben mijn interesse in het wetenschappelijk onderzoek blijvend gestimuleerd. Bedankt ook, voor het kritisch nalezen van mijn teksten en om mij de kans te bieden mijn werk op wetenschappelijke congressen voor te stellen. *Prof. Dr. Thomas De Beer* wens ik te bedanken voor zijn begeleiding en steun in de “wondere wereld” van Design of Experiments en Multivariate Data Analyse, welke een groot deel van mijn onderzoeksproject mee vorm hebben gegeven. Bedankt, voor uw kritisch inzicht, suggesties en verhelderende gesprekken en de kans die u me geboden heeft om deel uit te maken van enkele interessante projecten binnen uw onderzoeksgroep. *Prof. Dr. Annick Ludwig* wil ik graag bedanken om mijn interesse in het wetenschappelijk onderzoek te wekken. Het was u die de allereerste aanzet gegeven heeft. Bedankt daarvoor.

Graag wens ik bij deze ook de mensen van GEA Process Engineering, CourtoyTM te bedanken. In het bijzonder *Ir. Jan Vogeleer*, *Ir. Jurgen Boeckx* en *Dr. Ir. Frederik Detobel* voor de interesse die zij in mijn project hebben getoond. Bedankt ook aan *Dirk*, *Fabrice*, *Benny*, *Hugo*, ... en al jullie collega's, om praktische en technische ondersteuning te bieden op die momenten dat de experimenten net even minder vlot verliepen.

Bedankt aan de mensen waar ik tijdens mijn onderzoeksproject nauw mee heb samen gewerkt. Thank you *Maunu* (VTT Technical Research Centre of Finland) and *Ana* (Laboratorium voor Farmaceutische Proces Analytische Technologie, Universiteit Gent) for the pleasant and fruitful collaboration. Bedankt ook aan mijn thesisstudenten *Sara*, *Caroline*, *Bernard*, *Carolien* en *Jeroen* voor jullie hulp, inzet, interesse en enthousiasme tijdens jullie onderzoekstage.

Het labo zou niet hetzelfde zijn zonder die mensen die dagelijks administratieve en technische ondersteuning bieden. Daarom, bedankt *Bruno*, *Katharine* en *Ilse*, *Marc* en *Christine* voor ook aan mij die ondersteuning te bieden!

Aan al mijn collega's, bedankt voor de aangename en productieve sfeer. In het bijzonder, bedankt aan mijn bureaugenoten voor de vele interessante discussies, ook de occasionele niet-werkgerelateerde. *Lien, Valérie* en *Jurgen*, het was aangenaam te weten dat ik bij jullie altijd terecht kon, voor praktische hulp, maar ook voor een goed gesprek, een lach en een traan. Bedankt ook aan alle "PAT'ers", en in het bijzonder *Margot, Tinne* en *Fien*. Het was leuk en leerrijk om met jullie samen te werken. Ook een woord van dank aan mijn collega's die het labo al verlaten hebben na het succesvol beëindigen van hun doctoraat. *Barbara, An, Nele* en *Charlotte*, bedankt om mij wegwijs te maken op het labo en voor de aangename sfeer tijdens het begin van mijn doctoraat.

Bovenal is dit proefschrift het resultaat van de steun, liefde en vriendschap die ik krijg van alle mensen die me het dichtst bij het hart liggen. Vandaar: bedankt om er voor mij te zijn, dit werk is, meer dan jullie beseffen, ook van jullie! *Muchas gracias, Damian, Monica* and your children for your friendship and support! Bedankt, *Jessica*, voor je niet aflatende steun en onvoorwaardelijke vriendschap. Jouw regelmatige telefoontjes vanuit Duitsland hebben mij gestimuleerd om door te zetten, ook op momenten dat het wat minder ging. Ik weet zeker dat ook jij binnenkort met succes je proefschrift zal beëindigen! Bedankt ook aan *mijn schoonouders* voor hun oprechte interesse en steun. Hoewel ik best weet dat het niet altijd even makkelijk was om te kaderen waar ik nu exact mee bezig was, bleven jullie steeds enthousiast mijn verhalen aanhoren. Mijn broer(tje) *David*, mijn zus(je) *Patricia*, en *Patrick*. Bedankt voor jullie oprechte interesse en steun tijdens mijn doctoraat, maar ook al lang daarvoor. Ik ben net zo fier op jullie als jullie op mij. *Mijn ouders*, bedankt voor... alles! Voor de levenslessen die jullie mij hebben meegegeven, het doorzettingsvermogen en het relativiseringsvermogen, de kansen en de vrijheid die jullie mij hebben geboden om mij te ontwikkelen op de manier die ik zelf wilde. *Papa*, ik ben er zeker van dat jij ergens op de eerste rij zit. Deze is voor jou! Tot slot en niet in het minst, *Peter*. Bedankt voor je eindeloze geduld en begrip, om er voor mij te zijn en te luisteren als ik weer eens heel enthousiast was, of het net even niet zag zitten. Bedankt om altijd voor me klaar te staan. In goede en kwade dagen... Voor zoveel kleine dingen, Bedankt! Ik zie je graag!

Liesbeth,

September 2014

TABLE OF CONTENTS

ABBREVIATIONS AND SYMBOLS	1
OUTLINE AND AIMS	9
CHAPTER 1 INTRODUCTION	13
1. HISTORY OF TABLET COMPRESSION	14
2. COMPACTION EQUIPMENT IN MANUFACTURING	15
2.1. Eccentric tableting machines	15
2.2. Rotary tablet presses	16
2.3. Special presses and latest designs	18
3. COMPACTION EQUIPMENT IN RESEARCH AND DEVELOPMENT	21
3.1. Compaction simulators	21
3.1.1. Hydraulic compaction simulators	21
3.1.2. Mechanical compaction simulators	24
3.2. Instrumented manufacturing presses	25
4. STUDYING AND MODELING THE COMPACTION PROCESS	26
4.1. Data acquisition	26
4.1.1. In research and development	28
4.1.2. In scale-up and production	29
4.2. Design of Experiments	32
4.3. Multivariate Data Analysis	33
4.4. The roll of additional PAT-tools in the compaction process	33
REFERENCES	35
CHAPTER 2 THE MODUL TM P	49
1. PRESS DESIGN AND LAY-OUT	50
2. POWDER FEEDING SYSTEM	53
3. MECHANISM OF COMPRESSION	55
4. INSTRUMENTATION AND COLLECTION OF DATA	58
5. CONTROL MECHANISM AND PAT INTEGRATED IN THE PRESS	59
5.1. Control of the variation in tablet characteristics	59
5.1.1. Weight control	60

TABLE OF CONTENTS

5.1.2. Force control	61
5.1.3. Displacement control	62
5.2. Control of the relation between tablet characteristics and process parameters	62
5.3. Operation principles available on the press	62
REFERENCES	64
CHAPTER 3	<u>EFFECT OF THE PADDLE MOVEMENT IN THE FORCED FEEDER ON</u>
	<u>LUBRICANT SENSITIVITY</u>
	67
1. INTRODUCTION	69
2. MATERIALS AND METHODS	69
2.1. Materials	69
2.2. Preparation of powder mixtures	69
2.3. Powder characterization	71
2.4. Preparation of tablets	72
2.4.1. Tabletability	72
2.4.2. Effect of the paddle speeds	72
2.5. Monitoring of set and dependent machine parameters	73
2.6. Tablet evaluation	74
3. RESULTS AND DISCUSSION	75
3.1. Tabletability	75
3.2. Effect of the paddle speeds	76
4. CONCLUSIONS	84
REFERENCES	85
CHAPTER 4	<u>REDUCTION OF TABLET WEIGHT VARIABILITY BY OPTIMIZING</u>
	<u>PADDLE SPEED IN THE FORCED FEEDER OF A HIGH-SPEED ROTARY</u>
	<u>TABLET PRESS</u>
	91
1. INTRODUCTION	93
2. MATERIALS AND METHODS	95
2.1. Materials	95
2.2. Preparation of powder mixtures	95
2.3. Preparation of tablets	96
2.4. Powder characterization	97
2.4.1. Particle size analysis	97
2.4.2. Density	97

2.4.3. Flow properties	97
2.5. Tablet evaluation	98
2.6. Volume of powder in the feeder	98
2.7. Design of Experiments	98
3. RESULTS AND DISCUSSION	100
3.1. Evaluation of the powder characteristics	100
3.2. Experimental design analysis	101
3.2.1. Weight	101
3.2.2. Weight variability	104
3.2.3. Volume of powder in the feeder	105
3.3. Process optimization	106
4. CONCLUSIONS	109
REFERENCES	110
<u>CHAPTER 5</u>	<u>INFLUENCE OF EXTENDED DWELL TIME DURING PRE- AND MAIN</u>
	<u>COMPRESSION ON THE PROPERTIES OF IBUPROFEN TABLETS</u>
	<u>113</u>
1. INTRODUCTION	115
2. MATERIALS AND METHODS	116
2.1. Materials	116
2.2. Granule characterization	116
2.3. Preparation of tablets	117
2.3.1. Mechanism of compression	117
2.3.2. Collection of data	118
2.3.3. Tableability	119
2.3.4. Influence of extended dwell time	120
2.4. Data analysis	122
2.4.1. Analysis of process parameters	122
2.4.2. Tablet evaluation	128
2.4.3. Multivariate Data Analysis	131
3. RESULTS AND DISCUSSION	131
3.1. Granule characteristics	131
3.2. Tableability	132
3.3. Multivariate Data Analysis	133
3.3.1. Principal Component Analysis	133
3.3.2. Partial Least Squares	139

TABLE OF CONTENTS

3.4. Disintegration testing and SEM	144
4. CONCLUSIONS	145
ACKNOWLEDGEMENTS	146
REFERENCES	147
<u>CHAPTER 6</u>	<u>ASSESSMENT AND PREDICTION OF TABLET PROPERTIES USING</u>
	<u>TRANSMISSION AND BACKSCATTERING RAMAN SPECTROSCOPY</u>
	<u>AND TRANSMISSION NIR SPECTROSCOPY</u>
	153
1. INTRODUCTION	155
2. MATERIALS AND METHODS	156
2.1. Materials	156
2.2. Preparation of powder mixtures	157
2.3. Granulation	157
2.4. Tableting	157
2.5. Design of Experiments	158
2.6. Granule characterization	159
2.7. Tablet evaluation by reference analyzing techniques	160
2.8. Prediction of tablet properties using spectroscopic techniques	161
2.9. Influence of granulation parameters on granule properties, tablet properties and tableting process parameters	162
3. RESULTS AND DISCUSSION	164
3.1. Prediction of tablet properties using spectroscopic techniques	164
3.1.1. Physical properties	164
3.1.2. Theophylline content and hydration level	166
3.2. Influence of granulation process parameters on granule properties	169
3.3. Influence of granulation process parameters on tablet properties and tableting process parameters	171
4. CONCLUSIONS	173
REFERENCES	174
<u>GENERAL CONCLUSIONS AND FUTURE PERSPECTIVES</u>	<u>179</u>
<u>SUMMARY</u>	<u>185</u>
<u>SAMENVATTING</u>	<u>191</u>
<u>CURRICULUM VITAE</u>	<u>197</u>

ABBREVIATIONS AND SYMBOLS

ABBREVIATIONS

API	Active Pharmaceutical Ingredient
BRaman	Backscattering Raman
CCD	Charged Couple Device
CDAAS	Data Acquisition and Analysis System
cGMP	current Good Manufacturing Practices
CMA	Critical Material Attributes
COST	Changing One factor at a Time
CPP	Critical Process Parameters
CQA	Critical Quality Attributes
DCP	Dibasic calcium phosphate dihydrate
DEM	Discrete Element Method
DoE	Design of Experiments
ECM	Exchangeable Compression Module
FDA	Food and Drug Administration
IBC	Intermediate Bulk Container
ICH	International Conference on Harmonization
LVDT sensor	Linear Variable Displacement Transducer
MCC	Microcrystalline cellulose
MgSt	Magnesium stearate
MLR	Multiple Linear Regression
MSC	Multiplicative Scatter Correction
MVA	Multivariate Data Analysis
NIR	Near Infrared
PAT	Process Analytical Technology
PC	Principal Component
PCA	Principal Component Analysis
PLS	Partial Least Squares

ABBREVIATIONS AND SYMBOLS

PVP	Polyvinylpyrrolidone
QbD	Quality by Design
R&D	Research and Development
rpm	Rotations per minute
SEM	Scanning Electron Microscopy
SNV	Standard Normal Variate
tpm	Tablets per minute
TRaman	Transmission Raman
WOL	Wash-Off-Line

SYMBOLS

1st der	First derivative
AUC_{con} (kN*ms)	Area under the curve of the consolidation phase
AUC_{decomp} (kN*ms)	Area under the curve of the decompression phase
AUC_{total} (kN*ms)	Area under the curve of the complete force-time profile
bot (mm)	Position of bottom roller
BT (°C)	Barrel temperature
CAR (%)	Cumulative axial recovery of the tablets after a storage period of 7 days
CD (mm)	Maximum displacement of the upper roller
CF (kN)	Maximum compression force exerted on powder under compression
CF_r (kN)	Air pressure in air compensator at the upper roller
CI (%)	Compressibility index
d (mm)	Diameter
d10 (μ m)	Diameter at which 10 % (m/m) of a sample is comprised of smaller particles
d50 (μ m)	Diameter at which 50 % (m/m) of a sample is comprised of smaller particles
d90 (μ m)	Diameter at which 90 % (m/m) of a sample is comprised of smaller particles
Diff (CAR-IAR) (%)	Difference between the IAR_{t0} and CAR
Diff d (mm)	Difference in diameter between $t0$ and $t7$

Diff H (mg)	Difference in hardness between t0 and t7
Diff T (mm)	Difference in thickness between t0 and t7
Diff TS (mPa)	Difference in tensile strength between t0 and t7
Diff W (mg)	Difference in weight between t0 and t7
Dis (s)	Disintegration time
ϵ (%)	Porosity (of tablet after ejection)
ϵ_{ID} (%)	Porosity of tablet during compression, minimum distance between punches
EF (kN)	Maximum ejection force measured during the ejection phase
ER (%)	Elastic recovery
F (N)	Diametral crushing force of a tablet
F_{bdw} (kN)	Force at the beginning of the dwell time
F_{curve} (kN)	Maximum force of a force-time profile when no displacement is used
F_{ejec} (kN)	see "EF"
F_{edw} (kN)	Force at the end of the dwell time
F_{max} (kN)	Maximum force
F_{min} (kN)	Minimum force
$F_{plateau}$ (kN)	Mean force of F_{25dw} , F_{50dw} , F_{75dw}
F_{top} (kN)	Maximum force of a force-time profile when displacement is used
F_{25dw} (kN)	Force at 25 % of the dwell time
F_{50dw} (kN)	Force at 50 % of the dwell time
F_{75dw} (kN)	Force at 75 % of the dwell time
Fill (mm)	Fill depth, which determines the weight
Fria (%)	Friability
H (N)	Hardness
h (mm)	Height
h_{BT} (mm)	Minimum distance between upper and lower punch during compression
Hardening (%)	Change in TS of the tablets upon storage
IAR (%)	Immediate axial recovery
IAR_{pre} (%)	Immediate axial recovery after the decompression phase at precompression

ABBREVIATIONS AND SYMBOLS

IAR_{main} (%)	Immediate axial recovery after the decompression phase at main compression
IAR_{t0} (%)	Immediate axial recovery of the tablets after ejection from the die
LFR (g/min)	Liquid feed rate
mbot (mm)	Position of bottom roller at main compression
MCD (mm)	Maximum displacement of the upper roller during precompression
MCF (kN)	Maximum main compression force exerted on powder under compression
MCF_r (kN)	Air pressure in air-compensator of the upper roller at main compression
mtop (mm)	Position of top roller at main compression
pad1 (rpm)	Speed of paddle 1 in the forced feeder
pad2 (rpm)	Speed of paddle 2 in the forced feeder
PCD (mm)	Maximum displacement of the upper roller during precompression
PCF (kN)	Maximum precompression force exerted on powder under compression
PCF_r (kN)	Air pressure in the air-compensator of the upper roller at precompression
prebot (mm)	Position of bottom roller at precompression
pretop (mm)	Position of top roller at precompression
Q^2 (%)	Predictive squared correlation coefficient
ρ (mg/mm ³)	Density (of tablet after ejection)
ρ_{app} (mg/mm ³)	Apparent density
ρ_{bulk} (g/cm ³)	Bulk density
ρ_{ID} (mg/mm ³)	Density of tablet during compression, minimum distance between punches
ρ_{tapped} (g/cm ³)	Tapped density
ρ_{true} (mg/mm ³)	True density
R (mm)	Radius
R_h (mm)	Radius of the punch head flat
R_p (mm)	Radius of the pitch diameter
R^2 (%)	Coefficient of determination

RH (%)	Relative humidity
RMSEP	Root Mean Squared Error of Prediction
S_{con}	Slope of the consolidation phase
S_{decomp}	Slope of the decompression phase
SC	Screw configuration
Speed (tpm)	Tableting speed
Stdev	Standard deviation
T (mm)	Thickness
T_{ID} (mm)	Minimum in-die thickness during compression
T_{AD} (mm)	In-die thickness immediately after the decompression phase
t/ρ_{mean}	Ratio of F_{max} to $F_{mplateau}$
t_{begin} (ms)	Start of a signal on a force-time profile
t_{con} (ms)	Consolidation time
t_{decomp} (ms)	Decompression time
t_{dw} (ms)	Dwell time
t_{end} (ms)	End of a signal on a force-time profile
t_{Fmax} (ms)	Time when maximum force occurs on a force-time profile
t_{Fmin} (ms)	Time when minimum force occurs on a force-time profile
t_{lag} (ms)	Time between pre- and main compression, measured on lower roller
t_{total} (ms)	Contact time
t_0	Value measured immediately after production
t_7	Value measured after a storage period of seven days
t_{25dw} (ms)	First quarter of the dwell time
t_{50dw} (ms)	Middle of the dwell time
t_{75dw} (ms)	Third quarter of the dwell time
top (mm)	Position of top roller
TS (MPa)	Tensile strength
v_t (tpm)	see "Speed"
V (mm ³)	Volume (of tablet after ejection)
V_{ID} (mm ³)	Volume of tablet during compression, minimum distance between punches

ABBREVIATIONS AND SYMBOLS

V_0 (cm ³)	Bulk volume of powder
V_{1250} (cm ³)	Volume of powder after 1250 taps
VC (%)	Variation coefficient
W (mg)(g)	Weight
ω (rpm)	Turret speed
X (g/s)	Net material clearing from the feeder

OUTLINE AND AIMS

Despite the high quantities of tablets produced daily, a lot of the established processes and formulations are the results of (suboptimal) trial-and-error experiments, contributing to the image that the entire field of pharmaceutical powder technology is more “an art than a science” [1]. Also, a large number of contributing papers to the field date from roughly two or three decades ago. Although the operation mode and press lay-out stayed basically unchanged since its invention, the instrumentation improved largely in terms of quality, accuracy and sensitivity. Moreover, due to the increased competition through generic manufacturing and the shift towards a more patient-centered production, more advanced tablet formulations exhibiting e.g. prolonged, extended, delayed or immediate release profiles have emerged.

This, together with the Process Analytical Technology (PAT) – initiative, proposed by the American Food and Drug Administration (FDA) in 2004, encourages a shift towards a more scientifically based technology. The goal of the initiative is to stimulate the pharmaceutical industry to “design and develop processes that can consistently ensure a predefined quality at the end of the manufacturing process”. By identifying all sources of variation of importance for the product performance and quality, and by increased process understanding and continuous monitoring, quality could be built rather than tested into the product [2]. Together with the International Conference on Harmonization (ICH) Q8 guideline on Pharmaceutical Development, focusing on the Quality-by-Design (QbD) concept, it forms the regulatory framework to catalyze the shift of the pharmaceutical industry towards a redesigning of the current approach [3-5].

Seen in the light of these new movements within the tablet manufacturing area, it appears obvious that there is a need for new knowledge to fund a base for a thorough understanding of the continuous tableting process. This thesis aims to contribute in this large context by the investigation of the tableting process on a high-speed rotary tablet press. The goal was to increase the understanding of the influence of the properties of the starting material and process parameters on dependent process parameters and tablet properties. Since the PAT-initiative stimulates the introduction of new analytical tools to enhance process

understanding and product quality, additional analytical chemistry tools, next to the built-in instrumentation were used. Moreover, due to the large amount of data obtained, Design of Experiments (DoE) and Multivariate Data Analysis (MVA) were administered to perform experiments and analyze data in a structured manner. Three main topics were addressed:

- The role of the forced feeder: its influence on the properties of the starting material, on the die-filling process and on the final tablet properties.
- The mechanism of (double) compression: its influence on dependent process parameters and on the final tablet properties.
- The role of additional analytical chemistry tools in a continuous tableting process: its applicability to assess tablet properties, produced from starting material with different characteristics.

REFERENCES

- [1] H. Leuenberger, M. Lanz, Pharmaceutical powder technology – from art to science: The challenge of the FDA’s Process Analytical Technology initiative, *Adv. Powder Technol.* 16 (2005) 3-25.
- [2] United States Food and Drug Administration (FDA), Guidance for industry - PAT - A framework for innovative pharmaceutical development, manufacturing, and quality assurance, in, 2004.
- [3] International Conference on Harmonization (ICH) of technical requirements for registration of pharmaceuticals for human use, Topic Q8(R2): Pharmaceutical Development, in, Geneva, 2009.
- [4] S.N. Politis, D.M. Rekkas, The evolution of the manufacturing science and the pharmaceutical industry, *Pharm. Res.* 28 (2011) 1779-1781.
- [5] L.X. Yu, G. Amidon, M.A. Khan, S.W. Hoag, J. Polli, G.K. Raju, J. Woodcock, Understanding pharmaceutical quality by design, *AAPS J.* 16 (2014) 771-783.

1

INTRODUCTION

1. HISTORY OF TABLET COMPRESSION

Powder compression is a manufacturing process used in a broad range of industries, such as powder metallurgy, industrial ceramics, pharmaceuticals, food, detergents, fertilizers, batteries, magnets, nuclear and hard metals. Compaction can be described as the process whereby a loose powder is placed in a die and pressed between punches to form a coherent mass. The process is fast, economic and lends itself to high-volume production. Dependent on the complexity of the powder compact (e.g. complex parts as automotive gearbox components versus pharmaceutical tablets) production rates range from tens to millions per hour [1].

The earliest reference to a dosage form resembling the tablet is found in the Arabic medical literature and dates from the tenth century. Drug particles were compressed between the ends of engraved ebony rods while force was applied by a hammer. In 1843, British Patent 9977 was granted to William Brockendon for “manufacturing pills and medicinal lozenges by causing materials when in a state of granulation, dust or powder, to be made into form and solidified by pressure in dies”. The use of “compressed pills” increased rapidly since then, and by 1874 both rotary and eccentric presses were in use, with an operation mode fundamentally the same as the presses used today [1, 2].

Although in use for many years, it was not until the middle of the 1950’s that a systematic study began of those factors which might affect tablet properties. The initiation of this new approach was stimulated by the invention of the instrumented tablet press. Higuchi and his group instrumented upper and lower compression, ejection and punch displacement on an eccentric tablet press, and pioneered with this the study of the compaction process [3-5]. Since then, a number of patents related to press instrumentation and control followed. The pharmaceutical industry has attained a greater understanding of the compression process, due to this instrumented tablet presses and sophisticated data collection systems, together with the development of mathematical models [5, 6].

2. COMPACTION EQUIPMENT IN MANUFACTURING

2.1. Eccentric tableting machines

The eccentric tableting machine, a single-station press, is still in use for low-volume production of simple geometries or for the production of complex multi-level parts. In these presses (Figure 1.1), the powder is fed into a die from a hopper and a feed shoe (I). The feed shoe moves above the die opening and powder flows under gravitation into the die. Alternatively, the feed shoe can be equipped with vibrational or shaking devices or paddles inside to improve powder flow and die filling. After die filling, the feed shoe is withdrawn and while the bottom punch (II) stays stationary, the top punch (III) moves down into the die (a). After compression (b), top and bottom punch move up. The bottom punch herewith pushes the tablet out of the die (c). Subsequently, the lower punch position decreases again. The feed shoe slides over the die for refilling and pushes the compressed tablet from the die table (d). During compaction, the top punch is motor driven by an eccentric, while the bottom punch is maintained stationary. Consequently, the force is exerted in an unilateral direction (i.e. only by the upper punch) [1, 2, 7].

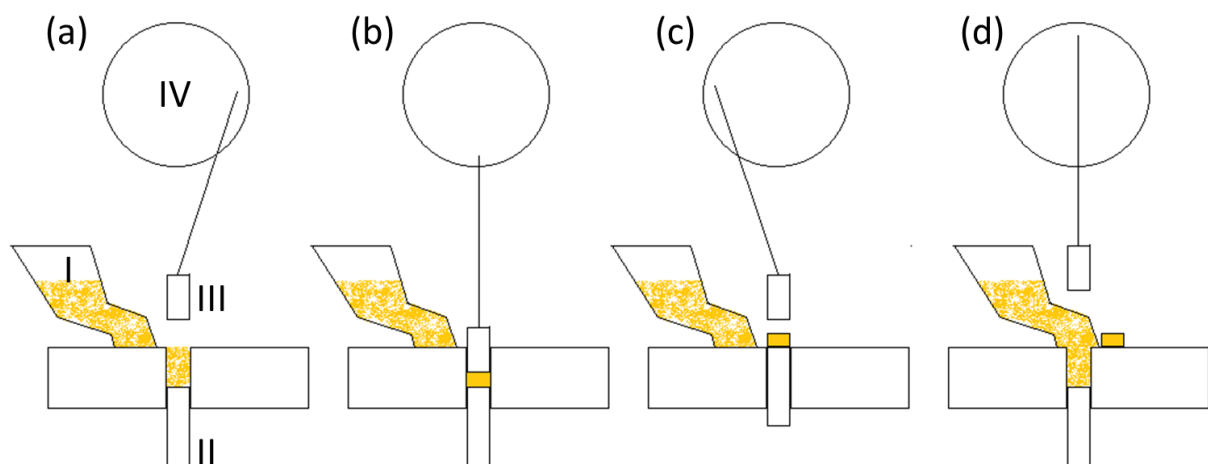


Figure 1.1: Schematic representation of an eccentric press. (I) feed shoe, (II) bottom punch, (III) top punch, (IV) eccentric motor driven wheel. (a) top punch moves down after die is filled, (b) compression step, (c) top and bottom punch move up, bottom punch pushes tablet out of the die, (d) feed shoe moves over die, pushing the tablet from the die table. (Adapted from [7])

In an eccentric tablet press, a relative small amount of press parameters determines the compression cycle and the final tablet characteristics. Firstly, the weight is controlled by the lower punch position. Since die filling is a volumetric process (in every type of tablet press),

the weight of the tablet is determined by the volume in the die. The die is confined by the die diameter, which obviously stays unchanged during a tableting campaign, and the height of the powder column, determined by the position of the lower punch. The tablet thickness, and with that the compression force exerted on the powder bed, is managed by the penetration depth of the top punch. The compression rate can be adapted by changing the speed of the eccentric wheel. Finally, the ejection point, which ideally is flush with the die table, is controlled by the highest position of the lower punch. Sometimes this latter needs adaption, when for instance punches with deep curvatures are installed.

2.2. Rotary tablet presses

Rotary tablet presses are used for high-volume production (millions of tablets per hour) of relatively simple powder parts. Nearly all production of pharmaceutical tablets nowadays takes place on these presses [1-3, 6]. A detailed description of the design of this machine is given in Chapter 2. The main differences with the eccentric presses are outlined in Table 1.1. Briefly, the powder is fed from a hopper and feeder which is mounted stationary on the die table. The die and punches reside in a rotating turret and pass through the filling station, precompression and main compression rollers and the ejection station [8].

Table 1.1: Main differences between the eccentric and rotary tablet press.

Features	Eccentric press	Rotary tablet press
Feeder	Moving	Stationary
Die table	Stationary	Moving
Number of punch stations	1	10 - 100
Compression direction	Unilateral (top punch)	Bilateral (top and bottom punch)
Compression stations	1 (main)	(mostly) 2 (pre- and main)
Tableting speed	$\pm 600 - 3600$ tabl/hour	$\pm 72000 - 1500000$ tabl/hour

A typical feed frame on a high speed rotary tablet press is a closed chamber which contains at least two paddle wheels. Dependent on the manufacturer and press type the amount of paddles, their design (amount of paddle fingers and shape), their direction of movement in relation to the turret movement, the clearance between them and between the paddles and top and base plate can vary. Also their speed regulation can be independent from each other and tablet speed, or interrelated.

Furthermore, the position of the hopper inlet into the feeder can vary [9-12]. Prior to weight adjustment, commonly the die is “overfilled”. The punch is lowered a little further than necessary to achieve the desired weight, to make sure that the die is completely filled. Before leaving the feeder, the punch moves up at the dosing cam (i.e. where the position is set to volumetrically control the weight) and the excess of powder is expelled.

On rotary tablet presses, the compression process generally consists out of two compression steps, pre- and main compression. At precompression a lower force is applied, mainly with the aim of removing excess of air present between the powder particles. Even so, with a precompression step the total time the powder is compressed is prolonged, contributing to stronger tablets [3, 8, 13-15]. Furthermore, next to a difference in the amount of compression stations between eccentric and rotary presses, there is also a fundamental difference in the compression method. Whereas the bottom punch stays stationary during compression in an eccentric machine and force is applied unilateral, compression in a rotary press happens bilateral. While the upper punch is lowered into the die by the upper compression roller, the lower punch is raised by the lower compression roller. Finally, the ejection step is basically the same for both types of presses. The lower punch is raised, herewith pushing the compressed tablet out of the die.

Although seemingly simple, compression on a rotary tablet press is a complicated engineering process, as a large amount of process parameters can be varied, irrespective of the press and tooling set, in contrast to an eccentric tablet press [8]. Weight control is not only managed by the position of the lower punch, but also the installed overfill cam and the speed of the paddles should be taken into account, as well as the clearance between the feeder and the die table. The compression step can be influenced by both the position of the upper and lower roller, as the distance between them controls the thickness and hence the compression force. Furthermore, their position relatively to the die table determines the in-die compression position, from which is known to influence the final tablet characteristics [8, 16, 17]. Next to the ejection point, the slope of the ejection cam is also important, as this, together with the tableting speed, determines the ejection rate.

2.3. Special presses and latest designs

Most special tablet presses can be categorized as adapted models of the rotary press, as described above.

By using multitip tooling (i.e. several punch tips on one punch) the productivity of small tablets can distinctly be increased, as with each compression more tablets are formed at the same time. This approach is also possible on an eccentric press [1, 7]. Another way to increase the productivity without changing the tableting speed, is by using a double-sided configuration, which is obviously only possible on a rotary press. Here, two ejection and two feeder positions are mounted on the press. With every rotation of the turret, the die is filled and emptied twice, herewith doubling the productivity. The newly inserted feeder and outlet can be placed between the pre- and main compression roller of an existing press. Hence, every tablet is formed by only one compression step. A more common approach is the use of dedicated presses, which have a total of four pair of compression rollers.

Similar adaptations allow the production of bilayer tablets. Here, an extra feeder is installed between the precompression and main compression station. At the die fill position, the powder of the first layer is introduced into the die. During precompression, this layer is compressed at a low force (i.e. tamping), hence forming initial bonds and determining the fill depth of the second layer. The second powder is subsequently brought into the die, after which the total powder column is compressed to form the final tablet. Tri-layer presses have also been developed, using the same principles. These multi-layer tablets are popular in the pharmaceutical industry, as they can be used for dosing incompatible active pharmaceutical ingredients (APIs) in one unit, or for compressing granules or a powder blend exhibiting different release rates of the same API. Furthermore, the compression coating process (i.e. dry coating or powder coating) can be considered as a special case of bi-layer tableting. The precompression station is replaced by a feeding device for small tablets. At the first die filling station, a small amount of powder is fed into the die. Subsequently the small (core) tablet, which is compressed on a separate press running at the same production speed, is introduced on top of the first layer. More powder is introduced at the second die fill position, followed by (pre- and main) compression and ejection [1, 7]. A schematic overview of the design of these presses is provided in Figure 1.2.

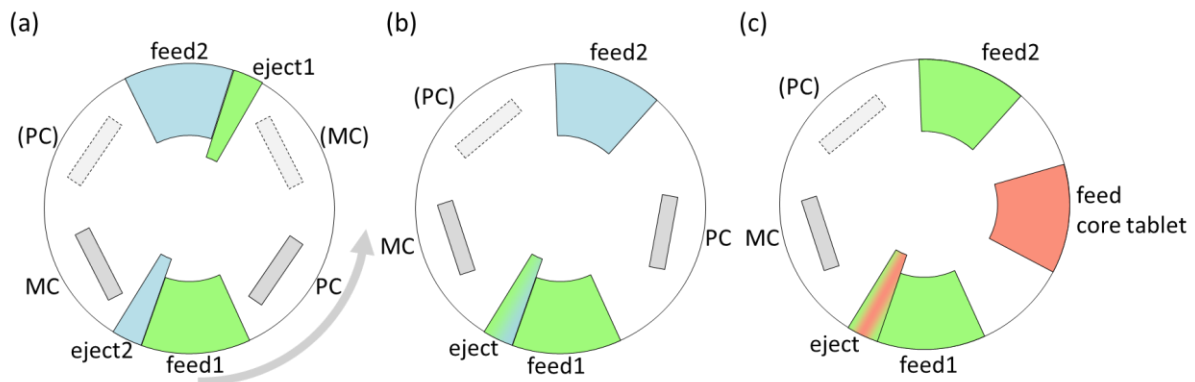


Figure 1.2: Schematic topview of the design of a (a) double-sided compression machine, (b) bilayer compression machine, (c) compression coating machine. Grey arrow in (a) depicts direction of die table movement for all. feed: feeder; eject: ejection station; PC: precompression; MC: main compression. (Adapted from [1])

Most rotary presses use die feed systems with paddles as described previously. However, there is one rotary machine which applies a different filling mechanism. In the IMA Comprima tablet press (I.M.A. (Industria Macchine Automatiche), Ozzano dell'Emilia, Bo, Italy) die filling is achieved via a centrifugal die filling system. The powder is fed into the center of the die table. The powder flows under the effect of centrifugal forces through radial channels inside the die opening. Die fill is facilitated by rapid separation of the punches. Both upper and lower punches lower after die filling, herewith closing the die. After compression between the compression rollers, the tablet is ejected at the lower opening of the die. This system is currently in use in the industry for large-scale manufacturing, but is restricted by the flow of the powder blend, as a free-flowing behavior is essential for optimal product yield [1, 7, 18].

Finally, since many manufacturers understand the need and importance of extended dwell time (i.e. the period during which the punch head flat (land) is in direct contact with the compression roller), some advances are made in the last decades regarding this topic. Foremost, the addition of an extra compression step, by the introduction of the precompression roller, is the greatest change in comparison to the first rotary tablet presses [3]. Nearly all rotary presses are equipped with two compression stations. However, some manufacturers offer other possibilities. Korsch (Berlin, Germany) for instance, equips his machines with a compression dwell bar. The bar is installed between the precompression and main compression station and maintains the pressure on the tablet exerted at

precompression, with that extending the (pre-)compression dwell time. The tablet presses of the newest line of Fette Compacting (Schwarzenbeck, Germany) can be installed with four pair of compression rollers, herewith subjecting the powder to four consecutive compression events. The tableting machines of GEA Process Engineering, Courtoy™ (Halle, Belgium) use a completely different approach to extend the dwell time, which is outlined in detail in Chapter 2. Briefly, the upper rollers are attached to an air piston, which allows vertical movement in an air cylinder. When during a compression run the reaction force exerted by the powder exceeds the air pressure in the cylinder, upward movement of the upper compression roller is possible. As the upper roller is displaced, the contact time between the punch head flat and the roller is prolonged. Hence the dwell-time is extended. Also tooling manufacturers try to anticipate on these specific demands of the pharmaceutical industry, by offering punches (Figure 1.3) with a specially designed punch head. By physically enlarging the head flat (land), this surface will stay longer into contact with the compression roller, hence prolonging the dwell-time.

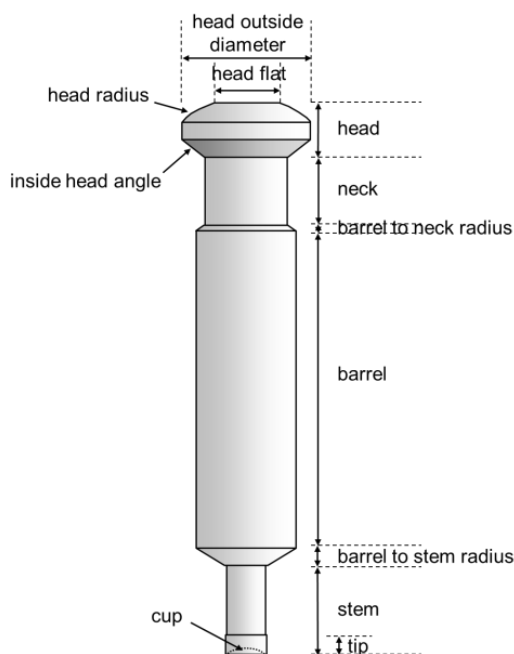


Figure 1.3: General tooling terminology. Representation of upper punch. (Adapted from [19])

3. COMPACTION EQUIPMENT IN RESEARCH AND DEVELOPMENT

3.1. Compaction simulators

A fundamental understanding of the compaction mechanism can assist in the formulation of powders. The amount of drug substance available in the early stages of formulation design and process development is usually limited and the use of full-scale rotary presses not possible, as the latter requires commonly large quantities of powder to fill the feed frame and operate the press at steady-state conditions. For this purpose, dedicated devices were invented [1, 7, 17].

3.1.1. Hydraulic compaction simulators

A first large group of these specially designed instrumented presses are the hydraulic compaction simulators, from which a schematic representation is given in Figure 1.4. The set-up consists of a die table, two independent servo-hydraulic systems driving upper and lower punch controlled by a computer and a load frame (i.e. supporting column for die table and the crossheads with punches).

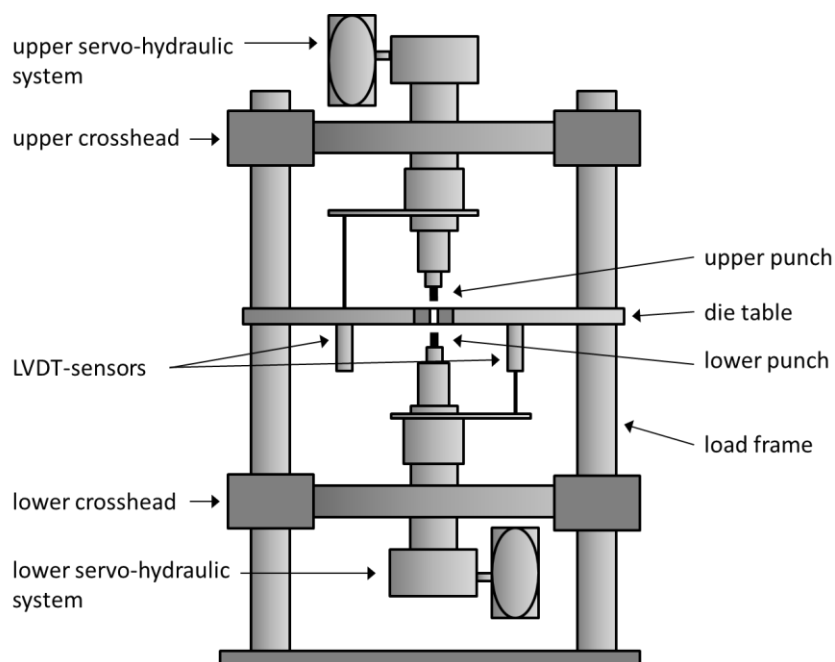


Figure 1.4: Schematic representation of a hydraulic compaction simulator. (Adapted from [1])

The machine is equipped with different control mechanisms, sensors and load cells, in order to carefully control and gain insight in the compression process. Force on and movement of

the punches (speed and path) is determined by the hydraulic system and crossheads coupled to the computer, as well as the fill depth and ejection height. The (transmission of) force exerted on the powder bed is measured by load cells on upper and lower punch and by radial die wall sensors. The movement of the punches is recorded by linear variable displacement transducers (LVDT sensors). Finally, the ejection force can be determined by the load cell on the lower punch. The latest designs (i.e. third generation compaction simulators) offer some additional features. The ESH Powder Compaction Simulator for instance (Huxley Bertram Engineering, Cambridge, UK) is equipped with automatic powder hoppers (also bilayer tableting is possible), a tablet take-off arm which measures the take-off force and a storage carousel. External systems can be coupled to control the temperature of the punch and die for non-ambient testing. The Merlin compaction simulator (Merlin Powder Characterisation, Leicestershire, UK) furthermore, offers the possibility to measure internal tablet temperature during compaction and tablet adhesion.

Compaction simulators were designed to mimic the compression cycle of any prescribed shape by using the hydraulic control mechanisms. The simulation can be achieved by two mechanisms. Either the force (load control) or the movement of the punches (position control) are controlled. When using the load control, in theory a force-time profile of a production machine can be mimicked. However, compaction simulators are seldom used for that goal. Too many factors influence the force-time profile on a rotary tablet press (e.g. the material under compression, tooling, geometry of the machine, tableting speed) which cannot all be theoretically calculated or programmed into the machine. Using an instrumented punch to collect data from a production press and feed these into the compaction simulator is a possible approach, but recalculation is not straight forward and the information is limited to a particular punch size and shape. Moreover, in early stages of product formulation, mostly not enough material is available to run the product on a rotary tablet press and collect data to transfer to the compaction simulator.

A second, far more used approach, is running the machine in position control. The rationale behind this technique is when the punches are forced to move in the same pattern as in a production press, the force-time curve will automatically follow [5]. There are three possible methods to investigate the punch movement. Firstly, prerecorded data from any tablet press can be used. This approach faces the same challenges as with the force-time profile:

- The instrumentation on the production press must allow accurate recording of the movement of the punches, which is rarely a standard feature. Alternatively an instrumented punch can be used. The Intelli-Punch for instance (Merlin Powder Characterisation, Leicestershire, UK), fits into any standard production press and replaces one punch of the normal tooling set. It measures the punch displacement and transmits the profile to a remote receiver, which is connected to a computer. The obtained “real” displacement profile data can be imported directly into the compaction simulator for further research. However, this technique is not always so straight forward, as reported in literature [5, 20, 21].
- The punch movements depend on many factors and the information is limited to the machine, tooling and material used.
- The formulation being developed is available in only limited quantities, restricting experiments on the production machine.

Instead of prerecorded data, artificial punch displacement profiles can be used. Compaction studies were done using for example the “single-ended” profile (i.e. when the lower punch is stationary like in an eccentric press) or the “saw tooth” profile (i.e. constant speed profile where punch displacement speed is constant) [22-25]. Finally, theoretical profiles can be administered. These profiles can be calculated from the press and punch geometry and the tableting speed. The resulting sinusoidal equation is used in order to simulate punch movement in a tablet press.

Due to the above mentioned constraints regarding the use of prerecorded data and the discrepancies between the actual profiles on a rotary press and the theoretical and artificial profiles from a compaction simulator, hydraulic compaction simulators are not the preferred equipment for scaling-up experiments, troubleshooting or simulation of high-speed production processes. However, they are ideally suited for basic compaction research and material characterization, as they are precision instruments that generate accurate results with only a small amount of material needed. A lot of parameters can be controlled and set freely, independently from one another, making these machines versatile tools for fundamental compaction research [5, 7].

3.1.2. Mechanical compaction simulators

A second group of compaction simulators can be defined as mechanical compaction simulators. These machines make no use of hydraulic systems. As with the latter, either the force (load control) or the movement of the punches (position control) can be controlled.

The first type of this machine was the linear mechanical rotary tableting machine simulator, the Presster™ (MCC (Measurement Control Corporation), New Jersey, USA). A single pair of punches moves linearly forth and back between compression wheels on a lower and upper punch track. A production press geometry can be simulated by matching the diameter of the (replaceable) compression rollers. Likewise, press speed, tablet weight (by adjusting fill depth) and thickness and force (by adjusting distance between the rollers) can be set and controlled mechanically [26]. The standard instrumentation allows measurement of the upper punch force, upper and lower punch movement and the compaction speed. Optionally, the machine can be equipped with precompression rollers, an ejection cam with adjustable angle and instrumentation measuring ejection force, lower punch force, radial die wall pressure and take-off forces.

Another group of mechanical compaction simulators has a design resembling the design of the hydraulic compaction simulators. Upper and lower punch and die table are positioned in a load frame, and the punches can only move in vertical direction. In contrast to the hydraulic systems, the movement of the punches is controlled electrically. In the Stylcam (Medelpharm, Beynost, France) for instance, electrically driven cams determine the movement of the punches. The cams are positioned under the lower compression wheel and allow the simulation of different tableting machines and their dwell times due to different acceleration of the punches. Precompression is simulated by compressing a tablet twice. Instrumentation is comparable to the other compaction simulators [27-29]. The latest designs of these machines (e.g. Styl'one Evolution, Medelpharm, Beynost, France) can almost be defined as "tableting robots". They offer the same features as other mechanical compaction simulators, but can additionally be equipped with up to three feeders for 5-layer-tablets, a feeder for core tablets for compression coating, special tooling (e.g. multitip tooling) and an external lubrication mechanism. Different types of feeders can be used (hand fill, gravity fill, forced feeder) and punch movement can be either set uniaxial or biaxial.

Furthermore, with a maximum output of 1200 tablets/hour, these machines are suitable for the manufacturing of clinical batches.

The mechanical compaction simulators simulate to a greater extent the tableting process on rotary tableting machines than the hydraulic compaction simulators. However, some mechanisms cannot be accounted for. The die filling step for instance, with the combination of gravitational, suction, forced and centrifugal forces is difficult, if not impossible, to mimic on a stationary (or linear) single-punch system. The great advantage of these machines is the small quantity of product needed, which makes them an interesting tool in the early development formulation experiments.

3.2. Instrumented manufacturing presses

Another possibility is the instrumentation of the presses used in manufacturing. This approach has some advantages and disadvantages over the use of dedicated machines for research and development.

One of the advantages is the reduction in scale-up time and related costs. Commonly a formulation is developed on laboratory-scale machinery. After the introduction of the formulation into the next scale-up step and final production-scale, often problems arise due to the differences (in geometry, mode of operation, tooling, speed,...) between the used equipment. Ultimately, this can lead to the need of completely reformulating the product [5, 30]. The less scale-up steps that have to be taken and the earlier a product can be run on production-scale, the faster problems can be identified. This also lowers the risk of encountering further upstream hurdles. Moreover, as the tableting process is by definition a continuous process, the scale factor is only determined by the process time and not by the dimensions of the equipment (as the scale factor between different steps is generally limited to a factor 10) [31]. The reduction of floor space can be seen as another benefit. Although small table-top presses (both rotary and eccentric) for use in research and development (R&D) are available, the larger equipment is mostly preferred, since it mimics to a closer extent the geometries and the applied forces of the production presses. Furthermore, extra personnel costs and training can be avoided. Compaction simulators, small-scale and production presses become more sophisticated, which often means more difficult to operate. This increases the requirements for skilled labor for operation and interpretation of

the results. Finally, the instrumentation of production presses is also cost-saving, as compaction simulators are often related to a capital investment. Evidently, the implementation of sensitive and accurate control and measuring devices in production equipment is neither an inexpensive decision, but is more likely to be profitable in the long term. As the pharmaceutical industry moves towards the implementation of Quality by Design (QbD), the implementation of tools to enhance process control and understanding during pharmaceutical development and manufacturing will gain importance [32, 33].

The instrumentation of manufacturing presses also encounters some drawbacks. Not in the least, it imposes some large engineering challenges. Major improvements in the quality, accuracy and sensitivity of instrumentation, data acquisition and analyzing techniques have been made over the last decades. The implementation of these sophisticated instruments in high-speed presses is not an easy task [26]. Besides the practical implications, tools also have to be robust enough to withstand electrical current fluctuations and vibrations. Moreover, easy calibration and validation procedures are preferable, as change-over and cleaning of the press requires fast disassembly and installation of press parts to ensure optimized product yields. As for research and development, another point of consideration is the availability of these machines in a production environment. Since a high output is important, machines are preferably run at the highest possible capacity for the largest amount of time. Interrupting a production campaign in a controlled environment for preliminary experiments with a non-approved test formulation is inconceivable. Consequently, at least one other identical press should be available for R&D purposes, which implies a large investment. Finally, another major disadvantage of using instrumented manufacturing presses in an early stage of development remains the necessity of a large amount of material [26]. Although the latest designs of rotary presses are capable of running with only one punch pair, still a few hundreds of grams of product is needed to fill the forced feeder, in order to be able to simulate a production run as close as possible.

4. STUDYING AND MODELING THE COMPACTION PROCESS

4.1. Data acquisition

Without taking into account the instrumentation in place for monitoring and controlling the process to guarantee fluent production and prevent damage to the press (e.g. sensors

measuring the pull-up force of the upper punch at ejection to control punch lubrication), a modern rotary press can be equipped with a large amount of sensors and measuring devices generating information directly related to the material under compression (Table 1.2).

Table 1.2: Measured values on an instrumented rotary tablet press.

Force

Shear force in the feeder
 Compression force on the roll*
 Compression force on the upper punch*
 Compression force on the lower punch*
 Radial die wall force*
 Ejection force
 Take-off force

Distance

Overfill depth
 Fill depth
 Underfill depth
 Compression depth*
 Movement of the upper roll*
 Movement of the upper punch*
 Movement of the lower punch*
 Distance between upper and lower punch under compression*
 Distance between upper and lower punch after compression*
 Ejection position

Time

(Speed)

Paddle speed(s)
 Tableting speed

Temperature

Temperature of die
 Temperature of upper punch
 Temperature of lower punch
 Temperature of tablet

*Different values for pre- and main compression

The instrumentation itself, their implementation and the systems to convert the measurements into useable information are a research field (engineering and IT) on itself, which lay beyond the scope of this research project. In-depth information and research performed on this topic can be found elsewhere [4, 5, 7, 20, 34-56]. Obviously, the output offers a wealth of data which can be used in different manners, depending on the purpose.

4.1.1 In research and development

In early development, the main goal is to gain insight in the basic material properties, with the latter referring to the compaction behavior of the material (elastic, plastic or by fragmentation) and the formation of bonds under applied pressure [57, 58]. An extensive body of literature is published about this topic in the last decades.

From the force-time profiles, attempts were undertaken to gain information on elasticity by evaluating the area under the curve and the shape of the force-time profile [59-62]. Other researchers tried to fit different functions (Weibull function, Fraser-Suzuki function) to the force-time data to differentiate between the deformation behavior of materials [63, 64]. Force is furthermore applied to calculate the ratio between the radial and axial transmission and equations were derived to study the compaction behavior under pressure [46, 65-70].

Displacement-time profiles are generally used to calculate the fast elastic recovery of material under pressure. As the position of both punches in the die is known, the distance between them can easily be calculated. Comparing the distance between the punches at maximum pressure with the distance immediate after compression (after the decompression phase) allows calculation of the elastic expansion [22, 23, 71].

Force-displacement measurements have also been a popular method for studying the compression process during tableting. The curves are obtained from measurements of punch force and displacement. The general assumption is that it should be possible to correlate the energy input, or work of compression, with the deformation and bonding properties of materials. In many of the studies, the work of compression is calculated as the total area under the upper punch force versus upper punch displacement curve, but also other techniques (e.g. calculation of the first derivative) are applied [29, 72, 73].

Another applied technique is the combination of force-displacement and displacement-time profiles in one model, or the combination of force, displacement and time in 3D-plots [74]. In the latter, force is expressed as pressure, time is normalized and from the displacement data the porosity according to Heckel is calculated [75-77]. Furthermore, viscoelastic behavior and the capping of compacts is often studied by equations and models (e.g. the Drucker-Prager Cap model) using force-time, displacement-time and force-displacement data [27, 28, 78, 79].

The equation of Heckel is the most extensively used model, with the underlying porosity-pressure known as the Heckel plot [24, 25, 50, 80-82]. The equation for the linear compression process follows first-order kinetics. Although so intensively administered for the description of powder compression, several authors have underlined the shortcomings of this equation, which finds its origin in the description of metal powders, for the characterization of pharmaceutical materials [83-87]. Other equations to describe the volume or porosity reduction or density increase under pressure were presented by Walker, Cooper-Eaton, Kawakita, Carstensen, Leuenberger, Shapiro and Adams, which are also commonly used by researchers to study the mechanical properties of particles [58, 88-100].

A lot of research in this field is dedicated to establishing correlations between the different functions. Sonnergaard for instance investigated the relation between tableability (tensile strength (TS) versus pressure) and compressibility (porosity versus pressure) characterized by the Walker coefficient [100]. Other researchers performed similar experiments in order to determine relations, for instance between tableability and the Heckel function; between TS, elastic recovery (ER) and Heckel values; between TS, ER and Heckel, Walker and Kawakita values and others [22, 26, 66, 96, 97, 102-104].

4.1.2. In scale-up and production

In contrast to the above mentioned techniques, the main goal in scale-up experiments and production is to gain insight in the correlation between the output data and the resulting tablet characteristics. When the influence of the process parameters (e.g. applied force, displacement, speed and temperature) on critical quality attributes (CQA) of the end product is known, the established correlations can be used to control, check and steer the production process. Process parameters can for instance be correlated with tablet

properties to obtain information about the tableability, the compressibility and the compactibility (solid fraction versus TS) [105]. More advanced methods include the use of X-ray computed tomography to investigate the density distributions inside the tablet and correlation to press parameters and other tablet properties [106].

The force-time profiles carry a large amount of information, which can be used to optimize the production process. In addition to the absolute force value and the variability, the shape of the force-time profile is of great importance as it directly affects tablet properties such as hardness and friability, as shown by Yliruusi et. al [107]. Other forces as the radial die-wall pressure, the ejection force and the take-off force can give information about sticking of material to the punches or die-wall [70]. These observations can be used for instance to study the capping tendency of material, optimize a formulation during a lubricant study, or in production to raise the external lubrication spray-rate. Increase in shear forces in the feeder of the tablet press can be an indication of segregation or uncontrolled packing of powder, which can require a change in paddle speed, paddle design or even in formulation composition.

The displacement-time profiles generate information about the in-die thickness under compression and after decompression, which can be linked with the ER of the material [22, 23, 71].

A very important factor in the tableting process is the tableting speed. The influence of nearly all other factors on the tablet properties changes with tableting speed. The rate of force application has a major influence on the force-time profile and the resulting tablet properties, for instance strength and capping tendency of compacts. In particular for plastic and viscoelastic materials this effect is observed [23, 82, 104, 108-113]. Tableting speed also influences the lag-time (the time between the precompression and main compression phase), which was also found to influence the tablet strength [114]. Furthermore, the production speed influences to a great extent the die fill process [8, 10]. Finally, increasing the tableting speed will contribute to more machine vibrations and a faster temperature rise of the tooling and consequently the tablet.

Next to the absolute value of a process parameter, the variability (i.e. fluctuation) of the data are of equal importance. Fluctuations are inherent to a dynamic process. Monitoring

that variance and gaining insight in its influence on the CQA of the end product allows justified actions to be undertaken (i.e. in a feed-back and feed-forward loop).

In all of the above mentioned, the characteristics of the starting material should also be taken into account, as they equally contribute to the quality of the end product. This approach fits into the QbD concept, which states that a process is generally considered well-understood when (1) all critical sources of variability are identified and explained, (2) variability is managed by the process, and (3) product quality attributes can be accurately and reliably predicted [115].

Table 1.3: Overview (not exhaustive) of the input material attributes, the process parameters and the quality attributes of the tableting process. (Adapted from [33])

Input material attributes	Process parameters	Quality attributes
Particle/granule size and distribution	Type of press (model, geometry, number of stations)	Tablet appearance
Fines/oversize	Hopper design, height, angle, vibration	Tablet weight
Particle/granule shape		Weight uniformity
Cohesive/adhesive properties	Feeder mechanism (gravity/forced feed, shape of wheels, direction of rotation, number of paddles)	Content uniformity
Electrostatic properties		Hardness/tablet breaking force/tensile strength
Hardness/plasticity		Thickness/dimensions
Bulk/tapped density	Feed frame type and speed	Tablet porosity/density/solid fraction
Viscoelasticity	Fill depth	Friability
Brittleness	Tooling design (e.g. dimension, score configuration, quality of the metal)	Tablet defects
Elasticity		Moisture content
Solid form/polymorph	Maximum punch load	Disintegration
Moisture content	Press speed	Dissolution profile
	Precompression force	
	Main compression force	
	Punch penetration depth	
	Ejection force	
	Dwell time	

A process parameter is considered critical (i.e. a critical process parameter (CPP)) when its absolute value and its variability has an impact on a CQA and therefore should be monitored or controlled to ensure the process produces the desired quality. Consequently, the state of a process and the quality of the end product depends on its CPP's and the critical material attributes (CMA's) of the input materials. An overview (not exhaustive) of these parameters for the tableting process is provided in Table 1.3 [32, 33].

4.2. Design of Experiments

Due to the large amount of process parameters that can be varied and their interactions, a rational and structural approach is necessary for conducting experiments which provide the maximum amount of relevant information (about the process parameters, their relation to each other and their influence on the product attributes), in the most efficient way. The traditional method of changing one factor at a time (COST-approach) has a lot of constraints, as it does not only require a large number of observations, but it also fails to reveal potential interactions between the factors, which is fundamental in understanding the system's behaviour [116, 117]. Moreover, the COST-approach is also not capable of identifying the optimum combination of parameters leading to the desired responses. Design of Experiments (DoE) is an approach in which the controlled input factors of the process are systemically (and simultaneously) varied in order to obtain the maximum of information, with only a limited number of experiments. The effects on the output variables and the most influential factors can be identified. DoE has a mathematical foundation behind the experimental procedures and yields the maximum information for a given amount of data. Moreover, this approach not only allows to investigate the *experimental space* (i.e. the area which spans the parameter ranges from which information needs to be gathered) in a structured way (screening) but also to make founded decisions on which values the factors should have to ensure that the response is close to the target value (optimization) with a minimum of uncertainty (robustness). Consequently, the final *process design space* can be defined, as the multi-dimensional combination and interaction of input variables and process parameters that have demonstrated to provide quality assurance [33, 116, 118-120].

4.3. Multivariate Data Analysis

By conducting experiments in an ordered way, masses of data are obtained. Product quality, itself laid out in different tablet characteristics, is multivariate, since it depends on achieving the desired values of all variables simultaneously [116]. Appropriate analytical tools for extracting meaningful information from these large amount of raw data is necessary. It is no longer efficient (and possible) to analyse data by simply looking at them or by plotting them in simple univariate graphs. More sophisticated, computer-based methods are needed if the data analysis is to be accomplished within a reasonable time [121]. For large datasets, Multivariate Data Analysis (MVA) is an appropriate technique to get a first insight in the data. Principal Component Analysis (PCA) is a multivariate method widely used for extracting relevant information from complex data sets by reducing their dimensionality [22, 58, 74, 93, 97]. Briefly, PCA transforms the original variables into a smaller number of uncorrelated (i.e., orthogonal) variables (i.e. principal components (PC's)), which are obtained as linear combinations of the original variables. Each PC is uncorrelated and orthogonal to all other PC's. The first PC represents the largest part of the variance of the data. The second component is computed orthogonal to the first and has the second largest possible variance. The rest of the components is computed likewise [116, 122]. Consequently, each PC represents a source of variability that is independent of the others sources [74, 121]. Partial Least Squares (PLS) is another multivariate technique. In contrast to PCA, which is a multivariate projection method designed to extract and display the systematic variation in a data matrix X, PLS is used to connect the information in two blocks of variables, X and Y, to each other. PLS is a regression extension of PCA, and a method for constructing predictive models, when the variables are many and highly collinear. This prediction is achieved by extracting a set of orthogonal factors from the independent variables which have the best predictive power [116, 121, 123].

4.4. The roll of additional PAT-tools in the compaction process

According to the Food and Drug Administration's (FDA) initiative of Process Analytical Technologies (PAT), PAT is a system for designing, analyzing and controlling manufacturing through timely measurements (i.e. during processing) of critical quality and performance attributes of raw and in-process materials and processes. The goal of this approach is

ensuring final product quality, which focuses on building quality into the product and manufacturing processes, as well as continuous process improvement [32, 33, 115, 124, 125]. Application of PAT involves four key components [126]:

- Multivariate data acquisition and analysis
- Process analytical chemistry tools
- Process monitoring and control
- Continuous process optimization and knowledge management

The instrumentation integrated in a tablet press as mentioned above, already offers a large amount of data which enables monitoring and controlling the process. However, additional techniques can provide essential information which is not possible to obtain via the existing instrumentation and can greatly assist in further fine-tuning and optimizing the causal relationships. For that purpose, the PAT initiative stimulates the introduction of new analytical chemistry tools [32, 115, 127]. Examples of the chemistry tools are vibrational spectroscopic techniques such as Near Infrared spectroscopy (NIR) and Raman spectroscopy. Although already readily applied in other industries (e.g. food, paper, polymer, medical diagnostics,...), it is still emerging as a tool for analysis of pharmaceutical processes and formulations [127]. The chemical engineering scientists acknowledge the amount of work needed to develop reliable and robust technologies for chemical compound identification and physical information, both for the materials under process as the end product. Moreover, chemometrics (i.e. extracting relevant information from the obtained spectra) and data management also constitute challenges that still require research [128]. In the light of the QbD approach, which stimulates the use of accurate, rapid, non-destructive techniques for the analysis of pharmaceutical processes and starting-, intermediate- and end products, it is likely that chemical imaging and other techniques will be increasingly adopted in the pharmaceutical industry [12, 127, 129, 130].

REFERENCES

- [1] K. Pitt, C. Sinka, Tableting, in: A.D. Salman, M.J. Hounslow, J.P.K. Seville (Eds.), Handbook of powder technology: Granulation, Elsevier, Amsterdam, 2007, pp. 735-778.
- [2] N.A. Armstrong, Tablet manufacture, in: J. Swarbrick (Ed.), Encyclopedia of pharmaceutical technology, Informa Healthcare USA Inc., New York, 2007, pp. 3653-3672.
- [3] N.A. Armstrong, Time-dependent factors involved in powder compression and tablet manufacture, *Int. J. Pharm.* 49 (1989) 1-13.
- [4] T. Higuchi, E. Nelson, L.W. Busse, The physics of tablet compaction 3: design and construction of an instrumented tableting machine, *J. Am. Pharm. Assoc.* 43 (1954) 344-348.
- [5] M. Levin, Tablet press instrumentation, in: J. Swarbrick (Ed.), Encyclopedia of pharmaceutical technology, Informa Healthcare USA Inc., New York, 2007, pp. 3684-3706.
- [6] M. J. Bogda, Tablet compression: Machine theory, design and process troubleshooting, in: J. Swarbrick (Ed.), Encyclopedia of pharmaceutical technology, Informa Healthcare USA Inc., New York, 2007, pp. 3611-3629.
- [7] K.M. Picker-Fryer, Tablet production systems, in: S.C. Gad (Ed.), Pharmaceutical manufacturing handbook: Production and processes, John Wiley & Sons Inc., New Jersey, pp. 1053-1098.
- [8] I.C. Sinka, F. Motazedian, A.C.F. Cocks, K.G. Pitt, The effect of processing parameters on pharmaceutical tablet properties, *Powder Technol.* 189 (2009) 276-284.
- [9] R. Mendez, F. Muzzio, C. Velazquez, Study of the effects of feed frames on powder blend properties during the filling of tablet press dies, *Powder Technol.* 200 (2010) 105-116.
- [10] A.S. Narang, V.M. Rao, H. Guo, J.A. Lu, D.S. Desai, Effect of force feeder on tablet strength during compression, *Int. J. Pharm.* 401 (2010) 7-15.
- [11] I.C. Sinka, L.C.R. Schneider, A.C.F. Cocks, Measurement of the flow properties of powders with special reference to die fill, *Int. J. Pharm.* 280 (2004) 27-38.

- [12] H.W. Ward, D.O. Blackwood, M. Polizzi, H. Clarke, Monitoring blend potency in a tablet press feed frame using near infrared spectroscopy, *J. Pharm. Biom. Anal.* 80 (2013) 18-23.
- [13] O. F. Akande, J.L. Ford, P.H. Rowe, M.H. Rubinstein, The effects of lag-time and dwell-time on the compaction properties of 1:1 paracetamol/microcrystalline cellulose tablets prepared by pre-compression and main compression, *J. Pharm. Pharmacol.* 50 (1998) 19-28.
- [14] E.N. Hiestand, J.E. Wells, C.B. Peot, J.E. Ochs, Physical processes in tableting, *J. Pharm. Sci.* 66 (1977) 510-519.
- [15] C.E. Ruegger, M. Celik, The influence of varying precompaction and main compaction profile parameters on the mechanical strength of compacts, *Pharm. Dev. Technol.* 5 (2000) 495-505.
- [16] I. Akseli, N. Ladyzhynsky, J. Katz, X. He, Development of predictive tools to assess capping tendency of tablet formulations, *Powder Technol.* 236 (2013) 139-148.
- [17] I.C. Sinka, K.G. Pitt, A.C.F. Cocks, The strength of pharmaceutical tablets, in: A.D. Salman, M. Ghadiri, M.J. Hounslow (Eds.), *Handbook of powder technology: Particle breakage*, Elsevier, Amsterdam, 2007, 941-970.
- [18] P.L. Catellani, P. Santi, E. Gasperini, S. Ciceri, G. Dondi, P. Colombo, Centrifugal die filling system in a new rotary tablet machine, *Int. J. Pharm.* 88 (1992) 285-291.
- [19] A. Bauer-Brandl, Tooling for tableting, in: J. Swarbrick (Ed.), *Encyclopedia of pharmaceutical technology*, Informa Healthcare USA Inc., New York, 2007, pp. 3782-3796.
- [20] C. Matz, A. Bauer-Brandl, T. Rigassi, R. Schubert, D. Becker, On the accuracy of a new displacement instrumentation for rotary tablet presses, *Drug Dev. Ind. Pharm.* 25 (1999) 117-130.
- [21] J. Ilkka, Instrumentation of rotary tablet machine by a portable measuring system, In: A. Munoz-Ruiz, H. Vromans (Eds.), *Data acquisition and measurement techniques*, Interpharm Press, Buffalo Grove, 1998.

- [22] R.V. Haware, I. Tho, A. Bauer-Brandl, Evaluation of a rapid approximation method for the elastic recovery of tablets, *Powder Technol.* 202 (2010) 71-77.
- [23] P.V. Marshall, P. York, J.Q. Maclaine, An investigation of the effect of the punch velocity on the compaction properties of ibuprofen, *Powder Technol.* 73 (1993) 171-177.
- [24] F.X. Muller, L.L. Augsburger, The role of the displacement-time waveform in the determination of Heckel behaviour under dynamic conditions in a compaction simulator and a fully instrumented rotary tablet machine, *J. Pharm. Pharmacol.* 46 (1994) 468-475.
- [25] F. Kiekens, A. Debunne, C. Vervaet, L. Baert, F. Vanhoutte, I. Van Assche, F. Menard, J.P. Remon, Influence of the punch diameter and curvature on the yield pressure of MCC-compacts during Heckel analysis, *Eur. J. Pharm. Biopharm.* 22 (2004) 117-126.
- [26] S.L. Cantor, S.W. Hoag, L.L. Augsburger, Evaluation of the mechanical properties of extrusion-spheronized beads and multiparticulate systems, *Drug Dev. Ind. Pharm.* 35 (2009) 683-693.
- [27] H. Diarra, V. Mazel, V. Busignies, P. Tchoreloff, FEM simulation of the die compaction of pharmaceutical products: influence of visco-elastic phenomena and comparison with experiments, *Int. J. Pharm.* 453 (2013) 389-394.
- [28] V. Mazel, V. Busignies, H. Diarra, P. Tchoreloff, Measurements of elastic moduli of pharmaceutical compacts: a new methodology using double compaction on a compaction simulator, *J. Pharm. Sci.* 101 (2012) 2220-2228.
- [29] F. Michaut, V. Busignies, C. Fouquereau, B. Huet De Barochez, B. Leclerc, P. Tchoreloff, Evaluation of a rotary tablet press simulator as a tool for the characterization of compaction properties of pharmaceutical products, *J. Pharm. Sci.* 99 (2010) 2874-2885.
- [30] J.B. Schwartz, Scale-up of the compaction and tableting process, In: M. Levin (Ed.), *Pharmaceutical process scale-up*, Marcel Dekker, New York, 2002, pp. 221-238.
- [31] C. Vervaet, J. Vercruyse, J.P. Remon, T. De Beer. Continuous processing of pharmaceuticals, in: J. Swarbrick (Ed.), *Encyclopedia of Pharmaceutical Science and Technology*, fourth ed., Taylor and Francis, New York, 2013, 644-655.

[32] International Conference on Harmonization (ICH) of technical requirements for registration of pharmaceuticals for human use, Topic Q8(R2): Pharmaceutical Development, in, Geneva, 2009.

[33] L.X. Yu, G. Amidon, M.A. Khan, S.W. Hoag, J. Polli, G.K. Raju, J. Woodcock, Understanding pharmaceutical quality by design, AAPS J. 16 (2014) 771-783.

[34] P.R. Watt, Tablet press instrumentation, Manuf. Chem. 54 (1983), 42-&.

[35] J. Barra, E. Doelker, Instrumentation of an eccentric tablet press, in: A. Munos-Ruiz, H. Vromans (Eds.), Data Acquisition and measurement techniques, Interpharm Press Inc., Buffalo Grove, 1998, pp.189-238.

[36] K. Marshall, Compression and consolidation of powdered solids, in: L. Lachman, H.A. Lieberman, J.L. Kanig (Eds.), The theory and practice of industrial pharmacy, third ed., Lea&Febiger, Philadelphia, 1986, pp.66-99.

[37] D. Sixsmith, Instruments for tablet technology, Manuf. Chem. Aer. N. 48 (1977) 17-21.

[38] G. Schwartz, The instrumented tablet press: uses in research and production, Pharm. Tech. 5 (1981) 102-132.

[39] K. Marshall, Instrumentation of tablet and capsule filling machines, Pharm. Tech. 7 (1983) 68-82.

[40] K. Marshall, Monitoring punch forces and punch movements as an aid to developing robust tablet formulations, Drug Dev. Ind. Pharm. 15 (1989) 2153-2176.

[41] P.R. Watt, N.A. Armstrong, Tablet and capsule machine instrumentation, Pharmaceutical Press, London, 2008.

[42] P.R. Watt, Tablet machine instrumentation in pharmaceuticals: Principles and practice, Ellis Horwood, Chichester, 1988.

[43] H.S. Thacker, Instrumentation of tablet machines, in: N.G. Stanley-Wood (Ed.), Enlargement and compaction of particulate solids, Butterworths, London, 1983, pp.227-240.

- [44] G. Bubb, Tablet press instrumentation in the research and development environment, in: M. Celik (Ed.), *Pharmaceutical Powder Compaction Technology*, second ed., Informa Healthcare USA Inc., New York, 2011, pp.74-98.
- [45] C. Yeh, S.A. Altaf, S.W. Hoag, Theory of force transducer design optimization for die wall stress measurement during tablet compaction: optimization and validation of split-web die using finite element analysis, *Pharm. Res.* 14 (1997) 1161-1170.
- [46] E. Doelker, D. Massuelle, Benefits of die-wall instrumentation for research and development in tableting, *Eur. J. Pharm. Biopharm.* 58 (2004) 427-444.
- [47] H. G. Cocolas, N.G. Lordi, axial to radial pressure transmission of tablet excipients using a novel instrumented die, *Drug Dev. Ind. Pharm.* 19 (1993) 2473-2497.
- [48] A.W. Hölzer, J. Sjörgen, Instrumentation and calibration of a single punch press for measuring the radial force during tableting, *Int. J. Pharm.* 3 (1979) 221-230.
- [49] P.D. Huckle, M.P. Summers, The use of strain gauges for radial stress measurement during tableting, *J. Pharm. Pharmacol.* 37 (1985) 722-725.
- [50] M. Cespi, M. Misici-Falzi, G. Bonacucina, S. Ronchi, G.F. Palmieri, The effect of punch tilting in evaluating powder densification in a rotary tablet machine, *J. Pharm. Sci.* 97 (2008) 1277-1284.
- [51] G.F. Palmieri, E. Joiris, G. Bonacucina, M. Cespi, A. Mercuri, Differences between eccentric and rotary tablet machines in the evaluation of powder densification behaviour, *Int. J. Pharm.* 298 (2005) 164-175.
- [52] A.S. Rankell, T. Higuchi, Physics of tablet compression. XV. Thermodynamic and kinetic aspects of adhesion under pressure, *J. Pharm. Sci.* 58 (1968) 574-577.
- [53] M.T. DeCrosta, J.B. Schwartz, R.J. Wigent, K. Marshall, Thermodynamic analysis of compact formation; compaction, unloading, and ejection. I. Design and development of a compaction calorimeter and mechanical and thermal energy determinations of powder compaction, *Int. J. Pharm.* 198 (2000) 113-134.

[54] M.T. DeCrosta, J.B. Schwartz, R.J. Wigent, K. Marshall, Thermodynamic analysis of compact formation; compaction, unloading, and ejection. II. Mechanical energy (work) and thermal energy (heat) determinations of compact unloading and ejection, *Int. J. Pharm.* 213 (2001) 45-62.

[55] J. Kelolainen, J. Ilkka, P. Paronen, Temperature changes during tableting measured using infrared thermoviewer, *Int. J. Pharm.* 92 (1993) 157-166.

[56] K.M. Picker-Fryer, A.G. Schmidt, Does temperature increase induced by tableting contribute to tablet quality, *J. Therm. Anal. Calorim.* 77 (2004) 531-539.

[57] M. Celik, C.E. Driscoll, An overview of the effects of some physico-chemical and mechanical characteristics of particulates on the compaction and post-compaction properties of compacts, *Drug Dev. Ind. Pharm.* 19 (1993) 2119-2141.

[58] J. Nordström, I. Klevan, G. Alderborn, A protocol for the classification of powder compression characteristics, *Eur. J. Pharm. Biopharm.* 80 (2012) 209-216.

[59] P.C. Schmidt, P.J. Vogel, Force-time-curves of a modern rotary tablet machine I. Evaluation techniques and characterization of deformation behaviour of pharmaceutical substances, *Drug Dev. Ind. Pharm.* 20 (1994) 921-934.

[60] P.C. Schmidt, M. Leitritz, Compression force/time-profiles of microcrystalline cellulose, dicalcium phosphate dihydrate and their binary mixtures – a critical consideration of experimental parameters, *Eur. J. Pharm. Biopharm.* 44 (1997) 303-313.

[61] P.J. Vogel, P.C. Schmidt, Force-time curves of a modern rotary tablet machine II. Influence of compression force and tableting speed on the deformation mechanisms of pharmaceutical substances, *Drug Dev. Ind. Pharm.* 19 (1993) 1917-1930.

[62] J.K. Yliruusi, P. Merkkü, L. Hellen, O.K. Antikainen, A new method to evaluate the elastic behavior of tablets during compression, *Drug Dev. Ind. Pharm.* 23(1997) 63-68.

[63] P. Konkel, J.B. Mielck, Associations of parameters characterizing the time course of the tableting process on a reciprocating and on a rotary tableting machine for high-speed production, *Eur. J. Pharm. Biopharm.* 45 (1998) 137-148.

- [64] G. Shlieout, M. Wiese, G. Zessin, A new method to evaluate the consolidation behavior of pharmaceutical materials by using the Fraser-Suzuki function, *Drug Dev. Ind. Pharm.* 25 (1999) 29-36.
- [65] S. Abdel-Hamid, M. Koziolok, G. Betz, Study of radial die-wall pressure during high speed tableting: effect of formulation variables, *Drug Dev. Ind. Pharm.* 38 (2012) 623-634.
- [66] S. Abdel-Hamid, G. Betz, Study of radial die-wall pressure changes during pharmaceutical powder compaction, *Drug Dev. Ind. Pharm.* 37 (2011) 387-395.
- [67] J.C. Cunningham, I.C. Sinka, A. Zavaliangos, Analysis of tablet compaction. I. Characterization of mechanical behavior of powder and powder/tooling friction, *J. Pharm. Sci.* 93 (2004) 2022-2039.
- [68] E.N. Hiestand, Principles, tenets and notions of tablet bonding and measurements of strength, *Eur. J. Pharm. Biopharm.* 44 (1997) 229-242.
- [69] A.W. Hölzer, J. Sjörgen, Friction coefficients of tablet masses, *Int. J. Pharm.* 7 (1981) 269-277.
- [70] H. Takeuchi, S. Nagira, H. Yamamoto, Y. Kawashima, Die wall pressure measurement for evaluation of compaction property of pharmaceutical materials, *Int. J. Pharm.* 274 (2004) 131-138.
- [71] N.A. Armstrong, R.F. Haines-Nutt, Elastic recovery and surface area changes in compacted powder systems, *J. Pharm. Pharmacol.* 24 (1972) 135P-136P.
- [72] V. Busignies, B. Leclerc, P. Porion, P. Evesque, G. Couarraze, P. Tchoreloff, Compaction behaviour and new predictive approach to the compressibility of binary mixtures of pharmaceutical excipients, *Eur. J. Pharm. Biopharm.* 64 (2006) 66-74..
- [73] S.F. Gharaibeh, A. Aburub, Use of first derivative of displacement versus force profiles to determine deformation behavior of compressed powders, *AAPS PharmSciTech.* 14 (2013) 398-401.

- [74] R. Roopwani, I.S. Buckner, Understanding deformation mechanisms during powder compaction using principal component analysis of compression data, *Int. J. Pharm.* 418 (2011) 227-234.
- [75] K.M. Picker, Three-dimensional modeling to determine properties of tableting materials on rotary machines using a rotary tableting machine simulator, *Eur. J. Pharm. Biopharm.* 50 (2000) 293-300.
- [76] K.M. Picker, F. Bikane, An evaluation of three-dimensional modeling of compaction cycles by analyzing the densification behavior of binary and ternary mixtures, *Pharm. Dev. Technol.* 6 (2001) 333-342.
- [77] K.M. Picker, The 3D model: explaining densification and deformation mechanisms by using 3D parameter plots, *Drug Dev. Ind. Pharm.* 30 (2004) 413-425.
- [78] F. Muller, Viscoelastic models, in: G. Alderborn, C. Nystrom (Eds.), *Pharmaceutical powder compaction technology*, Marcel Dekker Inc, New York-Basel, 1996, pp.99-132.
- [79] C.Y. Wu, B.C. Hancock, A. Mills, A.C. Bentham, S.M. Best, J.A. Elliott, Numerical and experimental investigation of capping mechanisms during pharmaceutical tablet compaction, *Powder Technol.* 181 (2008) 121-129.
- [80] R.W. Heckel, An analysis of powder compaction phenomena, *Trans. Metall. Soc. AIME*, 221 (1961) 1001-1008.
- [81] R.W. Heckel, Density-pressure relationships in powder compaction, *Trans. Metall. Soc. AIME*, 221 (1961) 671-675.
- [82] R.J. Roberts, R.C. Rowe, The effect of punch velocity on the compaction of a variety of materials, *J. Pharm. Pharmacol.* 37 (1985) 377-384.
- [83] S. Mallick, Rearrangement of particle and compactibility, tableability and compressibility of pharmaceutical powder: a rational approach, *J. Sci. Ind. Res.* 73 (2014) 51-56.

- [84] R.J. Roberts, R.C. Rowe, The compaction of pharmaceutical and other model materials – a pragmatic approach, *Chem. Eng. Sci.* 42 (1987) 903-911.
- [85] C.M. Gabaude, M. Guillot, J.C. Gautier, P. Saudemon, D. Chulia, effects of true density, compacted mass, compression speed and punch deformation on the mean yield pressure, *J. Pharm. Sci.* 88 (1999) 725-730.
- [86] J.M. Sonnergaard, Impact of particle density and initial volume on mathematical compression models, *Eur. J. Pharm. Sci.* 11 (2000) 307-315.
- [87] J.M. Sonnergaard, A critical evaluation of the Heckel equation, *Int. J. Pharm.* 193 (1999) 63-71.
- [88] M.J. Adams, M.A. Mullier, J.P.K. Seville, Agglomerate strength measurement using a uniaxial confined compression test, *Powder Technol.* 78 (1994) 5-13.
- [89] J.T. Carstensen, J.M. Geoffroy, C. Dellamonica, Compression characteristics of binary mixtures, *Powder Technol.* 62 (1990) 119-124.
- [90] A.R. Cooper, L.E. Eaton, Compaction behaviour of several ceramic powders, *J. Am. Ceram. Soc.* 5 (1962) 97-101.
- [91] N.D. Gentis, B.Z. Vranic, G. Betz, Assessing compressibility and compactibility of powder formulations with near-infrared spectroscopy, *Pharm. Dev. Technol.* 18 (2013) 156-171.
- [92] K. Kawakita, K.H. Ludde, Some considerations on powder compression equations, *Powder Technol.* 61 (1971) 61-68.
- [93] I. Klevan, J. Nordström, A. Bauer-Brandl, G. Alderborn, On the physical interpretation of the initial bending of a Shapiro-Knopicky-Heckel compression profile, *Eur. J. Pharm. Biopharm.* 71 (2009) 395-401.
- [94] H. Leuenberger, The compressibility and compactibility of powder systems, *Int. J. Pharm.* 12 (1982) 41-55.
- [95] H. Leuenberger, The compactibility of powder systems. A novel approach, *Powder Technol.* 37 (1984) 209-218.

- [96] S. Patel, A.M. Kaushal, A.K. Bansal, Effect of particle size and compression force on compaction behavior and derived mathematical parameters of compressibility, *Pharm. Res.* 24 (2007) 111-124.
- [97] J. Rojas, S. Hernandez, Effect of the compaction platform on the densification parameters of tableting excipients with different deformation mechanisms, *Chem. Pharm. Bull.* 62 (2014) 281-287.
- [98] I. Shapiro, Compaction of powders 10. Development of a general compaction equation, *Adv. PM Part.* 3 (1993) 229-243.
- [99] E.E. Walker, The properties of powder, Part VI. The compressibility of powders, *Trans. Faraday Soc.* 19 (1923) 73-82.
- [100] S.F. Yap, M.J. Adams, J.P.K. Seville, Z. Zhang, Single and bulk compression of pharmaceutical excipients: evaluation of mechanical properties, *Powder Technol.* 185 (2008) 1-10.
- [101] J.M. Sonnergaard, Quantification of the compactibility of pharmaceutical powders, *Eur. J. Pharm. Biopharm.* 63 (2006) 270-277.
- [102] I. Ilic, B. Govedarica, R. Sibanc, R. Dreu, S. Srcic, Deformation properties of pharmaceutical excipients determined using an in-die and out-die method, *Int. J. Pharm.* 446 (2013) 6-15.
- [103] I. Klevan, J. Nordström, I. Tho, G. Alderborn, A statistical approach to evaluate the potential use of compression parameters for classification of pharmaceutical powder materials, *Eur. J. Pharm. Biopharm.* 75 (2010) 425-435.
- [104] C.E. Ruegger, M. Celik, The effect of compression and decompression speed on the mechanical strength of compacts, *Pharm. Dev. Technol.* 5 (2000) 485-494.
- [105] C.K. Tye, C. Sun, G.E. Amidon, Evaluation of the effects of tableting speed on the relationships between compaction pressure, tablet tensile strength, and tablet solid fraction, *J. Pharm. Sci.* 94 (2005) 465-472.

- [106] I.C. Sinka, S.F. Burch, J.H. Tweed, J.C. Cunningham, Measurement of density variations in tablets using X-ray computed tomography, *Int. J. Pharm.* 271 (2004) 215-224.
- [107] J.K. Yliruusi, O.K. Antikainen, New parameters derived from tablet compression curves. Part I. Force-Time curve, *Drug Dev. Ind. Pharm.* 23 (1997) 69-79.
- [108] S.D. Bateman, M.H. Rubinstein, H.S. Thacker, Properties of paracetamol tablets produced using high precompression pressures, *J. Pharm. Pharmacol.* 41S (1989) 32P.
- [109] G.P. Cook, M.P. Summers, Effect of compression speed on tensile strength of tablets of binary mixtures containing aspirin, *J. Pharm. Pharmacol.* 42 (1990) 462-467.
- [110] K. Danjo, H. Kimura, A. Otsuka, Influence of punch velocity on the compressibility of granules, *Drug Dev. Ind. Pharm.* 22 (1996) 933-942.
- [111] J.S.M. Garr, M.H. Rubinstein, An investigation into the capping of paracetamol at increasing speeds of compression, *Int. J. Pharm.* 72 (1991) 117-122.
- [112] L.E. Holman, H. Leuenberger, Effect of compression speed on the relationship between normalized solid fraction and mechanical properties of compacts, *Int. J. Pharm.* 57 (1989) R1-R5.
- [113] M. Monedero, M.R. Jimenez-Castellano, M.V. Velasco, A. Munoz-Ruiz, Effect of compression speed and pressure on the physical characteristics of maltodextrin tablets, *Drug Dev. Ind. Pharm.* 24 (1998) 613-621.
- [114] W.R. Vezin, H.M. Pang, K.A. Khan, S. Malkowsda, The effect of pre-compression in a rotary machine on tablet strength, *Drug Dev. Ind. Pharm.* 9 (1983) 1465-1475.
- [115] United States Food and Drug Administration (FDA), Guidance for industry - PAT - A framework for innovative pharmaceutical development, manufacturing, and quality assurance, in, 2004.
- [116] E. Korakianiti, D. Rekkas, Statistical thinking and knowledge management for quality-driven design and manufacturing in pharmaceuticals, *Pharm. Res.* 28 (2011) 1465-1479.
- [117] R. Ackoff, towards a system of systems concepts, *Manage. Sci.* 17 (1971) 661-671.

[118] J. Lepore, J. Spavins, Product quality lifecycle implementation (PQLI) innovations. PQLI design space, *J. Pharm. Innov.* 3 (2008) 79-87.

[119] L. Eriksson, E. Johansson, N. Kettaneh-Wold, C. Wikström, S. Wold, *Design of Experiments - Principles and Applications*, third ed., Umea, Sweden, 2008.

[120] L.X. Yu, Pharmaceutical quality by design: Product and process development, understanding, and control, *Pharm. Res.* 25 (4) (2014) 781-791.

[121] L. Eriksson, E. Johansson, N. Kettaneh-Wold, J. Trygg, C. Wikström, S. Wold, *Multi- and Megavariate data analysis, part I, basic principles and applications*, second ed., Umea, 2006.

[122] H. Abdi, L.J. Williams, Principal component analysis, *Comp. Stat.* 2 (2010) 433-459.

[123] K. Muteki, V. Swaminathan, S.S. Sekulic, G. L. Reid, De-risking pharmaceutical tablet manufacture through process understanding, latent variable modeling, and optimization technologies, *AAPS PharmSciTech.* 12 (2011) 1324-1334.

[124] A. Mishra, S. Banerjee, N. Bhatwadekar, P. Mahajan, Process analytical technology (PAT): Boon to pharmaceutical industry, *Pharm. Rev.* 6 (2008).

[125] W. Chew, P. Sharatt, Trends in process analytical technology, *Anal. Methods-UK*, 2 (2010) 1412-1438.

[126] L.X. Yu, R.A. Lionberger, A.S. Raw, R. D'Costa, H. Wu, A.S. Hussein, Application of process analytical technology to crystallization process, *Adv. Drug Deliv. Rev.* 56 (2004) 349-369.

[127] A.A. Gowen, C.P. O'Donnell, P.J. Cullen, S.E.J. Bell, Recent applications of chemical imaging to pharmaceutical process monitoring and quality control, *Eur. J. Pharm. Biopharm.* 69 (2008) 10-22.

[128] G.V. Reklaitis, J. Khinast, F. Muzzio, *Pharmaceutical engineering science – new approaches to pharmaceutical development and manufacturing*, *Chem. Eng. Sci.* 65 (2010) iv-vii.

[129] K. Jarvinen, W. Hoehe, M. Jarvinen, S. Poutiainen, M. Juuti, S. Borchert, In-line monitoring of the drug content of powder mixtures and tablets by near-infrared spectroscopy during the continuous direct compression tableting process, *Eur. J. Pharm. Sci.* 48 (2013) 680-688.

[130] B.J. Maranzano, G.K. B.C. Hancock, Rapid method for measuring the mechanical properties of pharmaceutical compacts, *Powder Technol.* 236 (2013) 205-210.

2

THE MODUL™ P

All tableting experiments described in this thesis are conducted on the ModulTM P (Figure 2.1), a product of GEA Process Engineering, CourtoyTM, situated in Halle, Belgium. In this chapter, a general description of the machine design and the set-up of the system as installed at Ghent University is provided. The component units that were subject of research are described in more detail. Finally, the most relevant instrumentation and control mechanisms integrated in the press and the method of data collection is highlighted.



Figure 2.1: The ModulTM P, with the ECM removed from the machine. (Courtesy of GEA, CourtoyTM)

1. PRESS DESIGN AND LAY-OUT

A schematic overview of the compression cycle is provided in Figure 2.2 and Figure 2.3. The tableting process can generally be divided into three distinct stages: (a) die filling, (b) compaction and (c) ejection. Powder from the forced feeder is distributed into the dies at the filling station. After weight adjustment, the punches pass through the pre- and main compression rollers. After compression, the top punch moves upwards and the tablet is ejected by the lower punch as it passes through the ejection cam mechanism. Tablet scrape-off occurs immediately after ejection by an ejection finger, which leads the tablets towards the ejection chute.

Powder is fed gravitationally to the machine from an overhead 20L bin (hopper) through a chute into the forced feeder (Figure 2.4). Since overhead pressure, which can increase drastically if large overhead hoppers are used, can have an influence on die filling, the chute can be equipped with a rotary valve and level sensor. This avoids unwanted pressure build-

up in the chute by physically interrupting the powder column. The valve opens when the powder underneath the valve drops under a certain level.

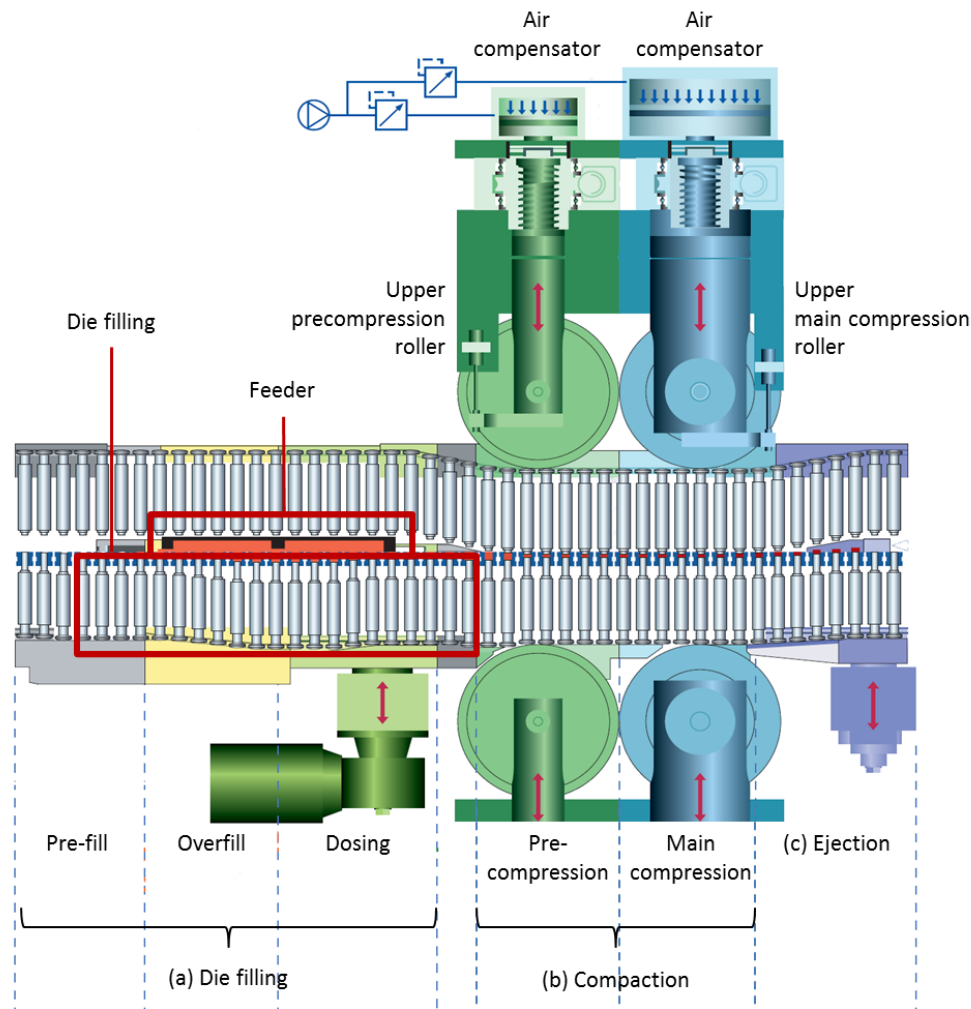


Figure 2.2: Schematic linear overview of the compression cycle. (Courtesy of GEA, Courtoy™)

The upper and lower punches reside in the upper and lower punch guide, respectively. The dies are inserted in the die table and secured by die lock screws. Upper punch guide, die table and lower punch guide are manufactured out of one solid block of forged steel, assuring perfect alignment of the three parts. As the entire assembly (turret) rotates, the movement of the upper and lower punches are controlled by cam tracks and compression rollers [1]. The Modul™ P is equipped with a 20 station mixed die table. Either Euro B (10 positions) or Euro D tooling (10 positions) can be installed. Even so, experiments can be performed with a full tooling set down to just one punch, making this machine a versatile tool for research and development.

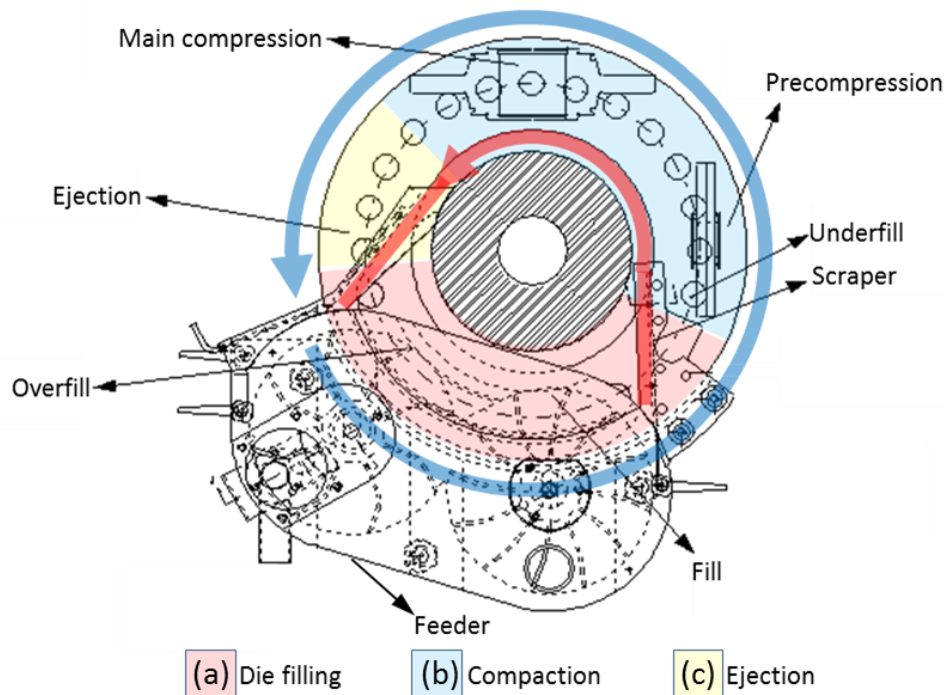


Figure 2.3: Schematic top-view representation of the compression cycle. Blue arrow depicts the movement of the turret; Red arrow depicts material recirculation. (Courtesy of GEA, Courtoy™)

The machines' name (Modul™) is derived from the built in exchangeable compression module (ECM). The ECM design reduces the compression zone with its entire contents to a single, removable machine module (Figure 2.1). This provides a physical separation and isolation of the compression area from the other press zones. Only the compression zone is exposed to material, thus reducing cleaning and change-over time of the tablet press, as the contaminated ECM can be removed after a production campaign and cleaned off-line, while a new ECM can be installed and production can resume immediately. Recently, the Wash-Off-Line ECM (WOL-ECM) extended the product line available on the Modul™ P. This WOL-ECM, designed for the production of tablets containing potent drugs, has an adapted design. Water-jet heads, connected to a water preparation skid, can be introduced into the ECM to knock down all airborne particles and wash away most of the material residue, before the ECM is opened for further manual cleaning and drying [2].

After tablets are scraped off by the ejection finger, they leave the press through the ejection chute. This chute has commonly three different outlets and is equipped with a motor driven tablet diverter. One outlet is used for rejected tablets (i.e. produced with process parameters exceeding the preset ranges (see 5. Control mechanisms and PAT integrated in

the press)). The other two are connected to tablet recipients or additional peripheral equipment for further handling or analysing of tablets.

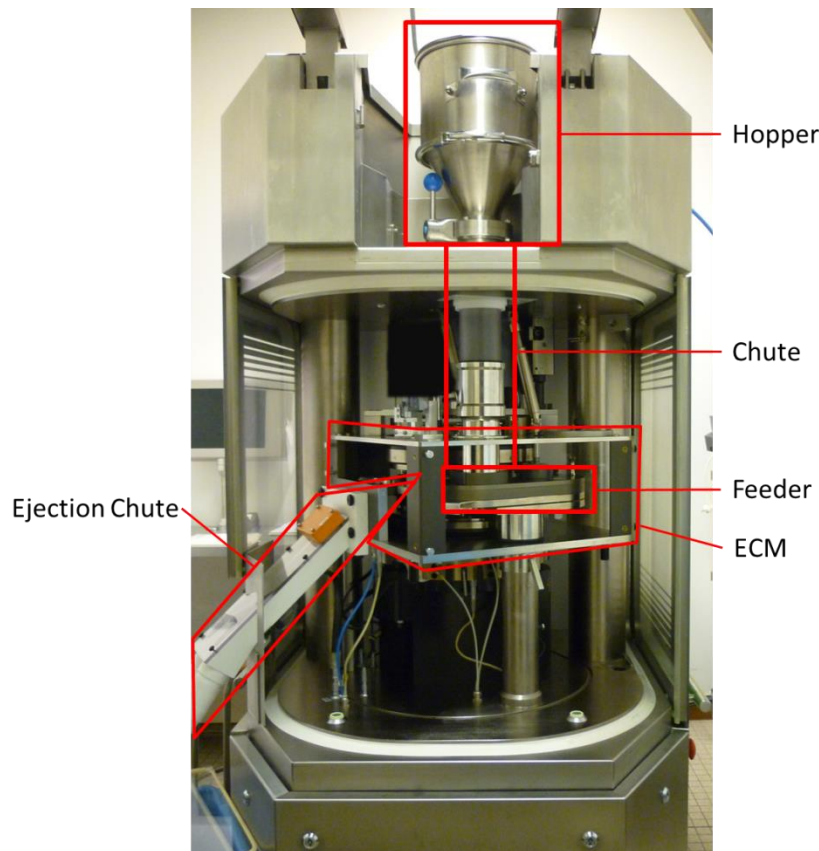


Figure 2.4: Overview of the compression zone (ECM) and all peripherals in contact with the material.

Besides the upper and lower rollers and compression zone, the machine also contains a mechanical section, which is situated underneath the latter, and an electrical section. The electrical section is brought to the back of the machine and separated from the rest of the machine. This avoids negative influence of the compression zone (machine vibrations and heat of production) on the electrical parts and allows a through-the-wall set-up in manufacturing.

2. POWDER FEEDING SYSTEM

The punch movement at the filling station is guided by cam tracks. While the upper punch stays at a fixed position as it travels over the forced feeder, the lower punch describes a different moving pattern, from which a schematic overview is given in Figure 2.5.

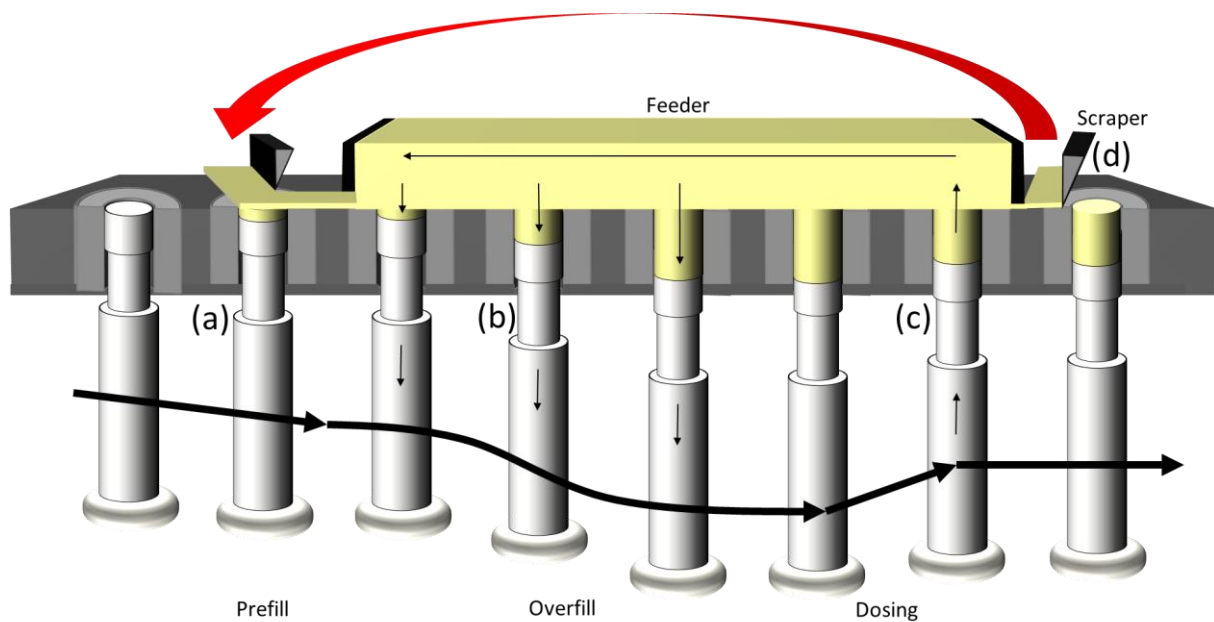


Figure 2.5: Schematic overview of the lower punch movement at the filling station: (a) prefill; (b) overfill; (c) dosing; (d) scrape-off and subsequent underfill. (Courtesy of GEA, Courtoy™)

As the lower punch enters the feeder, it is lowered by the overfill cam (b in Figure 2.5). The overfilling depth is dependent on the installed overfill cam. At this point, the die cavity contains more material than necessary in order to achieve a uniform tablet weight. After overfilling the die cavity, the lower punch is raised to a preset height as it passes into the dosing unit, herewith pushing excess material back into the feeder (c in Figure 2.5). Immediately behind the feeder, the scraper lying flush with the die table (d in Figure 2.5) scrapes off the last excess of material from the clearance between forced feeder and die table (0.05 mm), which is redirected into the recirculation channel in the middle of the turret. Subsequently, the punch is again lowered (3.00 mm) (underfill in Figure 2.3) to minimize uncontrolled material loss due to centrifugal forces before the upper punch seals the die cavity under the precompression roll. Material directed to the recirculation channel follows the movement of the turret and is subsequently introduced back into the feeder (red arrow in Figure 2.3) just before the overfill position. Here, the punch is already slightly lowered (3.00 mm) (a in Figure 2.5), favoring the flow of the recirculated material immediately into the passing dies [1].

The feed frame itself consists of a top and base plate and two coplanar paddle wheels (Figure 2.6). Powder is delivered from the hopper into the feed frame via an opening in the top plate. The first wheel, the feeding wheel (a in Figure 2.6) has eight curved paddles and is

located above the overfilling station. It transports powder from the powder feeding chute towards the overfilling region. The second wheel, the metering wheel (b in Figure 2.6), has twelve curved paddles and is located at the filling station. This wheel recovers the excess of powder ejected from the dies after weight adjustment and returns this powder to the feeding wheel. Both wheels are motor driven and rotate in opposite directions. Their speed can be adjusted independently from one another and from the turret speed.

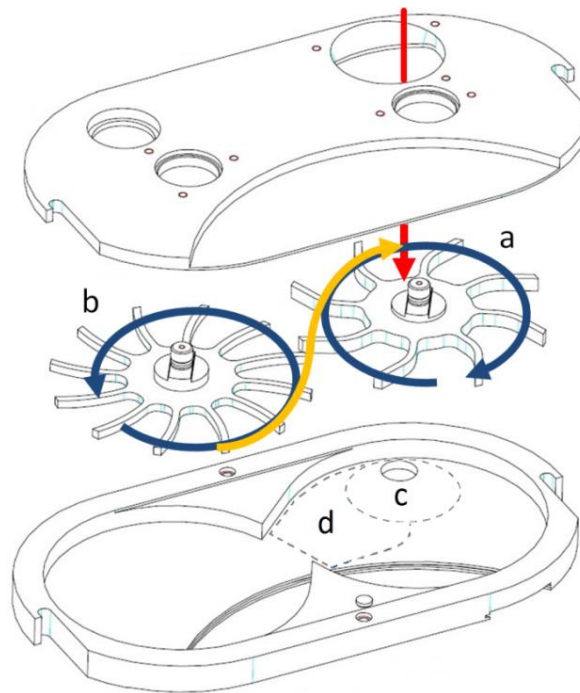


Figure 2.6: Schematic overview of the feed frame with two paddles: (a) feeding paddle (paddle 1); (b) metering paddle (paddle 2); (c) infeed; (d) recirculation area of the feeding paddle. Arrows depict schematically the movement of the powder through the feed frame. (Courtesy of GEA, Courtoy™)

3. MECHANISM OF COMPRESSION

The Modul™ P is equipped with two pairs of compression rollers, all with the same diameter (Figure 2.2). At the precompression station the punches apply an initial force on the powder, and subsequently, between the main compression rollers the final compression takes place, usually at a higher load compared to the precompression phase [1, 3, 4].

Most rotary presses operate by maintaining fixed roller positions during compression. The upper roller remains in a fixed position, which determines the penetration depth of the upper punch and consequently the in-die tableting position. By adjusting the position of the lower roller, the compression force is determined and hence, the thickness of the compact

under compression. Furthermore, for a given tablet press and tooling, the kinetics of the punch movement depend only on the tableting speed. As a result the total contact time (the period when the upper punch is in contact with the powder), the consolidation time (the period during which the punches approach each other), the dwell-time (the period during which the punch head flat (land) is in direct contact with the compression roller), the decompression phase (the time during which the punches move away from each other) and the lag-time (the time between precompression and main compression phase) are defined by the tangential velocity of the punch [3, 5-20].

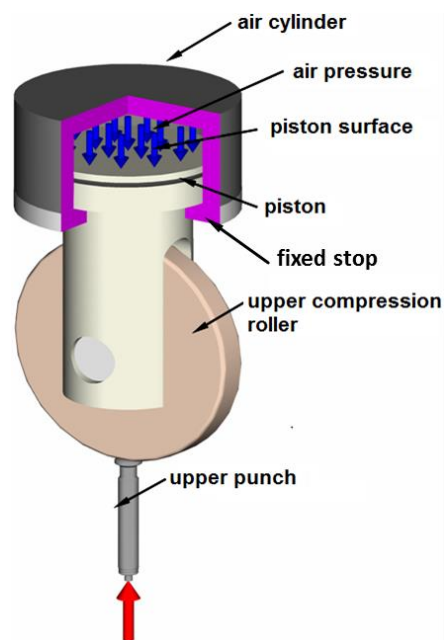


Figure 2.7: Schematic representation of the pneumatic air compensator. (Courtesy of GEA, CourtoyTM)

In contrast, using the MODUL P high-speed rotary tablet press these parameters can be controlled independently from the tableting speed, due to an air compensator which allows displacement of the upper compression rollers (Figure 2.7). The upper rollers are attached to an air piston, which allows vertical movement in an air cylinder. During a compression run the air pressure in the cylinder (CF_r) is set at a constant value due to a control system of pressure valves and expansion vessels. The piston, and consequently the upper roller, is pushed downwards by the air pressure against a fixed stop, being the bottom of the air cylinder. The adjustable position of the lower roller is controlled similar to a conventional tablet press with fixed rollers. During compression, the upper punch initially moves downwards into the die when in contact with the upper roller. As the lower punch is pushed upwards by the lower roller, the powder bed in the die consolidates and the compression

force increases. When the reaction force exerted by the powder on the upper punch exceeds the force exerted by the counter pressure (i.e. the air pressure on the piston), upward movement of the upper compression roller is possible. The complete assembly of bottom punch, powder slug and top punch moves simultaneously, following the lower compression roller and consequently raises the upper roller. The distance by which the upper roller is displaced only depends on the position of the lower compression roller. The dwell-time is now not only defined by the land, the pitch diameter and the turret speed, but also by the displacement. As the upper roller is displaced, the contact time between the punch head flat and the roller is prolonged. Hence the dwell-time is extended in comparison to the fixed roller set-up, although tableting speed is constant. If, however, a higher air pressure than the force exerted by the powder is set in the cylinder of the air compensator, the upper roller does not move, and the system behaves as a set-up with fixed rollers [21, 22]. An overview of the different positions and movements of rollers and punches is provided in Figure 2.8.

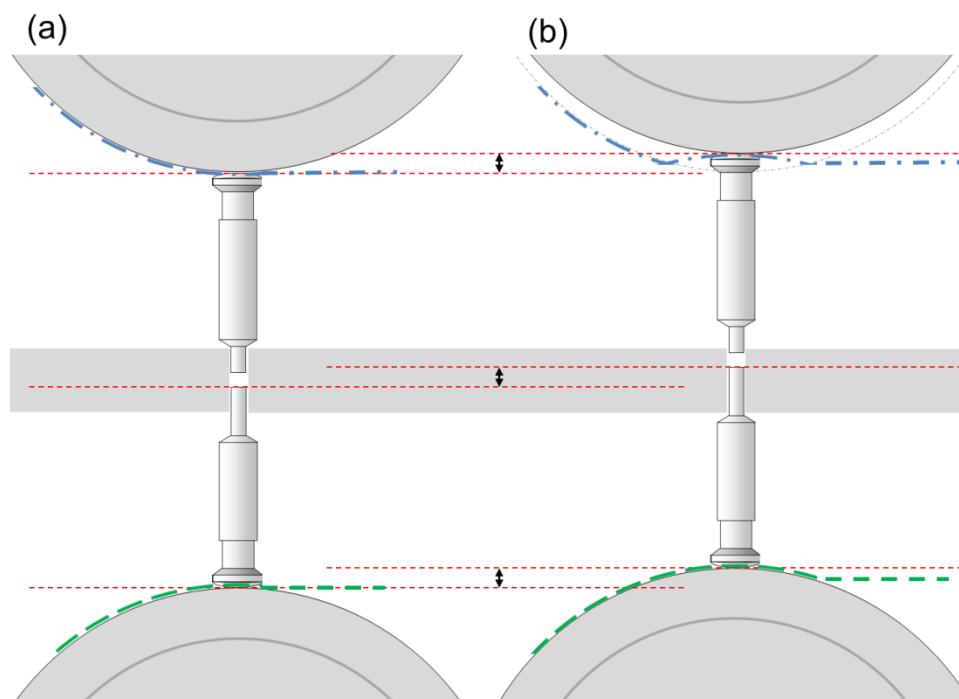


Figure 2.8: Schematic overview of the different positions and movements of rollers and punches (a) with fixed rollers and (b) with moving rollers, highlighted by red lines and arrows. -·-·- depicts the punch movement of the upper punch, - - - depicts the movement of the lower punch.

It is necessary to mention that the term ‘displacement’ in this thesis is strictly used to describe *the movement of the upper roller*, and *not* the movement of the punches, as it is done in all previous research regarding tablet compression on high speed rotary tablet presses.

4. INSTRUMENTATION AND COLLECTION OF DATA

A modern rotary tableting machine is a complex engineering system with numerous sensors and measuring devices installed, allowing real-time monitoring and control of the tableting process. A built-in sensor at the dosing station for instance, measures the resistance at which the bottom punch moves from the overfill to the dosing height. If the resistance is too high, an alarm is generated and the press is stopped. The same happens at the ejection station with the upper punch which is pulled up in the ejection cam after main compression. A high resistance can be an indication of low punch lubrication or wear of the bottom punches, as fine powder particles are able to settle between the flank of the punch tip and the die wall. Although the former are of high importance to guarantee a fluent compression process and prevent damage to the press, the signals which are more closely monitored and administered to characterize the compression cycle, like also done in this research project, are those directly related to the material under compression, being the compression forces (pre- and main compression force (PCF; MCF)), the ejection force (EF), the displacement of the upper rollers (pre- and main compression displacement (PCD; MCD)) and the movement of the punches.

Strain gauge-based load cells are used for force measurement at pre- and main compression and at ejection. Load cells underneath the lower compression rollers and the ejection cam measure the compression force and ejection force, respectively. Displacement of pre- and main compression rollers is measured by linear variable displacement transducers (LVDT sensors), which are connected to the upper compression rollers. Punch stroke movement is monitored by LVDT sensors, which are placed inside the turret and are fixed to one keyed punch set by means of clamps. Wireless data transmission and power supply ensures continuous data acquisition with no need to stop the process to download data. Calibration of the system is done by an interpolation method. The output voltage of the sensor and the physical value (displacement or force) are determined during static measurements and their linear relationship calculated.

Collection and analysis of these data is performed with a data acquisition and analysis system (CDAAS). The CDAAS software is an application which measures and samples the signals (PCF, MCF, PCD, MCD, EF and punch strokes) at high frequency (up to 100kHz) with

16bit A/D conversion. It allows calibration, filtering, visualization and recording of the processed sensor signals and reviewing and analyzing of recorded data. An overview of the hardware set-up is depicted in Figure 2.9.

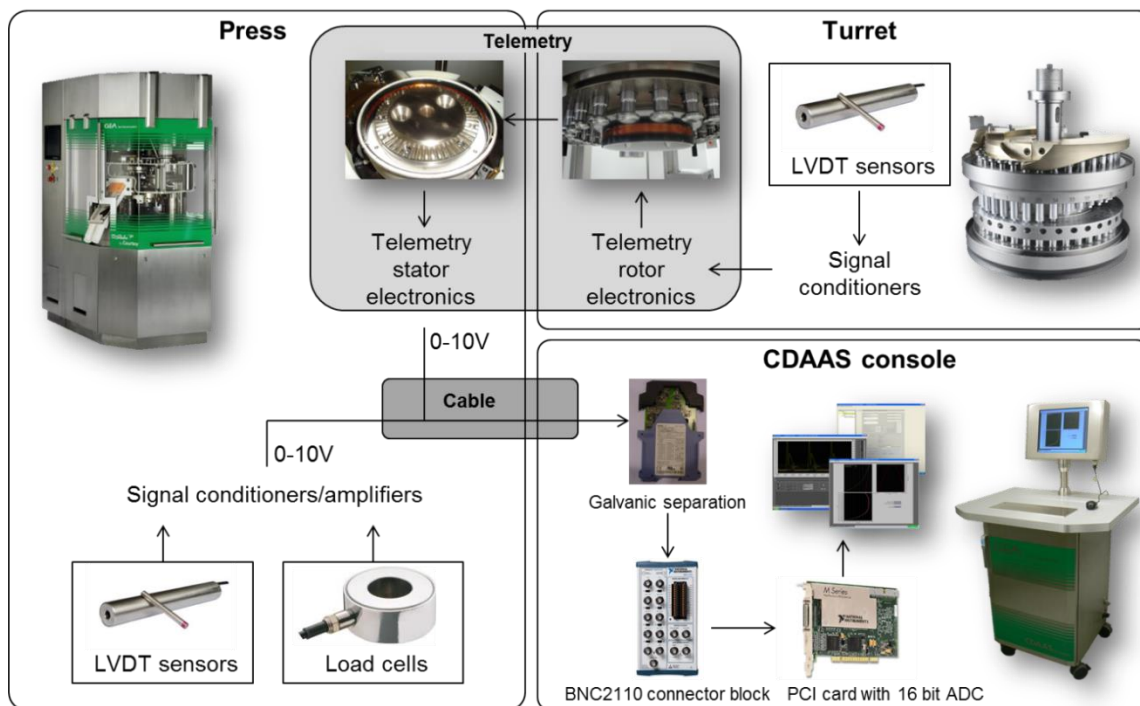


Figure 2.9: Schematic overview of hardware set-up on the tablet press. (Courtesy of GEA, Courtoy™)

5. CONTROL MECHANISMS AND PAT INTEGRATED IN THE PRESS

Under ideal circumstances, the weight and hardness of a tablet stays constant with a set fill depth and distance between the punches or displacement, respectively. This however is seldom the case. Environmental changes (relative humidity, temperature), temperature raise of the press parts and tooling and changes to the material under compression (segregation, inhomogeneity of the blend, particle size changes upon shear) all contribute to variations in tablet weight and hardness and also to a fluctuating relation between the tablet characteristics and the process parameters. Therefore, control mechanisms are available to control tablet weight and hardness and compensate for these fluctuations, thus guaranteeing tablets with the desired quality attributes.

5.1. Control of the variation in tablet characteristics

A tableting machine cannot determine the weight or hardness of tablets directly. This information is gained indirectly, by linking process parameters to these tablet characteristics. Depending if the machine is run with fixed or moving rollers, other process parameters are

utilized for this. In advance, the tolerance limits of the process parameters are set manually or calculated automatically. A mean value and two upper and two lower limits determine the actions undertaken by the press, as depicted in Figure 2.10. As long as a value varies between the upper and lower correction limit, no action is undertaken by the press. When the nominal value (i.e. the mean value of all tablets produced during one rotation) exceeds this correction limit, the machine will bring the nominal value back to the preset value and in between the correction limits (C in Figure 2.10). Each time a single tablet exceeds the reject limits, this tablet will be rejected (i.e. redirected at the ejection chute to the outlet of rejected tablets) (R in Figure 2.10). When three out of four consecutive tablets in one rotation (i.e. production out of tolerance) or three out of four tablets from one punch of four consecutive rotations (i.e. punch failure) are rejected, the press is stopped (S). The controls available on the press are weight, force and displacement control.

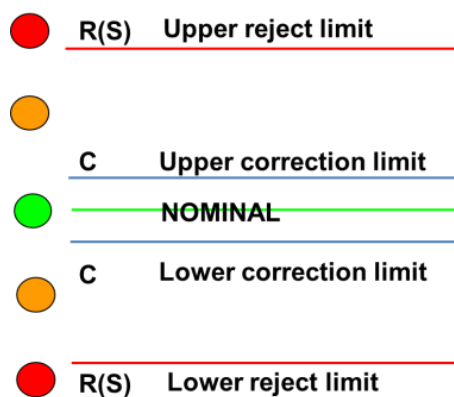


Figure 2.10: Schematic overview of the different limits and the actions undertaken by the tablet press. C: correction; R: reject; S: stop. (Courtesy of GEA, Courtoy™)

5.1.1. Weight control

When the fixed rollers set-up is used, the weight control is linked to the force on main compression. Whenever the main compression force exceeds the tolerance limits as depicted in Figure 2.10, the machine will react by changing the fill depth. The fill depth will be increased when the lower control limit is exceeded and decreased when the upper control limit is exceeded. Since force and weight have an exponential relationship, the tolerance limits need to be set manually. Firstly, a tablet with the nominal weight is produced and the distance between the rollers adapted to reach the desirable compression force. Subsequently, the fill depth is changed to intentionally produce an overweighed and underweighted tablet and the corresponding forces are set as the upper and lower rejection

limit, respectively. The correction limits are automatically calculated and set at 25 % of the reject limit. An example of these settings is provided in Figure 2.11 (“Fixed”). Due to the exponential relationship, the sensitivity of this principle decreases with tablet weight and/or compression force. Consequently, force measurement for weight control is always done at main compression, where the compression force and sensitivity are highest [23].

	Weight	Fixed	Moving
● Upper reject limit	309.00 mg	15.00 kN	0.40 mm
● Upper correction limit	302.25 mg	12.75 kN	0.28 mm
● NOMINAL	300.00 mg	12.00 kN	0.25 mm
● Lower correction limit	297.75 mg	11.50 kN	0.22 mm
● Lower reject limit	291.00 mg	10.00 kN	0.10 mm

Figure 2.11: Example of the relation between tablet weight and the compression force at main compression (for fixed roller set-up) and displacement at precompression (for moving roller set-up).

When compression is performed with the moving rollers set-up, the displacement is used as the process parameter to control weight variation (“Moving” in Figure 2.11). In contrast to the force-weight relationship, a linear relationship between displacement and weight is assumed. This allows automatic calculation of the reject limits, avoiding the need of manually producing an under- and overweighed tablet. This approach is preferentially performed at low compression forces where the density of the compressed powder is rather low. At low compression force, a given small change in weight will result in a larger change in displacement than at high compression force, resulting in a higher sensitivity. Consequently, displacement measurement for tablet weight control is always performed at precompression. By using this control at the precompression station, the main compression station can be used for additional (force or displacement) control loops [23].

5.1.2. Force control

Another possibility with the fixed roller set-up is the control of the compression force. Instead of a feedback coupling to the fill depth, the force on main compression is linked to the position of the bottom roller at that same station. Whenever the main compression force exceeds the tolerance limits as depicted in Figure 2.10, the machine will react by

changing the position of the lower roller at main compression, and consequently the distance between the punches. The roller will be raised when the lower control limit is exceeded and lowered when the upper control limit is exceeded. Force control is not possible with moving rollers, as the compression force is determined by the force in the air compensator and an adaption of the distance between the punches only changes the displacement.

5.1.3. Displacement control

In contrast to the force control, displacement control is only possible with moving rollers. Instead of a feedback coupling to the fill depth, the displacement on main compression is linked to the position of the bottom roller at that same station. The purpose of this control is to maintain the displacement or diverted dwell time, dependent on which mode is chosen (see 5.3. Operation principles available on the press).



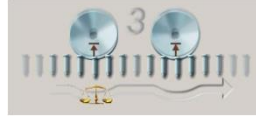
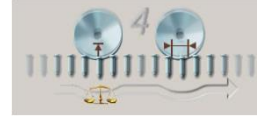

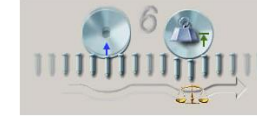
5.2. Control of the relation between tablet characteristics and process parameters

During a compression run, environmental changes, heating of the press and changes to the material under compression can change the set relation between the tablet characteristics and the process parameters as described above. Therefore, external control mechanisms are necessary. Weight, thickness and hardness of the tablets have to be checked periodically and coupled back to the machine to confirm or reset the established relation. If the control is done manually, the operator has to sample regularly a few tablets and determine their weight, hardness and thickness off-line. Another option is to couple an in-line tablet analyzer to the outlet of the press. Tablet samples are taken and analyzed automatically and the results are introduced into the control loop, after which the machine makes the appropriate adaptations.

5.3. Operation principles available on the press

A combination of the above control mechanisms results in six possible operation principles, i.e. six fixed combinations from which an overview is provided in Table 2.1.

Table 2.1: Overview of the six operation principles and control mechanisms available on the Modul™ P. (Courtesy of GEA, Courtoy™)

	Mode 1 Classic Courtoy Method	Mode 2 Courtoy Dual Control Force Method	Mode 3 Courtoy Dual Control Displacement Method	Mode 4 Courtoy Dual Control Dwell Time Method	Mode 5 Classic Method	Mode 6 Hybrid Method
						
Operation principle						
Precompression	Moving roller	Moving roller	Moving roller	Moving roller	Fixed roller	Moving roller
Main compression	Fixed roller	Fixed roller	Moving roller	Moving roller	Fixed roller	Fixed roller
Control						
Precompression	Weight control by displacement measurement	Weight control by displacement measurement	Weight control by displacement measurement	Weight control by displacement measurement	Not used	Not used
Main compression	Not used	Force control by force measurement	Displacement control by displacement measurement (with increasing machine speed, MCD stays the same, dwell time decreases)	Dwell time control by displacement measurement (with increasing machine speed, MCD increases, dwell time stays the same)	Weight control by force measurement	Weight control by force measurement

REFERENCES

- [1] M. J. Bogda, Tablet compression: Machine theory, design, and process troubleshooting, in: J. Swarbrick (Ed.), Encyclopedia of pharmaceutical technology, Informa Healthcare USA Inc., New York, 2007, pp. 3611-3629.
- [2] J. Vogeleeer, J. Boeckx, The new tableting facility, *Pharm. Tech. Eur.* 15 (2003), 25-30.
- [3] O. F. Akande, J.L. Ford, P.H. Rowe, M.H. Rubinstein, The effects of lag-time and dwell-time on the compaction properties of 1:1 paracetamol/microcrystalline cellulose tablets prepared by pre-compression and main compression, *J. Pharm. Pharmacol.* 50 (1998) 19-28.
- [4] C.E. Ruegger, M. Celik, The influence of varying precompaction and main compaction profile parameters on the mechanical stenth of compacts, *Pharm. Dev. Technol.* 5 (2000) 495-505.
- [5] N.A. Armstrong, Tablet manufacture, in: J. Swarbrick (Ed.), Encyclopedia of pharmaceutical technology, Informa Healthcare USA Inc., New York, 2007, pp. 3653-3672.
- [6] R.V. Haware, A. Bauer-Brandl, I. Tho, Comparative evaluation of the powder and compression properties of various grades and brands of microcrystalline cellulose by multivariate methods, *Pharm. Dev. Tech.* 15 (2010) 394-404.
- [7] T.M. Jones, The physicochemical properties of starting materials used in tablet formulation, *Int. J. Pharm. Tech. Prod. Manuf.* 2 (1981) 17-24.
- [8] P. Konkel, J.B. Mielck, Associations of parameters characterizing the time course of the tableting process on a reciprocating and on a rotary tableting machine for high-speed production, *Eur. J. Pharm. Sci.* 45 (1998) 137-148.
- [9] M. Leitritz, M. Krumme, P.C. Schmidt, Force-time curves of a rotary tablet press. Interpretation of the compressibility of a modified starch containing various amounts of moisture, *J. Pharm. Pharmacol.* 48 (1996) 456-462.
- [10] M. Levin, Tablet press instrumentation, in: J. Swarbrick (Ed.), Encyclopedia of pharmaceutical technology Informa Healthcare USA Inc., New York, 2007, pp. 3684-3706.

- [11] A. Munoz-Ruiz, M.R. Jimenez-Castellanos, J.C. Cunningham, A.V. Katdare, Theoretical estimation of dwell and consolidation times in rotary tablet machines, *Drug Dev. Ind. Pharm.* 18 (1992), 2011-2028.
- [12] A.S. Narang, V.M. Rao, H. Guo, J.A. Lu, D.S. Desai, Effect of force feeder on tablet strength during compression, *Int. J. Pharm.* 401 (2010) 7-15.
- [13] C.E. Rowlings, A.Y. Leung, P.C. Sheen, Resolution of the material and machine contributions to the area to height ratio obtained from force-time powder compression data II: Rotary tablet press, *Pharm. Acta Helv.* 72 (1997) 125-130.
- [14] C.E. Ruegger, M. Celik, The effect of compression and decompression speed on the mechanical strength of compacts, *Pharm. Dev. Technol.* 5 (2000) 485-494.
- [15] P.C. Schmidt, P.J. Vogel, Force-time-curves of a modern rotary tablet machine I. Evaluation techniques and characterization of deformation behaviour of pharmaceutical substances, *Drug Dev. Ind. Pharm.* 20 (1994) 921-934.
- [16] P.C. Schmidt, M. Leitritz, Compression force/time-profiles of microcrystalline cellulose, dicalcium phosphate dihydrate and their binary mixtures – a critical consideration of experimental parameters, *Eur. J. Pharm. Biopharm.* 44 (1997) 303-313.
- [17] I.C. Sinka, F. Motazedian, A.C.F. Cocks, K.G. Pitt, The effect of processing parameters on pharmaceutical tablet properties, *Powder Technol.* 189 (2009) 276-284.
- [18] C.K. Tye, C. Sun, G.E. Amidon, Evaluation of the effects of tableting speed on the relationships between compaction pressure, tablet tensile strength, and tablet solid fraction, *J. Pharm. Sci.* 94 (2005) 465-472.
- [19] P.J. Vogel, P.C. Schmidt, Force-time curves of a modern rotary tablet machine II. Influence of compression force and tableting speed on the deformation mechanisms of pharmaceutical substances, *Drug Dev. Ind. Pharm.* 19 (1993) 1917-1930.
- [20] J.K. Yliruusi, O.K. Antikainen, New parameters derived from tablet compression curves. Part I. Force-Time curve, *Drug Dev. Ind. Pharm.* 23 (1997) 69-79.

[21] J. Vogeeler, Rotary tablet press, Eur. Pharm. Manuf. 1 (2008).

[22] J. Van Evelghem, Improving tablet quality with compression to equal force technology, Pharm. Tech. (Suppl.) 32 (2008) 26-29.

[23] J. Vogeeler, Part two: Rotary tablet press, Eur. Pharm. Manuf. 3 (2008).

3

EFFECT OF THE PADDLE MOVEMENT

IN THE FORCED FEEDER

ON LUBRICANT SENSITIVITY

Abstract

The purpose of this research was to investigate the influence of paddle speed on the tensile strength of tablets prepared out of blends of microcrystalline cellulose and magnesium stearate. Four powder mixtures were prepared, one of them consisting out of pure microcrystalline cellulose, the others out of a mixture of microcrystalline cellulose and magnesium stearate in a concentration of 0.5 % with the difference between the three latter mixtures being the method of blending (low shear 3 minutes; low shear 15 minutes; high shear 5 minutes). After blending the mixtures were compressed into tablets. All parameters of the tableting cycle were kept constant except the speed of the paddles in the forced feeder. The tablets were stored overnight and their weight, hardness, thickness, diameter and friability was determined. The results indicate that the preparation method has an influence on the sensitivity of the mixture to the change of paddle speed. The tensile strength of the tablets made out of pure microcrystalline cellulose did not change with changing paddle speed. The tablets prepared by low shear mixing became softer with increasing paddle speed, albeit to a different extent, depending on the blending time. For the tablets prepared out of the mixture which was blended with the high shear blender, no change in hardness could be observed with changing paddle speed, but was overall low, suggesting that overlubrication of microcrystalline cellulose already occurred during the preceding blending step. Furthermore, analysis of the machine parameters allowed evaluation of the influence of the paddles on the flowability, initial packing and compactability of the powder mixtures. The results elucidated the influence of magnesium stearate but, except at the filling station, the differences in paddle speed did not further contribute to differences in the tableting process (packing, compactability, lubrication). In the production of tablets with powder mixtures containing magnesium stearate, not only care has to be taken at the blending step prior to tableting, but also at the tableting process itself, as the paddle speed in the feeder can have an important effect on the tensile strength, a critical quality attribute, of the tablets produced.

KEYWORDS: Tableting, Lubricant, Magnesium stearate, Tensile strength, Forced feeder, Blending.

1. INTRODUCTION

The negative effect of magnesium stearate as a tablet lubricant on the hardness of tablets containing components with a plastic deforming behavior is a well-known phenomenon [1-6]. The extent of this effect mainly depends on the magnesium stearate concentration, mixing time and mixing intensity [2, 7-9]. During tablet manufacturing the lubricant concentration and the mixing procedure (type of mixer, mixing time and intensity, mixing order) is mostly well defined, taking into account the possible negative effects of magnesium stearate [10-13]. However, the paddle speed of the feeder influences the shear rate and material residence time inside the forced feeder of the tablet press, but its influence on the lubricant effect during tablet compression is often neglected [14-17]. This study highlights the influence of the paddle speed in the forced feeder of a high speed tablet press on the tensile strength of microcrystalline cellulose (MCC) tablets containing magnesium stearate (MgSt). Furthermore, as machine parameters were set to obtain an equal tablet weight and compression force for all powder mixtures, analysis of the obtained results for these settings allowed evaluation of the influence of the paddles on the flowability, initial packing in the die and compactability of the powder mixtures.

2. MATERIALS AND METHODS

2.1. Materials

Microcrystalline cellulose (Avicel[®] PH-102, FMC Biopolymer, Cork, Ireland) was selected as the model powder for materials exhibiting plastically deforming behavior. Magnesium stearate was purchased from Fagron (Waregem, Belgium).

2.2. Preparation of powder mixtures

An overview of the composition and mixing method of the four blends is provided in Table 3.1. 4 kg of each blend was prepared. Prior to blending, the MCC was sieved by hand through a 3000 µm sieve to break up large agglomerates which might have been formed during storage. MgSt was placed on a 100 µm sieve and shaken at an amplitude of 2 mm for 30 minutes, using a sieve shaker (Retsch VE 1000, Haan, Germany).

Table 3.1: Composition and mixing method of the four powder mixtures.

Mixture	A	B	C	D
Microcrystalline cellulose (%)	100.0	99.5	99.5	99.5
Magnesium stearate (%)	-	0.5	0.5	0.5
Mixing method	-	Low shear	Low shear	High shear
Mixing time (min)	-	3	15	5

Low shear mixing was performed using a 20 L tumbling mixer (Inversina, Bioengineering, Wald, Switzerland). Besides the rotational and translational movement of a conventional tumbling mixer, this mixer uses inversional motion which leads to more efficient mixing and decreases the possibility of segregation [18-20]. Tumbling mixers are commonly used for the mixing and blending of granules or free-flowing powders with lubricants, glidants and disintegrants prior to tableting. There are many different designs of tumbling mixers. In industry, intermediate bulk containers (IBC's) are commonly used for both mixing and immediate feeding of the machine. Shear occurs as a velocity gradient is produced by rotation of the mixing container about an axis. As the powder bed tumbles it dilates, allowing diffusive mixing to occur. The operational speed, size and filling degree of these low shear blenders are all process factors influencing the mixing pattern inside the container.

A 10 L high shear mixer (Gral10, GEA Pharma Systems - Collette™, Wommelgem, Belgium) was used for the high shear mixing of the powder blend. The centrally mounted impeller blade at the bottom of the mixer rotates at high speed, throwing the material towards the mixer bowl wall by centrifugal force. The material is then forced upwards before dropping back down towards the center of the mixer. The components mix owing to high shear forces (arising from the high impeller velocity) and the expansion in bed volume that allows diffusive mixing. In pharmaceutical product manufacturing, this type of mixer is used for the mixing of cohesive powders or more commonly for single-pot processing. In the latter, mixing, granulation and drying takes place in the same piece of equipment, thereby removing the need to transfer the product [20-22]. Because of the high-speed movement within the mixer-granulator which can fracture material easily and the problems associated with overmixing of lubricants, this type of mixer is not normally used for blending lubricants

[20]. However, its use in this research is justified, as it was the intention to obtain an overlubricated blend.

The low shear mixer was run for 3 or 15 minutes, depending on the mixture (Table 3.1), at 25 rotations per minute (rpm) with a filling degree of approximately 60 %. The high shear blending was performed at 400 rpm. In order to also obtain a filling degree of 60 %, the amount of powder for the high shear mixer was divided in half. After blending, the powder blend was allowed to settle for 5 minutes before unloading the mixer, in order to reduce material loss due to airborne particles. Room temperature and relative humidity (RH) were logged.

2.3. Powder characterization

Particle size analysis was done by sieve analysis ($n=3$), using a sieve shaker (Retsch VE 1000, Haan, Germany). 30 g of powder was placed on a nest of sieves (50, 100, 125, 150 and 250 μm) and shaken at an amplitude of 0.2 mm for 2 minutes. The amount of powder retained on each sieve was determined.

The bulk (ρ_{bulk}) and tapped density (ρ_{tapped}) of 30 g of powder was determined in a 100 ml graduated cylinder ($n=3$). The powder was poured from a height of 40 cm through a stainless steel funnel with a 10 mm orifice into the graduated cylinder, mounted on a tapping device (J. Engelsmann, Ludwigshafen am Rhein, Germany). Bulk and tapped densities were calculated as $30 \text{ g} / V_0$ and $30 \text{ g} / V_{1250}$, respectively. These values were used to calculate the compressibility index (CI) in order to assess the tendency of a powder to consolidate [23].

Scanning electron microscopy (SEM) was used to study the shape and size distribution of the powders particles. A small amount of powder was mounted on metal stubs with carbon tape and coated with gold by means of a sputter coater (Emitech SC7620, Quorum Technologies, East Grinstead, UK). Photomicrographs were taken with a scanning electron microscope (FEI QuantaTM 200F, FEI, Hillsboro, USA) operated at an acceleration voltage of 20 kV. The granules were observed at a magnification of 100x.

2.4. Preparation of tablets

2.4.1. Tableability

A preliminary study was performed to determine the main compression force (MCF) for further experiments. Tableability is examined by plotting tensile strength (TS) against MCF [15, 24, 25]. Although very useful, the obtained correlation is not an intrinsic material characteristic and the profile depends upon the press, tooling and settings used (e.g. tableting speed, paddle speed in the forced feeder, fill depth) [15, 26-28]. Therefore, the same machine and tooling was used throughout the study.

Tablets of pure MCC were prepared using a MODUL™ P tablet press (GEA Process Engineering - Courtoy™, Halle, Belgium) equipped with an overfill cam of 10 mm. As the die table (turret) rotates, powder is fed from the forced feeder into the dies at the overfilling station. After weight adjustment at the filling station, the punches (n=10, standard euro B, Ø 8 mm, flat faced bevel edge) move further through the pre- and main compression station to the ejection cam, where the tablets are removed from the die table by a tablet stripper [29]. The fill depth was adjusted to obtain tablets of 150 mg, in accordance with the subsequent experiments. Tableting speed was set at 400 tablets per minute (tpm) and force feeder speeds were kept constant at 25 rpm – 40 rpm. Precompression force (PCF) was controlled at 2 kN and precompression displacement (PCD) at 0.2 mm. Main compression displacement (MCD) was kept at 0.0 mm for all experiments and MCF was varied from 3 to 31 kN. For each experiment the machine was run for 2 minutes, with sampling during the second minute. Room temperature (21.0 ± 2.0 °C) and RH (30.0 ± 2.0 %) were controlled. Tablets were stored overnight in open tablet trays in a desiccator (filled with a saturated solution of magnesium chloride hexahydrate (Fagron, Waregem, Belgium)) at 23.1 ± 1.0 °C and 30.0 ± 2.0 % RH prior to analysis.

2.4.2. Effect of the paddle speeds

For the evaluation of the effect of the paddle speeds, the different powder mixtures (Table 3.1) were compressed into tablets. The two paddles of the machine are located in the feed frame at the filling station, as described in detail in Chapter 2 (2. Powder feeding system). Paddle speeds were varied according to Table 3.2. All other machine settings were set and

left unchanged during an experiment (Table 3.3). As in the tableability study, fill depth was adjusted to obtain tablets of 150 mg. Tableting speed was set at 400 tpm. PCF was controlled at 2 kN and PDC at 0.2 mm. MCD was kept at 0.0 mm for all experiments and the MCF was controlled at 9 kN, based on the results of the preliminary tableability test.

Table 3.2: Combination of paddle speeds used for the different experiments.

Paddle speed (rpm)	1	2	3	4
Paddle 1	10	25	40	60
Paddle 2	20	40	70	100

When starting an experimental run, the hopper and feeder were filled with the powder blend. Every experiment the machine was started and run for one minute before adjusting fill depth and parameters controlling the compression force and displacement. Subsequently, the machine was run for another five minutes with sampling during the last minute. To exclude the direction of the run order as a confounding factor, experiments were conducted from the lowest to the highest paddle speed (Table 3.2, from experiment 1 to 4) and vice versa. Room temperature (21.0 ± 2.0 °C) and RH (30.0 ± 2.0 %) were controlled. Tablets were also stored overnight before analysis.

2.5. Monitoring of set and dependent machine parameters

The machine settings which were kept constant (Table 3.3) were logged on the tableting machine. Fill depth was set to obtain a tablet weight of 150 mg. Although this value is set at the beginning of each experimental run and kept constant, its absolute value is dependent on the flow properties of the mixture. Consequently, it is actually a response and monitoring and analyzing this value provides insight in the lubrication effect of the paddles. The same reasoning is followed for the position of the bottom roller (bot) and the pressure in the air-compensator (PCF_r , MCF_r), since a combination of these two parameters together with the powder characteristics determines the compression force (PCF, MCF) and the compression displacement (PCD, MCD) with which tablets are compressed at pre- and main compression, respectively. As the goal was to keep the PCF (2 kN), MCF (9 kN), PCD (0.2 mm) and MCD (0.0 mm) at a fixed value, the pressure in the air-compensator and position of the bottom punch had to be adapted for each run to reach these values.

On the other hand, since PCF, MCF, PCD and MCD are dependent on the above machine settings, they can be identified as dependent process parameters. These values, together with the ejection force (EF), were recorded with a data acquisition and analysis system (CDAAS), from which a description is given in Chapter 2 (4. Instrumentation and collection of data). The maximum values of ten successive signals for each parameter were determined and the mean value and standard deviation calculated. An overview of these dependent machine settings is also provided in Table 3.3.

Table 3.3: Overview of the set and dependent machine settings included in the data analysis.

Key	Meaning
Set machine settings	
speed (tpm)	Tableting speed
pad1 (rpm)	Speed of paddle 1 in the forced feeder
pad2 (rpm)	Speed of paddle 2 in the forced feeder
fill (mm)	Fill depth, which determines the weight
PCF _r (kN)	Air pressure in the air-compensator of the upper roller at precompression
MCF _r (kN)	Air pressure in the air-compensator of the upper roller at main compression
prebot (mm)	Position of bottom roller at precompression
mbot (mm)	Position of bottom roller at main compression
Dependent machine settings	
PCF (kN)	Maximum precompression force exerted on powder under compression
MCF (kN)	Maximum main compression force exerted on powder under compression
PCD (kN)	Maximum displacement of the upper roller during precompression
MCD (kN)	Maximum displacement of the upper roller during main compression
EF (kN)	Maximum ejection force measured during the ejection phase

2.6. Tablet evaluation

Tablets (n=20) were weighed and their hardness, thickness and diameter was determined (Sotax HT 10, Basel, Switzerland). The tablet tensile strength (TS) (MPa) was calculated using Equation (3.1) [30].

$$TS = \frac{2F}{\pi dT} \quad (3.1)$$

where F, d and T denote the diametral crushing force (N), the tablet diameter (mm) and the tablet thickness (mm), respectively.

Tablet friability was determined (n=3) on 43 tablets using a friabilator described in the European Pharmacopoeia 7.0 (Pharma Test PTF-E, Hainburg, Germany), at a speed of 25 rpm for 4 minutes. Tablets were dedusted and weighed prior to and after the test. Tablet friability was expressed as the percentage weight loss.

3. RESULTS AND DISCUSSION

3.1. Tableability

Figure 3.1 depicts the tableability curve obtained when compressing pure MCC into tablets, by plotting TS against MCF. 9 kN was chosen as the MCF to perform further experiments. The tableability curve is linear at compression pressures less than 9 kN. Above 9 kN, the curve gradually levels off to a plateau, where a further increase in the compaction force does not contribute to a higher tensile strength. The higher energy put in the system is not used for additional bond formation and can, in some cases with highly elastic material, even decrease the strength of formed bonds, as elastic expansion at higher compression forces is favored.

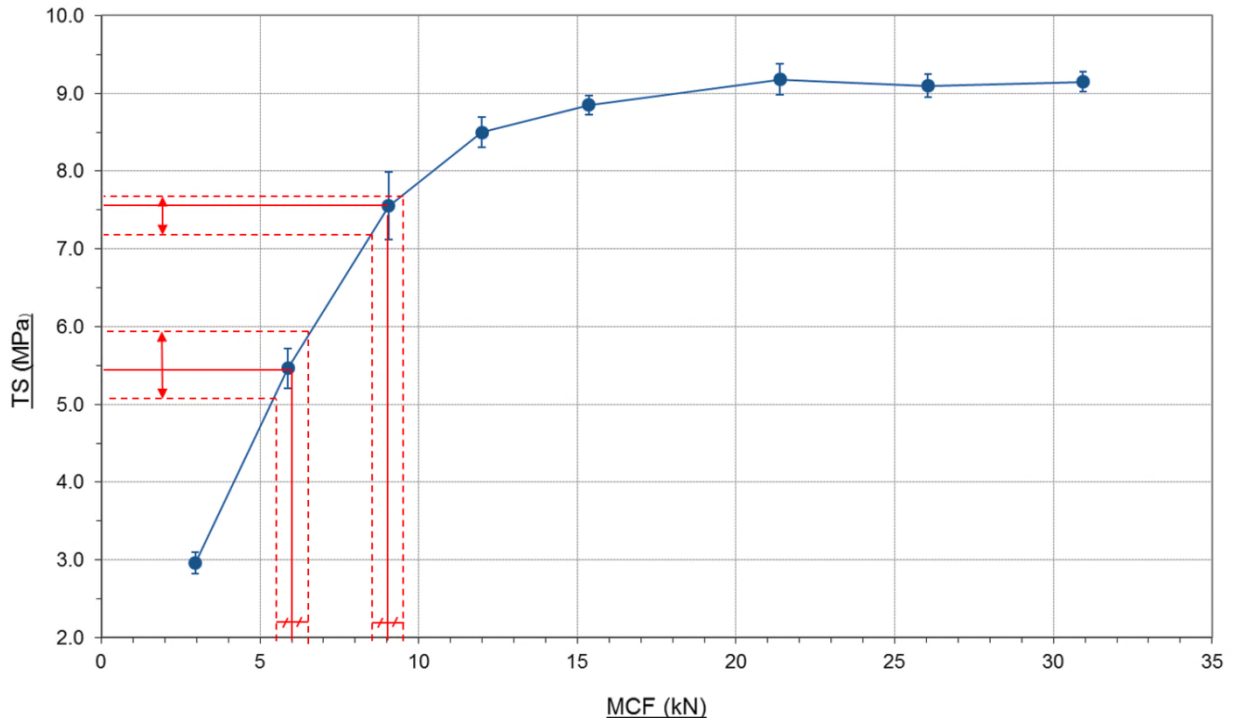


Figure 3.1: Tableability curve of pure MCC. Each point depicts the mean \pm stdev (n=20). The arrows indicate the range over which tensile strengths (TS) changes when main compression force (MCF) varies 0.5 kN.

The preferred compression force from a manufacturing point of view is the lowest force (i.e. the least energy input) at which tablets complying with quality- and bioavailability requirements can be produced. MCC is known for its compression behavior, with the formation of strong tablets at relatively low compression forces [2]. Hence, a lower compression force could be selected. The variability in TS however, is significantly larger when a variation (e.g. 0.5 kN) in MCF occurs at lower compression forces (Figure 3.1). Since this could be a confounding factor in the interpretation of the influence of magnesium stearate on tensile strength, a force closer to the plateau of the curve was chosen.

3.2. Effect of the paddle speeds

A schematic overview of the machine parameters, both set and dependent, the tablet characteristics and their relation to each other is outlined in Table 3.4. Since water content has a major influence on the mechanical properties of MCC, this parameter was also taken into account [2, 3, 31-33]. As all samples (also pure MCC) were exposed to the same ambient conditions for an equal period, the moisture content was not regarded as a confounding factor. During blending experiments and powder characterization, the RH and temperature were $54.0 \pm 5.4 \%$ and $20.1 \pm 2.0 \text{ }^\circ\text{C}$, while during tableting, storing and analyzing of tablets, RH and temperature were controlled at $30.0 \pm 2.0 \%$ and $21.5 \pm 2.0 \text{ }^\circ\text{C}$, respectively.

The influence of the paddle speed on the tensile strength is depicted in Figure 3.2. The tensile strength of tablets without MgSt was not affected by the paddle speed (mixture A). Following low shear blending of MCC and MgSt the tensile strength decreased using a higher paddle speed (mixture B). The higher mixing intensity in the forced feeder increased the lubricant effect on the plastically deforming MCC. The effect of paddle speed was less pronounced using a longer mixing time (mixture C), but the tensile strength of the tablets was lower due to increased coating of the MCC fibers during blending. Following high shear blending of MCC and MgSt no effect of the paddle speed was observed, indicating that the powder mixture was already overblended during the mixing step (mixture D). Overall, irrespective of the paddle speeds, the influence of MgSt on the tensile strength is pronounced, as the tensile strength of the tablets containing MgSt is lower than the tablets lacking lubricant.

Table 3.4: Schematic overview of the set and dependent machine parameters, the tablet characteristics and their relation to each other. The preset factors are highlighted with grey background. Key: see Table 3.3.

Tablet characteristics	Dependent machine parameters	Set machine parameters	Relation
		speed (tpm)	
TS (MPa) ± stdev		pad1 (rpm) – pad2 (rpm)	Influence of the lubricating properties of the paddles ↓ Affects
Friability (%) ± stdev			
Weight (mg) ± stdev		fill (mm)	Influence of MgSt on flowability of the powder
	PCF (kN) ± stdev	PCF _r (kN)	Influence of MgSt on initial packing of the powder
	PCD (mm) ± stdev	prebot (mm)	
	MCF (kN) ± stdev	MCF _r (kN)	Influence of MgSt on compactibility of the powder
	MCD (mm) ± stdev	mbot (mm)	
	EF (kN) ± stdev		Influence of MgSt on lubrication of the powder

Depends on →

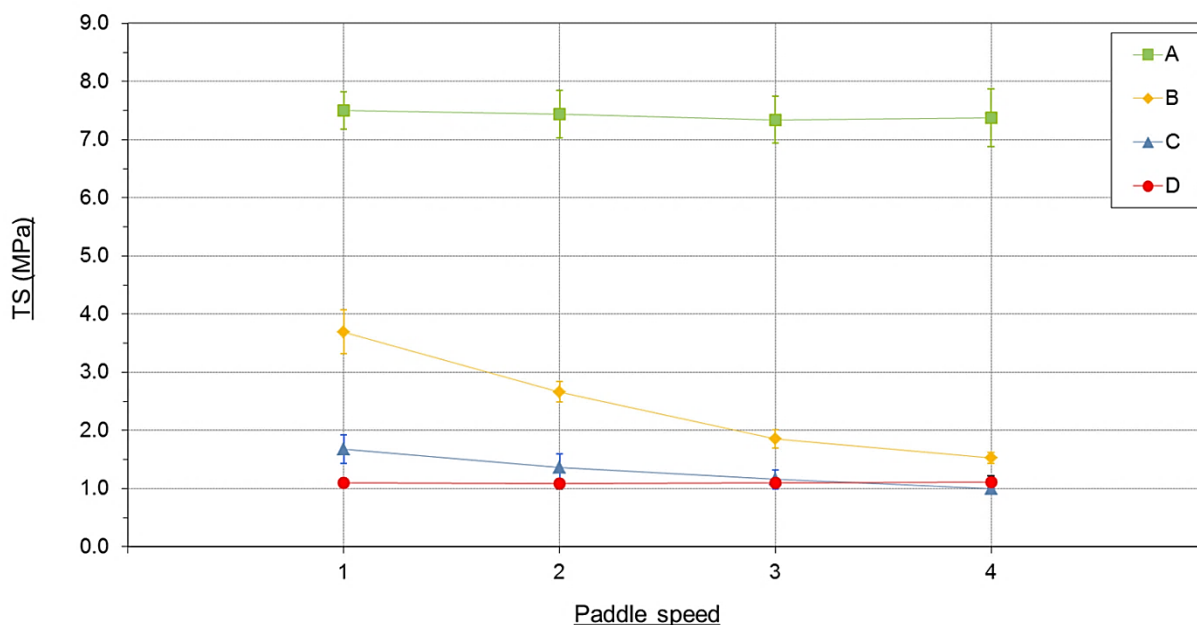


Figure 3.2: Influence of the paddle speed on TS of tablets. Each point depicts the mean \pm stdev (n=20).

When taking into account the structure of MCC, it could be argued that the observed results are not solely dependent on the presence of MgSt, but on a combination of the influence of the blending step (prior to and during tableting) on the particle size distribution of MCC and the distribution of MgSt. MCC consists of porous microfibrilles, which are easily broken down [3, 9]. During the blending step, shear is introduced in the powder bed. When shear increases, either by altering the blending step prior to tableting (by increasing the mixing time or intensity) or during tableting by increasing the paddle speed, particles will fracture more extensively.

Table 3.5: Flow properties and particle size distribution of the powders. Values depict the mean \pm stdev (n=3).

Mixture	A	B	C	D
V_0 (ml)	89.67 \pm 0.58	81.83 \pm 0.29	75.33 \pm 0.58	65.83 \pm 0.29
V_{1250} (ml)	71.00 \pm 0.87	65.83 \pm 0.29	61.83 \pm 0.29	55.00 \pm 0.00
ρ_{bulk} (g/cm ³)	0.33 \pm 0.00	0.37 \pm 0.00	0.40 \pm 0.00	0.46 \pm 0.00
ρ_{tapped} (g/cm ³)	0.42 \pm 0.01	0.46 \pm 0.00	0.49 \pm 0.00	0.55 \pm 0.00
Compressibility index (CI) (%)	20.82 \pm 0.46	19.55 \pm 0.07	17.92 \pm 0.55	16.45 \pm 0.37
Particle size distribution				
d10 (μm)	54.7 \pm 3.2	50.8 \pm 7.3	37.5 \pm 7.1	31.7 \pm 0.6
d50 (μm)	154.7 \pm 2.9	148.2 \pm 14.8	122.5 \pm 13.6	117.5 \pm 0.5
d90 (μm)	232.5 \pm 2.0	232.0 \pm 2.0	227.8 \pm 2.8	227.0 \pm 0.5

This is supported by the results of the particle size distribution of the different blends, as presented in Table 3.5. Also the SEM-pictures (Figure 3.3) illustrate the difference in particle size distribution. However, as reported in literature, tablets prepared from different size fractions of pure MCC did not differ in the time they needed to disintegrate or their tensile strength [3, 9]. This indicates that, even when MCC particles are broken down during the preceding blending step or in the forced feeder, this does not attribute to the differences seen in TS. Moreover, due to their small size, MCC microfibrilles have a relatively large surface to volume ratio [34]. Consequently, when the concentration of MgSt and the blending conditions remain the same, the smaller the lubricating effect for smaller host particles will be [2]. When the influence of MgSt on different sieve-fractions was compared, all results in literature report an increase in TS for smaller particle sizes. This demonstrates that in this experiment the observed (negative) results of TS can be mainly attributed to the difference in the blending step of magnesium stearate, and not to the change in particle size of MCC [2, 3, 9, 12].

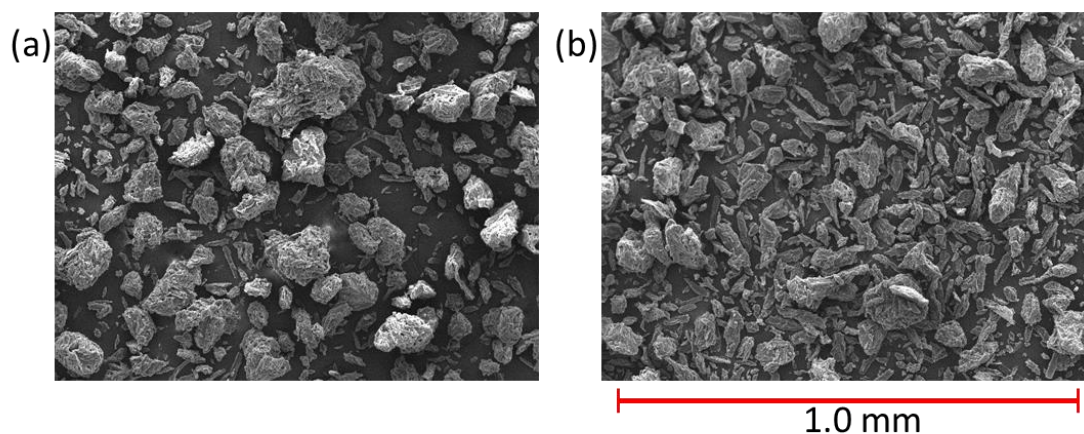


Figure 3.3: SEM-pictures illustrating the difference in particle size distribution: (a) mixture A, (b) mixture C.

An overview of the obtained values of set and dependent machine parameters and tablet characteristics is presented in Table 3.6. Regardless the paddle speed, the friability for all mixtures was low. The tablets prepared out of the high shear blended mixture (mixture D) had a somewhat higher friability. These results show that the resistance to crushing, expressed by the tensile strength, and the susceptibility to abrasion, represented by the friability, are not completely interdependent and care should be taken not to generalize results obtained by determining only one characteristic.

Table 3.6: Overview of the obtained values of set and dependent machine parameters and the tablet characteristics. Values depict the mean \pm stdev (n=3 for friability; n=20 for weight; n=10 for PCF, PCD, MCF, MCD and EF). Key: see Table 3.3.

Mixture	Paddle speed	Friability (%)	Flowability		Initial packing				Compactibility				Lubrication
			Fill (mm)	Weight (mg)	PCF _r (kN)	prebot (mm)	PCF (kN)	PCD (mm)	MCF _r (kN)	mbot (mm)	MCF (kN)	MCD (mm)	EF (kN)
A	1	0.25 \pm 0.02	7.72	151.59 \pm 0.85	1.56	4.87	2.16 \pm 0.19	0.19 \pm 0.01	25.15	4.62	9.29 \pm 0.39	0.00	0.26 \pm 0.02
	2	0.23 \pm 0.01	7.56	151.70 \pm 0.75	1.56	4.87	2.11 \pm 0.13	0.20 \pm 0.01	25.15	4.63	9.28 \pm 0.35	0.00	0.26 \pm 0.02
	3	0.24 \pm 0.01	7.54	151.45 \pm 0.70	1.56	4.87	2.08 \pm 0.10	0.19 \pm 0.01	25.15	4.62	9.40 \pm 0.48	0.00	0.25 \pm 0.01
	4	0.17 \pm 0.04	7.54	151.23 \pm 0.66	1.56	4.87	2.19 \pm 0.14	0.19 \pm 0.01	25.15	4.62	9.32 \pm 0.32	0.00	0.26 \pm 0.02
B	1	0.05 \pm 0.00	6.88	150.07 \pm 0.52	1.80	4.85	2.06 \pm 0.09	0.19 \pm 0.01	25.21	4.59	8.97 \pm 0.39	0.00	0.08 \pm 0.01
	2	0.11 \pm 0.01	6.71	151.12 \pm 0.95	1.80	4.85	2.07 \pm 0.14	0.19 \pm 0.01	25.21	4.60	8.99 \pm 0.49	0.00	0.08 \pm 0.01
	3	0.20 \pm 0.02	6.60	150.75 \pm 0.69	1.80	4.86	2.11 \pm 0.15	0.20 \pm 0.01	25.23	4.60	8.98 \pm 0.43	0.00	0.09 \pm 0.01
	4	0.28 \pm 0.01	6.59	151.23 \pm 0.99	1.80	4.86	2.17 \pm 0.19	0.19 \pm 0.01	25.23	4.60	9.01 \pm 0.53	0.00	0.08 \pm 0.00
C	1	0.13 \pm 0.01	6.25	150.74 \pm 0.77	1.80	4.77	2.10 \pm 0.15	0.18 \pm 0.01	25.38	4.59	9.12 \pm 0.35	0.00	0.09 \pm 0.01
	2	0.21 \pm 0.01	6.17	150.15 \pm 0.74	1.80	4.76	2.14 \pm 0.14	0.19 \pm 0.01	25.38	4.59	8.96 \pm 0.40	0.00	0.08 \pm 0.01
	3	0.22 \pm 0.03	6.14	149.74 \pm 1.24	1.80	4.75	2.10 \pm 0.16	0.18 \pm 0.01	25.37	4.59	9.13 \pm 0.50	0.00	0.08 \pm 0.00
	4	0.10 \pm 0.05	6.15	150.29 \pm 1.09	1.80	4.76	2.18 \pm 0.14	0.18 \pm 0.01	25.36	4.59	9.14 \pm 0.44	0.00	0.09 \pm 0.00
D	1	0.39 \pm 0.01	6.27	150.32 \pm 0.63	1.80	4.81	2.11 \pm 0.15	0.20 \pm 0.01	25.21	4.60	9.15 \pm 0.58	0.00	0.09 \pm 0.00
	2	0.40 \pm 0.01	6.26	150.17 \pm 0.89	1.80	4.80	2.02 \pm 0.17	0.19 \pm 0.01	25.21	4.60	9.24 \pm 0.54	0.00	0.09 \pm 0.00
	3	0.34 \pm 0.03	6.29	150.83 \pm 0.88	1.80	4.80	2.12 \pm 0.18	0.19 \pm 0.01	25.21	4.59	8.91 \pm 0.52	0.00	0.08 \pm 0.00
	4	0.35 \pm 0.02	6.30	150.42 \pm 1.09	1.80	4.80	2.12 \pm 0.13	0.19 \pm 0.01	25.21	4.59	8.94 \pm 0.52	0.00	0.08 \pm 0.00

When looking at the obtained weight and the weight variability, there can be concluded that for all experiments tablets with the desired weight could be produced. All powders possess sufficient flow, regardless of the paddle speed, since there are no visible trends or differences in the weight variability. This is supported by the values of the compressibility index (Table 3.5), according to which all powder blends can be classified as fairly flowing powders. When looking at the fill depth necessary to obtain the desired weight, conclusions about the fill density can be drawn. In general, the fill depth can be ranked as Mixture A > Mixture B > Mixture D > Mixture C. This indicates that the fill density of the mixture lacking the lubricant is the lowest, followed by the mixture subjected to low shear for a short period of time and the mixture blended with high shear and finally the mixture which was blended by low shear for 15 minutes. As bulk density is dependent on particle size, the higher fill depth of D compared to C is somewhat surprising, especially since the results of powder flow (Table 3.5) indicate otherwise. Moreover, smaller particles commonly exhibit worse flow properties and this opposes the observed results [2, 3]. However, both effects can be explained by the glidant properties of MgSt, as decreasing friction between particles results in a higher bulk density [10, 35-37].

The mixture lacking MgSt (Mixture A) has a poor flowability, shown by a large fill depth and the dependence of the paddle speed, as fill depth gradually decreases as the paddle speed increases [38]. Also the flow of the mixture subjected for a short period to low shear (Mixture B) shows dependence of the paddle movement. But since the overall fill depth is lower compared to mixture A, the flow can be considered to be improved, due to the presence of MgSt. The flow of the other two mixtures is not affected by the paddle speed, indicating that these materials are free-flowing. The lower fill depth of mixture D compared to mixture C can be ascribed by taking into account the specific surface of the MCC particles. In mixture C, although exerted for a longer period, the shear is less than in mixture D. As a consequence more particles are broken down into their primary particles (Table 3.5) and the concentration of MgSt is not sufficient to completely cover the large free surface area, herewith contributing less than in mixture C to the flowability [3]. It should be mentioned that the results of the flow properties determined via bulk and tapped density and via the parameter settings of the machine show some deviation, especially for Mixture C and D. Although the former is very useful to obtain in a fast way an initial indication of the flow

performance, these determinations are static measurements, whereas the powder flow in a forced feeder is a dynamic process. Different mechanisms act simultaneously on the powder bed, which cannot be captured by the existing conventional techniques to measure and quantify powder flow [38-41]. Since the capacity of a glidant is mainly expressed in moving material, it is possible that this property is more pronounced in the forced feeder, during actual die filling, than it is during the static flow measurements.

As the PCF and PCD for all tablets are comparable, the PCF_r and position of the lower punch give information about the effect of magnesium stearate on the initial densification of the powders under compression. The position of the bottom punch mainly provides information about the interparticulate voids. The smaller the value, the smaller the interparticulate space. This value is the largest for the mixture lacking the lubricant, which indicates more space between the particles and can be linked to a larger particle size of the MCC particles. For the other mixtures, the same reasoning can be followed as with the fill depth. For mixture B and C, a smaller particle size and the presence of MgSt are translated in a denser packing, due to the ability of MgSt coated particles to more easily slip by one another and pack into a denser formation [10]. Since the glidant ability of MgSt in blend D is hampered due to the large specific surface of the individual MCC particles, the initial packing is not as dense as with mixture C.

The PCF_r gives information about the ability of MgSt to reduce die-wall friction. As die-wall friction is reduced, the net energy introduced in the process will be more efficiently used. Since the difference between PCF_r and PCF is smaller for mixtures B-D than for A, this means less energy is lost when MgSt is used, which could be attributed to its lubricating potential [42]. Another contributing factor to the observed effect is the ability of MgSt to reduce air entrapment [43]. The initial volume of mixture A is larger for the same weight than for the other mixtures. As already mentioned, this assumes more void spaces (i.e. more air) and a less dense packing of the particles. So for a same displacement (PCD) more air will be pressed out between the particles for mixture A than for the other mixtures. The lower the value of PCF_r when reaching a similar displacement (PCD) under an equal load (PCF), the lower the densification will be. From these results can be concluded that during precompression mainly release of entrapped air and particle rearrangement takes place for mixture A, whereas for the other mixtures already bond formation and deformation of

particles occurs. Finally, few researchers report the ability of MgSt to reduce elasticity and/or to promote plastic behavior [6, 7, 44]. This might also explain partially the lower value of PCF_r for an equal displacement under an equal load. In accordance to the findings of other researchers, this mechanism is not affected by the particle size of MCC, which can be concluded from the equal value for PCF_r for mixture B, C and D [2]. Comparing mixture A with the other mixtures, it can be seen that this value is lower, i.e. elasticity higher. However, results obtained by other researchers are not always consistent and straightforward, nor a full explanation for these observations is given. Therefore, no clear statement about this effect can be made.

The results of the main compression should be interpreted with a different rationale as the precompression results. Since no displacement is generated, the MCF_r has no added value in the interpretation of the results. It is set at a high value, to inhibit roller displacement. As such, the only factor of importance is the position of the bottom punch. As this value changes, when the force exerted on the powder bed (MCF) stays the same, this indicates a change in compactability. Since the particle size of MCC does not influence this factor, an observed effect is mainly caused by the presence of MgSt [7]. Although a difference between mixture A and mixture B-D can be observed, this difference is rather small. Therefore, a reduction of die-wall friction in the presence of MgSt is the main cause of this effect, rather than a change in compactability, as is also reported by other authors [6, 45].

Finally, the effect of MgSt on the ejection force reveals a clear effect of the lubricating properties of MgSt, since there is a large difference between the mixture lacking the lubricant and the other mixtures [46]. This reduction in EF is equally distinct for all mixtures with MgSt and all paddle speeds. The desired effect (i.e. lowering the die-wall friction at ejection) is thus already reached after only 3 minutes of blending in a low shear mixer [47].

From a manufacturing point of view, mixture B is the closest one related to a real life setting. It is also this mixture which is most susceptible to a change in paddle speeds. Moreover, as already mentioned, MCC has a good compression behavior and forms strong tablets at relatively low compression forces. It is likely to assume when adding active pharmaceutical ingredients also possessing a plastically deformation behavior, the negative effect of MgSt on the TS will be even more elucidated. Furthermore, next to the reduction of TS, MgSt is

also known to increase the disintegration and dissolution time and reduce the adhesion of film-coats to tablet surfaces [47-49]. Instead of incorporating the lubricant into the powder mixture, external lubrication by spraying MgSt immediately on the punch tips and dies could decrease its detrimental effects [50-52]. However, some challenges arise to incorporate this system into existing tableting machines currently lacking the system. This will contribute to the need of gaining further understanding in the internal lubrication of formulations.

4. CONCLUSIONS

By analyzing the data collected at the different stations on the tableting machine, it can be concluded that the presence of MgSt clearly influences the tableting process (differences between mixture A and mixtures B-D). The paddle speeds on the other hand, did not contribute to large changes in the tableting process (packing, compactability, lubrication), except at the filling station. This is in contrast to the different blending steps prior to tableting. However, the paddle speeds have an influence on the shear rate and material residence time inside the forced feeder, inducing an effect on the flowability of the powders and on the tensile strength of the tablets produced, and with that on the quality of the end product. This study illustrates that the paddles are more than just an aid to force material into a die, and the passage of the material through the forced feeder can be considered as an additional blending step. Their influence should not be underestimated. When manufacturing tablets containing magnesium stearate, not only the blending step prior to tableting should be optimized (adding magnesium stearate at the end of the blending cycle, using a low lubricant concentration, mixing using low shear blenders), but also the mixing effect of the feeder should be taken into account.

REFERENCES

- [1] G.K. Bolhuis, C.F. Lerk, H.T. Zijlstra, A.H. De Boer, Film formation by magnesium stearate during mixing and its effect on tableting, *Pharm. Weekblad* 110 (1975) 517-560.
- [2] E. Doelker, Comparative compaction properties of various microcrystalline cellulose types and generic products, *Drug Dev. Ind. Pharm.* 19 (1993) 2399-2471.
- [3] E. Doelker, D. Massuell, F. Vuillez, P. Humbert-Droz, Morphological, packing, flow and tableting properties of new avicel types, *Drug Dev. Ind. Pharm.* 21 (6) (1995) 643-661.
- [4] P.J. Jarosz, E. L. Parrott, Effect of lubricants on tensile strengths of tablets, *Drug Dev. Ind. Pharm.* 10 (1984) 259-273.
- [5] S. Lakio, B. Vajna, I. Farkas, H. Salokangas, G. Marosi, J. Yliruusi, Challenges in detecting magnesium stearate distribution in tablets, *AAPS PharmSciTech.* 14 (2013) 435-444.
- [6] K. Zuurman, K. Van der Voort Maarschalk, G.K. Bolhuis, Effect of magnesium stearate on bonding and porosity expansion produced from materials with different consolidation properties, *Int. J. Pharm.* 179 (1999) 107-115.
- [7] R.V. Haware, A. Bauer-Brandl, I. Tho, Comparative evaluation of the powder and compression properties of various grades and brands of microcrystalline cellulose by multivariate methods, *Pharm. Dev. Technol.* 15(4) (2010) 394-404.
- [8] P.J. Jarosz, E. L. Parrott, Effect of lubricants on axial and radial work of failure, *Drug Dev. Ind. Pharm.* 8 (1982) 445-453.
- [9] J.G. van der Watt, The effect of the particle size of microcrystalline cellulose on tablet properties in mixtures with magnesium stearate, *Int. J. Pharm.* 36 (1987) 51-54.
- [10] J. Kushner, F. Moore, Scale-up model describing the impact of lubrication on tablet tensile strength, *Int. J. Pharm.* 399 (2010) 19-30.
- [11] J. Kushner, Incorporating Turbula mixers into a blending scale-up model for evaluating the effect of magnesium stearate on tablet tensile strength and bulk specific volume, *Int. J. Pharm.* 429 (2012), 1-11.

- [12] K. Pingali, R. Mendez, D. Lewis, B. Michniak-Kohn, A. Cuitino, F. Muzzio, Mixing order of glidant and lubricant – influence on powder and tablet properties, *Int. J. Pharm.* 409 (2011) 269-277.
- [13] J.G. van der Watt, M.M. de Villiers, The effect of V-mixer scale-up on the mixing of magnesium stearate with direct compression microcrystalline cellulose, *Eur. J. Pharm. Biopharm.* 43 (1997) 91-94.
- [14] R. Mendez, F. Muzzio, C Velazquez, Study of the effects of feed frames on powder blend properties during the filling of tablet press dies, *Powder Technol.* 200 (2010) 105-116.
- [15] A.S. Narang, V.M. Rao, H. Guo, J.A. Lu, D.S. Desai, Effect of force feeder on tablet strength during compression, *Int. J. Pharm.* 401 (2010) 7-15.
- [16] K. Pingali, R. Mendez, D. Lewis, B. Michniak-Kohn, A. Cuitino, F. Muzzio, Evaluation of strain-induced hydrophobicity of pharmaceutical blends and its effect on drug release rate under multiple compression conditions, *Drug Dev. Ind. Pharm.* 37 (2011) 428-435.
- [17] J. Wang, H. Wen, D. Desai, Lubrication in tablet formulations, *Eur. J. Pharm. Biopharm.* 75 (2010) 1-15.
- [18] P. Porion, N. Sommier, A. Faugere, P Evesqu, Dynamics of size segregation and mixing of granular materials in a 3D-blender by NMR imaging investigation, *Powder Technol.* 141 (2004) 55-68.
- [19] N. Sommier, P. Porion, P. Evesque, B. Leclerc, P. Tchoreloff, G. Couarraze, Magnetic resonance imaging investigation of the mixing-segregation process in a pharmaceutical blender, *Int. J. Pharm.* 222 (2001) 243-258.
- [20] A. Twitchell, Mixing, in: M.E. Aulton (Ed.), *Pharmaceutics: The science of dosage form design*, Churchill Livingstone, London, 2002, pp. 181-196.
- [21] M. Cavinato, R. Artoni, M. Bresciani, P. Canu, A.C. Santomosa, Scale-up effects on flow patterns in the high shear mixing of cohesive powders, *Chem. Eng. Sci.* 102 (2013) 1-9.

- [22] H. Nakamura, H. Fujii, S. Watano, Scale-up of high shear mixer-granulator based on discrete element analysis, *Powder Technol.* 236 (2013) 149-156.
- [23] R.L. Carr, Evaluating flow properties of solids, *Chem. Eng.* 72 (1965) 163-168.
- [24] C. C. Sun, D.J.W. Grant, Influence of crystal structure on the tableting properties of sulfamerazine polymorphs, *Pharm. Res.* 18 (2001) 274-280.
- [25] E. Joiris, P. Di Martino, C. Berneron, A.M. Guyot-Hermann, J.C. Guyot, Compression behavior of orthorhombic paracetamol, *Pharm. Res.* 15 (1998) 1122-1130.
- [26] C.K. Tye, C. Sun, G.E. Amidon, Evaluation of the effects of tableting speed on the relationships between compaction pressure, tablet tensile strength, and tablet solid fraction, *J. Pharm. Sci.* 94 (2005) 465-472.
- [27] S.L. Cantor, S.W. Hoag, L.L. Augsburger, Evaluation of the mechanical properties of extrusion-spheronized beads and multiparticulate systems, *Drug Dev. Ind. Pharm.* 35 (2009) 683-693.
- [28] C.E. Ruegger, M. Celik, The effect of compression and decompression speed on the mechanical strength of compacts, *Pharm. Dev. Technol.* 5 (2000) 485-494.
- [29] I.C. Sinka, F. Motazedian, A.C.F. Cocks, K.G. Pitt, The effect of processing parameters on pharmaceutical tablet properties, *Powder Technol.* 189 (2009) 276-284.
- [30] J.T. Fell, J.M. Newton, Determination of Tablet Strength by Diametral-Compression Test, *J. Pharm. Sci.* 59 (1970) 688-691.
- [31] A. Crouter, L. Briens, The effect of moisture on the flowability of pharmaceutical excipients, *AAPS PharmSciTech.* 15 (2014) 65-74.
- [32] C. C. Sun, Mechanism of moisture induced variations in true density and compaction properties of microcrystalline cellulose, *Int. J. Pharm.* 346 (2008) 93-101.
- [33] C. C. Sun, True density of microcrystalline cellulose, *J. Pharm. Sci.* 94 (2005) 2132-2334.

- [34] H. Iijima, K. Takeo, Microcrystalline cellulose: an overview. In: G.O. Phillips, P.A. Williams (Eds.), Handbook of hydrocolloids, Woodhead Publishing Ltd. Cambridge, 2000, pp. 331-346.
- [35] E.C. Abdullah, D. Geldart, The use of bulk density measurements as flowability indicators, Powder Technol. 102 (1999) 151-165.
- [36] F. Podczeczek, Y. Miah, The influence of particle size and shape on the angle of internal friction and the flow factor of unlubricated and lubricated powders, Int. J. Pharm. 144 (1996) 187-194.
- [37] M.V. Velasco, A. Munoz-Ruiz, M.C. Monedero, M.R. Jimenez-Castellanos, Study of flowability of powders. Effect of the addition of lubricants, Drug Dev. Ind. Pharm. 21 (1995) 2385-2391.
- [38] E. Peeters, T. De Beer, C. Vervaet, J.P. Remon, Reduction of tablet weight variability by optimizing paddle speed in the forced feeder of a high-speed rotary tablet press, Drug Dev. Ind. Pharm. (2014) doi: 10.3109/03639045.2014.884121.
- [39] Q. Li, C. Rudolph, B. Weigl, A. Earl, Interparticle van der Waals force in powder flowability and compactibility, Int. J. Pharm. 280 (2004) 77-93.
- [40] X. Xie, V.M. Puri, Uniformity of powder die filling using a feed shoe: a review, Particul. Sci. Technol. 24 (2006) 411-426.
- [41] Y. Yaginuma, Y. Ozeki, M. Kakizawa, S.I. Gomi, Y. Watanabe, Effects of powder flowability on die-fill properties in rotary compression, J. Drug Deliv. Sci. Tec 17 (2007) 205-210.
- [42] R.C. Hwang, E.L. Parrott, Effect of lubricant on wear rate of tablets, Drug Dev. Ind. Pharm. 19 (1993) 1379-1391.
- [43] F. Ebba, P. Piccerelle, P. Prinderre, D. Opota, J. Joachim, Stress relaxation studies of granules as a function of different lubricants, Eur J. Pharm. Biopharm. 52 (2001) 211-220.

- [44] D.E. Wurster, S. Likitlersuang, Y. Chen, The influence of magnesium stearate on the Hiestand tableting indices and other related mechanical properties of maltodextrines, *Pharm. Dev. Technol.* 10 (2005) 461-466.
- [45] B. van Veen, G.K. Bolhuis, Y.S. Xu, K. Zuurman, H.W. Frijlink, Compaction mechanism and tablet strenth of unlubricated and lubricated (silicified) microcrystalline cellulose, *Eur. J. Pharm. Biopharm.* 59 (2005) 133-138.
- [46] S. Patel, A.M. Kaushal, A.K. Bansal, Lubrication potential of magnesium stearate studied on instrumented rotary tablet press, *AAPS PharmSciTech.* 8 (2007) E1-E8.
- [47] J. Kikuta, N. Kitamori, Effect of mixing time on the lubricating properties of magnesium stearate and the final charactersitics of the compressed tablets, *Drug Dev. Ind. Pharm.* 20 (1994) 343-355.
- [48] V.M. Lethola, J.T. Heinamaki, P. Nikupaavo, J.K. Yliruusi, Effect of some excipients and compression pressure on the adhesion of aqueous-based hydroxypropyl methylcellulose film coatings to tablet sufraces, *Drug Dev. Ind. Pharm.* 21 (1995) 1365-1375.
- [49] P.J. Sheskey, R.T. Robb, R.D. Moore, B.M. Boyce, Effect of lubricant level, method of mixing, and duration of mixing on a controlled-release matrix tablet containing hydroxypropyl methylcellulose, *Drug Dev. Ind. Pharm.* 21 (1995) 2151-2165.
- [50] T. Jahn, K.J. Steffens, Press chamber coating as external lubrication for high speed rotary presses: lubricant spray rate optimization, *Drug Dev. Ind. Pharm.* 31 (2005) 951-957.
- [51] M. Otsuka, M. Sato, M. Matsuda, Comparative evaluation of tableting compression behaviors by methods of internal and external lubricant addition: Inhibition of enzymic activity of trypsin reparation by using external lubricant addition during the tableting compression process, *AAPS PharmSci.* 3 (2001) 1-11.
- [52] T. Yamamura, T. Ohta, T. Taira, Y. Ogawa, Y. Sakai, K. Moribe, K. Yamamoto, Effect of automated external lubrication on tablet properties and the stability of eprazinone hydrochloride, *Int. J. Pharm.* 370(2009) 1-7.

4

REDUCTION OF TABLET WEIGHT VARIABILITY BY OPTIMIZING PADDLE SPEED IN THE FORCED FEEDER OF A HIGH-SPEED ROTARY TABLET PRESS

E. Peeters, T. De Beer, C. Vervaet, J.P. Remon, Reduction of tablet weight variability by optimizing paddle speed in the forced feeder of a high-speed rotary tablet press, Drug Development and Industrial Pharmacy, (2014) doi:10.3109/03639045.2014.88412

Abstract

Tableting is a complex process due to the large number of process parameters that can be varied. Knowledge and understanding of the influence of these parameters on the final product quality is of great importance for the industry, allowing economic efficiency and parametric release. The aim of this study was to investigate the influence of paddle speeds and fill depth at different tableting speeds on the weight and weight variability of tablets. Two excipients possessing different flow behavior, microcrystalline cellulose (MCC) and dibasic calcium phosphate dihydrate (DCP), were selected as model powders. Tablets were manufactured via a high speed rotary tablet press using design of experiments (DoE). During each experiment also the volume of powder in the forced feeder was measured. Analysis of the DoE revealed that paddle speeds are of minor importance for tablet weight but significantly affect volume of powder inside the feeder in case of powders with excellent flowability (DCP). The opposite effect of paddle speed was observed for fairly flowing powders (MCC). Tableting speed played a role in weight and weight variability, whereas changing fill depth exclusively influenced tablet weight. The DoE approach allowed predicting the optimum combination of process parameters leading to minimum tablet weight variability. Monte Carlo simulations allowed assessing the probability to exceed the acceptable response limits if factor settings were varied around their optimum. This multi-dimensional combination and interaction of input variables leading to response criteria with acceptable probability reflected the design space.

KEYWORDS: Critical process variables, Design space, Die filling, Direct compression, Flowability, Forced feeder, Process optimization, Tableting.

1. INTRODUCTION

Solid dosage forms, and primarily tablets, are the most widely used systems for oral drug delivery, mainly due to their ease of manufacturing, accurate dosing and high patient compliance [1-5]. Today, tablets still account for more than 80 % of all pharmaceutical preparations [6].

The tableting process on a high speed rotary tableting press can generally be divided into three distinct stages: die filling, compaction and ejection [7-9]. This study focuses on the first stage of the tableting cycle, the die filling, which is a crucial control variable. The amount of powder in the die determines the weight of the tablet, hence the drug content [10]. The reproducibility of the process is also very important, as weight variations contribute to variations in drug content and other critical quality attributes, including tensile strength, porosity and drug release [11, 12].

Accurate die filling is a complicated process comprising different mechanisms, which act simultaneously and contribute to the complexity of this step in the compression cycle [3, 7, 8, 13]. These mechanisms include gravity feed (powder falls into the die), forced feed (rotating wheels in the feeding shoe transfer powder into the die, but induce shear stress in the powder bed), suction fill (at the overfilling station the lower punch is rapidly lowered, creating a partial vacuum which pulls the powder into the die cavity), weight control (after the die is overfilled, the lower punch moves upwards to eject some of the powder), centrifugal forces (caused by the rotational movement of the turret), vibrations of the press and overhead pressure (pressure on the powder in the feeder and die caused by the weight of the powder in the hopper and tubing) [3, 7, 8, 13].

Irrespective of the tooling and the machine settings, powder flow is another important factor influencing the die filling process. The flow behavior of a powder is determined by powder characteristics and operating conditions. Also environmental conditions, the pre-conditioning of the powder and applied loads should be taken into account [1, 3, 8, 11, 13-16].

For a number of researchers the die filling process has also been of particular interest. In early experiments, Ridgway et al. [17] constructed an automatic weight-control device. Their

findings contributed to the development of the closed-loop weight-control systems used in rotary tableting machines today. Wu et al. [18] used transparent stationary dies and moving feeding shoes of simple and complex geometries to study the powder flow of different metallurgical powder components in air and vacuum. His experiments showed that powder characteristics, shoe speed, die geometry and airflow play an important role in the die filling process. Sinka et al. [13] applied the same system in an attempt to characterize the flow behavior of pharmaceutical powders in dies and made similar observations as Wu et al. [18]. Mendez et al. [10] used a fixed feed frame and a moving die disc system to examine the effect of blend composition, shoe properties and die parameters on flow properties, uniformity of die filling and applied shear of pharmaceutical blends. This study showed that the amount of powder entering the dies depended on blend flow properties, the speed of the paddles in the feed frame and die disc speed. Furthermore they concluded that blend properties changed after passing the feeder and the flowability of lubricated blends improved significantly as the feed frame speed was increased. Also research in the field of computer modeling focused on the flow behavior of powder systems in dies [9, 19].

While this former research contributed to the understanding of die filling on high speed rotary presses, the majority of these experiments were conducted on simplified systems. Although attempts were made to simulate a real-life setting, often important parameters were not taken into account or intentionally disregarded. Wu et al. [9], for instance, ignored the effects of airflow, air pressure and cohesive forces in his Discrete Element Method (DEM) simulations, whilst other researchers draw their conclusions about die filling on a high speed rotary tablet press from passive die filling experiments (moving fill shoe and steady die) [13, 18]. Hence no set-up covered the complete range of factors involved in this complex process. Furthermore, the existing conventional techniques for measuring flowability do not directly provide relevant and applicable information for the selection of press parameters during die filling on a rotary tablet press [20]. Therefore, the experiments in this study were performed on an industrial tableting machine whereby all possible mechanisms affecting die filling are involved, without simplifications.

Although a complex process, the die filling process for a given tablet press is mainly controlled by four parameter settings: turret speed (tableting speed), speed of the first paddle wheel (paddle speed 1), speed of the second paddle wheel (paddle speed 2) and fill

depth. The aim of this current research was to investigate the influence of these important control variables on the weight and weight variability of tablets manufactured using an industrial high-speed rotary tablet press. The volume of powder in the feeder was monitored to assess the powder densification in the feeding shoe. Moreover, these results were correlated with specific powder characteristics, utilizing two commonly used powders with different flow behavior: microcrystalline cellulose and dibasic calcium phosphate dehydrate [5, 21-24]. A design of experiments (DoE) was used to study the effect of the four selected process variables at the die filling station of a rotary tablet press.

2. MATERIALS AND METHODS

2.1. Materials

Microcrystalline cellulose (Avicel® PH-102, FMC Biopolymer, Cork, Ireland) and dibasic calcium phosphate dihydrate (Emcompress®, JRS Pharma, Budenheim, Germany) were selected as model powders. A lubricant, sodium stearyl fumarate (Lubrisanaq®, Pharmatrans Sanaq, Basel, Switzerland) was added (0.5 % to microcrystalline cellulose and 1 % to dibasic calcium phosphate dihydrate). These powder mixtures are further referred to as MCC and DCP, respectively.

2.2. Preparation of powder mixtures

Both mixtures (MCC_{start}; DCP_{start}) were prepared by low shear mixing (15 minutes, 25 rotations per minute (rpm)) in a 20 L stainless steel drum with a filling degree of 60 %, using a tumbling mixer (Inversina, Bioengineering, Wald, Switzerland).

Since powder flow is an important factor influencing the die filling process and can be affected by operating conditions and applied loads, it was investigated whether the shear forces in the forced feeder had an influence on the powder properties [16]. To mimic this process, the forced feeder was filled with powder and both paddles were run at maximum (140 rpm) speed for 2 minutes, while the die table was kept stationary (MCC_{shear}; DCP_{shear}). For each powder, the experiments were performed in triplicate.

2.3. Preparation of tablets

Tablets were prepared using a MODULTM P tablet press (GEA Process Engineering - CourtoyTM, Halle, Belgium) equipped with an overfill cam of 16 mm and a feed frame as described in detail in Chapter 2 (2. Powder feeding system) and shown in Figure 4.1. As the die table (turret) rotates, powder is fed from the forced feeder into the dies at the overfilling station. After weight adjustment at the filling station, the punches (n=10, Ø 12 mm, concave radius 24 mm) pass through the pre- and main compression station and the ejection cam mechanism.

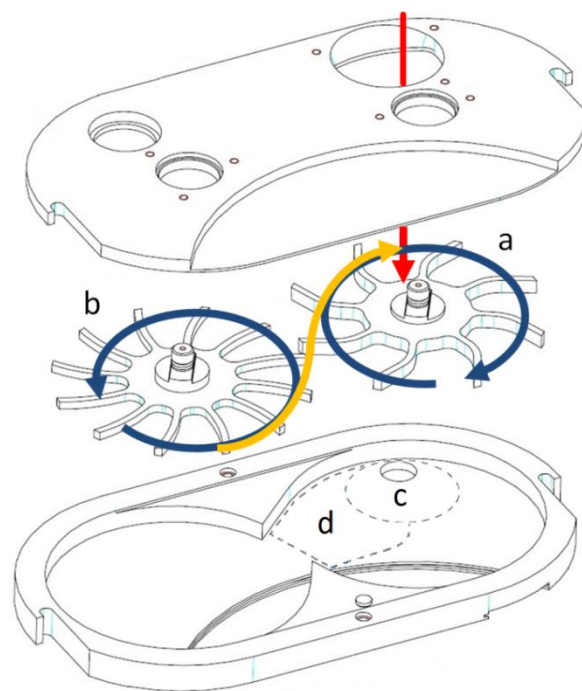


Figure 4.1: Schematic overview of the feed frame with two paddles: (a) feeding paddle; (b) metering paddle; (c) infeed; (d) recirculation area of the feeding paddle. Arrows depict schematically the movement of the powder through the feed frame. (Courtesy of GEA, CourtoyTM)

In order to avoid confounding factors, each experiment was run on an empty and cleaned tablet press. The machine was filled (MCC_{start} ; DCP_{start}) and run for 1 minute. Then tablets were sampled during 30 seconds. Room temperature (21 ± 2 °C) and relative humidity (RH) (30 ± 2 %) were controlled.

2.4. Powder characterization

2.4.1. Particle size analysis

Particle size analysis was done by sieve analysis, using a sieve shaker (Retsch VE 1000, Haan, Germany). 100 g of powder mixture was placed on the upper sieve of the installed set (50, 90, 125, 180, 250, 300, 500 and 710 μm) and shaken at an amplitude of 2 mm for 5 minutes. The amount of powder retained on each sieve was determined. All batches were measured in triplicate.

2.4.2. Density

The density of the powders was measured using a helium pycnometer (Accupyc 1330 pycnometer, Micrometrics Instruments, Norcross Georgia, USA). Each sample was measured in triplicate, with ten purges and ten runs per measurement. Prior to the measurements, the apparatus was calibrated. All tests were performed at 22 ± 2 °C.

2.4.3. Flow properties

In the flow-through-an-orifice method, the time required for the powder (an amount equivalent to 150 ml) to flow through a stainless steel funnel with a 10 mm orifice was measured using a powder flow tester (Pharma Test PTG-S2, Hainburg, Germany). Each sample was measured in triplicate. The results were expressed as the amount of powder (in g) per second that flowed through the orifice.

The bulk and tapped density of the powder mixture (25 g and 60 g for MCC and DCP, respectively) was determined in a 100 ml graduated cylinder, mounted on a tapping machine (J. Engelsmann, Ludwigshafen am Rhein, Germany). The initial volume (V_0) as well as the volume after 1250 taps (V_{1250}) was recorded. Each sample was measured in triplicate. Bulk and tapped densities were calculated as the amount of powder (g)/ V_0 and the amount of powder (g)/ V_{1250} , respectively. These values were used to calculate the compressibility index (CI) (%) (Equation (4.1)):

$$CI = \left(\frac{\rho_{1250} - \rho_0}{\rho_{1250}} \right) \times 100 \quad (4.1)$$

2.5. Tablet evaluation

Immediately after production of the tablets, the tablet weight ($n=50$) was determined. The variation coefficient (VC) (%) as an indication of weight variability was calculated.

2.6. Volume of powder in the feeder

After each experiment, the powder remaining in the hopper and tubing above the feed shoe was removed. The powder left in the forced feeder was collected and poured into a 1000 ml graduated cylinder to determine the bulk volume.

2.7. Design of Experiments

A D-optimal design with 26 experiments, including 3 repeated center points, was used to study the influence of four process variables (factors) - fill depth (mm), tableting speed (tablets per minute (tpm)), paddle speed 1 (rpm) and paddle speed 2 (rpm) - on the responses weight (mg), weight variability (%) and volume of powder in the forced feeder (ml). Table 4.1 shows the experimental space within which the selected DoE parameters were varied. The factor ranges were selected based on preliminary experiments and by taking into account the operational ranges of the tablet press.

Table 4.1: Overview of the upper and lower levels of the process variables.

Process variable	Lower level	Upper level
Fill depth (mm)	8	12
Tableting speed (tpm)	250	1000
Paddle speed 1 (rpm)	20	140
Paddle speed 2 (rpm)	20	140

As the feeding wheel delivers the powder to the dies and the metering wheel recuperates the powder at the filling station, it is important that the rotation speed of the feeding wheel is lower than the speed of the metering wheel to avoid overfilling and compaction in the forced feeder. Hence, a constraint was introduced in the design: paddle speed 1 must be lower than or equal to paddle speed 2. Due to this constraint, the experimental space became irregular and a D-optimal design was selected [25]. An overview of the DoE is given in Table 4.2.

Table 4.2: Overview of the performed experimental design. Values of the responses depict the mean for weight (n=50) and VC for weight variability (n=50). n=1 for volume of powder in the feeder.

Run	Factors				Responses					
	Fill depth (mm)	Tableting speed (tpm)	Paddle speed 1 (rpm)	Paddle speed 2 (rpm)	Weight (mg)		Weight variability (%)		Volume of powder in the feeder (ml)	
					MCC	DCP	MCC	DCP	MCC	DCP
1	8	250	140	140	428.1	981.9	0.63	0.58	570	495
2	12	250	140	140	613.0	1436.4	0.35	0.40	550	545
3	8	250	20	60	367.1	977.5	0.80	0.51	500	430
4	12	250	20	100	528.7	1408.0	1.12	0.27	410	335
5	12	250	20	140	517.6	1401.4	1.35	0.34	330	325
6	12	250	60	60	551.0	1430.0	0.47	0.37	522	505
7	10	625	60	100	442.6	1173.8	1.29	0.46	445	410
8	10	625	80	140	442.5	1182.3	1.35	0.52	430	390
9	9.33	250	20	140	412.6	1131.4	1.02	0.5	350	325
10	12	1000	140	140	502.9	1339.4	1.79	1.07	430	465
11	10	625	60	100	435.1	1194.3	1.45	0.45	430	410
12	8	1000	100	140	354.0	907.6	1.47	1.71	420	415
13	10	625	60	100	432.8	1193.9	1.44	0.56	435	415
14	10	625	20	80	432.2	1184.7	1.06	0.47	385	350
15	8	500	20	20	376.0	978.4	0.32	0.36	460	485
16	9.33	1000	140	140	418.4	1046.1	1.65	1.49	460	460
17	12	1000	20	140	458.4	1224.8	1.60	1.18	265	255
18	8	250	60	140	380.0	985.0	0.90	0.62	415	415
19	12	1000	20	20	470.5	1309.1	1.93	1.55	420	420
20	8	250	100	100	405.6	985.2	0.67	0.40	540	510
21	8	1000	20	140	335.0	889.6	1.58	1.28	300	275
22	8	1000	20	20	367.0	911.0	2.06	1.74	480	490
23	10.66	250	20	20	480.7	1280.1	0.45	0.39	525	490
24	8	750	140	140	389.0	951.5	1.31	0.80	540	510
25	8	1000	60	60	353.4	906.6	2.17	1.55	500	490
26	8	500	20	140	352.3	963.4	0.84	0.67	540	310

The results of the DoE experiments were analyzed using the MODDE 9.1 software (Umetrics, Umeå, Sweden). After evaluating the effects, DoE models were calculated for each response herewith deleting the non-significant coefficients. Furthermore, after defining the desired responses (weight 450 mg and 1000 mg for MCC and DCP respectively; weight variability lower than 1.5 % as acceptable limit; volume of powder in the feeder not exceeding the maximal volume of the feeder to avoid packing) (Table 4.3), the optimum combination of factors yielding tablets with these desired responses was determined from the DoE models. Subsequently the probability to exceed the acceptable response limits was assessed via Monte Carlo simulations by varying the factor settings around these determined optima.

Table 4.3: Overview of the optimal responses and their limits.

Response		Lower limit	Optimal response	Upper limit
Weight (mg)	MCC	441	450	459
	DCP	980	1000	1020
Weight variability (%)		N/A	N/A	1.5
Volume of powder in the feeder (ml)		N/A	N/A	500

3. RESULTS AND DISCUSSION

3.1. Evaluation of the powder characteristics

For DCP, no difference in powder properties could be observed between the starting material (DCP_{start}) and the powder subjected to shear (DCP_{shear}), as summarized in Table 4.4. The particle size (distribution) of MCC on the other hand, was clearly affected by the applied shear, with significantly smaller particles being formed due to shearing forces. This effect can be explained by the structure of MCC particles, which are a mixture of primary particles and agglomerates of needle-like micro crystals [5, 6, 24, 26]. The agglomerates are broken down by the shear inside the forced feeder, resulting in a higher amount of primary particles. Nevertheless, the flow properties were not significantly affected by this change in particle size distribution. Consequently, the flow of the starting material (MCC_{start} ; DCP_{start}) and the powders subjected to shear (MCC_{shear} ; DCP_{shear}) could be considered equal.

MCC and DCP could be distinguished on the basis of their flow properties, as shown in Table 4.4. The values of flowability show that the DCP powder flows almost seven times faster through an orifice than MCC. Likewise, based on the CI values, the MCC mixture was identified as a fairly flowing powder, while the DCP mixture had excellent flow properties (Carr) [27].

Table 4.4: Flow properties, true density and particle size distribution of the powders. Values depict the mean \pm stdev (n=3).

	MCC		DCP	
	Start	Shear	Start	Shear
Flowability (g/s)	2.17 \pm 0.06	2.44 \pm 0.13	14.64 \pm 0.33	14.72 \pm 0.14
Bulk density (g/cm ³)	0.34 \pm 0.00	0.35 \pm 0.00	0.97 \pm 0.00	0.94 \pm 0.01
Tapped density (g/cm ³)	0.41 \pm 0.00	0.41 \pm 0.00	1.04 \pm 0.00	1.04 \pm 0.01
Compressibility index (CI) (%)	18.09 \pm 0.31	15.35 \pm 0.59	7.41 \pm 0.56	8.92 \pm 1.13
True density (g/cm ³)	1.55 \pm 0.00	1.55 \pm 0.00	2.31 \pm 0.00	2.31 \pm 0.00
Particle size distribution				
d10 (μ m)	106.6 \pm 1.4	29.2 \pm 0.8	103.1 \pm 1.5	102.8 \pm 0.9
d50 (μ m)	167.2 \pm 1.1	109.5 \pm 0.5	160.2 \pm 0.2	160.6 \pm 0.7
d90 (μ m)	240.8 \pm 1.5	212.8 \pm 1.8	257.9 \pm 1.1	258.5 \pm 1.3

Start: properties of the starting material; Shear: properties of the material subjected to shear forces by filling the forced feeder with powder and running both paddles for 2 minutes at maximum speed (140 rpm).

3.2. Experimental design analysis

3.2.1. Weight

In order to analyze the influence of the critical parameters on the tablet weight an effect plot (Figure 4.2) for this response was constructed. An effect plot displays the change in the response when a factor varies from its low level to its high level, with all other factors kept constant at their average [25]. As expected, for both powders a higher fill depth significantly (confidence interval does not include zero) increased the tablet weight, as the volume of the die increased. Obviously the absolute increase of tablet weight is higher for DCP compared to MCC tablets (430 mg versus 145 mg), owing to its higher density. However, as the increase in percentage of tablet weight at higher fill depth is 43.0 and 32.2 % for DCP and MCC mixtures, respectively, this difference in weight is not only caused by the true density

of both powders. A better packing of DCP particles in comparison to MCC particles also contributed to the weight gain at higher filling depth. This observation can be linked to the low CI of DCP (Table 4.4) which indicates that the powder consolidation upon tapping is limited as the unsettled particles are already quite tightly packed and interparticular voids are small (i.e. high bulk density).

A negative effect was observed for the tableting speed. An increase of this parameter from the lowest (250 tpm) to the highest (1000 tpm) value significantly decreased the tablet weight. At higher tableting speeds, the die is exposed to the powder bed for a shorter period of time, allowing a shorter filling time. These results were also obtained by other researchers [10, 20]. Although the absolute reduction in tablet weight is larger for DCP (90 mg versus 60 mg), the reduction in terms of percentage for the MCC powder was slightly larger (13.3 % versus 9 %), due to the better flowability of the DCP mixture (i.e. faster die filling), which was also observed by Mendez et al. [10]. Another contributing factor can be the higher centrifugal forces generated at higher tableting speed. As the powder bed in the die is freely exposed at the surface of the turret after the filling station (the upper punch seals the die opening only at the (pre-) compression station), powder can be ejected from the die during this short exposure.

For the MCC mixture, paddle speed 1 had a significant positive effect on the tablet weight, in contrast to the DCP mixture where the effect of paddle speed 1 is insignificant. This is related to the flowability of both powders. Paddle 1 assists the powder into the dies, while paddle 2 removes the excess of material at the filling station. Due to the good flowability of the DCP mixture, paddle 1 did not affect the flow of this powder into the die opening. In contrast, varying the paddle speed 1 changed the die filling of MCC, indicating that this powder is more subjected to force feeding than gravity feeding, mainly because of its poor flowability. The interaction effect between the tableting speed and paddle speed 1, as depicted in Figure 4.3, supported this theory. At a high tableting speed, an increase in paddle speed 1 only resulted in a minor increase in tablet weight, whereas at low tableting speeds the effect of paddle speed 1 was significant. Due to the poor flowability of MCC, the highest impact of force feeding is observed at low tableting speeds. At high speeds, the turret moves too fast, and even a high paddle speed 1 is unable to force as much powder into the die as at low tableting speeds. These results suggest that the flowability of powders is the rate

limiting step in die filling [10]. From this it could be expected that, besides paddle speed, also paddle design (e.g. shape and amount of fingers) can play a major role in the flow behavior of powders in the feed shoe.

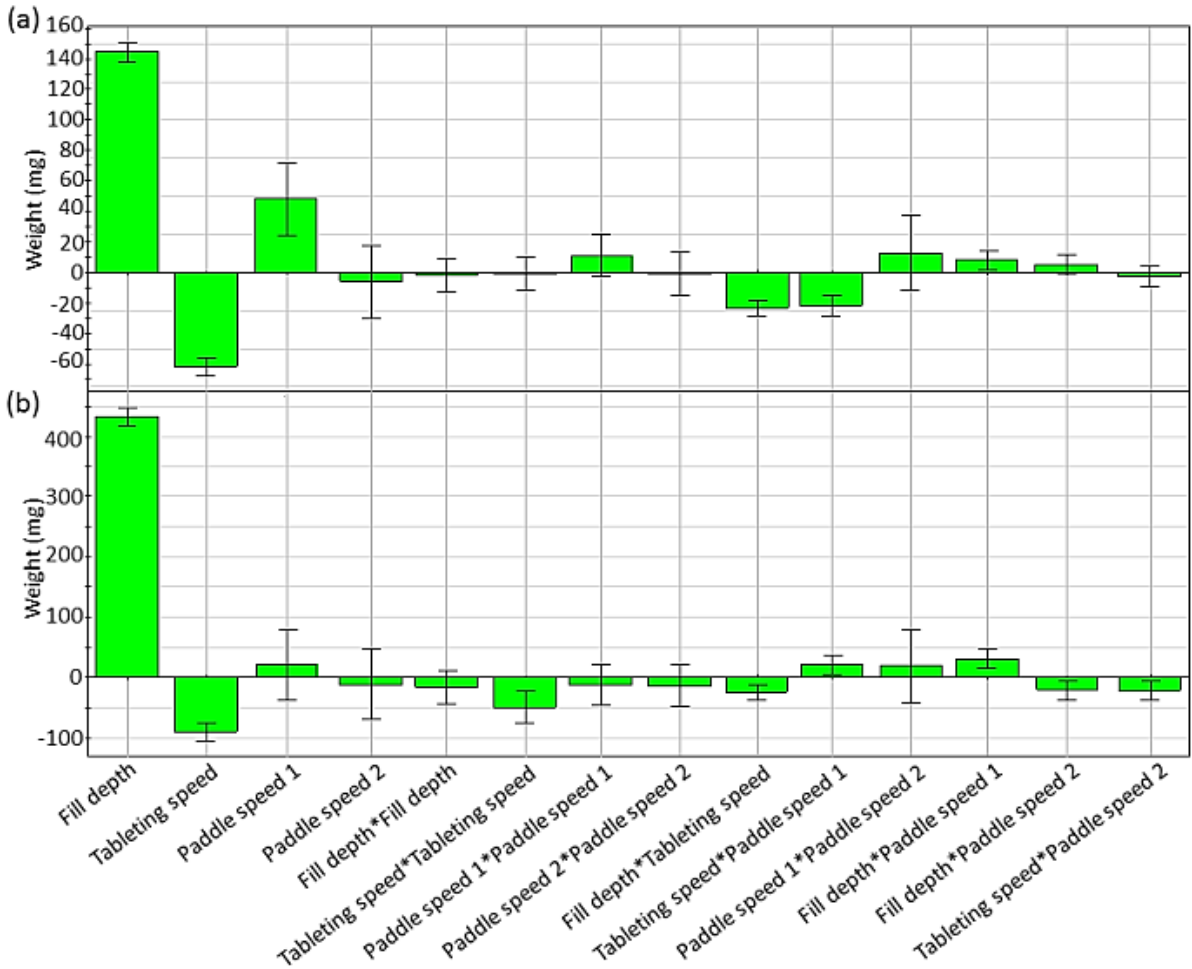


Figure 4.2: Effect plot of tablet weight. (a) MCC, (b) DCP.

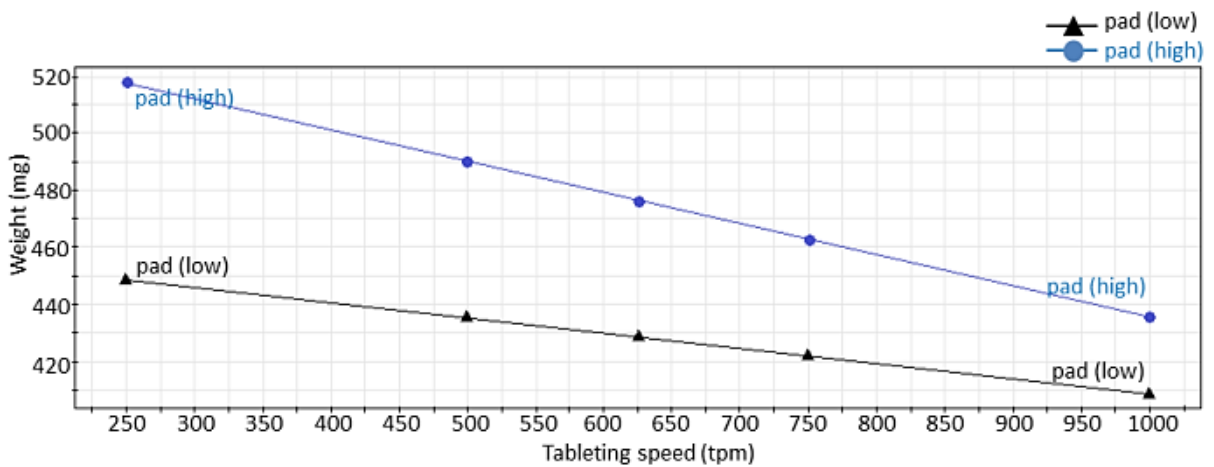


Figure 4.3: Interaction plot of tableting speed and paddle speed 1 for the weight of MCC tablets. Pad (high): paddle speed 1 = 140 rpm; Pad (low): paddle speed 1 = 20 rpm.

3.2.2. Weight variability

The influence of the critical parameters on the tablet weight variability is graphically presented in Figure 4.4. As also observed by Mehrotra et al. [19] and Yaginuma et al. [20], a higher tableting speed caused a significant increase in tablet weight variability for both powder mixtures. This result could be linked with the lower tablet weight at higher tableting speeds. A decrease in the weight suggests a lower fill density of the powders or an incomplete filling of the dies at higher tableting speed, an observation already reported in literature [10, 20]. This effect combined with more material loss after filling due to higher centrifugal forces increased weight variability. Although no significant difference was observed between the absolute increase in weight variability, it should be mentioned that the overall weight variability for MCC tablets is higher than for DCP tablets (Table 4.2), which is linked to their powder flow properties.

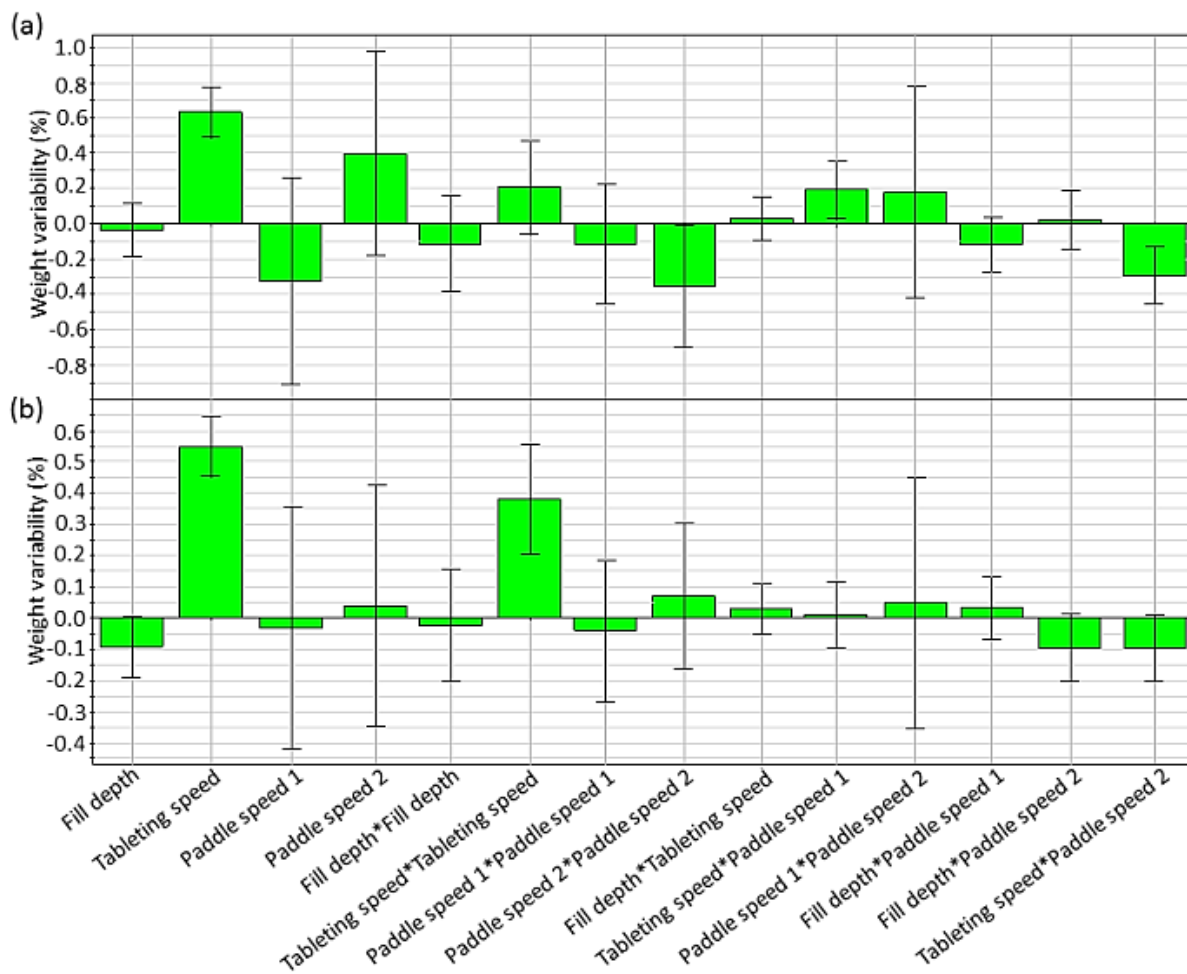


Figure 4.4: Effect plot of tablet weight variability. (a) MCC, (b) DCP.

3.2.3. Volume of powder in the feeder

For the DCP mixture, as shown in Figure 4.5, paddle 1 and paddle 2 had a significant positive and negative effect, respectively, on the volume of powder in the forced feeder. A higher paddle speed 1 increased the transfer rate of powder towards the dies. However, as the production rate remained constant and the speed of paddle 1 had no influence on tablet weight (Figure 4.2), the consumption rate of the powder is not affected. As a result more powder must be recirculated back to the powder infeed (Figure 4.1c), and the powder volume in the recirculation area (Figure 4.1d) of paddle wheel 1 will increase, hence the total volume of powder in the feeder. An increase in the speed of paddle wheel 2 on the other hand resulted in a higher rate at which expelled powder at the dosing station is removed. However, since the production speed remains constant, the rate at which powder is expelled from the dies during dosing does not change. This resulted in more powder transferred towards paddle wheel 1 where the powder is reused to fill the passing dies and consequently in a reduced volume of powder in the feeder.

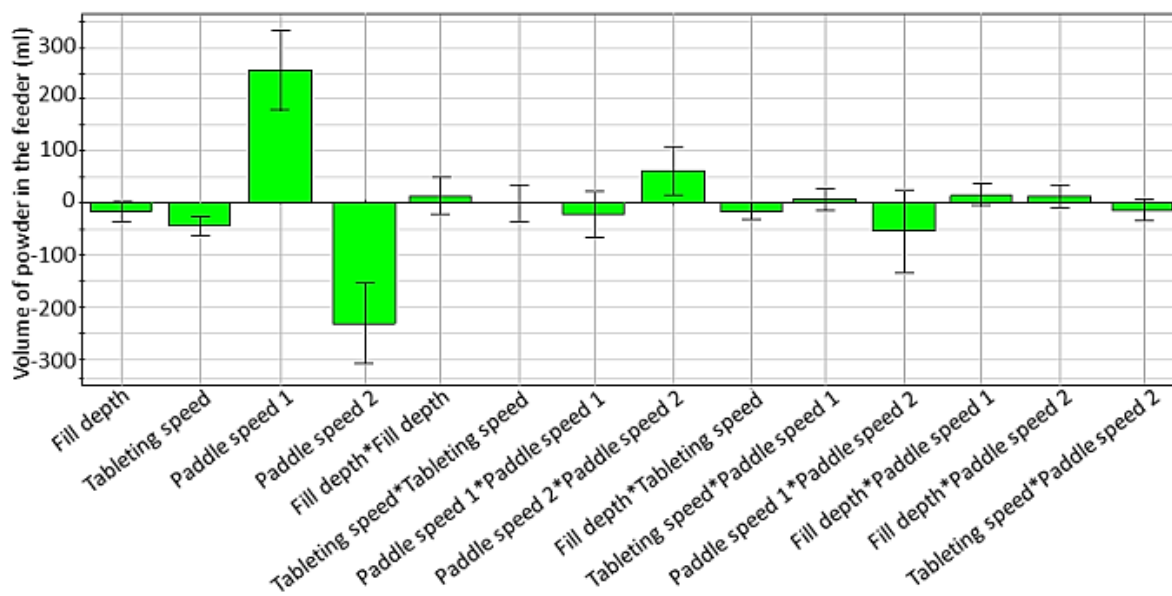


Figure 4.5: Effect plot of volume of powder in the feeder for the DCP powder.

Also the tableting speed has a small negative effect on the volume of DCP powder inside the forced feeder. At higher tableting speed more dies pass the filling station, and - although the tablet weight is lower at these settings in comparison to lower tableting speeds - the overall

material clearing from the feeder per unit of time is higher, resulting in less powder left in the feeder. This hypothesis can be supported mathematically by Equation (4.2):

$$x = \frac{(W \times 1000 \times v_t)}{60} \quad (4.2)$$

where x is the net material clearing from the feeder (g/s), W the mean tablet weight (mg) and v_t the tableting speed (tpm). With the Modde software it could be determined that, keeping all other parameters constant at their mean value, the weight for the DCP tablets is 1207 and 1116 mg at 250 and 1000 tpm respectively, which is in agreement with the results shown in Figure 4.2 where a weight decrease of about 90 mg was observed if the tableting speed increases from 250 to 1000 tpm. Applying Equation (4.2), the net material clearing from the feeder is 5.03 g/s at 250 tpm and 18.61 g/s at 1000 tpm.

For the MCC mixture, none of the factors had a significant effect (data not shown) on the volume of powder present in the feeder. Although differences in the absolute values can be observed (Table 4.2), these could not be linked to changes in factor settings, hence it was not possible to model this effect. This observation might be explained by the high CI of MCC. Powder is not only set into motion by the movement of the paddles, but also densified. For specific runs, mainly at high paddle speeds, some packing of powder in the feed shoe could be observed.

3.3. Process optimization

Using the Modde optimizer, it was possible to calculate the combination of factors (fill depth, tableting speed, paddle speed 1 and paddle speed 2) yielding tablets which meet all the specifications (weight, weight variability and volume of powder in the feeder) as defined in Table 4.3. The sweet spot plots (Figure 4.6) show the regions for all combinations of examined variables where these targets are reached. Due to the lower flowability of the MCC mixture and the different effects of process variables, the sweet spot area is smaller for the MCC formulation compared to the DCP mixture.

The optimal response criteria (Table 4.3) can be met when several combinations of fill depth, tableting speed and paddle speeds are applied. Since the risk of not meeting the target specifications is higher when a combination of variables close to the border of the sweet

spot is selected, one is advised to work at the center of the sweet spot. However, since the highest possible tableting speed is preferred from a production point of view, the following optimum combination of factors were selected by the Modde optimizer: (i) for MCC: fill depth = 10.36 mm; tableting speed = 900 tpm; paddle speed 1 = 114 rpm and paddle speed 2 = 140 rpm; and (ii) for DCP: fill depth = 9.35 mm; tableting speed = 1000 tpm; paddle speed 1 = 20 rpm and paddle speed 2 = 140 rpm.

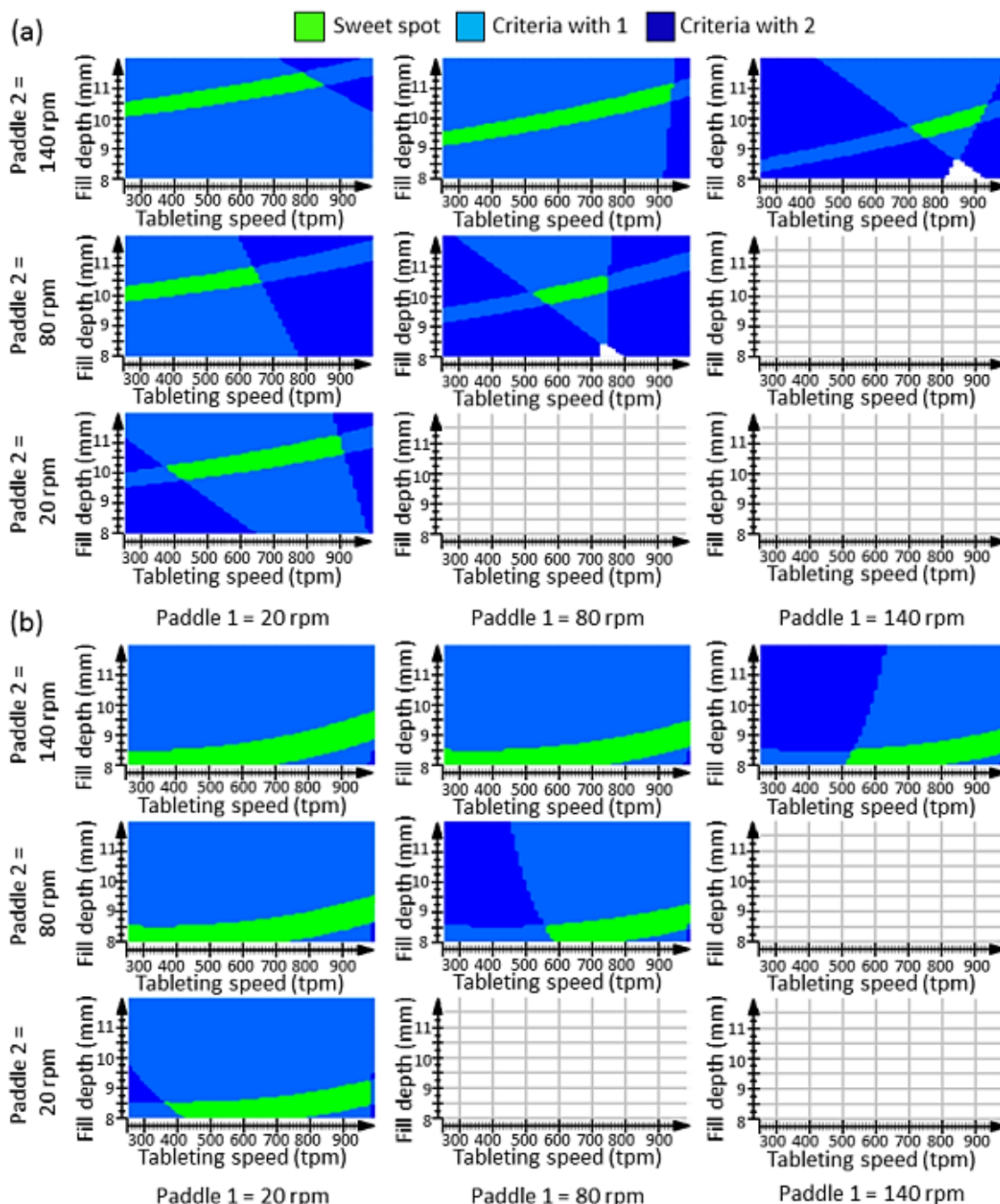


Figure 4.6: Sweet spot plots for (a) MCC and (b) DCP, showing the combination of process parameters which yield tablets with the required responses.

Limitations with a sweet spot plot presentation are the number of dimensions and the lack of probability estimate in the predicted surface [25]. Performing Monte Carlo simulations on the established optimum factor settings for the MCC formulation showed there is a probability of 0.009 % for tablet weight, 33.14 % for weight variability and 0.043 % for volume of powder in the feeder to exceed the specification limit values when the optimum process settings are used (Figure 4.7a). Performing Monte Carlo simulations for the DCP formulation showed there is a probability of 1.43 % for the tablet weight, 18.73 % for the weight variability and 0.001 % for the volume of powder in the feeder to exceed the specification limit values when the optimum process settings for this powder are used (Figure 4.7b). Although the probability for exceeding the weight variability specification limit seems rather large (33.14 % and 18.73 % for MCC and DCP respectively), it should be mentioned that the chosen limit of weight variability is quite narrow (1.5 %). If a variation coefficient of 2 % is selected, the probability of exceeding this specification limit is close to zero.

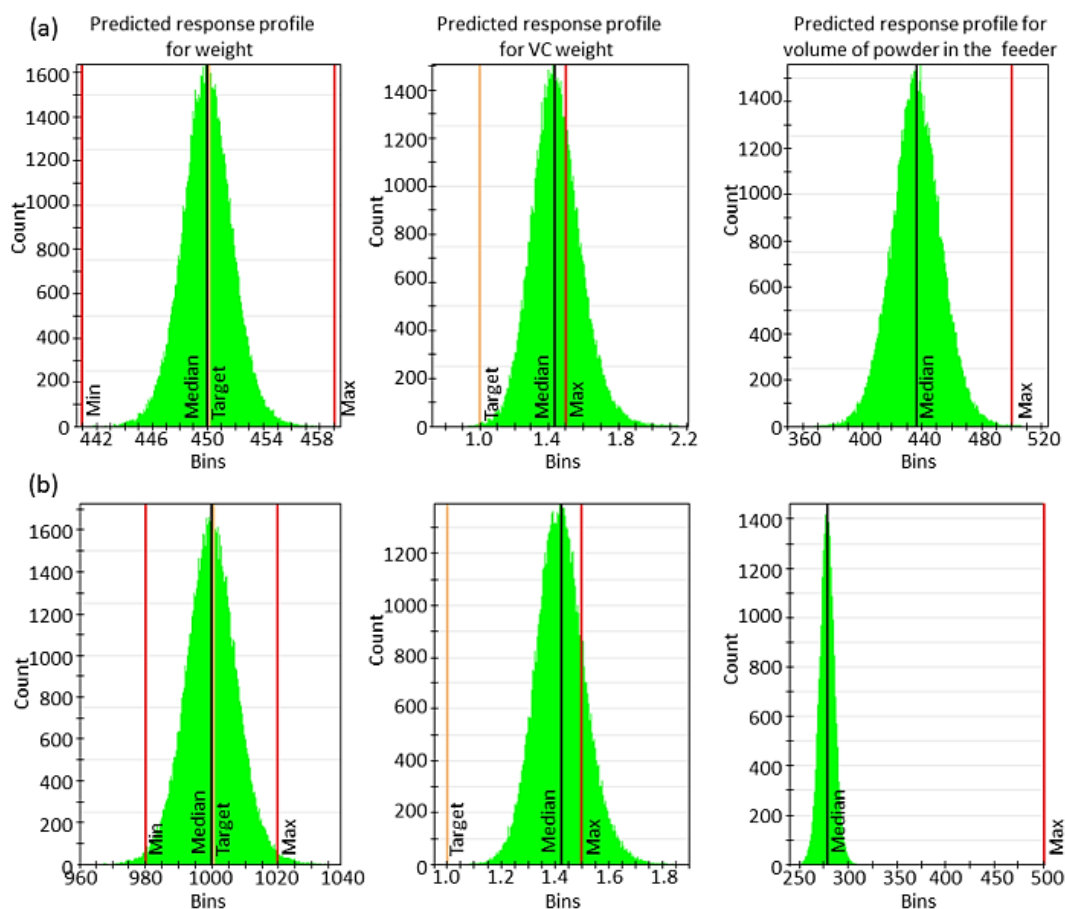


Figure 4.7: Monte Carlo simulations for (a) MCC and (b) DCP.

Due to the different mechanisms that influence the die filling on a rotary tablet press and their relation to each other, it is difficult to study the contribution of all these factors separately. Even compaction simulators cannot cover all events influencing this process (e.g. centrifugal forces). As shown in this research, the best practical approach is to conduct a series of experiments in an ordered way on an industrial tablet press, whereby all possible mechanisms involved are covered, without simplifications. Even if the contribution of a certain effect cannot be completely distinguished (e.g. effect of tableting speed due to inadequate filling or centrifugal forces), it can be accounted for. DoE is a powerful tool to identify in a quick and simple way the critical process parameters in a die filling process. It is also an essential instrument to set up a prediction model which includes powder characteristics and process parameters. Although these experiments can be repeated easily and fast, it should be mentioned that the obtained results cannot be extrapolated to other machines nor to the same machine with other tooling or another formulation.

4. CONCLUSIONS

Using DoE, this study indicated that the paddle speeds in the forced feeder are of minor importance for tablet weight (variability) in case of powders with excellent flowability (DCP), whereas the paddle speeds affected tablet weight of fairly flowing powders (MCC). The opposite phenomenon could be seen on the volume of powder in the feeder. Tableting speed played a role in the tablet weight and weight variability, whereas changing fill depth exclusively influenced the tablet weight for both powders. The DoE approach also allowed predicting the optimum combination of studied process parameters yielding the lowest tablet weight variability. Using Monte Carlo simulations the robustness of the process was assessed. This multi-dimensional combination and interaction of input variables (factor ranges) reflected the design space which results in acceptable response criteria with a reasonable probability.

REFERENCES

- [1] M.C. Gohel, P.D. Jogani, A review of co-processed directly compressible excipients, *J. Pharm. Pharm. Sci.* 8 (2005) 76-93.
- [2] C.Y. Wu, O.M. Ruddy, A.C. Bentham, B.C. Hancock, S.M. Best, J.A. Elliott, Modelling the mechanical behaviour of pharmaceutical powders during compaction, *Powder Technol.* 152 (2005) 107-117.
- [3] I.C. Sinka, F. Motazedian, A.C.F. Cocks, K.G. Pitt, The effect of processing parameters on pharmaceutical tablet properties, *Powder Technol.* 189 (2009) 276-284.
- [4] N.A. Armstrong, Tablet manufacture, in: J. Swarbrick (Ed.), *Encyclopedia of pharmaceutical technology*, Informa Healthcare USA Inc., New York, 2007, pp. 3653-3672.
- [5] D.J. Mastropietro, H. Omidian, Prevalence and trends of cellulose in pharmaceutical dosage forms, *Drug Dev. Ind. Pharm.* 39 (2013) 382-392.
- [6] M. Jivraj, L.G. Martini, C.M. Thomson, An overview of the different excipients useful for the direct compression of tablets, *Pharm. Sci. Technol. To.* 3 (2000) 58-63.
- [7] S. Jackson, I.C. Sinka, A.C.F. Cocks, The effect of suction during die fill on a rotary tablet press, *Eur. J. Pharm. Biopharm.* 65 (2007) 253-256.
- [8] L.C.R. Schneider, I.C. Sinka, A.C.F. Cocks, Characterisation of the flow behaviour of pharmaceutical powders using a model die-shoe filling system, *Powder Technol.* 173 (2007) 59-71.
- [9] C.Y. Wu, DEM simulations of die filling during pharmaceutical tableting, *Particuology* 6 (2008) 412-418.
- [10] R. Mendez, F. Muzzio, C. Velazquez, Study of the effects of feed frames on powder blend properties during the filling of tablet press dies, *Powder Technol.* 200 (2010) 105-116.
- [11] X. Xie, V.M. Puri, Uniformity of powder die filling using a feed shoe: a review, *Particul. Sci. Technol.* 24 (2006) 411-426.

- [12] N.A. Armstrong, Tablet manufacture by direct compression, in: J. Swarbrick (Ed.), Encyclopedia of pharmaceutical technology Informa Healthcare USA Inc., New York, 2007, pp. 3673-3683.
- [13] I.C. Sinka, L.C.R. Schneider, A.C.F. Cocks, Measurement of the flow properties of powders with special reference to die fill, *Int. J. Pharm.* 280 (2004) 27-38.
- [14] S.F. Burch, A.C.F. Cocks, J.M. Prado, J.H. Tweed, Die fill and powder transfer, in: P.R. Brewin, O. Coube, P. Doremus, J.H. Tweed (Eds.), Modelling of powder die compaction, Springer-Verlag London Limited, London, 2008, pp. 131-150.
- [15] R. Kapil, D.N. Kapoor, S. Dhawan, Flow, compressive, and bioadhesive properties of various blends of poly(ethylene oxide), *Drug Dev. Ind. Pharm.* 36 (2010) 45-55.
- [16] K. Pingali, R. Mendez, D. Lewis, B. Michniak-Kohn, A. Cuitino, F. Muzzio, Evaluation of strain-induced hydrophobicity of pharmaceutical blends and its effect on drug release rate under multiple compression conditions, *Drug Dev. Ind. Pharm.* 37 (2011) 428-435.
- [17] K. Ridgway, J.J. Deer, P.L. Finlay, C. Lazarou, Automatic weight-control in a rotary tableting machine, *J. of Pharm. Pharmacol.* 24 (1972) 203-210.
- [18] C.Y. Wu, L. Dihoru, A.C.F. Cocks, The flow of powder into simple and stepped dies, *Powder Technol.* 134 (2003) 24-39.
- [19] A. Mehrotra, B. Chaudhuri, A. Faqih, M.S. Tomassone, F.J. Muzzio, A modeling approach for understanding effects of powder flow properties on tablet weight variability, *Powder Technol.* 188 (2009) 295-300.
- [20] Y. Yaginuma, Y. Ozeki, M. Kakizawa, S.I. Gomi, Y. Watanabe, Effects of powder flowability on die-fill properties in rotary compression, *J. Drug Deliv. Sci. Tec.* 17 (2007) 205-210.
- [21] J.T. Carstensen, C. Ertell, Physical and chemical properties of calcium phosphates for solid-state pharmaceutical formulations, *Drug Dev. Ind. Pharm.* 16 (1990) 1121-1133.

- [22] S. Edge, D.F. Steele, A.S. Chen, M.J. Tobyn, J.N. Staniforth, The mechanical properties of compacts of microcrystalline cellulose and silicified microcrystalline cellulose, *Int. J. Pharm.* 200 (2000) 67-72.
- [23] E. Fischer, Calcium-phosphate as a pharmaceutical excipient, *Manuf. Chemist* 63 (1992) 25-27.
- [24] C.C. Diaz-Ramirez, L. Villafuerte-Robles, Surrogate functionality of celluloses as tablet excipients, *Drug Dev. Ind. Pharm.* 36 (2010) 1422-1435.
- [25] L. Eriksson, E. Johansson, N. Kettaneh-Wold, C. Wikström, S. Wold, *Design of Experiments - Principles and Applications*, third ed., MKS Umetrics AB, Umea, 2008.
- [26] G.K. Bolhuis, Z.T. Chowhan, Materials for direct compaction, in: G. Alderborn, C. Nyström (Eds.), *Pharmaceutical Powder Compaction Technology*, Marcel Dekker Inc., New York, 1996, pp. 419-500.
- [27] R.L. Carr, Evaluating flow properties of solids, *Chem. Eng.* 72 (1965) 163-168.

5

**INFLUENCE OF EXTENDED DWELL TIME
DURING PRE- AND MAIN COMPRESSION
ON THE PROPERTIES OF
IBUPROFEN TABLETS**

Abstract

The low melting point, poor flow, physico-mechanical properties (particle size distribution, shape, particle surface roughness) and deformation mechanism of ibuprofen in combination with its high dose in tablets all contribute to the problems observed during the compaction of ibuprofen-based formulations. Since ibuprofen is plastically and elastically deforming, the rate of compaction plays an important role in both the final tablet properties and the risk of capping, laminating and sticking to the punches. While the compaction rate in most tableting machines is only determined by the tableting speed, the high speed rotary tableting machine used in this research project (MODUL™ P, GEA Process Engineering - Courtoy™, Halle, Belgium) can adjust and control the dwell time independently from the tableting speed, using an air compensator which allows displacement of the upper (pre-) compression roller. The effect of this machine design on process parameters and tablet properties was investigated. Granules containing 80 % ibuprofen were compressed into tablets at 250, 500 and 1000 tablets per minute via double compression (pre- and main compression) with or without extended dwell time. Prior to tableting, granule properties were determined. Process parameters and tablet properties were analyzed using Multivariate Data Analysis. Principal Component Analysis provided an overview of the main phenomena determining the tableting process and Partial Least Squares Analysis unveiled the main variables contributing to the observed differences in the tablet properties.

KEYWORDS: Tableting, Rotary tablet press, Displacement, Force-Time profile, Extended dwell time, Multivariate data analysis.

1. INTRODUCTION

Ibuprofen is widely used for the treatment of rheumatoid arthritis, osteoarthritis and mild and moderate pain, in daily doses ranging from 0.2 to 2.4 g [1]. For high-dosed tablets, the physico-mechanical properties of the pure component play a major role in the tableting process [2, 3]. As a result, the processing of ibuprofen into tablets still encounters problems due to its low melting point, poor flow and deformation mechanism [3-5]. Various attempts were made to improve the tableting behavior of ibuprofen formulations (flowability, tabletability, compactibility) by recrystallization, dry granulation (roller compaction, pressure swing granulation) or dry coating [3-11]. Although these methods contribute to the understanding of the tableting behavior of ibuprofen, the applicability in production settings is limited, due to the rather moderate improvements and long processing times of some methods.

Since the common crystal form (needle-like shape) of ibuprofen undergoes plastic and elastic deformation, the rate of compaction plays an important role in both the final tablet properties and the risk of capping, laminating and sticking to the punches [2, 12, 13]. Besides the compaction rate, also the punch tip geometry, roughness and embossment, as well as the composition of the punch tip coating (i.e. boron-alloy, chrome,...) have an influence on the sticking tendency [14, 15]. Consequently, in industrial manufacturing the production process is optimized either by optimizing the tooling, or reducing the rate of compaction, or both [2, 12-15].

In most tableting machines, the compaction rate (i.e. consolidation phase, dwell time, decompression phase) can only be adjusted by changing the tableting speed [16]. However, using the MODULTM P high-speed rotary tablet press (GEA Process Engineering - CourtoyTM, Halle, Belgium) the dwell time can be adjusted and controlled independently of the tableting speed, due to an air compensator which allows displacement of the upper (pre-) compression roll. This design, which has not yet been thoroughly studied in literature, could affect the processability of materials exhibiting a rate-dependent compression behavior, like ibuprofen [2, 12, 13, 17, 18].

The aim of this study was to get a thorough understanding of this compression method (i.e. speed-independent extended dwell time). Using a commercial ibuprofen formulation the

influence of extended dwell time independent of compression speed on the dependent machine parameters and on the tablet properties was examined. Due to the large amount of data obtained (process parameters and tablet characteristics), multivariate data analysis was used to analyze and present results in a structured manner.

2. MATERIALS AND METHODS

2.1. Materials

Granules, containing 80 % ibuprofen, were kindly donated by Sanico (Turnhout, Belgium), and used as received. The granules were produced by fluid bed wet granulation. A premixed blend of the active pharmaceutical ingredient (API) and a binder were agglomerated with water as the granulation liquid. After drying, a glidant, lubricant and anti-adhesive were added externally.

2.2. Granule characterization

Particle size analysis was done by sieve analysis ($n=3$), using a sieve shaker (Retsch VE 1000, Haan, Germany). 200 g of granules was placed on a nest of sieves (50, 100, 150, 250, 300, 500, 710, 1000 and 1120 μm) and shaken at an amplitude of 2 mm for 10 minutes. The amount of granules retained on each sieve was determined. The density (ρ_{true}) of the granules was measured ($n=3$) using a helium pycnometer (Accupyc 1330 pycnometer, Micrometrics Instruments, Norcross, Georgia, USA), with ten purges and ten runs per measurement. The bulk (ρ_{bulk}) and tapped density (ρ_{tapped}) of 30 g of granules was determined in a 100 ml graduated cylinder ($n=3$). The powder was poured from a height of 40 cm through a stainless steel funnel with a 10 mm orifice into the graduated cylinder, mounted on a tapping device (J. Engelsmann, Ludwigshafen am Rhein, Germany). Bulk and tapped densities were calculated as $30 \text{ g} / V_0$ and $30 \text{ g} / V_{1250}$, respectively. These values were used to calculate the compressibility index (CI) in order to assess the tendency of a powder to consolidate [19]. Scanning electron microscopy (SEM) was used to study the shape and surface of the granules. A small amount of granules was mounted on metal stubs with carbon tape and coated with gold by means of a sputter coater (Emitech SC7620, Quorum Technologies, East Grinstead, UK). Photomicrographs were taken with a scanning

electron microscope (FEI QuantaTM 200F, FEI, Hillsboro, USA) operated at an acceleration voltage of 20 kV. The granules were observed at magnifications of 1000x and 5000x.

2.3. Preparation of tablets

2.3.1. Mechanism of compression

All tablets were prepared by double compression (i.e. a precompression and main compression step). At the precompression station the punches apply an initial force on the powder, and subsequently, under the main compression rollers the final compression takes place, usually at a higher load compared to the precompression phase [20-22]. The role of the precompression is to reduce air-entrapment during the final compression step. Also the duration of compression is increased by effectively extending the dwell time via precompression, yielding stronger tablets [21-24].

The mechanism of compression with the moving and fixed roller set-up is thoroughly described in Chapter 2 (3. Mechanism of compression). Basically, in a fixed roller set-up, for a given tablet press and tooling, the kinetics of the punch movement depend only on the tableting speed. As a result the total contact time (the period when the upper punch is in contact with the powder), the consolidation time (the period during which the punches approach each other), the dwell time (the period during which the punch head flat is in direct contact with the compression roller), the decompression phase (the time during which the punches move away from each other) and the lag-time (the time between precompression and main compression phase) are defined by the tangential velocity of the punch [16, 21-23, 25-38].

In contrast, using the MODULTM P high-speed rotary tablet press these parameters can be controlled independently from the tableting speed, due to an air compensator which allows displacement of the upper compression rollers (Figure 5.1). The upper rollers are attached to an air piston, which allows vertical movement in an air cylinder. The air pressure in the cylinder (CF_r) is set at a constant value due to a control system of pressure valves and expansion vessels. This system with moving rollers has major implications on the control systems and kinetics of punch movement, compared to a system with fixed rollers. The shape of the force-time profiles, and mainly the dwell time, is affected [18, 20, 29, 33, 39].

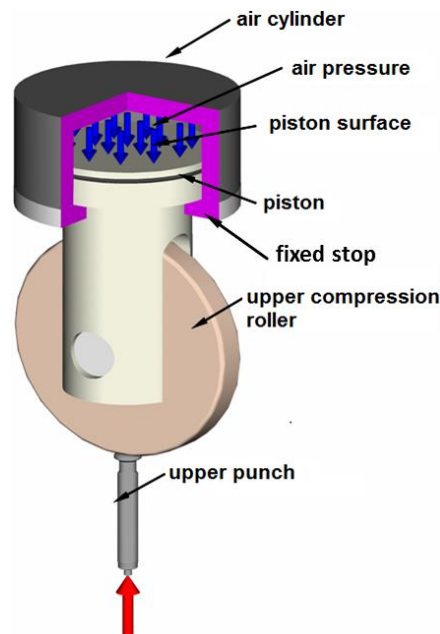


Figure 5.1: Schematic representation of the pneumatic air compensator. (Courtesy of GEA, CourtoyTM)

The dwell time is not only defined by the land, the pitch diameter and the turret speed, but also by the displacement. As the upper roller is displaced, the contact time between the punch head flat and the roller is prolonged. Hence the dwell time is extended in comparison to the fixed roller set-up, although tableting speed is constant. Another implication of this concept is the effect on the in-die tableting position since the lower roller will have a higher position in order to induce displacement. Therefore, the position of the powder slug in the die will be higher compared to a system with fixed rollers. Hence the distance travelled by the tablet before being ejected is less which can influence the stress applied on the powder bed, resulting in a different relaxation behaviour [23]. A schematic overview of the different positions and movements of rollers and punches is provided in Figure 5.2.

It is necessary to mention that the term ‘displacement’ in this research is strictly used to describe *the movement of the upper roller*, and *not* the movement of the punches, as it is done in all previous research describing force-time profiles.

2.3.2. Collection of data

Collection and analysis of the data was performed with a data acquisition and analysis system (CDAAS) (GEA Process Engineering - Courtoy, Halle, Belgium) as described in detail in Chapter 2 (4. Instrumentation and collection of data).

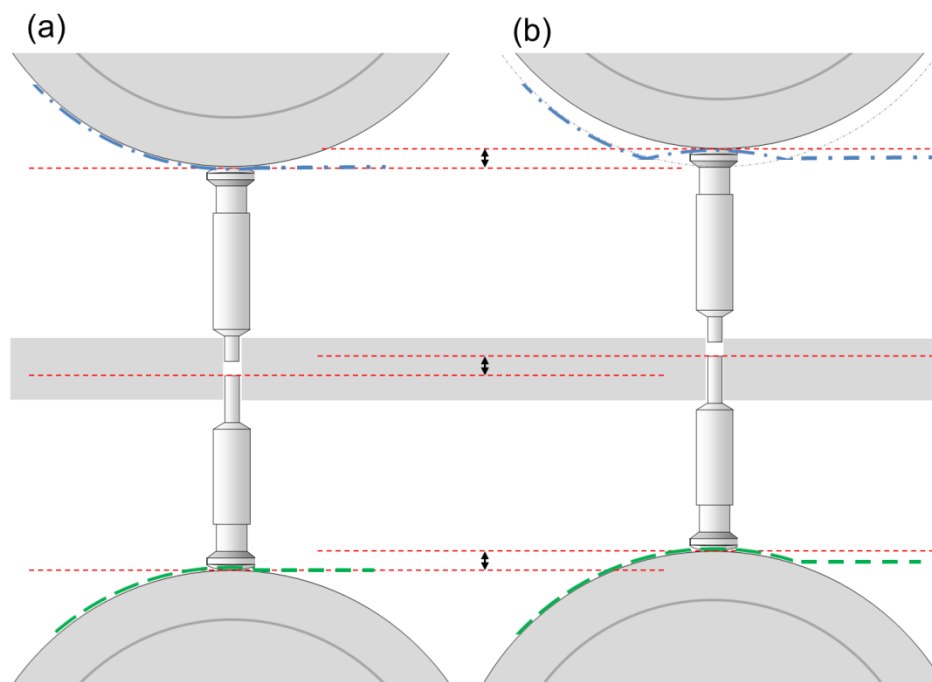


Figure 5.2: Schematic overview of the different positions and movements of rollers and punches (a) with fixed rollers and (b) with moving rollers, highlighted by red lines and arrows. ---- depicts the punch movement of the upper punch, --- depicts the movement of the lower punch.

2.3.3. Tableability

In order to determine the main compression force (MCF) at which the experiments should be performed, a preliminary tableability study was performed. Tableability may be defined as the capacity of a powder to be transformed into a tablet of specified strength under the effect of compaction pressure. It can be represented by a plot of tensile strength (TS) versus compaction pressure [31, 36, 40-43]. Although very useful, the obtained correlation is not an intrinsic material characteristics and the profile is dependent upon the press, tooling and settings used (e.g. tableting speed, paddle speed in the forced feeder, fill depth) [31, 32, 36, 42]. Therefore, the same tooling (n=10, standard euro B, \varnothing 12 mm, concave radius 24 mm) was used throughout the study. The fill depth was adjusted to obtain tablets of 500 mg, in accordance with the dwell time experiments. Tableting speed was set at 500 tablets per minute (tpm) and force feeder speeds were kept constant at 25 and 40 rotations per minute (rpm). Precompression force (PCF) was set at 2 kN and precompression displacement (PCD) at 0.2 mm. Main compression displacement (MCD) was kept at 0.0 mm for all experiments and MCF was varied from 3 to 30 kN with increments of 3 kN. An extra point at 42 kN MCF was added to examine the TS at a very high compression load. For each experiment the

machine was run for 2 minutes, with sampling during the second minute. Room temperature (21.0 ± 2.0 °C) and relative humidity (RH) (30.0 ± 2.0 %) were controlled.

2.3.4. Influence of extended dwell time

A series of experiments was conducted in order to investigate the effect of the extended dwell time induced by displacement. Experiments were repeated at three different tableting speeds to examine the effect of this parameter. Initially, the experimental set-up consisted of 12 experiments, in which three factors were varied (Table 5.1). PCF was kept constant at 2 kN and MCF was set at 12 kN, based on the results of the preliminary tableting test.

Table 5.1: Initial set-up of the experimental design.

Process variable	Lower level	Mid level	Upper level
Tableting speed (tpm)	250	500	1000
Precompression displacement (mm)	0	-	1
Main compression displacement (mm)	0	-	1

However, the shape of the force-time signal for tablets compressed with moving rollers induced some set-up modifications, as this profile deviated from the theoretical profile (Figure 5.3) [36]. This atypical shape is caused by the inertia of the system and is inherently connected to the design of the air compensator. A limited “overshoot” occurs before the plateau of the extended dwell is reached. Furthermore, the ratio between F_{top} and F_{mplateau} (defined as the mean value of $F_{25\text{dw}}$, $F_{50\text{dw}}$ and $F_{75\text{dw}}$ (see Table 5.3)) increases at higher tableting speed, which is by default due to the larger impact at higher punch velocities when the punches come into contact with the compression rolls.

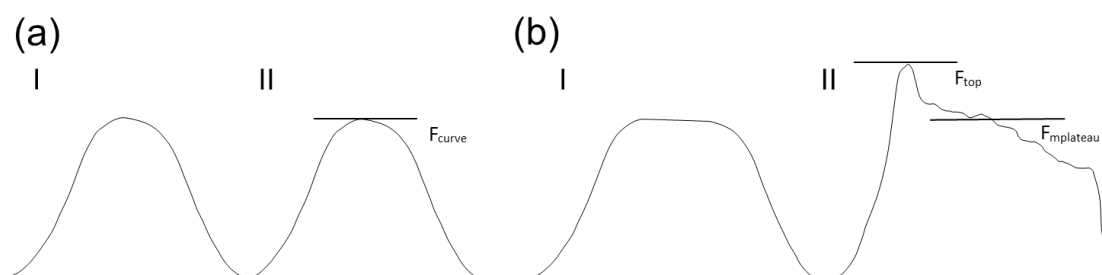


Figure 5.3: Representative illustration of theoretical (I) and observed (II) compression profile for tablets compressed without (a) and with (b) displacement.

As a result, two compression forces (F_{top} and $F_{mplateau}$) were taken into account for analysis and correlation with the tablet properties. Hence, PCF and MCF values of 2 kN and 12 kN, respectively, were maintained, in order to be able to compare the experiments between different tableting speeds. Moreover, depending on the tableting speed, the other compression force (with displacement) was determined as the resulting F_{top} by keeping the $F_{mplateau}$ on these preset values (i.e. experiment 3 in Figure 5.4). This ultimately resulted in an adjusted set-up with seven experiments per tableting speed (total of 20 experiments, experiment 12 was not performed), from which an overview is provided in Figure 5.4.

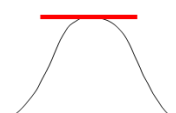
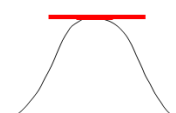
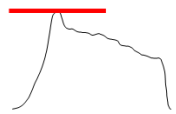
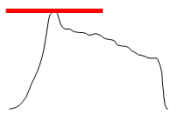
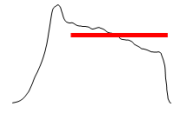
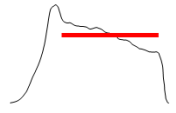
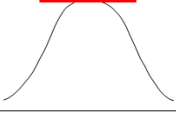
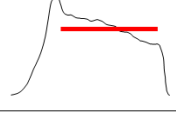
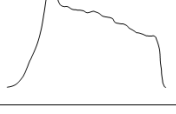
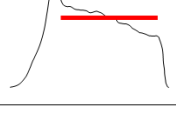
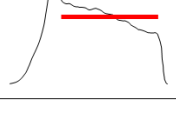
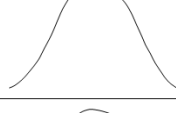
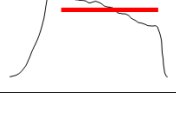
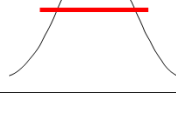
Speed (tpm)			Precompression		Main compression	
250	500	1000	Shape	Displacement	Shape	Displacement
Experiment						
1	8	15		no		no
2	9	16		yes		yes
3	10	17		yes		yes
4	11	18		no		yes
5	12	19		yes		yes
6	13	20		yes		no
7	14	21		yes		no

Figure 5.4: Schematic overview of the performed experiments. Red bars indicate the initial force (2 kN at precompression, 12 kN at main compression).

Tablets were prepared on the MODUL™ P, equipped with an overfill cam of 16 mm and using a set of punches as described earlier. The fill depth was adjusted prior to each experiment to obtain tablets of 500 mg. Tableting speed was set at 250, 500 or 1000 tpm, depending on the experiment. As paddle speed must be adjusted in function of tableting

speed in order to avoid speed-induced weight variability, force feeder speeds were set either at 10 rpm – 50 rpm, 25 rpm – 40 rpm or 35 rpm – 50 rpm [44]. PCF, PCD, MCF and MCD were set according to the experiment (Figure 5.4). In order to avoid confounding factors, each experiment was run on an empty and cleaned tablet press. The machine was run for 2 minutes, with sampling during the second minute. Room temperature ($21.0 \pm 2.0 \text{ }^\circ\text{C}$) and RH ($30.0 \pm 2.0 \%$) were controlled. A summary of the machine settings is given in Table 5.2.

Table 5.2: Overview of the machine settings. Settings included in the PCA and PLS-analysis are marked by \blacklozenge .

Key	Meaning	Incl.
speed (tpm)	Tableting speed	\blacklozenge
pad1 (rpm)	Speed of paddle 1 in the forced feeder	
pad2 (rpm)	Speed of paddle 2 in the forced feeder	
fill (mm)	Fill depth, which determines the weight	\blacklozenge
CF_r (kN)**	Air pressure in the air-compensator at the upper roller	\blacklozenge
bot (mm)**	Position of bottom roller	\blacklozenge
top (mm)**	Position of top roller	\blacklozenge

** Different values for pre- (P) and main compression (M).

2.4. Data analysis

2.4.1. Analysis of process parameters

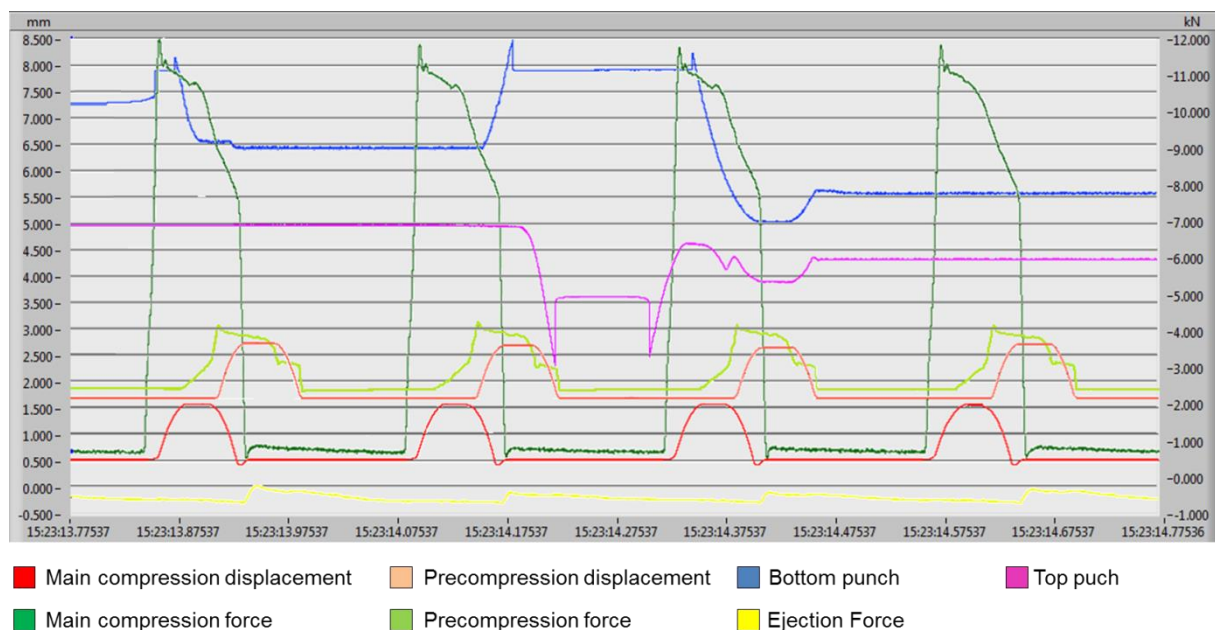


Figure 5.5: Example of the data-logging. X-axis represents time (ms), left and right Y-axis represent distance (mm) and force (kN), respectively. Offset on Y-axis is intentionally changed to permit better visibility of signals.

The CDAAS software stores the collected data from the seven signals as a continuous recording, with time (ms) on the X-axis. PCF, MCF and ejection force (EF) are plotted on one Y-axis (kN), whereas PCD, MCD, movement of bottom punch and movement of upper punch are plotted against distance (mm) (Figure 5.5).

Force-time profiles are already thoroughly addressed by other authors [16, 33-35, 37, 38]. Although these researchers provided insight and proposed applicable evaluation methods for force-time profiles on rotary tablet presses, all these studies were conducted with a fixed roller set-up. Consequently, the moving roller assembly used in this research and the resulting atypical force-time profile requires a modified analysis protocol. Moreover, since it is possible to compress tablets with both methods (fixed and moving rollers), parameters allowing quantitative comparison between both types of profiles had to be defined. A schematic overview of these parameters is given in Figure 5.6, which represents a force-time profile without and with displacement (i.e. fixed and moving rollers). Since the shape of the force-time profile without displacement was slightly different for main compression compared to precompression, a representation of both (Figure 5.6a and 5.6b) is provided. The force-time profiles with displacement were comparable for both stations (Figure 5.6c).

Firstly, the contact time (t_{total} , from t_{begin} to t_{end}) and the area under the curve of the complete profile (AUC_{total}) were defined as parameters [16, 34, 35]. Subsequently, the force-time profile was divided into three phases: the consolidation phase, the dwell time and the decompression phase [16, 34, 35, 37]. The method used to define these phases on the force-time curves depended if the run was performed with fixed or moving rollers. Using moving rollers, the onset and end of the displacement-time signal clearly marked the beginning and end point of the dwell time. This also allowed easy tracking of the consolidation and decompression phase. In runs with fixed rollers, there is no signal indicating when the punches are vertically aligned with the center of the pressure role. For each tableting speed (250, 500 and 1000 tpm) five consecutive force-time signals of the first run (experiment 1 in Figure 5.4, pre- and main compression without displacement) were aligned on the X-axis by means of an algorithm with five consecutive force-time signals of the second run (experiment 2 in Figure 5.4, pre- and main compression with displacement). As the middle of the displacement-time signal of experiment 2 marks the center of the role, by default it also marks the middle of the dwell time on the force-time profile for both aligned experiments.

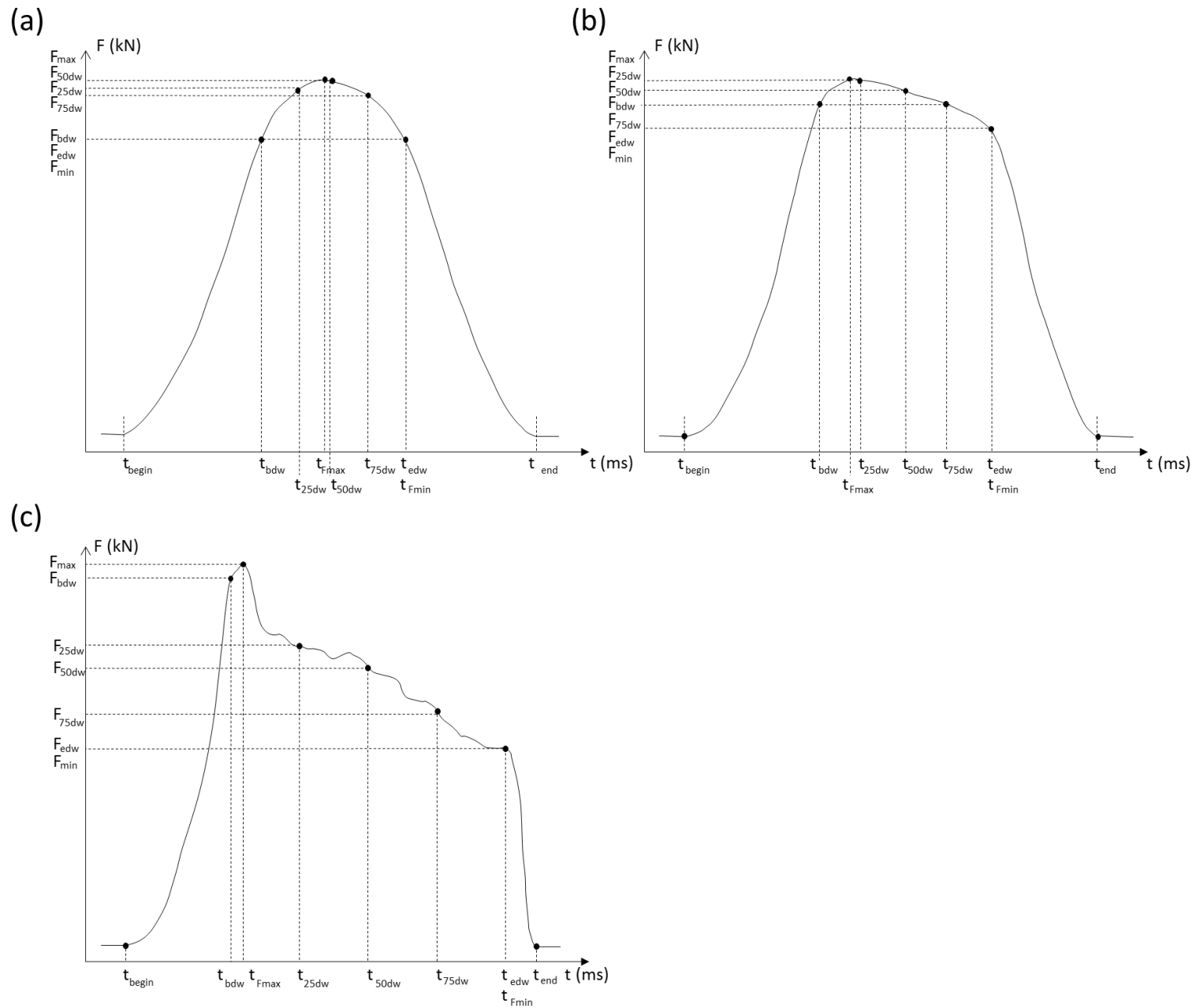


Figure 5.6: Schematic overview of the parameters determined from the force-time profiles for tablets compressed without displacement at main compression (a) and precompression (b) and with displacement (c) (both at pre- and main compression).

Knowledge about the middle of the dwell time (t_{50dw}) allows correct positioning of the dwell time on the force-time profile. The dwell time (t_{dw}) (ms) itself, for the force-time signals without displacement, was calculated according to Equation (5.1):

$$t_{dw} = \frac{6 \times 10^4 \times R_h}{\pi \times \omega \times R_p} \quad (5.1)$$

where R_h , R_p and ω denote the radius of the punch head flat (mm), radius of the pitch diameter (mm) and the turret speed (rpm), respectively.

In order to allow a faster determination of t_{50dw} for the other experiments without displacement, an empirical method was derived. For main compression, the dwell time of the force-time profiles without displacement were characterized by the same force at the beginning of the dwell time (F_{bdw}) as at the end (F_{edw}) (Figure 5.6a). Therefore, the onset and end of the dwell time were defined by the intersections between the force-time profile and a horizontal line with a length equal to the theoretical calculated dwell time. For precompression, the endpoint of the dwell time on the force-time profile without displacement was characterized by a rather sudden and sharp drop in the force profile (F_{edw}) (Figure 5.6b). Consequently, the onset of the dwell time was determined based on this sharp decrease of the force using a line parallel to the X-axis with a length equal to the theoretical dwell time.

Next to the dwell time (t_{dw}), the middle of the dwell time (t_{50dw}) and the forces at the beginning and the end of the dwell time (F_{bdw} and F_{edw} respectively), additional parameters for this phase were determined. The force at 25 % (F_{25dw}), 50 % (F_{50dw}) and 75 % (F_{75dw}) of the dwell time and the respectively absolute time-points (t_{25dw} , t_{50dw} , t_{75dw}) were determined. The same procedure was followed for the maximum and minimum force occurring during the dwell time (F_{max} , t_{Fmax} ; F_{min} , t_{Fmin}). The maximum force is also referred to as F_{curve} or F_{top} (Figure 5.3), depending on compression without or with compression, respectively. $F_{mplateau}$ was determined as the mean value of F_{25dw} , F_{50dw} and F_{75dw} . Furthermore, a dimensionless parameter describing the shape of the force-time profile, independent of the absolute force values used, was included. The t/p_{mean} ratio was defined as the ratio between F_{max} and $F_{mplateau}$.

For the consolidation phase, the consolidation time (t_{con} , from t_{begin} to t_{bdw}), the area under the curve (AUC_{con}) and the slope (S_{con}) were defined as parameters. The decompression phase was analyzed accordingly (t_{decomp} , from t_{edw} to t_{end} ; AUC_{decomp} ; S_{decomp}) [16, 25, 34, 35].

From the ejection profile (yellow line on Figure 5.5) only the maximum ejection force (F_{eject}) was considered.

As stated above, the displacement-time profiles (red and orange line on Figure 5.5) were used to measure the dwell time on the force-time profiles. Furthermore, the maximum displacement (CD) was taken into account for further analysis. The signals for bottom punch and top punch movement (blue and purple line on Figure 5.5) were used to calculate the in-die thickness of the powder plug. The minimum in-die thickness (T_{ID}) was calculated by determining the minimum distance between the bottom and upper punch during compression (h_{BT}), for both pre- and main compression. Furthermore, the distance between the punches immediately after pre- and main compression (T_{AD}) was measured in order to calculate the in-die immediate axial recovery (IAR) of the material after each compression step. Finally, based on the movement of the bottom punch, the time between the end of punch movement at precompression and the beginning of punch movement at main compression was defined as the lag-time (t_{lag}) [21, 22].

For each run, consecutive force-time ($n=10$), displacement-time ($n=10$) and punch motion ($n=3$) signals were manually analyzed. Data were then exported for further statistical pretreatment and computations prior to PCA analysis. A schematic overview of all parameters is given in Table 5.3.

Table 5.3: Overview of parameters derived from the logged data. The settings included in the PCA and PLS-analysis are marked: ♦ if only the absolute value was taken into account, ♦♦ if also the variation coefficient (VC) was included in the data.

Key	Meaning	Incl.
Force-Time profile**		
AUC _{total} (kN*ms)	Area under the curve of the complete profile	♦♦
t _{total} (ms)	Contact time	♦♦
AUC _{con} (kN*ms)	Area under the curve of the consolidation phase	♦
t _{con} (ms)	Consolidation time	♦
S _{con}	Slope of the consolidation phase	♦
AUC _{decomp} (kN*ms)	Area under the curve of the decompression phase	♦
t _{decomp} (ms)	Decompression time	♦
S _{decomp}	Slope of the decompression phase	♦
t _{dw} (ms)	Dwell time	♦♦
F _{bdw} (kN)	Force at the beginning of the dwell time	♦
F _{edw} (kN)	Force at the end of the dwell time	♦
t _{25dw} (ms)	First quarter of the dwell time	♦
F _{25dw} (kN)	Force at 25 % of the dwell time	♦
t _{50dw} (ms)	Middle of the dwell time	♦
F _{50dw} (kN)	Force at 50 % of the dwell time	♦
t _{75dw} (ms)	Third quarter of the dwell time	♦
F _{75dw} (kN)	Force at 75 % of the dwell time	♦
t _{Fmax} (ms)	Time when maximum force occurs	♦♦
F _{max} (kN)	Maximum force	♦♦
t _{Fmin} (ms)	Time when minimum force occurs	♦
F _{min} (kN)	Minimum force	♦
F _{mplateau} (kN)	Mean force of F _{25dw} , F _{50dw} , F _{75dw}	♦♦
t/p _{mean}	Ratio of F _{max} to F _{mplateau}	♦
Ejection profile		
F _{ejec} (kN)	Maximum ejection force	♦
Displacement-time profiles**		
CD (mm)	Maximum displacement of the upper roller	♦
Punch strokes		
h _{BT} (mm)**	Minimum distance between upper and lower punch during compression	♦
T _{ID} (mm)**	Minimum in-die thickness during compression	♦♦
T _{AD} (mm)**	In-die thickness immediately after the decompression phase	♦
t _{lag} (ms)	Time between pre- and main compression, measured on lower roller	♦

**Different values for pre- (P) and main (M) compression.

2.4.2. Tablet evaluation

An overview of the examined tablet characteristics is provided in Table 5.4. In order to obtain information about the influence of the tableting parameters on the granules both “in-die” as well as “out-of-die”, tablet evaluation was done immediately after production (t0) and after a storage period of seven days (t7). Friability, disintegration and SEM were only performed after the storage period. Tablets were stored in open tablet trays in a sealed container at 23.1 ± 1.0 °C and 30.0 ± 2.0 % RH.

Table 5.4: Overview of the tablet characteristics. The settings included in the PLS-analysis are marked: ♦ if only the absolute value was taken into account, ♦♦ if also the variation coefficient (VC) was included in the data.

Key	Meaning	Incl.
W (mg)*	Tablet weight	♦
T (mm)*	Tablet thickness	♦♦
d (mm)*	Tablet diameter	♦
H (N)*	Hardness	♦
TS (MPa)*	Tensile strength	♦♦
Fria (%)	Friability	♦
Dis (s)	Disintegration time	
V _{ID} ** (mm ³)	Volume of the tablets during compression, minimum distance between punches	♦
V* (mm ³)	Volume of the tablets after ejection	♦
ρ _{ID} ** (mg/mm ³)	Density of the tablets during compression, minimum distance between punches	♦
ρ* (mg/mm ³)	Density of the tablets after ejection	♦
ε _{ID} ** (%)	Porosity of the tablets during compression, minimum distance between punches	♦♦
ε* (%)	Porosity of the tablets after ejection	♦♦
IAR _{pre} (%)	Immediate axial recovery after the decompression phase at precompression	♦
IAR _{main} (%)	Immediate axial recovery after the decompression phase at main compression	♦
IAR _{t0} (%)	Immediate axial recovery of the tablets after ejection from the die	♦
CAR (%)	Cumulative axial recovery of the tablets after a storage period of 7 days	♦
Hardening (%)	Change in TS of the tablets upon storage	♦
Diff (CAR-IAR) (%)	Difference between the IAR _{t0} and CAR	♦
Diff W (mg)	Difference in weight between t0 and t7	♦
Diff T (mm)	Difference in thickness between t0 and t7	♦
Diff d (mm)	Difference in diameter between t0 and t7	♦
Diff H (N)	Difference in hardness between t0 and t7	♦
Diff TS (mPa)	Difference in tensile strength between t0 and t7	♦

* Different values for measurements immediately after ejection (t0) and after the storage period (t7).

** Different values for pre- (P) and main (M) compression.

Tablets (n=10) were weighed and their hardness, thickness and diameter was determined (Sotax HT 10, Basel, Switzerland). The tablet tensile strength (TS) (MPa) was calculated using Equation (5.2) [45].

$$TS = \frac{2F}{\pi dT} \quad (5.2)$$

where F, d and T denote the diametral crushing force (N), the tablet diameter (mm) and the tablet thickness (mm), respectively.

Tablet friability was determined on 13 tablets using a friabilator described in the European Pharmacopoeia 7.0 (Pharma Test PTF-E, Hainburg, Germany), at a speed of 25 rpm for 4 minutes. Tablets were dedusted and weighed prior to and after the test. Tablet friability was expressed as the percentage weight loss. The disintegration time of the tablets (n=9) was evaluated with the Pharma Test PTZ-E (Hainburg, Germany) as described in the European Pharmacopoeia 7.0. Tests were performed in distilled water at 37.0 ± 0.5 °C using disks. The disintegration time was determined as the time when no visible particles remained on the mesh wire.

In order to calculate the porosity (ϵ) (%) of the tablets, the apparent density (ρ_{app}) of the tablets was determined. For the in-die density determination, tablet volume (V) (mm^3) was calculated using Equation (5.3), according to the diameter of the die, dimensions of the punch tip and the in-die thickness (T_{ID}), derived from the distance between the top and bottom punch (h_{BT}). For out-of-die determination four dimensions of 10 tablets with known weight were measured with a projection microscope (Reichert, 96/0226, Vienna, Austria), as shown in Figure 5.7. Subsequently, the volume of the tablet was calculated according to Equation (5.3). Weight divided by the volume of the tablet resulted in the apparent density (ρ_{app}). Based on the true density of the granules (ρ_{true}) determined by helium pycnometry, the porosity of the tablets was calculated according to Equation (5.4).

$$V = \left[\pi \times \left(\frac{d}{2}\right)^2 \times h_2 \right] + 2 \times \left[\frac{1}{3} \times \pi \times \left(\frac{h_1-h_2}{2}\right)^2 \times \left[3 \times R - \left(\frac{h_1-h_2}{2}\right) \right] \right] \quad (5.3)$$

$$\epsilon = \left(1 - \frac{\rho_{app}}{\rho_{true}} \right) \times 100 \quad (5.4)$$

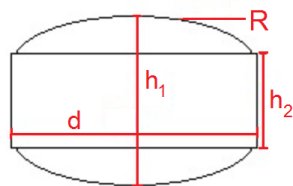


Figure 5.7: Four determined dimensions (R , d , h_1 and h_2) for the porosity calculation of tablets.

Several definitions are used to characterize immediate axial tablet expansion or recovery (IAR) (%) [26, 42, 43, 46]. In general, IAR describes the difference between the minimum tablet thickness under maximum compression force (T_{ID}) (mm) and the tablet thickness after the pressure is removed (T_A) (mm), as represented by Equation (5.5) [46].

$$IAR = \left(\frac{T_A - T_{ID}}{T_{ID}} \right) \times 100 \quad (5.5)$$

However, there is a discrepancy between the interpretation of different authors about that latter data point. Some authors define the tablet height at the end of the decompression phase, before the tablet is ejected from the die (T_{AD}) [26, 43, 47]. Others measure the tablet thickness immediately after ejection from the die (T_{t0}) [42, 48] or even after a defined period (e.g. 1 minute) after ejection (T_{tx}) [46, 48]. Since each of these different determinations contributes to the understanding of the behavior of the granules in the compression cycle, both definitions (before and after ejection) were used in this research. Consequently, three different values of IAR were obtained:

- IAR_{pre} : the immediate axial recovery after precompression, with T_A and T_{ID} the tablet thickness measured in-die immediately after the decompression phase (T_{AD}) and the minimum tablet thickness under maximum precompression force, respectively.
- IAR_{main} : similar to IAR_{pre} , but calculated for the main compression phase.
- IAR_{t0} : the axial relaxation of the tablet after ejection, where T_A denotes the tablet height immediately after ejection (T_{t0}) and T_{ID} the tablet height under maximum compression force at main compression (T_{IDM}).

Furthermore, after a recovery period of seven days, the cumulative axial recovery was calculated accordingly (Equation (5.6)) [46]:

$$CAR = \left(\frac{T_{t7} - T_{IDM}}{T_{IDM}} \right) \times 100 \quad (5.6)$$

with CAR the cumulative axial recovery (%), T_{t7} the tablet height after a storage period of seven days (mm) and T_{IDM} the tablet height under maximum compression force at main compression (mm), respectively. Additionally, the hardening of the tablets (%) upon storage was calculated using Equation (5.7):

$$\text{Hardening} = \left(\frac{TS_{t7} - TS_{t0}}{TS_{t0}} \right) \times 100 \quad (5.7)$$

with TS_{t0} and TS_{t7} the tablet tensile strengths (MPa) measured immediately after ejection from the die and after seven days of storage, respectively. In order to simplify the evaluation of the influence of the storage period on the tablet characteristics, a few additional parameters were defined. Diff(CAR-IAR), Diff W, Diff T, Diff D, Diff H and Diff TS represent the changes in axial relaxation, weight, thickness, diameter, hardness and tensile strength of the tablets during storage, respectively.

SEM was used to study the tablet surface. The tablets were mounted on metal stubs with carbon tape and further processed as described for the granule characterization. The tablets were observed at magnifications of 1000x and 2000x.

2.4.3. Multivariate data analysis

Principal Component Analysis (PCA) was performed on the machine settings and logged data obtained from the tableting press and CDAAS (X , Tables 5.2 and 5.3) in order to provide an overview of the performed experiments and investigate the correlations between all process variables. A Partial Least Squares (PLS) regression model was developed to explore the correlations between the machine settings and logged data (X) and the tablet properties (Y , Table 5.4). Variables were scaled to unit variance prior to analysis [49]. The multivariate model was developed with the Simca P+13 software (Umetrics AB, Umeå, Sweden).

3. RESULTS AND DISCUSSION

3.1. Granule characteristics

An overview of the flow properties, true density and particle size distribution of the granules is presented in Table 5.5. Based on their particle shape (Figure 5.8), it is evident that the ibuprofen crystals are needle-like shaped. This observation, in combination with the large

fraction of smaller particles detected in the mixture, contributed to the classification of this powder as a fairly flowing powder based on the CI values.

Table 5.5: Flow properties, true density and particle size distribution of the granules. Values depict the mean \pm stdev (n=3).

$\rho_{\text{bulk}}(\text{g}/\text{cm}^3)$	$\rho_{\text{tapped}}(\text{g}/\text{cm}^3)$	CI (%)	$\rho_{\text{true}}(\text{g}/\text{cm}^3)$	Particle size distribution		
				d10 (μm)	d50 (μm)	d90 (μm)
0.56 ± 0.00	0.67 ± 0.01	17.34 ± 0.59	1.24 ± 0.00	11.6 ± 0.6	66.2 ± 0.8	527.3 ± 3.5

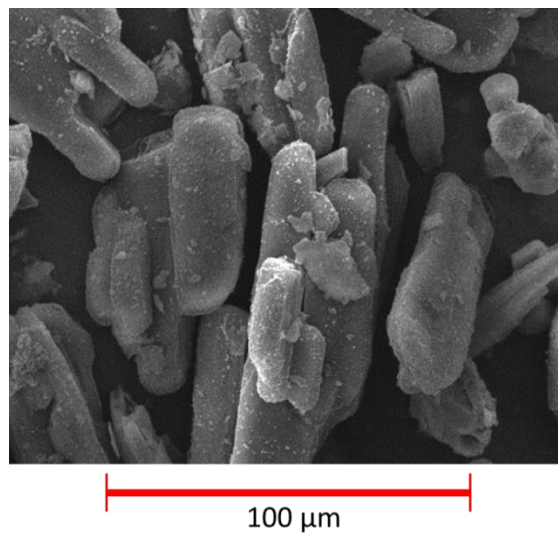


Figure 5.8: SEM-picture of the granules.

3.2. Tableability

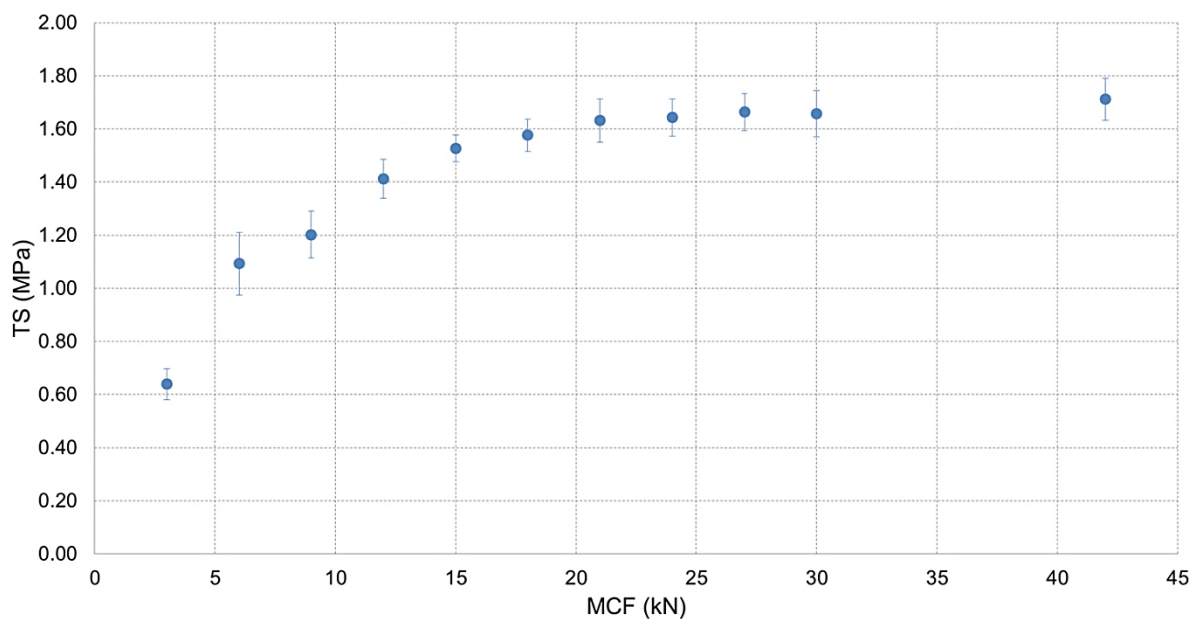


Figure 5.9: Plot representing the tableability. Tensile strength (TS) is plotted against main compression force (MCF). Each point depicts the mean \pm stdev (n=20).

The influence of MCF on TS is depicted in Figure 5.9. The TS increases with MCF at compression pressures less than 18 kN. Above 18 kN, the curve gradually levels off to a plateau, where a further increase in the compaction force does not contribute to a higher tensile strength. The higher energy put in the system is not used for additional bond formation and can, in some cases, even decrease the strength of formed bonds, as elastic expansion at higher compression forces is favored [2, 12, 13, 40]. The preferred compression force is the lowest force at which tablets with sufficient hardness can be produced. Consequently, 12 kN was chosen as MCF for further experiments. At this CF, TS still depends on CF and the hardness of tablets was sufficient to allow handling.

3.3. Multivariate Data Analysis

3.3.1. Principal Component Analysis

Four principal components (PCs) were fitted in the PCA model explaining 81.9 % (R^2) of the variation in the data. The first, second, third, and fourth PC explained 29.0 %, 24.9 %, 19.1 %, and 9.8 %, respectively.

Figure 5.10 depicts the scores of PC1 versus the scores of PC2. Three obvious clusters on the X-axis (PC1) are identifiable: experiments on the left side were performed at a speed of 250tpm, on the center at a speed of 500tpm and on the right at a speed of 1000tpm. PC1, the first PC in the model, is found by searching in the multivariate space for the direction of the largest variance. This elucidates again how important the tableting speed is in performing tableting experiments, as it contributes the most to the observed variance. To investigate in detail how the tableting speed is related to the other process parameters, a loading plot is constructed (Figure 5.11). Scores and loadings have a strong association, and both plots should be observed simultaneously. Observations in a particular place on the score plot have high values for the variables in the same place on the loading plot (positively correlated) and low values for the variables at the opposite side of the loading plot (negatively correlated). Moreover, the effect is more pronounced further away from the origin (i.e. from the middle) of the plot [49]. On the right side of the loading plot (Figure 5.11), four process variables cluster with the tableting speed (red full circle): fill, S_{con} (P), S_{con} (M) and T_{AD} (M). As tableting speed increases, the fill depth (fill) for powders not exhibiting a free-flowing behavior commonly has to be increased to allow sufficient die filling during the

short exposure time to the feeder in order to reach the desired weight. The positive correlation between the after-die thickness (T_{AD}) and the tableting speed confirms the observations of other researchers, who stated that an increased tableting speed is able to increase the immediate elastic expansion [12, 21, 26, 28, 42, 50]. S_{con} shows that the tableting speed is closely correlated to the shape of the force-time profile, as this value, representing the slope of the consolidation phase, for both pre- (P) and main compression (M) are significantly increased at high speed. This conclusion is further supported by the cluster situated at the left side of the loading plot, where nearly all other speed related variables of the force-time profile (the area under the curve (AUC) and the different time points (t)) are grouped (red dashed circle). These variables have a higher numerical value when the tableting speed is decreased.

When looking at the score of PC1 versus the scores of PC2 (Figure 5.10) along the Y-axis (PC2), two clusters can be distinguished. Loadings for PC2 (Figure 5.11) show that experiments with a lower score value (lower half of the score plot) were performed at a higher MCD (at the bottom of the loading plot (blue full line)) while experiments with higher PC2 scores (upper half of the score plot) were performed at a lower MCD, which is in accordance with the set-up of the experiments (see also Figure 5.4). Moreover, experiments with a high score value of PC2 have a high loading value for MCF_r , M_{bot} and M_{top} as these process parameters can be found at the top of the loading plot, opposite from the MCD (blue dashed circle). This is understandable, as the force in the air compensator (MCF_r) has to be lowered and the position of the lower roller has to be raised (M_{bot} decreased) to allow more upward vertical displacement (MCD) of the compression rollers. Obviously, with displacement, the position of the upper roller will also be raised (M_{top} decreased).

Several other variables are positively or negatively correlated to MCD as seen on Figure 5.11 (blue dotted circles). Firstly, the inverse correlation between MCD and the ejection force (F_{ejec}) is an interesting finding worth mentioning. An explanation for this observation can be that with displacement the ejection is facilitated (ejection force lowered), since compression happens higher in the die. Secondly, the model shows the relation between the MCD and the variability of the process. A cluster close to MCD on the loading plot with $VC t_{Fmax}$, $VC t_{dw}$ and $VC T_{IDM}$ highlight that during compression with displacement the variation in dwell time, in the point when maximum force occurs and in in-die thickness is larger than in experiments

where no displacement is used. On the opposite side of the loading plot however, a cluster of VC F_{mplateau}, VC F_{max} and VC AUC_{total} reveals that the value of these variables is lowered when displacement is used. From these observations can be concluded that during compression with a moving roller set-up, the variability in the process is not translated into variability in the force exerted on the powder bed, as is the case with a fixed roller set-up.

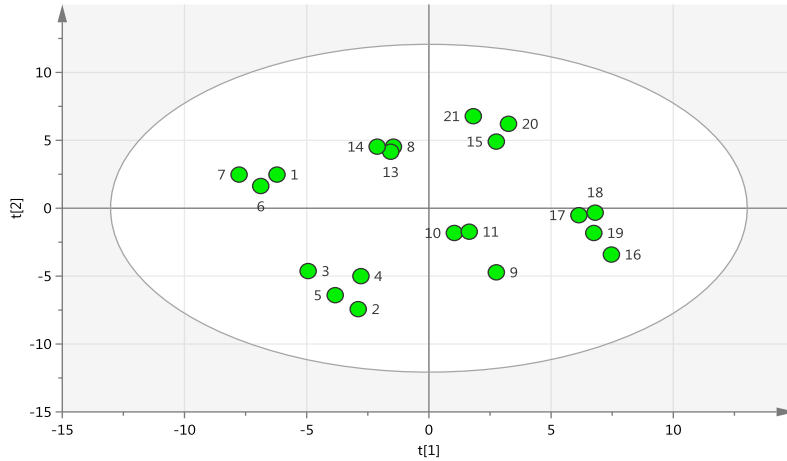


Figure 5.10: Score scatter plot of PC1 vs. PC 2. [t1] – scores of Principal Component 1; [t2] scores of Principal Component 2. Key: see Figure 5.4.

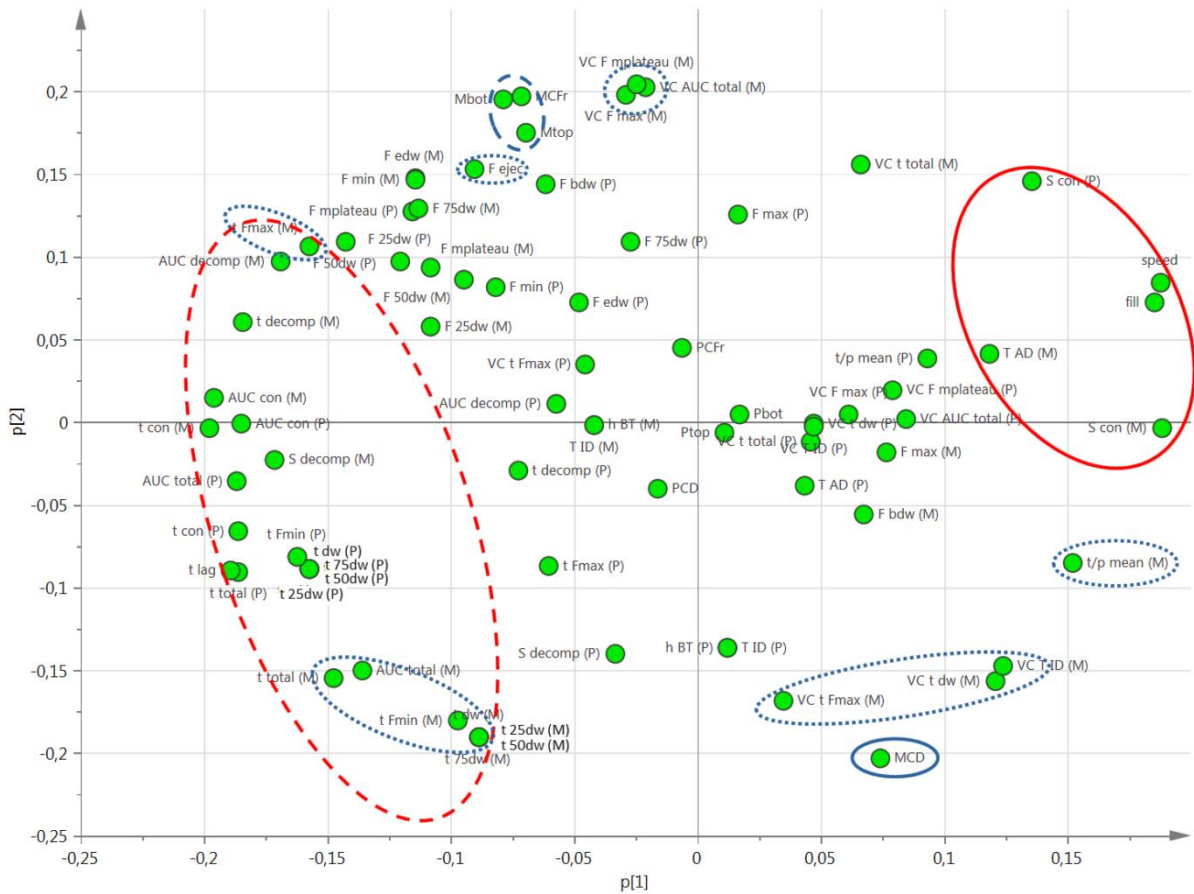


Figure 5.11: Loading scatter plot of PC1 vs. PC 2. [p1] – scores of Principal Component 1; [p2] – scores of Principal Component 2. Key: see Table 5.2 and Table 5.3.

Finally, the parameters positioned in the left lower corner of the loading plot are positively correlated to the MCD. From this can be concluded that during the experiments with displacement the compression event is statistically prolonged, as the total contact time (t_{total}), the dwell time (t_{dw}) and related values (AUC_{total} , $t_{25\text{dw}}$, $t_{50\text{dw}}$, $t_{75\text{dw}}$, t_{Fmin}) are increased. In contrast, t_{Fmax} can be found at the upper part of the loading plot, so negatively correlated with an increased displacement.

This observation becomes clear when looking at the difference in shape of the force-time profile with and without displacement (Figure 5.6a and Figure 5.6c). For all former parameters ($t_{25\text{dw}}$, $t_{50\text{dw}}$, $t_{75\text{dw}}$, t_{Fmin}) the difference between that data point and the beginning of the dwell time (t_{bdw}) becomes larger when using displacement. For the latter (t_{Fmax}) exactly the opposite effect can be seen. The fact that these process parameters are located on the loading plot more to the left instead of center bottom, indicates that both the tableting speed (PC1) and the displacement at main compression (PC2) are correlated with these parameters. This means that the influence of MCD will be more elucidated at lower tableting speeds. A similar conclusion can be drawn when looking at the position of t/p_{mean} on the loading plot. As it is located closer to the lower right corner, both a higher tableting speed and a higher displacement contribute to this value. As mentioned previously, the atypical shape of the force-time profile with displacement is caused by the inertia of the system and is inherently correlated to the design of the air compensator. Furthermore, the ratio between F_{top} and F_{mplateau} increases at higher tableting speed, which is by default due to the larger impact at higher punch velocities when the punches come into contact with the compression rolls. From this can be concluded that the t/p_{mean} ratio is a sensitive parameter to describe the shape of the force-time profile within the range of the parameter setting used.

Figure 5.12 depicts the scores of PC3 versus the scores of PC4 and accordingly, Figure 5.13 represents the loadings of PC3 versus the loadings of PC4. According to PC3 there are two obvious clusters which by looking at the loadings plots can be attributed to differences in the PCD. Experiments with a lower score value (left side of the score plot) were performed at a higher PCD (left side of the loading plot (blue full line)) while experiments with higher PC3 scores (right side of the score plot) were performed at a lower PCD, which is also in accordance with the set-up of the experiments (see also Figure 5.4). Some of the observed

relations show similarity with those observed between the score and loading plot according to PC2. For instance, experiments with a high score value according to PC3 have a high loading value for PCF_r , P_{bot} and P_{top} as these process parameters can be found at the complete right side of the loading plot, opposite from the PCD (blue dashed circle). The same rationale as with MCD can be followed to explain these observations.

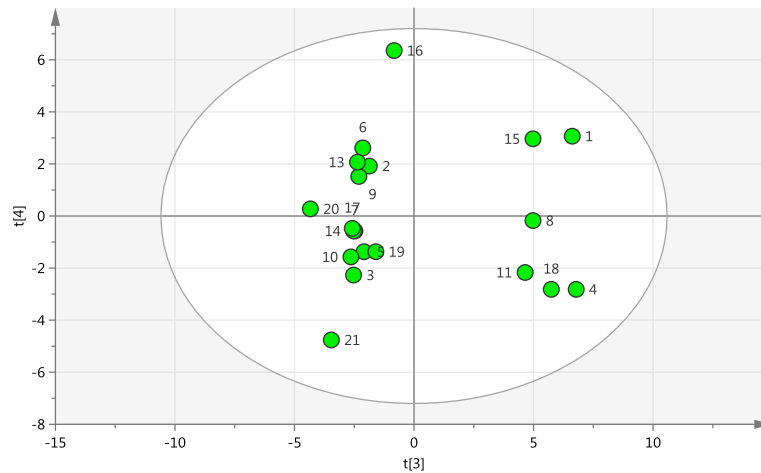


Figure 5.12: Score scatter plot of PC3 vs. PC 4. [t3] – scores of Principal Component 3; [t4] – scores of Principal Component 4. Key: see Figure 5.4.

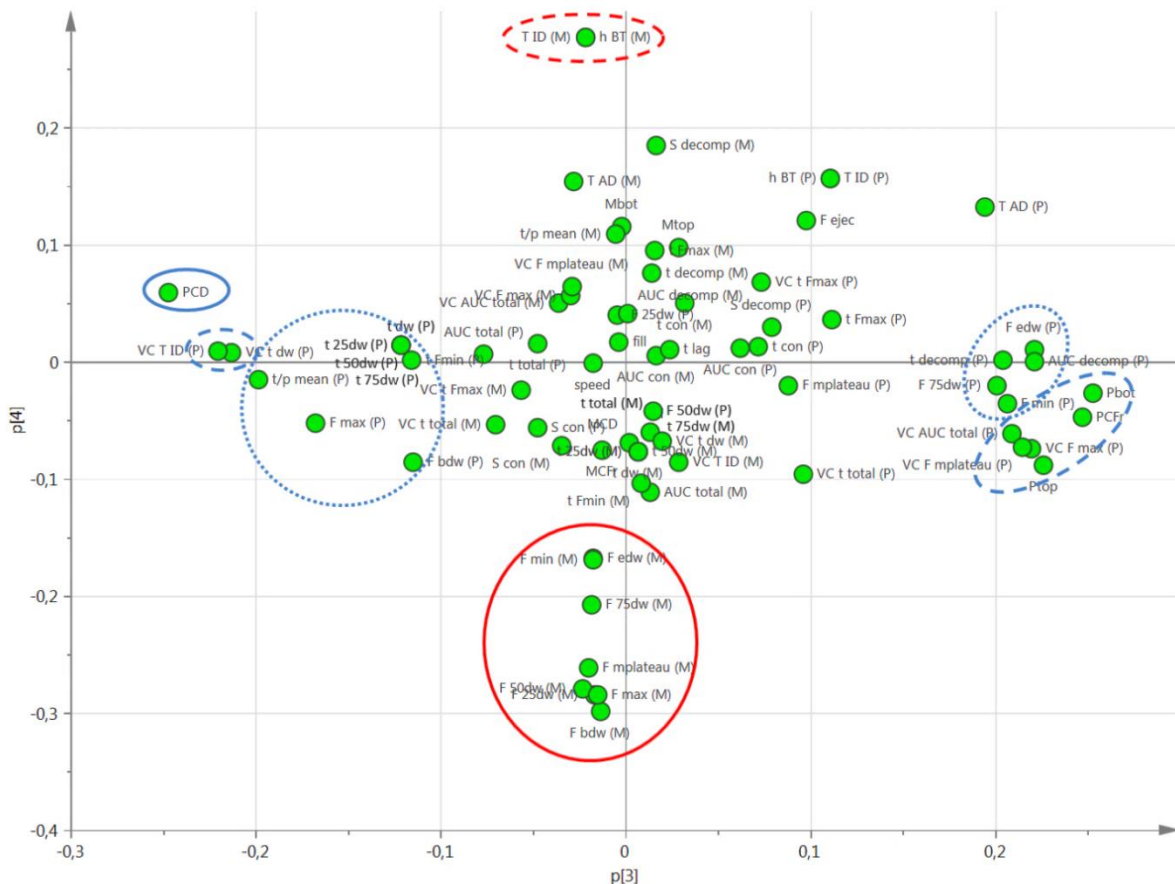


Figure 5.13: Loading scatter plot of PC3 vs. PC 4. [p3] – loadings of Principal Component 3; [p4] – loadings of Principal Component 4. Key: see Table 5.2 and Table 5.3.

Furthermore, the model shows the relation between the PCD and the variability of the process. A cluster close to PCD on the loading plot with VC t_{dw} and VC T_{IDP} highlight that during compression with displacement the variation in dwell time and in in-die thickness is larger than in experiments where no displacement is used. Also here a cluster of VC $F_{mplateau}$, VC F_{max} and VC AUC_{total} on the opposite side of the loading plot reveals that the value of these variables is lowered when displacement is used. From these observations can be concluded that also during precompression with the moving roller set-up, the variability in the process is not translated into variability in the force exerted on the powder bed, as is the case with the fixed roller set-up.

Several other variables are positively or negatively correlated to PCD as seen in Figure 5.13 (blue dotted circles). Their position on the loading plot can be explained by the difference in the shape of the force-time profile between compression with and without displacement (Figure 5.6b and Figure 5.6c). Firstly, the position of the t/p_{mean} close to the PCD confirms that this value is a suitable parameter to describe the shape of the force-time profile. Furthermore, for the Y-axis of the force-time profile (force), the location of F_{max} and F_{bdw} for precompression are logically, as these variables have a higher value when displacement is used. Since F_{75dw} , F_{min} and F_{edw} can be found on the opposite side of the plot, these variables are negatively correlated with MCD, F_{max} and F_{bdw} . When comparing Figure 5.6b and Figure 5.6c, indeed can be seen that these values are lower when displacement is used. F_{25dw} and F_{50dw} are not significantly altered by compressing with or without displacement, which is supported by the position of these variables in the loading plot, since they are located in the middle of the plot according to PC3. For the X-axis of the force-time profile (time), the dwell time (t_{dw}) and related values (t_{25dwl} , t_{50dw} , t_{75dw} , t_{Fmin}) are increased. In contrast, t_{decomp} can be found at the right side of the loading plot, so is negatively correlated with an increased displacement. From this can be concluded that also during precompression the dwell time with the moving-roller is prolonged.

When looking at the scores of PC3 versus the scores of PC4 (Figure 5.12) along the Y-axis (PC4), two clusters can be distinguished. Loadings for PC4 (Figure 5.13) show that experiments with a lower score value (lower half of the score plot) were performed at a higher MCF (at the bottom of the loading plot (red full line)) while experiments with higher PC4 scores (upper half of the score plot) were performed at a lower MCF, which is also in

accordance with the set-up of the experiments (Figure 5.4). Closely correlated variables to the MCF (F_{\max}) are clearly clustered (F_{bdw} , $F_{25\text{dw}}$, $F_{50\text{dw}}$, $F_{75\text{dw}}$, F_{mplateau} , F_{edw} , F_{min}), as can be seen on the loading plot. Moreover, experiments with a high score value according to PC4 have a high loading value for T_{IDM} and $h_{\text{BT(M)}}$ as these process parameters can be found at the top of the loading plot, opposite from the MCF (red dashed circle). This is expected, as the in-die thickness (T_{IDM}) and distance between the punches (h_{BT}) is decreased when higher compression forces are used.

Based on the PCA-analysis, a few general conclusions can be drawn. Firstly, tableting speed contributes to a large extent to the variance of PC1, the first PC in the model. This elucidates how important tableting speed is in performing tableting experiments, as it contributes the most to the observed variance. Mainly its influence on the shape of the force-time profile and the dwell time has to be considered. Secondly, this analysis shows that the moving roller set-up also influences to a great extent the tableting process. Using displacement, both on pre- and main compression, decreased the observed variability in the process and prolonged the dwell time significantly. For main compression displacement, a decrease of the ejection force with increased displacement can also be considered as an important effect. Moreover, the dimensionless parameter, t/p_{mean} ratio, can be considered a sensitive parameter to describe the shape of the force-time profile within the range of the parameter setting used. Finally, the main compression force contributes to a large extent to the variance captured by PC4. Since PC4 only explains 9.8 % of the variance in the model, it can be concluded that the tableting speed and displacement have a larger influence on the compression event (i.e. the other process variables) than the applied (main compression) force.

3.3.2. Partial Least Squares

In order to examine the influence of the process parameters on the tablet properties, a PLS model was constructed. PLS is a regression extension of PCA, which is used to connect the information in two blocks of variables, X (the process parameters) and Y (the tablet properties) [49]. In a first attempt to construct the model, all selected variation coefficients (VC) were included in the model (see Table 5.3 and Table 5.4). However, a negative Q^2 value was obtained for the first 2 PC's. This implies that the model has no predictive power when using only 2 PC's, and a third PC is necessary to force the model into cross validation

predictions. Since this approach has no rational basis, the model was adapted and all variation coefficients were excluded. In this new model, three principal components (PCs) were fitted in the PLS model explaining 66.8 % (R^2) and predicting 18.1 % (Q^2) of the variation.

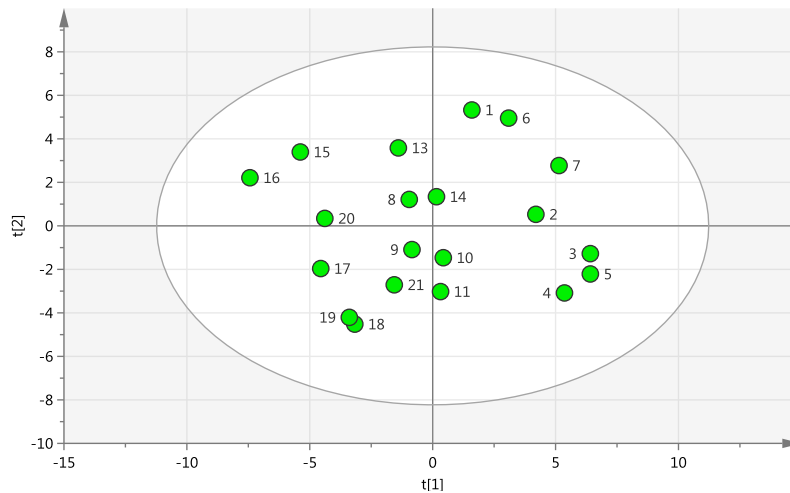


Figure 5.14: Score scatter plot of PC1 vs. PC 2. [t1] – scores of Principal Component 1; [t2] – scores of Principal Component 2. Key: see Figure 5.4.

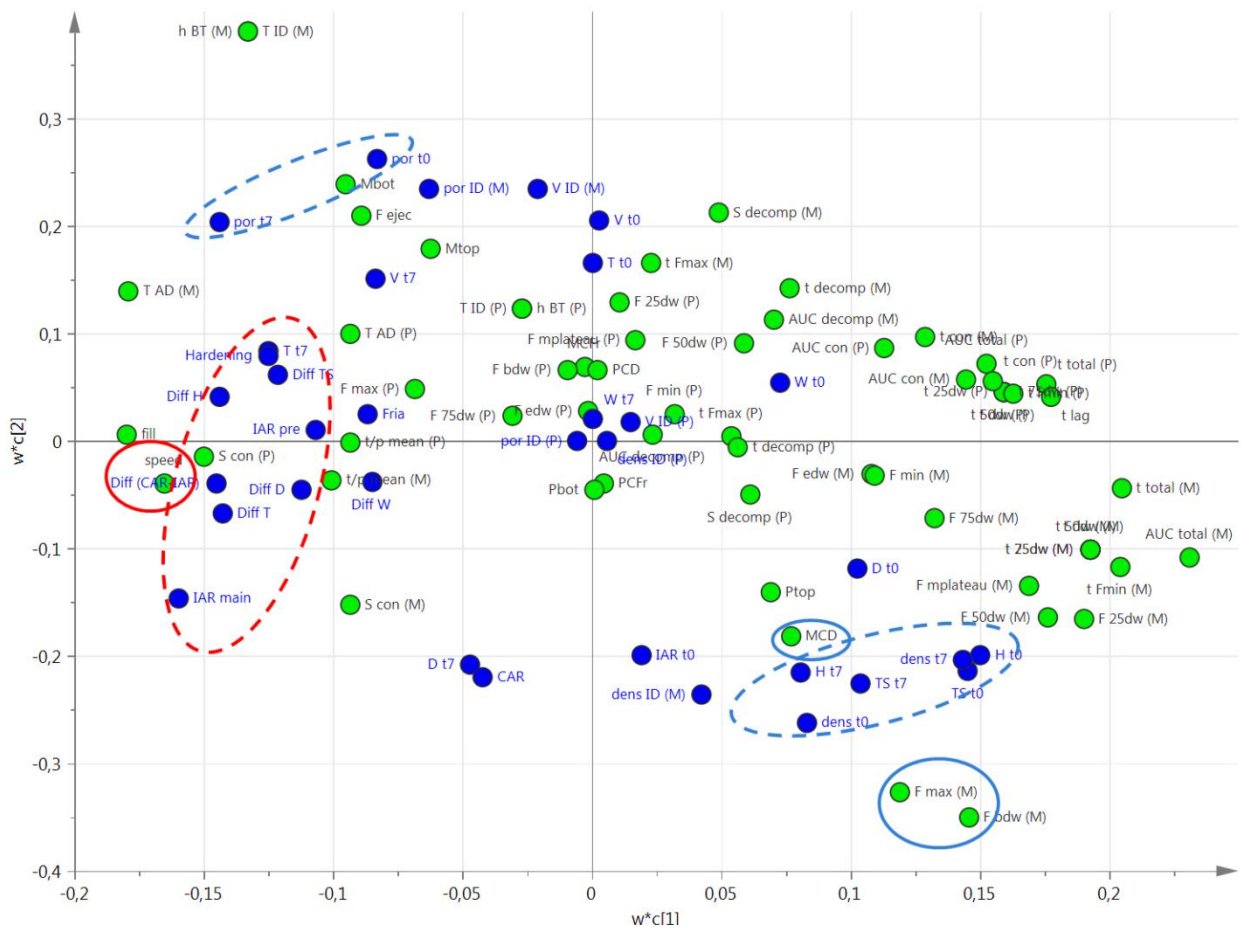


Figure 5.15: Loading scatter plot of PC1 vs. PC 2. $w*c[1]$ – loadings of Principal Component 1; $w*c[2]$ – loadings of Principal Component 2. Key: see Table 5.2, Table 5.3 and Table 5.4.

Scores of PC1 versus PC2 are depicted in Figure 5.14. Figure 5.15 is a plot of the loadings of PC1 versus the loadings of PC2. Again, three clusters on the X-axis (PC1) are identifiable: experiments on the left side were performed at a speed of 1000tpm, on the center at a speed of 500tpm and on the right at a speed of 250tpm. This is confirmed when looking at the loading plot, where the variable speed is positioned on the left side of the plot (red full circle). The loadings of the tablet properties located close to the variable speed are correlated with this process parameter (red dashed circle). Mainly all the "Diff" variables, which depict the difference between the mean value of the process parameter measured at t_0 and t_7 , are related to the tableting speed. Since these variables have a high value, this means that the values of these process parameters are higher after 1 week of storage, than measured immediately after production. The observations can be explained by the viscoelastic behavior of ibuprofen. IAR_{pre} and IAR_{main} have high values at high tableting speed. This means that the immediate axial recovery (in-die) is higher at higher tableting speeds, as also reported in literature [12, 21, 26, 28, 42, 50]. The axial recovery (relaxation) continues further after removal from the die and during storage (Diff (CAR-IAR)), as an increase in diameter (Diff d) and thickness (Diff T) can be observed. Not only the dimensions of the tablet change, but also an increase in tensile strength takes place, represented by Diff H, Diff TS and Hardening. This suggests that the tablet not only expands slowly due to the viscoelastic nature of the material, but that at the same time a reorganization of the material inside the tablet takes place, contributing to a higher tensile strength. Although already reported in literature, a clear explanation for this effect cannot be given [48]. Moreover, since the absolute values are small (e.g. for thickness a maximum increase of 0.11 mm, diameter 0.03 mm and TS 0.16 MPa) this does not necessarily imply any bio-relevant or critical qualitative changes.

When looking at the scores of PC1 versus the scores of PC2 (Figure 5.14) along the Y-axis (PC2), no clear clusters can be distinguished. Moreover, based on the experimental settings (Figure 5.4) and the loadings for PC2 (Figure 5.15) it is clear that more than one process parameter is contributing to the variance captured by PC2. The loading plot shows that experiments with a lower score value (lower half of the score plot) were performed at a higher MCD and a higher MCF (at the bottom of the loading plot (blue full circle)) while experiments with higher PC2 scores (upper half of the score plot) were performed at a lower

MCD and a lower MCF. The loadings of the tablet properties close to these two process variables are the hardness (H), TS and density (dens) of the tablets, both at t0 and t7 (blue dashed circle). The correlation with a higher compression force is obvious, the contribution of the prolonged dwell time (higher MCD) however as such cannot be determined. On the opposite side of the plot, the tablet porosity (t0 and t7) can be found, as this parameter is the inverse of density.

Scores of PC2 versus PC3 are depicted in Figure 5.16. Figure 5.17 is a plot of the loadings of PC2 versus the loadings of PC3. Although two clusters on the Y-axis (PC3) are identifiable, it is clear that more than one process parameter is contributing to the variance captured by PC3. The loading plot shows that experiments with a higher score value (upper half of the score plot) were performed at a higher MCF and a higher PCF (at the left upper corner and top of the loading plot (blue full circle)) while experiments with lower PC3 scores (lower right corner and bottom of the score plot) were performed at a lower MCF and a lower PCF. The loading of the tablet property close to the process variable PCF is the in-die density (dens ID (P)) (blue dashed circle). On the opposite side of the plot, the in-die porosity (por ID (P)) and in-die volume (V ID (P)) can be found. The loadings of the tablet properties close to the process variable MCF (blue dotted circle) are immediate axial recovery upon ejection (IAR t0) and the axial recovery after storage (CAR). From this can be concluded that when tablets are compressed at higher loads, the relaxation over time is prolonged. Moreover, based on these observations it is clear that different process parameters have a different influence on the relaxation behavior of material (i.e. the correlation between IAR_{pre} , IAR_{main} and tableting speed and the correlation between IAR_{t0} , CAR with MCF) and that it is important to take all these measurements into consideration. Other tablet properties related to a higher compression force are the density, hardness and TS. On the opposite side of the plot, the porosity, volume and thickness of the tablets are situated. It is interesting to note that the final tablet properties are mainly determined by the final compression (i.e. main compression) step and not so much by the precompression step, as the in-die properties at main compression (i.e. dens ID (M), por ID (M), V ID (M)) are closely related to the properties after ejection (and after storage). Since the process variable MCD is also located close to the loadings of the former tablet properties (density, TS, H) it is possible that a higher MCD contributes to these tablet characteristics, although clear conclusions cannot be drawn.

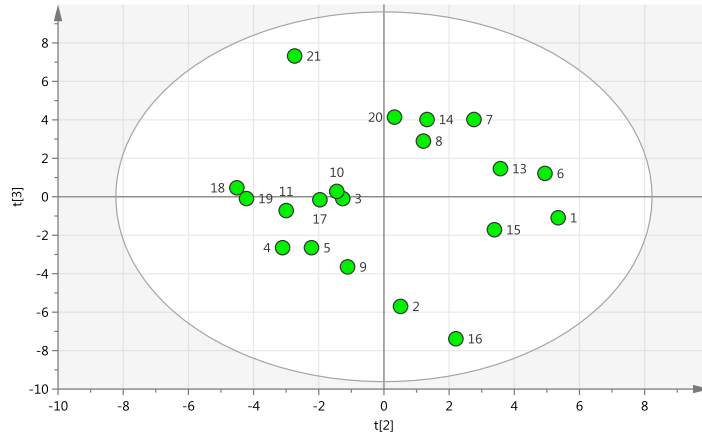


Figure 5.16: Score scatter plot of PC2 vs. PC 3. $t[2]$ – scores of Principal Component 2; $t[3]$ – scores of Principal Component 3. Key: see Figure 5.4.

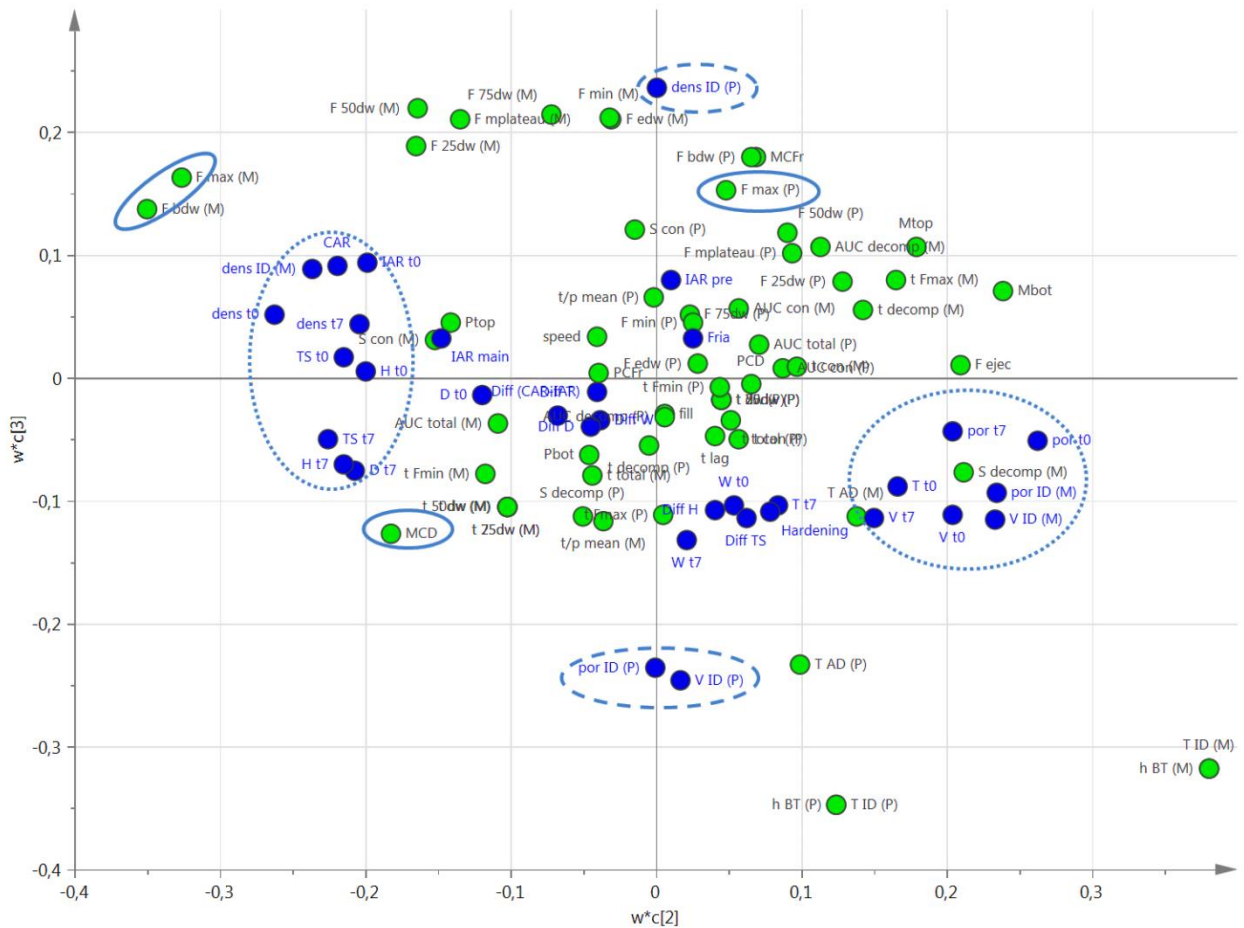


Figure 5.17: Loading scatter plot of PC2 vs. PC 3. $w*c[2]$ – loadings of Principal Component 2; $w*c[3]$ – loadings of Principal Component 3. Key: see Table 5.2, Table 5.3 and Table 5.4.

Overall, the PLS revealed that mainly the tableting speed and the main compression force attribute to the final tablet properties. Furthermore, the relation between process parameters and tablet properties is not straightforward, as the different variables all contribute simultaneously to the final tablet characteristic and the variation captured by the

different PC's cannot be linked to one particular process variable. Although displacement seems to contribute to (some of) the tablet characteristics, clear conclusions cannot be drawn. Finally, a special reference should be made to the elastic behavior of ibuprofen. The PLS revealed that a high compression speed and a high MCF both favor the elastic expansion (either in-die or after ejection). This effect is known to increase the capping tendency of tablets. Although not translated in the absolute values of hardness or friability, it should be mentioned that the detrimental effect of higher elastic recovery at high speeds and high compression forces was observed during friability and hardness testing. A large amount of tablets from experiment 3 and 5 at 1000 tpm (Figure 5.4) underwent capping upon radial pressure before breaking at the hardness test after the storage period (33 and 50 % respectively). Also, during the friability test, about half of these tablets broke into smaller pieces.

3.4. Disintegration testing and SEM

The data obtained from the disintegration test were not included in the PLS-analysis, as the observed differences were not bio-relevant, with the shortest disintegration time being 102.57 ± 26.09 s and the longest 167.95 ± 18.06 s. A trend could be observed however, depending on tableting speed and applied forces. The tableting speed had a negative influence on the disintegration time, whereas an increase of the compression force increased the time the tablets needed to disintegrate.

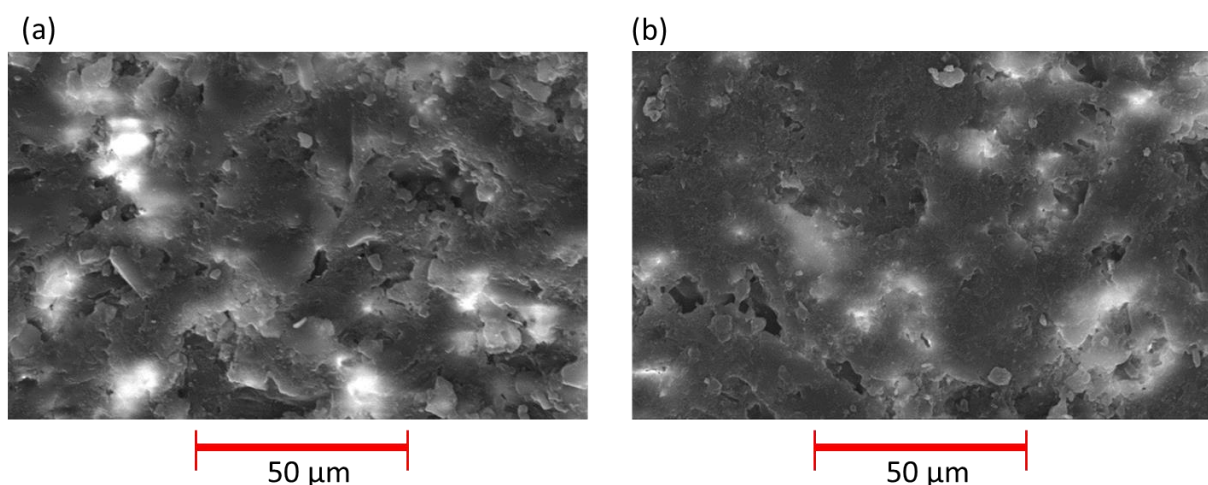


Figure 5.18: SEM-pictures of the surface of tablets produced at the same PCF (2 kN), MCF (12 kN), tableting speed (250 tpm), (a) without extended dwell on PC and MC; (b) with extended dwell on PC and MC.

An illustration of the obtained SEM-pictures is given in Figure 5.18. Overall, it could be concluded that the surfaces of the tablets were similar, although an influence of the tableting speed and the compression force could also here be observed. In those experiments where lower tableting speeds and higher compression forces were used, a slightly smoother surface was obtained. The difference becomes more pronounced when comparing the experiments (of each tableting speed) who were performed with and without displacement (extended dwell time), and this both on pre- and main compression, as depicted in Figure 5.18 for tablets produced at 250 tpm. The tablets produced with displacement (experiment 2) had markedly smoother surfaces than the tablets produced without (experiment 1). This observation might explain partly the lower ejection forces obtained with displacement at main compression, as could be concluded from the PCA-analysis. Smoother surfaces will adhere less to the punch tips and die-wall, reducing the force necessary to overcome this adherence and consequently lowering the ejection force.

4. CONCLUSIONS

Principal Component Analysis (PCA) provided an overview of the main underlying phenomena in the performed tableting experiments. The main source of variation in this dataset was captured in PC1 which is composed mainly by the changes caused by an alteration of the tableting speed. The second major direction of variation in the dataset (PC2) is the change in main compression displacement. PC3 is mainly composed by the displacement at precompression and correlated variables. At last, the main compression force contributes to a large extent to the variance captured by PC4. Partial Least Squares (PLS) revealed that mainly the tableting speed and the main compression force attribute to the final tablet properties and that the relation between process parameters and tablet properties is not straightforward, as the different variables all contribute simultaneously to the final tablet characteristics. Overall, this analysis provided a summary of the contribution of the moving roller set-up to the tableting process and tablet properties. This research project shows that a large amount of parameters influence the compression cycle and it is difficult, if not impossible, to study the contribution of all factors separately. Using an instrumented high speed rotary press, a large amount of information is obtained which contributes to the further understanding of this complex engineering process.

ACKNOWLEDGEMENTS

Authors would like to thank Sanico N.V. for their kind donation of the granules. Dr. Ir. Frederik Detobel and Benny Van der Steen from GEA Pharma Systems - Courtoy N.V. are gratefully acknowledged for the fruitful discussions and their technical support in this work.

REFERENCES

- [1] C. De Brabander, C. Vervaet, L. Van Bortel, J.P. Remon, Bioavailability of ibuprofen from hot-melt extruded mini-matrices, *Int. J. Pharm.* 271 (2004) 77-84.
- [2] P.V. Marshall, P. York, J.Q. Maclaine, An investigation of the effect of the punch velocity on the compaction properties of ibuprofen, *Powder Technol.* 73 (1993) 171-177.
- [3] N. Rasenack, B.W. Müller, Crystal habit and tableting behavior, *Int. J. Pharm.* 244 (2002) 45-57.
- [4] N.F. Abu Bakar, A. Mujumdar, S. Urabe, K. Takano, K. Nishii, M. Horio, Improvement of sticking tendency of granules during tableting process by pressure swing granulation, *Powder Technol.* 176 (2007) 137-147.
- [5] K. Kachrimanis, G. Kistis, S. Malamataris, Crystallisation conditions and physicommechanical properties of ibuprofen-Eudragit® S100 spherical crystal agglomerates prepared by the solvent-change technique, *Int. J. Pharm.* 173 (1998) 61-74.
- [6] P. Di Martino, M. Beccerica, E. Joiris, G.F. Palmieri, A. Gayot, S. Martelli, Influence of chystal habit on the compression and densification mechanism of ibuprofen, *J. Cryst. Growth* 243 (2002) 345-355.
- [7] H.A. Garekani, D. Sadeghi, A. Badiee, S.A. Mostafa, A.R. Rajabi-Siahboomi, Crystal habit modifications of ibuprofen and their physicommechanical characteristics, *Drug Dev. Ind. Pharm.* 27 (2001) 803-809.
- [8] P.K. More, K.S. Khomane, A.K. Bansal, Flow and compaction behaviour of ultrafine coated ibuprofen, *Int. J. Pharm.* 441 (2013) 527-534.
- [9] S. Patel, A.M. Kaushal, A.K. Bansal, Compaction behavior of roller compacted ibuprofen, *Eur. J. Pharm. Biopharm.* 69 (2008) 743-749.
- [10] N. Rasenack, B.W. Müller, Ibuprofen crystal with optimized properties, *Int. J. Pharm.* 245 (2002) 9-24.

- [11] L. Seton, M. Roberts, F. Ur-Rehman, Compaction of recrystallised ibuprofen, *Chem. Eng. J.* 164 (2010) 449-452.
- [12] A. Nokhodchi, M.H. Rubinstein, H. Larhrib, J.C. Guyot, The effect of moisture on the properties of ibuprofen tablets, *Int. J. Pharm.* 118 (1995) 191-197.
- [13] A. Nokhodchi, M.H. Rubinstein, H. Larhrib, J.C. Guyot, The effect of moisture content on the energies involved in the compaction of ibuprofen, *Int. J. Pharm.* 120 (1995) 13-20.
- [14] M. Roberts, J.L. Ford, G.S. MacLeod, J.T. Fell, G.W. Smith, P.H. Rowe, Effects of surface roughness and chrome plating of punch tips on the sticking tendencies of model ibuprofen formulations, *J. Pharm. Pharmacol.* 55 (2003) 1223-1228.
- [15] M. Roberts, J.L. Ford, G.S. MacLeod, J.T. Fell, G.W. Smith, P.H. Rowe, A.M. Dyas, Effects of punch tip geometry and embossment on the punch tip adherence of a model ibuprofen formulation, *J. Pharm. Pharmacol.* 56 (2004) 947-950.
- [16] M. Leitritz, M. Krumme, P.C. Schmidt, Force-time curves of a rotary tablet press. Interpretation of the compressibility of a modified starch containing various amounts of moisture, *J. Pharm. Pharmacol.* 48 (1996) 456-462.
- [17] J. Vogeeler, Rotary tablet press, *Eur. Pharm. Manuf.* 1 (2008).
- [18] J. Van Evelghem, Improving tablet quality with compression to equal force technology, *Pharm. Tech. (Suppl.)* 32 (2008) 26-29.
- [19] R.L. Carr, Evaluating flow properties of solids, *Chem. Eng.* 72 (1965) 163-168.
- [20] M. J. Bogda, Tablet compression: Machine theory, design, and process troubleshooting, in: J. Swarbrick (Ed.), *Encyclopedia of pharmaceutical technology* Informa Healthcare USA Inc., New York, 2007, pp.3611-3629.
- [21] O. F. Akande, J.L. Ford, P.H. Rowe, M.H. Rubinstein, The effects of lag-time and dwell-time on the compaction properties of 1:1 paracetamol/microcrystalline cellulose tablets prepared by pre-compression and main compression, *J. Pharm. Pharmacol.* 50 (1998) 19-28.

- [22] C.E. Ruegger, M. Celik, The influence of varying precompaction and main compaction profile parameters on the mechanical strength of compacts, *Pharm. Dev. Technol.* 5 (2000) 495-505.
- [23] I.C. Sinka, F. Motazedian, A.C.F. Cocks, K.G. Pitt, The effect of processing parameters on pharmaceutical tablet properties, *Powder Technol.* 189 (2009) 276-284.
- [24] E.N. Hiestand, J.E. Wells, C.B. Peot, J.E. Ochs, Physical processes in tableting, *J. Pharm. Sci.* 66 (1977) 510-519.
- [25] N.A. Armstrong, Tablet manufacture, in: J. Swarbrick (Ed.), *Encyclopedia of pharmaceutical technology* Informa Healthcare USA Inc., New York, 2007, pp.3653-3672.
- [26] R.V. Haware, I. Tho, A. Bauer-Brandl, Evaluation of a rapid approximation method for the elastic recovery of tablets, *Powder Technol.* 202 (2010) 71-77.
- [27] T.M. Jones, The physicochemical properties of starting materials used in tablet formulation, *Int. J. Pharm. Tech. Prod. Manuf.* 2 (1981) 17-24.
- [28] P. Konkel, J.B. Mielck, Associations of parameters characterizing the time course of the tableting process on a reciprocating and on a rotary tableting machine for high-speed production, *Eur. J. Pharm. Sci.* 45 (1998) 137-148.
- [29] M. Levin, Tablet press instrumentation, in: J. Swarbrick (Ed.), *Encyclopedia of pharmaceutical technology* Informa Healthcare USA Inc., New York, 2007, pp.3684-3706.
- [30] A. Munoz Ruiz, M.R. Jimenez-Castellanos, J.C. Cunningham, A.V. Katdare, Theoretical estimation of dwell and consolidation times in rotary tablet machines, *Drug Dev. Ind. Pharm.* 18 (1992) 2011-2028.
- [31] A.S. Narang, V.M. Rao, H. Guo, J.A. Lu, D.S. Desai, Effect of force feeder on tablet strength during compression, *Int. J. Pharm.* 401 (2010) 7-15.
- [32] C.E. Ruegger, M. Celik, The effect of compression and decompression speed on the mechanical strength of compacts, *Pharm. Dev. Technol.* 5 (2000) 485-494.

[33] C.E. Rowlings, A.Y. Leung, P.C. Sheen, Resolution of the material and machine contributions to the area to height ratio obtained from force-time powder compression data II: Rotary tablet press, *Pharm. Acta Helv.* 72 (1997) 125-130.

[34] P.C. Schmidt, P.J. Vogel, Force-time-curves of a modern rotary tablet machine I. Evaluation techniques and characterization of deformation behaviour of pharmaceutical substances, *Drug Dev. Ind. Pharm.* 20 (1994) 921-934.

[35] P.C. Schmidt, M. Leitritz, Compression force/time-profiles of microcrystalline cellulose, dicalcium phosphate dihydrate and their binary mixtures – a critical consideration of experimental parameters, *Eur. J. Pharm. Biopharm.* 44 (1997) 303-313.

[36] C.K. Tye, C. Sun, G.E. Amidon, Evaluation of the effects of tableting speed on the relationships between compaction pressure, tablet tensile strength, and tablet solid fraction, *J. Pharm. Sci.* 94 (2005) 465-472.

[37] P.J. Vogel, P.C. Schmidt, Force-time curves of a modern rotary tablet machine II. Influence of compression force and tableting speed on the deformation mechanisms of pharmaceutical substances, *Drug Dev. Ind. Pharm.* 19 (1993) 1917-1930.

[38] J.K. Yliruusi, O.K. Antikainen, New parameters derived from tablet compression curves. Part I. Force-Time curve, *Drug Dev. Ind. Pharm.* 23 (1997) 69-79.

[39] J. Vogeleer, Part two: Rotary tablet press, *Eur. Pharm. Manuf.* 3 (2008).

[40] C. Sun, D.J.W. Grant, Influence of crystal structure on the tableting properties of sulfamerazine polymorphs, *Pharm. Res.* 18 (2001) 274-280.

[41] C. Sun, M.W. Himmelpach, Reduced tableability of roller compacted granules as a result of granule size enlargement, *J. Pharm. Sci.* 95 (2006) 200-206.

[42] S.L. Cantor, S.W. Hoag, L.L. Augsburger, Evaluation of the mechanical properties of extrusion-spheronized beads and multiparticulate systems, *Drug Dev. Ind. Pharm.* 35 (2009) 683-693.

- [43] E. Joiris, P. Di Martino, C. Berneron, A.M. Guyot-Hermann, J.C. Guyot, Compression behavior of orthorhombic paracetamol, *Pharm. Res.* 15 (1998) 1122-1130.
- [44] E. Peeters, T. De Beer, C. Vervaet, J.P. Remon, Reduction of tablet weight variability by optimizing paddle speed in the forced feeder of a high-speed rotary tablet press, *Drug Dev. Ind. Pharm.* doi: 10.3109/03639045.2014.884121.
- [45] J.T. Fell, J.M. Newton, Determination of Tablet Strength by Diametral-Compression Test, *J. Pharm. Sci.* 59 (1970) 688-691.
- [46] N.A. Armstrong, R.F. Haines-Nutt, Elastic recovery and surface area changes in compacted powder systems, *J. Pharm. Pharmacol.* 24 (1972) 135P-136P.
- [47] A. Adolfsson, C. Nystrom, Tablet strength, porosity, elasticity and solid state structure of tablets compressed at high loads, *Int. J. Pharm.* 132 (1996) 95-106.
- [48] K.M. Picker, Time dependence of elastic recovery for characterization of tableting materials, *Pharm. Dev. Technol.* 6 (2001) 61-70.
- [49] L. Eriksson, E. Johansson, N. Kettaneh-Wold, J. Trygg, C. Wikström, S. Wold, Multi- and Megavariate data analysis, part I, basic principles and applications, second ed., Umea, 2006.
- [50] R.J. Roberts, R.C. Rowe, The effect of punch velocity on the compaction of a variety of materials, *J. Pharm. Pharmacol.* 37 (1985) 377-384.

6

ASSESSMENT AND PREDICTION OF TABLET PROPERTIES USING TRANSMISSION AND BACKSCATTERING RAMAN SPECTROSCOPY AND TRANSMISSION NIR SPECTROSCOPY

Abstract

The aim of this study was to investigate if backscattering Raman, transmission Raman and transmission Near Infrared (NIR) spectroscopy could be used for the prediction of the physical properties of tablets. Granules with different characteristics were produced on the Consigma™-25 continuous powder-to-tablet line by varying a number of granulation parameters (concentration of active pharmaceutical ingredient, liquid feed rate, barrel temperature and screw configuration) according to a full-factorial design of experiments. Granules were oven-dried and processed into tablets on a MODUL™ P high speed rotary tablet press. Tableting process parameters were adjusted to obtain tablets with a uniform tablet weight, thickness and diameter for all batches. From all tablets, transmission and backscattering Raman spectra and transmission NIR spectra were collected offline. Tensile strength, friability, disintegration time, apparent density and porosity were determined with traditional analyzing methods. Partial Least Squares (PLS) regression was utilized to model and correlate spectral information to tablet properties. Predictive PLS models for disintegration, friability, porosity and tensile strength could not be established. The utilized Process Analytical Technology (PAT) tools are not suitable for the prediction of the physical properties of tablets. Principal component analysis (PCA) was effectively utilized to distinguish between different theophylline concentrations and its hydration level. The differences between backscattering Raman, transmission Raman and NIR spectroscopy performance in the quantification of theophylline content by means of a PLS model was insignificant. Furthermore, Multiple Linear Regression analysis (MLR) allowed a successful investigation on how the changes in the granulation parameters affect granule properties, tablet properties and dependent tableting process parameters.

KEYWORDS: Continuous production, PAT, Granulation, Tableting, Tablet properties, Granule properties, NIR, Raman.

1. INTRODUCTION

Most pharmaceutical manufacturing nowadays is still performed using batch manufacturing processes. In contrast to other industries (e.g. petrochemical, chemical and food industries) who transferred to continuous manufacturing decades ago, the pharmaceutical industry has been reluctant to move from batch processing towards continuous processing. Rigorous regulatory constraints, amongst others, can be identified as one of the reasons for this [1-6]. However, since the publication of the Food and Drug Administration's (FDA) Pharmaceutical current Good Manufacturing Practices (cGMP) for the 21st century initiative, there has been a shift towards regulatory authorities encouraging the pharmaceutical industry to implement new technology. The International Conference on Harmonization (ICH) guidelines Q8, Q9 and Q10 together with the Process Analytical Technology (PAT) - Guidance for Industry and the Process Validation - Guidance for Industry introduced the concepts of Quality by Design (QbD) and the use of science and risk-based approaches to assure product quality [1, 7-11].

The production of tablets on a high speed rotary tablet press is by definition a classic example of a continuous process. As long as the machine is fed with material, tablets will be produced and ejected at the ejection station. The production speed of an industrial tablet press gives an extremely large output (i.e. several hundreds of thousands of tablets per hour). If analyzing methods guaranteeing the quality of the end product are optimized, this results in a shorter "time-to-market" and a cost and floor space reduction, as there is less need to storage. In theory however, tablet quality is still mainly assessed offline by performing traditional methods of analysis on tablets collected at the end of production. These methods are often destructive and involve sample pretreatment. As a consequence, the latter becomes the rate-limiting step and annuls the advantages of the fast continuous production process. Consequently, to allow real-time release, other techniques are necessary. Evidently, the use of PAT-tools is a vital element in this process.

In contrast to the classical analyzing methods, spectroscopic techniques offer a rapid, simple, non-invasive and non-destructive alternative requiring little or even no sample preparation. Near Infrared (NIR) and Raman spectra carry significant chemical and physical features of the samples but since these often overlap it is difficult to get information directly from the spectra. Therefore, multivariate data analysis tools such as Principal Component Analysis

(PCA) are essential to extract and summarize this information [12]. NIR reflectance and also transmittance measurements have proven to be reliable methods for the identification and quantification of active pharmaceutical ingredients (APIs) in tablets and for the prediction of tablet properties [13-20]. A few publications report the application of Raman spectroscopy for the determination of tablet properties [12, 20, 21]. It is crucial to emphasize that all of these studies were performed on tablets prepared using different compression forces, hence resulting in tablets with a different thickness or a different weight, depending on the followed approach (i.e. maintaining the weight results in tablets with decreased thickness when compression force is raised whereas maintaining the thickness requires an increased weight when compression force is raised). In an industrial manufacturing process however, the main objective is to maintain the preset tablet weight, thickness and diameter. As differences in weight, thickness and diameter are also known to affect signals detected via Raman and NIR spectroscopy, it was the objective of this study to adjust the tableting process parameters in order to obtain for all batches tablets of uniform weight, thickness and diameter. Hence, any differences observed in tablet characteristics could only be due the differences in granule characteristics.

The primary objective of the present study was to determine the applicability of NIR and Raman spectroscopy in the prediction of the physical properties of tablets, using the Partial Least Squares (PLS) approach. It was further investigated if these PAT-tools could also be used with the same capability to determine the concentration and hydrate level of the API (theophylline). Moreover, the influence of different granulation parameters on granule quality attributes, tablet quality attributes and associated tableting process parameters was studied.

2. MATERIALS AND METHODS

2.1. Materials

Theophylline anhydrate was selected as model API and purchased from Farma-Química Sur (Malaga, Spain). α -lactose monohydrate 200 M (Caldic, Hemiksem, Belgium) was used as filler for granulation and polyvinylpyrrolidone (PVP) (Kollidon[®] 30, BASF, Ludwigshafen, Germany) in a concentration of 2.5 % (w/w to the dry powder) as binder. Distilled water was used as the granulation liquid.

2.2. Preparation of powder mixtures

Prior to granulation, three premixes, with different theophylline concentrations (Table 6.1), were prepared by low shear mixing (20 minutes, 25 rotations per minute (rpm)) in a 20 L stainless steel drum with a filling degree of 60 %, using a tumbling mixer (Inversina, Bioengineering, Wald, Switzerland).

2.3. Granulation

Granulation experiments were performed using a high-shear co-rotating twin screw granulator, being the granulation unit of the ConsiGmaTM-25 continuous powder-to-tablet line (GEA Pharma Systems - ColletteTM, Wommelgem, Belgium), which has already been thoroughly described by other authors [1, 4, 6, 22, 23]. Depending on the experiment (Table 6.1), the concentration of theophylline (API conc), liquid feed rate (LFR), barrel temperature (BT) and amount of kneading elements (screw configuration (SC)) were changed [4]. The powder premix was gravimetrically dosed at a constant feed rate of 25 kg/h onto the screws (950 rpm) and the granulation liquid (distilled water) was pumped into the screw chamber in front of the first kneading element by two peristaltic pumps. After a calibration time of 60 sec, for each run 600 g of granules were collected at the outlet of the granulator. The wet granules were spread on a tray and oven-dried at 40 °C during 24 h. After drying, a part of the granules was used for granule characterization. The rest of the batch was used as such to produce tablets.

2.4. Tableting

Tablets were prepared by single compression (no precompression) using a high speed rotary tablet press (MODULTM P, GEA Pharma Systems - CourtoyTM, Halle, Belgium) equipped with ten punches ($\varnothing = 9$ mm, flat faced bevel edge, no embossing). In order not to impair Raman and NIR measurements, it was important that all tablets had the same thickness (4 mm), diameter (9 mm) and weight (300 mg). Fill depth was adjusted prior to each experiment to obtain the desired weight. Paddle speeds (10-20 rpm), tableting speed (200 tablets per minute (tpm)) and distance between the punches under compression (3.25 mm) were kept constant. Hence, observed differences in physical properties of the tablets are only caused by the differences in granule characteristics and not by the tableting process parameters.

Moreover, several tableting parameters (fill depth (fill), compression force (MCF) and variability of the compression force (VC MCF)) could also be defined as a response of the granule characteristics. Although the fill depth (fill) is set at the beginning of each experimental run and kept constant, its absolute value is dependent on the flow properties of the granules. The compression force and its' variability are parameters dependent on the compressibility and packing properties of the granules. Mean weight was kept constant for all experiments, but small variations are inherent to the dynamics of the process. Consequently, as weight variability could only be influenced by the granule characteristics (flow properties) since tableting speed and paddle speeds stayed the same throughout all experiments [24], this parameter was also taken into account as a response. The forced feeder was filled with 400 g of granules. The machine was run for 60 seconds and then tablets were sampled during 60 seconds. Room temperature (21 ± 2 °C) and relative humidity (RH) (30 ± 2 %) were controlled. Tablets were collected in bags, placed in an environmental controlled room (temperature = 21 ± 2 °C; RH = 30 ± 2 %) and allowed to relax for 24h. Prior to analysis, 72 tablets out of each bag were placed in tablet trays, with a separate slot for each tablet, assigning them an individual identity. This was preserved through all further analysis (Raman spectroscopy, NIR spectroscopy and reference analysis) in order to correlate results between different analytical techniques.

2.5. Design of Experiments

The experimental ranges for the Design of Experiments (DoE) factors (granulation parameters: API conc, LFR, BT and SC) were chosen based on a former study [22]. The concentration of theophylline was set at three levels (19.5, 29.25 or 39 % (w/w to the dry powder mix)) and achieved by preblending the API, 2.5 % PVP and the remaining amount of lactose by low shear mixing. Also the liquid feed rate was varied at three levels (36.2, 41.2 and 46.3 g/min) corresponding to a water concentration of 8, 9 and 10 % respectively, calculated on wet mass. The full length of the barrel was preheated, either to 25 or 35 °C. As fourth process parameter, the amount of kneading elements was varied between 4 and 12. When 12 kneading elements were used, two kneading zones each consisting of 6 kneading elements were assembled, separated by a conveying element and an extra conveying element after the second kneading block [25]. For both screw configurations (1x4, 2x6), the angle of the kneading elements was kept constant at 60°.

As the amount of process parameters was relatively low (four) as well as the levels at which they were explored (two or three), a full factorial design was justified. Furthermore, since each level of each process parameter could be combined with each level of another process parameter, the experimental region could be identified as regular, which is a requisite for a (full) factorial design. Since a full-factorial design gives the maximum amount of information compared to other designs as this arrangement enables the effect of one factor to be assessed independently of all the other factors [26], this approach was followed. The combination of 2 factors at three levels and 2 factors at two levels resulted in $(3^2 \times 2^2)$ 36 experiments. One repetition of the center point was added, which led to a total of 37 experiments. An overview of the DoE is given in Table 6.1.

2.6. Granule characterization

Particle size analysis was done by sieve analysis, using a sieve shaker (Retsch VE 1000, Haan, Germany). 65 g of granules were placed on the upper sieve of the set (150, 300, 500, 710, 1000, 1400 and 2000 μm) and shaken at an amplitude of 2 mm for 5 minutes, after which the amount retained on each sieve was determined. Fines and oversized agglomerates were defined as the fractions <300 and >2000 μm , respectively.

Granule friability was determined using a friabilator (Pharma Test PTF E, Hainburg, Germany) at a speed of 25 rpm for 10 minutes, by placing 10 g (W_{initial}) of granules together with 200 glass beads (mean diameter 4 mm) into the drum and subjecting them to falling shocks. Prior to determination, the granule fraction <150 μm was removed to assure the same starting conditions. After ending a test, the glass beads were removed and the weight of the granules retained on the 150 μm sieve (W_{final}) was determined. Each sample was measured in triplicate. The friability (%) was calculated using Equation (6.1).

$$\text{Friability} = \left(\frac{W_{\text{initial}} - W_{\text{final}}}{W_{\text{initial}}} \right) \times 100 \quad (6.1)$$

Bulk and tapped density of the granules (30 g) were determined in a 100 ml graduated cylinder. The granules were poured from a height of 40 cm through a stainless steel funnel with a 10 mm orifice into the graduated cylinder, mounted on a tapping machine (J. Engelsmann, Ludwigshafen am Rhein, Germany). The granules were allowed to settle loosely under the influence of gravity and the initial volume (V_0) was recorded. The sample was

tapped for 1250 times and the final volume (V_{1250}) was determined. Each sample was measured in duplicate. Bulk (ρ_{bulk}) and tapped (ρ_{tapped}) densities were calculated as $30 \text{ g} / V_0$ and $30 \text{ g} / V_{1250}$, respectively. These values were used to calculate the compressibility index (CI) (%) (Equation (6.2)) [27].

$$\text{CI} = \left(\frac{\rho_{\text{tapped}} - \rho_{\text{bulk}}}{\rho_{\text{tapped}}} \right) \times 100 \quad (6.2)$$

2.7. Tablet evaluation by reference analyzing techniques

Hardness, thickness and diameter of tablets ($n=20$) was determined with a semi-automated hardness tester (Sotax HT 10, Basel, Switzerland). The tablet tensile strength (TS) (MPa) was calculated according to Fell and Newton (Equation (6.3)) [28].

$$\text{TS} = \frac{2F}{\pi dT} \quad (6.3)$$

where F , d and T stand for the diametral crushing force (N), the tablet diameter (mm) and the tablet thickness (mm), respectively.

Tablet friability was determined using a friabilator described in European Pharmacopoeia 7.0 (Pharma Test PTF E, Hainburg, Germany), at a speed of 25 rpm for 4 minutes. Tablets ($n=22$) were dedusted and weighed prior to (W_{initial}) and after ending (W_{final}) a test. The percentage weight loss expresses the tablet friability and was calculated using Equation (6.1). In those cases where cracked, cleaved or broken tablets were detected after friability testing, it was reported in the results that these batches failed the test.

In order to calculate the porosity (ϵ) (%) of the tablets, the apparent density (ρ_{app}) of the tablets was determined. Five dimensions of ten tablets with known weight were measured with a projection microscope (Reickert, 96/0226, Vienna, Austria). Subsequently, the volume of the tablet (V) (mm^3) was calculated according to Equation (6.4).

$$V = \left[\left(\pi \times \left(\frac{d_1}{2} \right)^2 \times h_1 \right) + 2 \left(\frac{1}{3} \times \pi \times h_2 \times \left(\left(\frac{d_2}{2} \right)^2 + \left(\frac{d_3}{2} \right)^2 + \frac{d_2}{2} \times \frac{d_3}{2} \right) \right) \right] \quad (6.4)$$

With h_1 and d_1 the height and diameter of the central cylinder respectively and h_2 , d_2 and d_3 the height, diameter of lower base and diameter of upper base of the conical frustum

(horizontally sliced cone) respectively. Weight divided by the volume of the tablet resulted in the apparent density (ρ_{app}). Based on the true density of the granules (ρ_{true}) determined by helium pycnometry (Accupyc 1330 pycnometer, Micrometrics Instruments, Norcross Georgia, USA), with ten purges and ten runs per measurement ($n=3$), the porosity of the tablets was calculated according to Equation (6.5).

$$\varepsilon = \left(1 - \frac{\rho_{app}}{\rho_{true}} \right) \times 100 \quad (6.5)$$

Disintegration time was determined ($n=6$) using the apparatus described in European Pharmacopoeia 7.0 (PTZ-E Pharma Test, Hainburg, Germany). Tests were performed in distilled water at 37 ± 0.5 °C using disks.

2.8. Prediction of tablet properties using spectroscopic techniques

All 72 tablets from each DoE batch were measured with a NIR-Flex N500 transmission FT-NIR spectrometer (BUCHI, Switzerland) using the NIRWare software. This system contains a tablet holder, isolated from external light sources that can contain up to 10 tablets at a time. The tablet holder minimizes light scattering effects unrelated to the tablet physical properties, providing a robust measurement method. Spectra were collected with 128 scans over the range 11520 cm^{-1} to 6000 cm^{-1} with a resolution of 4 cm^{-1} and an acquisition time of 38 seconds.

The same tablets were also measured with a RamanRXN2 Analyzer (Kaiser optical systems) based on a 785 nm excitation laser with a power of 400mW and a charged coupled device (CCD). Samples were irradiated from above through a PhAT probe (backscattering geometry) and from underneath (using the transmission accessory), collecting the signal for Raman shifts in the range 150 cm^{-1} to 1890 cm^{-1} with a resolution of 0.3 cm^{-1} and an acquisition time of 15 s for the backscattering geometry and 55 s for the transmission geometry. Tablets were placed in an automated tablet holder to minimize light scattering effects unrelated to the tablet physical properties. The probe was fixed at a 25 cm distance from the holder. In order to prevent background noise, measurements were performed in complete darkness by covering both tablet holder and PhAT probe with a black cover. No human interference was necessary during the measurements, resulting in a very robust procedure.

PCA models were built to provide an overview of the collected data. Individual PLS models were developed for the prediction of the tablets' physical properties (friability, tensile strength, porosity and disintegration time) and also for the prediction of the concentration of theophylline. Models for the physical properties of tablets were developed individually for each concentration of theophylline in order to minimize the spectral variation originating from the change in the tablets chemical composition. Modelling was performed using SIMCA 13.0.3 (Umetrics, Umeå, Sweden). Given that the physical features of tablets have been described to influence spectra not only on the form of light scattering effects (i.e. baseline offset) but also on peak height or peak shifts, several different pretreatments were tested including Standard Normal Variate (SNV) and Multiplicative Scatter Correction (MSC) [18, 20]. First and second derivatives were also applied calculating 15-point quadratic Savitzky-Golay filters. Several wavenumbers were tested in order to find the optimal spectral range. The parameters utilized to examine the PCA models performance were R^2X and Q^2 . The performance assessment of PLS models was based on the R^2X , R^2Y , Q^2 and Root Mean Squared Error of Prediction (RMSEP).

2.9. Influence of granulation parameters on granule properties, tablet properties and tableting process parameters

In order to demonstrate the effect of granulation process parameters on granulation properties, tablet properties and dependent tableting parameters (fill, MCF, VC MCF), Multiple Linear Regression (MLR) analysis was performed using MODDE 9.1 (Umetrics, Umeå, Sweden).

Table 6.1: Overview of factor settings and characterization of granules and tablets from the experimental design.

Run	Batch	Factors				Responses of granules							Responses of tablets				Tableting parameters		
		Formulation	SC	BT	LFR	Fines n=1	Oversized n=1	Fria n=3	ρ_{bulk} n=2	ρ_{tapped} n=2	CI n=2	TS n=20	Fria n=1	Dis n=6	ϵ n=10	VC W n=20	Fill n=1	MCF n=10	VC MCF n=10
5	1111	19.50 / 78.00 / 2.50	1x4	25	36.2	34.1	9.0	19.7	0.403	0.464	13.1	1.5	0.2	199	26.1	1.9	10.00	6.63	14.5
33	1112	19.50 / 78.00 / 2.50	1x4	25	41.2	21.2	17.4	15.4	0.437	0.492	11.2	0.9	4.7*	112	25.4	1.7	9.80	5.61	19.4
3	1113	19.50 / 78.00 / 2.50	1x4	25	46.3	10.5	29.0	10.5	0.415	0.464	10.6	0.9	3.7*	188	29.0	1.6	9.35	5.41	13.5
26	1121	19.50 / 78.00 / 2.50	1x4	35	36.2	32.1	9.4	16.7	0.432	0.491	12.1	1.2	3.0*	144	28.2	1.6	9.05	5.50	19.5
25	1122	19.50 / 78.00 / 2.50	1x4	35	41.2	20.1	16.5	15.6	0.433	0.497	12.9	0.8	8.6*	108	30.4	1.7	9.05	5.68	17.4
4	1123	19.50 / 78.00 / 2.50	1x4	35	46.3	14.9	23.3	11.1	0.399	0.456	12.6	0.8	10.9	195	31.0	2.2	9.30	5.06	12.4
34	1211	19.50 / 78.00 / 2.50	2x6	25	36.2	23.4	11.8	14.5	0.448	0.501	10.5	1.2	3.1*	220	22.3	1.9	9.20	5.76	17.1
20	1212	19.50 / 78.00 / 2.50	2x6	25	41.2	16.1	19.4	10.9	0.438	0.494	11.4	1.3	0.2	272	28.8	1.8	9.28	5.27	18.9
7	1213	19.50 / 78.00 / 2.50	2x6	25	46.3	8.9	37.4	6.5	0.446	0.519	14.1	0.8	8.3*	178	30.0	1.7	9.05	6.11	12.2
8	1221	19.50 / 78.00 / 2.50	2x6	35	36.2	20.0	16.2	12.3	0.452	0.509	11.2	0.9	2.9*	218	29.4	1.8	8.90	6.00	22.4
6	1222	19.50 / 78.00 / 2.50	2x6	35	41.2	9.6	32.4	10.3	0.442	0.495	10.6	0.7	4.9*	175	31.5	1.7	9.00	5.06	18.2
1	1223	19.50 / 78.00 / 2.50	2x6	35	46.3	4.9	43.0	4.3	0.464	0.516	10.0	1.1	0.5	526	21.4	1.5	8.50	6.03	22.3
29	2111	29.25 / 68.25 / 2.50	1x4	25	36.2	36.5	7.8	19.7	0.451	0.496	9.0	1.9	0.1	436	24.8	2.0	9.10	5.22	22.2
19	2112	29.25 / 68.25 / 2.50	1x4	25	41.2	29.7	11.5	24.7	0.409	0.441	7.3	2.1	0.1	379	27.2	2.0	9.50	5.63	27.9
17	2113	29.25 / 68.25 / 2.50	1x4	25	46.3	16.6	23.9	15.3	0.439	0.489	10.2	1.9	0.4	355	27.0	2.1	9.50	5.70	23.0
35	2121	29.25 / 68.25 / 2.50	1x4	35	36.2	35.8	7.8	18.8	0.455	0.517	11.9	2.0	0.2	346	20.7	2.1	9.10	5.60	19.2
22	2122	29.25 / 68.25 / 2.50	1x4	35	41.2	23.9	15.5	17.3	0.450	0.513	12.2	2.1	0.1	423	27.2	1.9	8.90	5.47	22.3
14	2122R1 [○]	29.25 / 68.25 / 2.50	1x4	35	41.2	22.9	15.9	17.5	0.450	0.504	10.7	2.1	0.1	570	26.5	1.8	9.90	5.95	21.0
30	2123	29.25 / 68.25 / 2.50	1x4	35	46.3	20.1	14.9	10.8	0.401	0.456	12.0	1.8	1.1*	413	22.7	1.9	9.35	5.63	20.3
12	2211	29.25 / 68.25 / 2.50	2x6	25	36.2	33.4	7.6	14.8	0.463	0.517	10.5	2.1	0.3	519	26.8	1.9	8.72	5.56	22.5
28	2212	29.25 / 68.25 / 2.50	2x6	25	41.2	26.0	9.0	12.2	0.467	0.517	9.7	1.7	1.4*	559	22.6	2.0	8.75	5.23	23.0
23	2213	29.25 / 68.25 / 2.50	2x6	25	46.3	18.2	15.0	9.3	0.487	0.549	11.3	1.4	2.2*	382	27.6	1.7	8.63	5.57	19.1
2	2221	29.25 / 68.25 / 2.50	2x6	35	36.2	26.2	10.2	18.5	0.438	0.483	9.2	2.2	0.4	379	23.3	2.0	9.10	5.73	22.4
13	2222	29.25 / 68.25 / 2.50	2x6	35	41.2	18.2	17.9	9.2	0.469	0.529	11.3	1.9	0.5	589	25.9	1.9	9.00	5.65	20.4
10	2223	29.25 / 68.25 / 2.50	2x6	35	46.3	14.3	17.9	7.5	0.464	0.533	12.9	1.4	2.4*	388	30.1	2.2	9.60	4.98	20.2
18	3111	39.00 / 58.50 / 2.50	1x4	25	36.2	40.0	6.2	25.9	0.369	0.432	14.6	1.7	0.3	963	27.6	1.9	10.05	5.76	13.5
37	3112	39.00 / 58.50 / 2.50	1x4	25	41.2	27.3	12.9	25.1	0.417	0.479	12.9	1.6	0.1	927	21.3	2.2	9.85	5.45	18.8
36	3113	39.00 / 58.50 / 2.50	1x4	25	46.3	26.2	11.0	18.1	0.406	0.457	11.2	2.0	0.1	960	21.3	2.0	9.75	5.42	23.6
16	3121	39.00 / 58.50 / 2.50	1x4	35	36.2	36.7	7.5	22.8	0.407	0.466	12.7	2.2	0.1	653	28.0	1.9	9.75	5.57	17.2
27	3122	39.00 / 58.50 / 2.50	1x4	35	41.2	26.1	11.8	23.4	0.412	0.463	11.0	2.4	0.1	594	26.0	2.1	9.42	5.55	29.0
9	3123	39.00 / 58.50 / 2.50	1x4	35	46.3	22.8	14.3	16.9	0.417	0.456	8.6	2.0	0.2	768	28.5	2.3	9.45	5.75	19.9
31	3211	39.00 / 58.50 / 2.50	2x6	25	36.2	43.3	4.4	16.2	0.470	0.523	10.2	2.3	0.1	972	23.8	2.4	8.75	5.79	16.8
24	3212	39.00 / 58.50 / 2.50	2x6	25	41.2	28.2	8.1	16.3	0.473	0.528	10.4	2.4	0.1	571	27.1	1.9	8.70	5.60	20.5
32	3213	39.00 / 58.50 / 2.50	2x6	25	46.3	18.2	13.4	9.1	0.474	0.539	12.1	2.3	0.1	112	22.9	2.1	9.00	5.42	23.3
21	3221	39.00 / 58.50 / 2.50	2x6	35	36.2	29.1	7.6	16.0	0.440	0.496	11.4	2.6	0.2	935	27.6	2.2	9.30	5.23	23.9
11	3222	39.00 / 58.50 / 2.50	2x6	35	41.2	21.3	13.9	14.8	0.435	0.487	10.7	1.8	0.2	134	27.2	2.0	9.46	5.60	24.8
15	3223	39.00 / 58.50 / 2.50	2x6	35	46.3	15.8	14.2	12.1	0.451	0.489	7.8	1.6	0.1	157	27.6	1.7	9.40	6.38	15.8

Formulation: API/lactose/PVP (%)(w/w); SC: Number of kneading elements; BT: Barrel temperature (°C); LFR: Liquid feed rate (g/min); Fines: < 300 μm (%); Oversized: > 2000 μm (%); Fria: Friability (%); ρ_{bulk} : Bulk density (g/ml); ρ_{tapped} : Tapped density (g/ml); CI: Compressibility index (%); TS: Tensile strength (MPa); Dis: Disintegration time (sec); ϵ : Porosity (%); VC W: variation coefficient weight (%); Fill: fill depth (mm); MCF main compression force (kN); VC MCF: variation coefficient MCF (%) [○] at “Batch code” refers to the repetition of the center point; * at “Fria” depicts the tablet batches that failed the friability test. The values of the responses / parameters are the mean of all determinations in each batch.

3. RESULTS AND DISCUSSION

3.1. Prediction of tablet properties using spectroscopic techniques

3.1.1. Physical properties

PLS models were built separately for each of the measured properties and theophylline contents. Two thirds of the total number of observations was used for the model development while the other third was utilized for its validation. Table 6.2 depicts the best possible models found for correlating the tablets physical properties with the collected spectra. It can be observed that no acceptable models could be obtained since the RMSEP values are too high to be considered satisfactory. Even though the models captured almost all spectral variation, mostly it could not be correlated to any of the assayed tablets physical properties and, therefore, no good predictions could be obtained.

Earlier studies have shown a correlation between spectral information (both Raman and NIR) with tablet hardness, porosity and disintegration time. However, in these studies, tablets were prepared with the same formulation but compressed at different compression forces yielding tablets with different thickness, diameter and/or weight. Differently, in the current study tableting was performed in a way that all tablets had these properties (thickness, diameter and weight) kept constant. Given this, the differences in physical properties observed between the tablets could only be related to the properties of the tableted granules (size distribution, friability, amount of fines, amount of oversized particles) and thus are dependent on the granulation parameters as varied in the performed DoE. These findings suggested that the used PAT-tools were not able to capture these differences in physical properties between tablets. Hence, in manufacturing, where the variations in a stabilized process are also limited, changes in tablet characteristics would stay unnoticed. Moreover, it suggests that in research where tablets were compressed with different compression forces, the correlation seen between spectral data and tablet properties were not only due to (detectable) large differences in the extent of bonding and density, but also to differences in the dimensions (thickness) of the measured tablets.

Table 6.2: PLS models for the prediction of the tablet properties. The range is defined as the minimum and maximum values of the corresponding property measured in the individual tablets.

Physical property	Theophylline concentration (%/tablet)	Spectroscopic Technique	Range	Preprocessing	Wavenumber	# PC	R ² X (%)	R ² Y (%)	Q ² (%)	RMSEP
TS	19.50	BRaman	0.2 to 2.2 MPa	-	150-1890	2	99.0	17.0	15.8	0.351
		TRaman		-	150-1890	2	99.8	11.4	4.6	0.377
		NIR		-	8700-9500	3	100	46.3	43.6	0.367
	29.25	BRaman	0.5 to 2.8 MPa	-	150-1890	1	91.4	7.1	6.1	0.508
		TRaman		-	150-1890	2	98.8	27.7	26.8	0.414
		NIR		-	8700-9500	2	99.8	5.9	0.3	0.487
	39.00	BRaman	0.6 to 3.0 MPa	-	150-1890	7	99.8	52.9	42.0	0.357
		TRaman		-	150-1890	4	99.7	21.8	18.5	0.378
		NIR		-	8700-9500	2	99.8	2.7	1.3	0.516
Friab	19.50	BRaman	0.2 to 10.9 %	SNV	150-1890	13	99.2	96.0	93.7	0.868
		TRaman		SNV	150-1890	5	96.7	63.4	62.4	2.247
		NIR		-	8700-9500	6	100	49.8	47.7	2.401
	29.25	BRaman	0.1 to 2.4 %	SNV	150-1890	11	99.4	90.1	68.6	0.269
		TRaman		SNV	150-1890	10	99.2	98.0	93.1	0.293
		NIR		-	8700-9500	5	100	55.1	52.9	0.508
	39.00	BRaman	0.1 to 0.3 %	SNV	150-1890	13	99.6	94.8	91.7	0.022
		TRaman		SNV	150-1890	6	98.9	78.4	77.8	0.027
		NIR		-	8700-9500	5	100	48.4	47.5	0.040
ε	19.50	BRaman	19.9 to 33.8 %	SNV	150-1890	5	97.5	74.8	66.2	1.891
		TRaman		-	150-1890	2	99.9	50.9	45.2	1.392
		NIR		-	8700-9500	1	88.4	1.7	0.9	4.072
	29.25	BRaman	18.8 to 31.5 %	SNV	150-1890	10	99.3	91.9	78.3	1.910
		TRaman		-	150-1890	4	99.5	39.7	28.2	2.890
		NIR		-	8700-9500	4	100	28.7	19.3	3.152
	39.00	BRaman	19.1 to 28.5 %	SNV	150-1890	1	55.9	5.4	5.0	6.047
		TRaman		-	150-1890	1	92.0	0.6	0.7	5.459
		NIR		-	8700-9500	1	98.5	4.4	3.6	5.750
Dis	19.50	BRaman	73 to 611 s	1 st der	150-1890	5	96.5	84.2	74.5	69.795
		TRaman		1 st der	150-1890	7	99.6	99.5	90.7	57.152
		NIR		-	7500-11520	2	99.2	53.3	42.2	99.805
	29.25	Braman	228 to 717 s	1 st der	150-1890	2	83.2	23.9	17.3	94.671
		Traman		1 st der	150-1890	3	92.6	36.8	9.3	86.974
		NIR		-	7500-11520	2	96.3	20.8	9.2	108.875
	39.00	Braman	547 to 1590 s	1 st der	150-1890	6	98.0	93.4	83.9	124.085
		Traman		1 st der	150-1890	6	98.7	94.5	84.4	134.317
		NIR		-	7500-11520	2	98.5	67.9	64.3	152.224

TS: Tensile Strength; Friab: Friability; ε: Porosity; Dis: disintegration time; BRaman: Backscattering Raman; TRaman: Transmission Raman; NIR: transmission Near-Infrared; SNV: Standard Normal Variate; 1st der: 1st derivative; # PC: number of Principal Components; R²X (%): spectral variance captured by the model; R²Y (%): variance in the measured property captured by the model; Q²: total variation predicted by the model; RMSEP: Root Mean Square Error of Prediction.

3.1.2. Theophylline content and hydration level

All of the assayed techniques allowed a clear distinction between the 3 concentrations of theophylline in the tablets and also between the levels of theophylline anhydrate and monohydrate. The best PCA models for the visualization of this feature can be observed in Table 6.3.

Table 6.3: Selected PCA models for the visualization of theophylline content and hydration level and PLS models for the prediction of theophylline content.

Range (theo conc/tablet)	Model type	Spectroscopic technique	Pre-processing	Wavenumber (cm ⁻¹)	#PC	R ² X (%)	R ² Y (%)	Q ² (%)	RMSEP
13.9 % to 42.8 %	PCA	BRaman	SNV	400.2-600.9 and 1600.2-1800.9	3	99.4	N/A	99.4	N/A
		TRaman	SNV	400.2-600.9 and 1600.2-1800.9	3	99.6	N/A	99.6	N/A
		NIR	MSC	8700-9500	2	99.9	N/A	99.9	N/A
	PLS	BRaman	-	150-1890	3	99.2	98.4	98.4	0.986 %
		TRaman	SNV	150-1890	3	98.1	98.1	98.1	1.022 %
		NIR	-	8700-9500	3	100	98.1	98.1	0.972 %

BRaman: Backscattering Raman; TRaman: Transmission Raman; NIR: transmission Near-Infrared; SNV: Standard Normal Variate; MSC: Multiplicative Scatter Correction, # PC: number of Principal Components; R²X (%): spectral variance captured by the model; R²Y (%): variance in the measured property captured by the model; Q²: total variation predicted by the model; RMSEP: Root Mean Square Error of Prediction.

Figure 6.1 depicts the scores and loadings of the first 2 principal components (PC) of the PCA model obtained from the backscattering Raman data. On the score scatter plot it is possible to observe three different clusters according to PC1. The loadings of PC1 correspond to the difference between the pure analyte spectra of theophylline and lactose. The positive peak at 555 cm⁻¹ reveals that with an increase of PC1 scores there is a simultaneous increase of theophylline anhydrate concentration. Moreover, on the loadings of PC2 a positive peak of

theophylline monohydrate can be observed at 1686.9 cm^{-1} and a negative peak of theophylline anhydrate at 555 cm^{-1} . With the increase of PC2 scores, theophylline anhydrate content decreases and theophylline monohydrate increases. The PC1 and PC2 loadings of the transmission Raman model are identical and describe the same information as the backscattering mode.

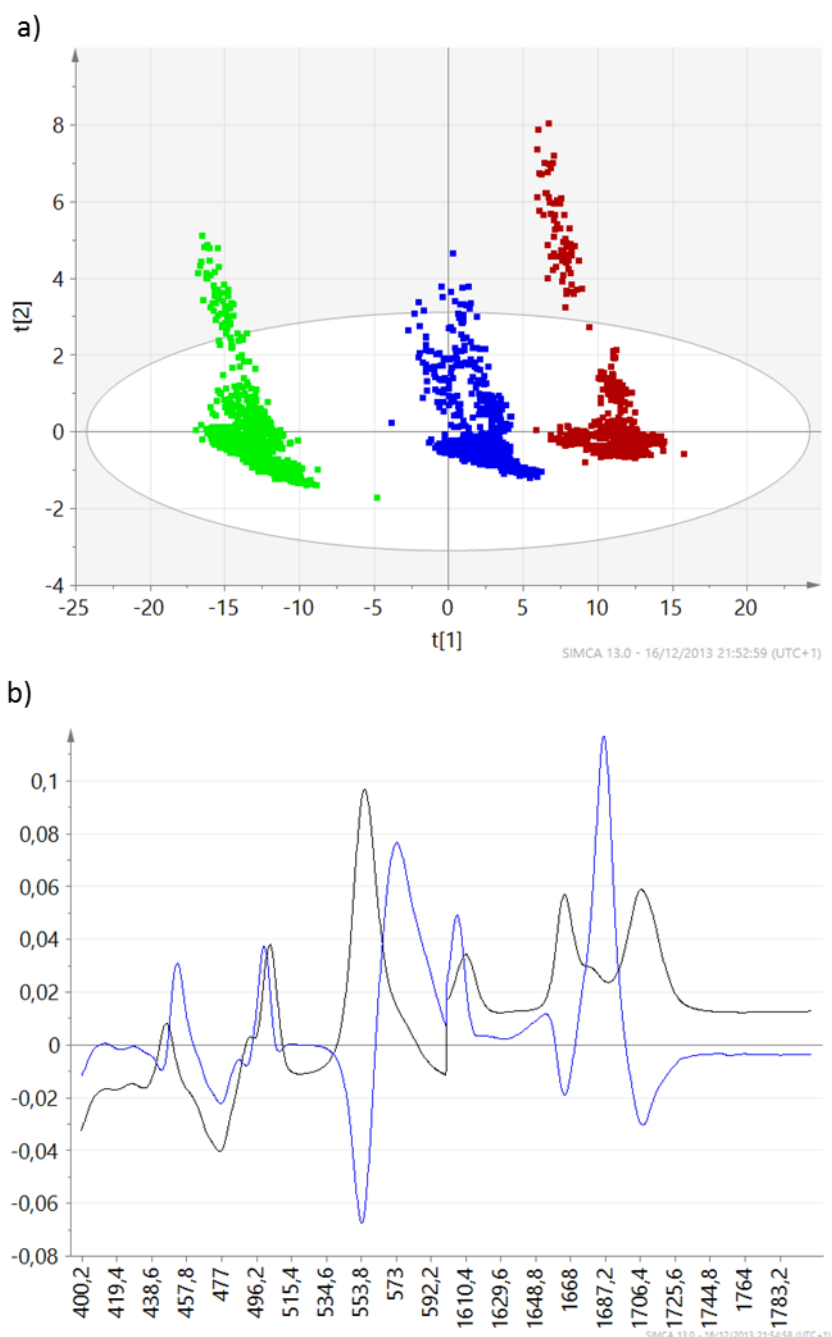


Figure 6.1: a) Score scatter plot of the first ($t[1]$) and second ($t[2]$) principal components of the PCA model on backscattering Raman data colored according to the concentration of theophylline: Green - 19.5 %; Blue - 29.25 %; Red - 39 % and b) PC1 loadings (black) and PC2 loadings (blue).

Regarding the PCA model obtained from NIR spectral data, clustering along PC1 is also present (Figure 6.2). Three individual clusters can be observed according to the concentration of theophylline. PC1 loadings contain a negative peak around 8900 cm^{-1} which is characteristic of theophylline and therefore the scores of this component are negatively correlated with the theophylline concentration. On the other hand, PC2 loadings are positive at 8936 cm^{-1} . This peak represents the theophylline hydration level, with higher scores as the theophylline hydration level increases (Figure 6.2). These conclusions agree with the findings of Fonteyne et al. [29].

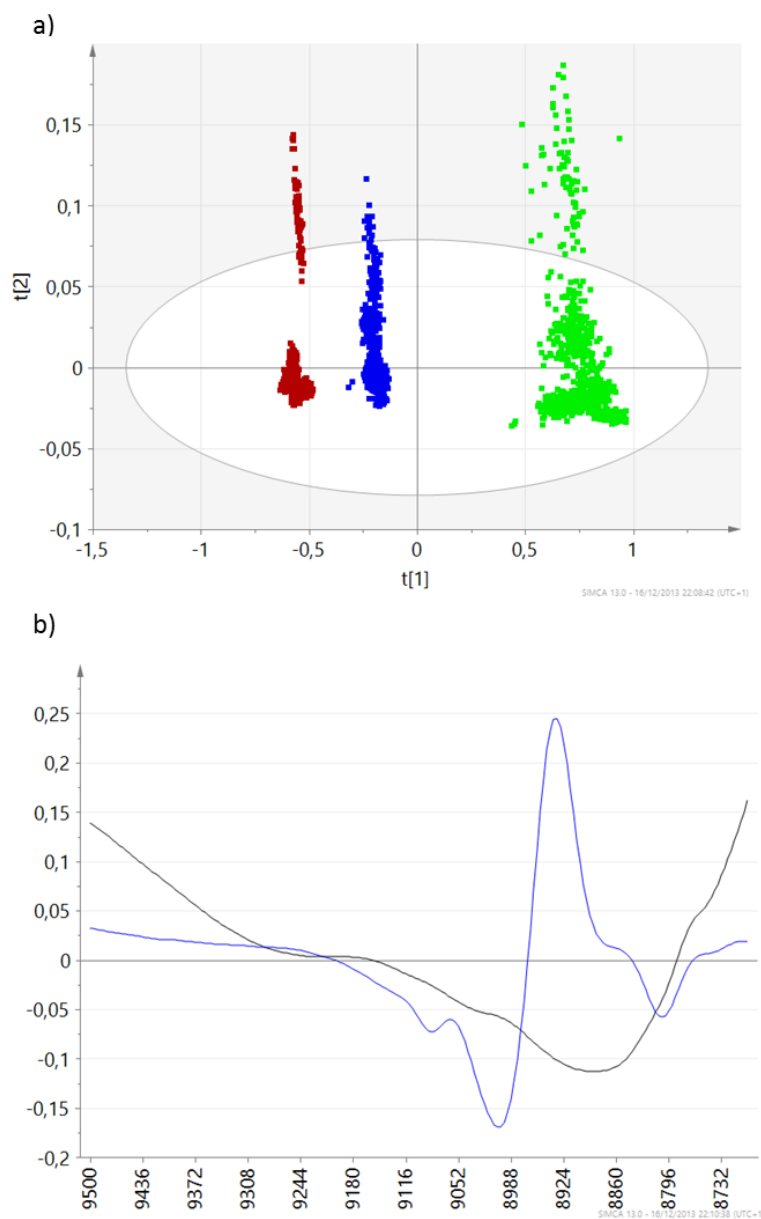


Figure 6.2: a) Score scatter plot of the first ([t1]) and second ([t2]) principal components of the PCA model on transmission NIR data colored according to the concentration of theophylline: Green - 19.5 %; Blue - 29.25 %; Red - 39 % and b) PC1 loadings (black) and PC2 loadings (blue).

PLS models were also built for the prediction of the theophylline content in the tablets. Forty eight of the 72 observations (tablets) were used from each batch to calculate the models and the remaining observations were utilized for validation. From all the tested pretreatments and wavenumber ranges the combinations providing the best model for each spectral technique were selected. Table 6.3 indicated that the captured variance in the spectra and in the theophylline content is similar for all models. The 3 spectroscopic techniques also present identical performance in predicting the content of theophylline with an error of prediction around 1 %.

3.2. Influence of granulation process parameters on granule properties

Based on the data of the particle size distribution (PSD), a significant relationship between amount of fines, amount of oversized agglomerates and all four process variables (API %, LFR, BT, SC) was detected (Figure 6.3a and b, Table 6.1). Due to the hydrophobic character of theophylline anhydrate, the formation of liquid bridges was hampered, resulting in smaller particles and hence a larger amount of fines. On the contrary, increasing the liquid feed rate, barrel temperature and the number of kneading elements yielded less fines (4.9 - 43.3 % < 300 μm) and more oversized agglomerates (4.4 - 43.0 % > 2000 μm). Due to a larger amount of available liquid, an increased solubility rate and a more intensive mixing of powder and granulation liquid, more liquid bridges could be formed between the powders. These results are in accordance with those obtained by other authors [1, 22, 30-33].

The friability of the granules (4.3 – 25.9 %) was clearly affected by the API %, LFR and SC (Figure 6.3c, Table 6.1). A lower theophylline concentration, higher liquid concentration and more kneading elements resulted in less friable granules. These results could also be linked with the formation of liquid bridges, which are a requisite for strong granules, resisting mechanical stress [22, 25, 30, 32, 33].

The granule bulk densities ranged from 0.369 to 0.487 g/ml and the tapped densities from 0.432 to 0.549 g/ml (Table 6.1). The number of kneading elements was the only process parameter significantly affecting these responses. Increasing the number of kneading elements yielded higher bulk and tapped densities, as more irregular-shaped coarse granules were formed, leading to a better packing [22]. Since the bulk and tapped densities were equally affected by the same process parameter, no significant effect of the process

variables on the flow properties, described by the compressibility index (CI), could be detected. Overall, compressibility indices only differed slightly from each other (7.3 - 14.6 %) (Table 6.1) and did not exceed 15 %, indicating a good flowability of the granules [34]. These conclusions were in agreement with the results obtained by Vercruyssen et al. and Djuric and Kleinebudde [22, 33].

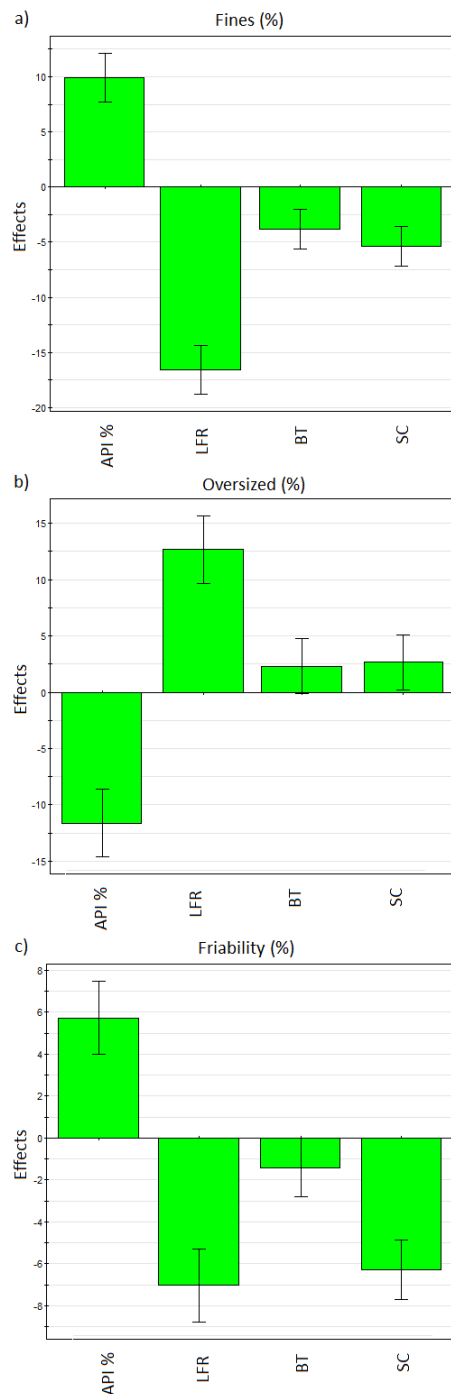


Figure 6.3: Effect plots for particle size distribution of granules ((a) Fines, (b) Oversized agglomerates) and (c) Friability. API %: Concentration of theophylline (%); LFR: Liquid feed rate (g/min); BT: Barrel temperature (°C); SC: Number of kneading elements.

3.3. Influence of granulation process parameters on tablet properties and tableting process parameters

The API % was the major factor of influence for all investigated responses. An overview of the results of the tablet analysis is given in Table 6.1. The responses could not only be linked with the granulation process parameters, but also with the granule characteristics.

For the results of tablet tensile strength, a clear influence of the theophylline concentration and, to a lesser extent, the liquid feed rate could be observed. A higher theophylline concentration and, in accordance with Keleb et al. and Tan et al., a lower water concentration yielded stronger tablets [35, 36]. The hydrophobic character of theophylline anhydrate and a low liquid feed rate during granulation hampered the formation of liquid bridges, resulting in more and smaller particles. As more fines were present, the (extragranular) specific surface area became larger [37-40]. Hence more interaction forces were likely to occur, contributing to higher tablet tensile strengths.

To explain the friability results, the same reasoning as for tensile strength applies. With more fines, the specific surface area increased and allowed more interaction between the granules, hence forming tablets with a higher resistance toward abrasion. This conclusion can be further supported by the observation that 9 out of 12 batches from the lowest API concentration failed the friability test. In these cases cracked, cleaved or broken tablets were detected after friability testing. For the tablets produced with the intermediate API concentration, this was only 4 out of 14. In contrast, none of the batches containing the highest amount of theophylline failed, with friability values ranging from 0.1 % to 0.3 %.

A significant positive influence of API %, LFR and SC on disintegration time was detected. The influence of theophylline concentration could be explained by its hydrophobicity, which hinders the percolation of liquid inside the granules. The effect of the water concentration and the amount of kneading elements could be related to the density of the granules. Higher liquid concentration stimulated the formation of liquid bridges in the granules and kneading elements improved the distribution of granulation liquid, resulting in granules with a higher density [22, 25, 30, 32, 33]. The denser tablet structure hampered the percolation of liquids inside the granules, resulting in tablets with a longer disintegration time (108 - 1576 s). Regarding tablet porosity (20.7 - 31.5 %), API %, LFR and BT were identified as significant

process variables. A low level of theophylline and a high level of liquid feed rate and barrel temperature resulted in tablets possessing a high porosity. These observations were also correlated with PSD, as the same set of process parameters yielded less fines. With less fines present, the intergranular pores during tableting are less likely to be filled, resulting in a lower overall porosity of the produced tablets. For the variation in tablet weight, illustrated by the variation coefficient (VC), the same argumentation can be followed with the API % as the significant process variable. Since die filling is a volumetric (and not gravimetric) process, the intergranular space plays an important role. When the theophylline concentration is high, more particles are present which are likely to fill this space, hence increasing the variability. However, although significant, the VC for all batches is rather small (<2.5 %) and far beneath the typically tolerated 4 % limit applied for high speed tableting. These results are all in strong accordance with previously published work on continuous granulation, which acknowledges the robustness of this process [22].

The data of the tableting process parameters (Table 6.1) identified a correlation between the dependent process parameters (fill depth (FD) (mm), main compression force (MCF) (kN), variation coefficient of main compression force (VC MCF) (%)) and the granule process parameters and resulting granule properties. A significant negative effect of the amount of kneading elements (SC) on fill depth can be detected. More kneading elements had a significant positive effect on bulk and tapped density: at a higher density of the packed granules, a smaller volume (i.e. a lower fill depth) is required to obtain the same weight (300 mg). None of the process parameters had a significant influence on MCF, which is in accordance with the results of CI. Furthermore, since differences in MCF between batches were limited (4.98-6.63 kN), these results illustrate again that all tablets were compressed at the same compression force. It should be mentioned that the absolute value of MCF is rather low, compared to commonly used compression forces (8-16 kN). By keeping this value low, it was possible to obtain tablets with different characteristics brought about by the different granule process parameter settings. At high compression forces, this information is likely lost. A significant positive effect of the API % on VC MCF was observed. These observations were also linked to PSD and tablet weight variability. Although correlated, the VC in tablet weight is much smaller than the VC in MCF, due to the exponential relation between these two tableting parameters.

4. CONCLUSIONS

The main goal of this study to predict tablet physical properties from backscattering Raman, transmission Raman and transmission NIR spectroscopic data was not possible to achieve. The utilized PAT-tools were not able to capture the differences in physical properties between tablets. This suggests that in previous research in which tablets were compressed with different compression forces, the correlation between spectral data and tablet properties was not only linked to differences in bonding and density, but also to differences in tablet dimension (thickness).

In accordance with previous research it was possible to predict the theophylline content by means of a PLS approach. All spectroscopic methods revealed a similar prediction performance with an RMSEP around 1 %. PCA models allowed a distinction between the three different levels of theophylline and a determination of the API's hydration level. Furthermore, the effect of several granulation process variables on granule quality, tablet quality and measured tableting parameters was evaluated by means of a DoE. For the granule properties, theophylline concentration and moisture content were identified as the most important parameters. The same effect of theophylline concentration was observed for the tablet properties. The dependent tableting parameters were mainly influenced by the API concentration (VC MCF) and the screw configuration (FD).

Even though it was not possible to predict tablet physical properties with the applied spectroscopic techniques, these PAT-tools have a significant added value when applied for the monitoring of a continuous process since API concentration is an important parameter influencing both granule and tablet properties and it is an important quality attribute for the end product. Based on the good models for this process parameter, implementation of NIR and/or Raman probes in a tablet production line will contribute to the monitoring, adaption and understanding of the process as well as to quality assurance of the end product.

REFERENCES

- [1] M. Fonteyne, J. Vercruysse, D.C. Díaz, D. Gildemyn, C. Vervaet, J.P. Remon, T.D. Beer, Real-time assessment of critical quality attributes of a continuous granulation process, *Pharm. Dev. Technol.* 18 (2011) 85-97.
- [2] K. Jarvinen, W. Hoehe, M. Jarvinen, S. Poutiainen, J. Juuti, S. Borchert, In-line monitoring of the drug content of powder mixtures and tablets by near-infrared spectroscopy during the continuous direct compression tableting process, *Eur. J. Pharm. Sci.* 48 (2013) 680-688.
- [3] H. Leuenberger, New trends in the production of pharmaceutical granules: batch versus continuous processing, *Eur. J. Pharm. Biopharm.* 52 (2001) 289-296.
- [4] J. Vercruysse, U. Delaet, I. Van Assche, P. Cappuyens, F. Arata, G. Caporicci, T. De Beer, J.P. Remon, C. Vervaet, Stability and repeatability of a continuous twin screw granulation and drying system, *Eur. J. Pharm. Biopharm.* 85 (2013) 1031-1038.
- [5] C. Vervaet, J.P. Remon, Continuous granulation in the pharmaceutical industry, *Chem. Eng. Sci.* 60 (2005), 3949-3957.
- [6] C. Vervaet, J.P. Remon, Continuous granulation, in: D.M. Parikh (Ed.), *Handbook of Pharmaceutical Granulation Technology*, Informa Healthcare USA Inc., New York, 2009, pp. 308-322.
- [7] International Conference on Harmonization (ICH) of technical requirements for registration of pharmaceuticals for human use, Topic Q8(R2): Pharmaceutical Development, in, Geneva, 2009.
- [8] International Conference on Harmonization (ICH) of technical requirements for registration of pharmaceuticals for human use, Topic Q9: Quality Risk Management in, Geneva, 2005.
- [9] International Conference on Harmonization (ICH) of technical requirements for registration of pharmaceuticals for human use, Topic Q10: Pharmaceutical Quality System, in, Geneva, 2008.

- [10] United States Food and Drug Administration (FDA), Guidance for industry - PAT - A framework for innovative pharmaceutical development, manufacturing, and quality assurance, in, 2004.
- [11] United States Food and Drug Administration (FDA), Guidance for industry - Process Validation: General principles and practices, in, 2011.
- [12] J. Johansson, S. Pettersson, S. Folestad, Characterization of different laser irradiation methods for quantitative Raman tablet assessment, *J. Pharm. Biomed. Anal.* 39 (2005) 510-516.
- [13] W. Kessler, D. Oelkrug, R. Kessler, Using scattering and absorption spectra as MCR-hard model constraints for diffuse reflectance measurements of tablets, *Anal. Chim. Acta* 642 (2009) 127-134.
- [14] Y. Chen, S.S. Thosar, R.A. Forbess, M.S. Kemper, R.L. Rubinovitz, A.J. Shukla, Prediction of drug content and hardness of intact tablets using artificial neural network and near-infrared spectroscopy, *Drug Dev. Ind. Pharm.* 27 (2001) 623-631.
- [15] M. Donoso, D.O. Kildsig, E.S. Ghaly, Prediction of tablet hardness and porosity using near-infrared diffuse reflectance spectroscopy as a nondestructive method, *Pharm. Dev. Technol.* 8 (2003) 357-366.
- [16] M. Donoso, E.S. Ghaly, Prediction of tablets disintegration times using near-infrared diffuse reflectance spectroscopy as a nondestructive method, *Pharm. Dev. Technol.* 10 (2005) 211-217.
- [17] N.K. Ebube, S.S. Thosar, R.A. Roberts, M.S. Kemper, R. Rubinovitz, D.L. Martin, G.E. Reier, T.A. Wheatley, A.J. Shukla, Application of near-infrared spectroscopy for nondestructive analysis of Avicel® powders and tablets, *Pharm. Dev. Technol.* 4 (1999) 19-26.
- [18] J.D. Kirsch, J.K. Drennen, Nondestructive tablet hardness testing by near-infrared spectroscopy: a new and robust spectral best-fit algorithm, *J. Pharm. Biomed. Anal.* 19 (1999) 351-362.

- [19] K. Morisseau, C. Rhodes, Near-infrared spectroscopy as a nondestructive alternative to conventional tablet hardness testing, *Pharm. Res*, 14 (1997) 108-111.
- [20] R.B. Shah, M.A. Tawakkul, M.A. Khan, Process analytical technology: Chemometric analysis of Raman and near-infrared spectroscopic data for predicting physical properties of extended release matrix tablets, *J. Pharm. Sci.* 96 (2007) 1356-1365.
- [21] H. Wang, C.K. Mann, T.J. Vickers, Effect of powder properties on the intensity of Raman scattering by crystalline solids, *Appl. Spectrosc.* 56 (2002) 1538-1544.
- [22] J. Vercruyssen, D. Córdoba Díaz, E. Peeters, M. Fonteyne, U. Delaet, I. Van Assche, T. De Beer, J.P. Remon, C. Vervaet, Continuous twin screw granulation: Influence of process variables on granule and tablet quality, *Eur. J. Pharm. Biopharm.* 82 (2012) 205-211.
- [23] L. Chablani, M. Taylor, A. Mehrotra, P. Rameas, W. Stagner, Inline real-time near-infrared granule moisture measurements of a continuous granulation–drying–milling process, *AAPS PharmSciTech.* 12 (2011) 1050-1055.
- [24] E. Peeters, T. De Beer, C. Vervaet, J.P. Remon, Reduction of tablet weight variability by optimizing paddle speed in the forced feeder of a high-speed rotary tablet press, *Drug. Dev. Ind. Pharm.* (2014) (doi:10.3109/03639045.2014.884121).
- [25] B. Van Melkebeke, C. Vervaet, J.P. Remon, Validation of a continuous granulation process using a twin-screw extruder, *Int. J. Pharm.* 356 (2008) 224-230.
- [26] L. Eriksson, E. Johansson, N. Kettaneh-Wold, C. Wikström, S. Wold, *Design of Experiments - Principles and Applications*, third ed., MKS Umetrics AB, Umea, 2008.
- [27] R.L. Carr, Evaluating flow properties of solids, *Chem. Eng.* (1965) 163-168.
- [28] J.T. Fell, J.M. Newton, Determination of tablet strength by the diametral-compression test, *J. Pharm. Sci.* 59 (1970) 688-691.
- [29] M. Fonteyne, S. Soares, J. Vercruyssen, E. Peeters, A. Burggraeve, C. Vervaet, J.P. Remon, N. Sandler, T. De Beer, Prediction of quality attributes of continuously produced granules using complementary PAT tools, *Eur. J. Pharm. Biopharm.* 82 (2012) 429-436.

- [30] R.M. Dhenge, R.S. Fyles, J.J. Cartwright, D.G. Doughty, M.J. Hounslow, A.D. Salman, Twin screw wet granulation: Granule properties, *Chem. Eng. J.* 164 (2010) 322-329.
- [31] A.S. El Hagrasy, J.R. Hennenkamp, M.D. Burke, J.J. Cartwright, J.D. Litster, Twin screw wet granulation: Influence of formulation parameters on granule properties and growth behavior, *Powder Technol.* 238 (2013) 108-115.
- [32] E.I. Keleb, A. Vermeire, C. Vervaet, J.P. Remon, Twin screw granulation as a simple and efficient tool for continuous wet granulation, *Int. J. Pharm.* 273 (2004) 183-194.
- [33] D. Djuric, P. Kleinebudde, Impact of screw elements on continuous granulation with a twin-screw extruder, *J. Pharm. Sci.* 97 (2008) 4934-4942.
- [34] A.M. Railkar, J.B. Schwartz, Evaluation and comparison of a moist granulation technique to conventional methods, *Drug Dev. Ind. Pharm.* 26 (2000) 885-889.
- [35] E.I. Keleb, A. Vermeire, C. Vervaet, J.P. Remon, Cold extrusion as a continuous single-step granulation and tableting process, *Eur. J. Pharm. Biopharm.* 52 (2001) 359-368.
- [36] L. Tan, A.J. Carella, Y. Ren, J.B. Lo, Process optimization for continuous extrusion wet granulation, *Pharm. Dev. Technol.* 16 (2011) 302-315.
- [37] M. Dumarey, H. Wikstrom, M. Fransson, A. Sparen, P. Tajarobi, M. Josefson, J. Trygg, Combining experimental design and orthogonal projections to latent structures to study the influence of microcrystalline cellulose properties on roll compaction, *Int. J. Pharm.* 416 (2011) 110-119.
- [38] M.G. Herting, P. Kleinebudde, Studies on the reduction of tensile strength of tablets after roll compaction/dry granulation, *Eur. J. Pharm. Biopharm.* 70 (2008) 372-379.
- [39] M. Šantl, I. Ilić, F. Vrečer, S. Baumgartner, A compressibility and compactibility study of real tableting mixtures: The impact of wet and dry granulation versus a direct tableting mixture, *Int. J. Pharm.* 414 (2011) 131-139.
- [40] C. Sun, M.W. Himmelpach, Reduced tableability of roller compacted granules as a result of granule size enlargement, *J. Pharm. Sci.* 95 (2006) 200-206.

GENERAL CONCLUSIONS AND FUTURE PERSPECTIVES

The goal of this research project was to increase the understanding of the influence of the starting material properties and process parameters on dependent process parameters and tablet properties, using a high-speed rotary tablet press (Modul™ P, GEA Process Engineering, Courtoy™, Halle, Belgium).

When manufacturing tablets containing magnesium stearate, not only the blending step prior to tableting should be optimized (adding magnesium stearate at the end of the blending cycle, using a low lubricant concentration, mixing using low shear blenders), but also the mixing effect of the feeder should be taken into account. By analyzing the data collected at the different stations on the tableting machine, it can be concluded that the presence of magnesium stearate clearly influences the tableting process. The paddle speeds on the other hand, did not contribute to large changes in the tableting process (packing, compactability, lubrication), except at the filling station. This was in contrast to the different blending methods prior to tableting. However, the paddle speeds have an influence on the shear rate and material residence time inside the forced feeder, inducing an effect on the flowability of the powders and on the tensile strength of the tablets produced, and with that on the quality of the end product. This illustrates that the paddles are more than just an aid to force material into a die, and the passage of the material through the forced feeder can be considered as an additional blending step.

The effect of the forced feeder was further investigated using two excipients possessing a different flow behavior, microcrystalline cellulose (MCC) and dibasic calcium phosphate dihydrate (DCP). Using DoE, the study indicated that the paddle speeds in the forced feeder are of minor importance for tablet weight (variability) in case of powders with excellent flowability (DCP), whereas the paddle speeds affected tablet weight of fairly flowing powders (MCC). The opposite phenomenon could be seen on the volume of powder in the feeder. Tableting speed played a role in the tablet weight and weight variability, whereas changing fill depth exclusively influenced the tablet weight for both powders. The DoE approach also allowed predicting the optimum combination of studied process parameters yielding the lowest tablet weight variability. Using Monte Carlo simulations the robustness of

the process was assessed. The multi-dimensional combination and interaction of input variables (factor ranges) reflected the design space which results in acceptable response criteria with a reasonable probability.

Also the influence of the compression step was studied. Granules, containing 80 % ibuprofen, known for its plastically and elastically deforming behavior, were compressed into tablets. By analyzing the data with Principal Component Analysis (PCA), it was seen that the main source of variation in the dataset was captured in PC1 which was composed mainly by the changes caused by an alteration of the tableting speed. The second major direction of variation in the dataset (PC2) was the change in main compression displacement. PC3 was mainly composed by the displacement at precompression and correlated variables. Finally, the main compression force contributes to a large extent to the variance captured by PC4. Based on the PCA-analysis, it could be concluded that the tableting speed is a crucial variable in performing tableting experiments, as it contributed the most to the observed variance. Mainly its influence on the shape of the force-time profile and the dwell time has to be considered. Secondly, the analysis showed that the moving roller set-up influenced to a great extent the tableting process. Using displacement, both on pre- and main compression, decreased the observed variability in the process and prolonged the dwell time significantly. For main compression displacement, lowering of the ejection force with increased displacement could also be considered as an important effect. Moreover, the dimensionless parameter, t/p_{mean} ratio, could be considered a sensitive parameter to describe the shape of the force-time profile within the range of the parameter setting used. Finally, by the contribution of PC4 to the observed variance, it could be concluded that the tableting speed and the displacement have a larger influence on the compression event (i.e. the other process variables) than the applied (main compression) force. Partial Least Squares (PLS) revealed that mainly the tableting speed and the main compression force attributed to the final tablet properties and that the relation between process parameters and tablet properties was not straight-forward, as the different variables all contributed simultaneously to the final tablet characteristics. Overall, the analysis provided a summary of the contribution of the moving roller set-up to the tableting process and tablet properties. The research project showed that a large amount of parameters influence the compression cycle and it is difficult, if not impossible, to study the contribution of all factors separately.

The main goal of the last study was to predict tablet physical properties from backscattering Raman, transmission Raman and transmission NIR spectroscopic data. The utilized PAT-tools were not able to capture the differences in physical properties between tablets. This suggests that in previous research in which tablets were compressed with different compression forces, the correlation between spectral data and tablet properties was not only linked to differences in bonding and density, but also to differences in tablet dimension (thickness). In accordance with previous research it was possible to predict the theophylline content by means of a PLS approach. All spectroscopic methods revealed a similar prediction performance with an RMSEP around 1 %. PCA models allowed a distinction between the three different concentration levels of theophylline and a determination of the API's hydration level. Furthermore, the effect of several granulation process variables on granule quality, tablet quality and measured tableting parameters was evaluated by means of a DoE. For the granule properties, theophylline concentration and moisture content were identified as the most important parameters. The same effect of theophylline concentration was observed for the tablet properties. The dependent tableting parameters were mainly influenced by the API concentration and the screw configuration. Even though it was not possible to predict tablet physical properties with the applied spectroscopic techniques, these PAT-tools have a significant added value when applied for the monitoring of a continuous process since API concentration is an important parameter influencing both granule and tablet properties and it is an important quality attribute for the end product. Based on the good models for this process parameter, implementation of NIR and/or Raman probes in a tablet production line will contribute to the monitoring, adaption and understanding of the process as well as to quality assurance of the end product.

Overall, this research project provided process knowledge about the tableting process on a high-speed rotary tablet press. Nevertheless, an extension of this project is necessary to further broaden process knowledge. Below, a few topics are identified for further investigation:

- Although the use of Design of Experiments was a good tool to optimize the die filling with the current feeder design, it has to be mentioned that the obtained results are product-, machine- and tooling specific. Moreover, some mechanisms were not addressed, e.g. the movement of the air in the feeder and its influence on the

movement of material; the influence of the overfill cams; the influence of the paddle design;... Further investigation is necessary to gain a thorough mechanistic understanding of the die filling process. Hence, this is crucial to ensure good tablet quality, high output and high process yields. Additional PAT-tools are believed to be a valuable instrument to further increase the process knowledge of this complicated process step in the compression cycle.

- Based on the results obtained in this research project, it is clear that the paddles have an influence on the properties of the starting material, the process parameters and the quality of the produced tablets. The current design of the feeder attributes to a great extent to undesirable effects, e.g. segregation, compaction in the feeder, breaking-up of granules due to shear forces, overblending of lubricant... These issues make the die-filling step in production often the rate-limiting step. This affects the maximum achievable production speed for a given product and consequently also the production capacity. Additionally, the current design typically has a 1 to 2 % powder yield loss, and with increasing costs for API's, this is a growing concern to the tablet production industry. Consequently, besides gaining understanding in the die-filling process with the current design of feeder, an optimization of the present powder hopper-, chute- and feeder design will be necessary to keep up with the emerging challenges.
- Based on the research involving the compression station and the moving roller set-up, it could be concluded that this compression mechanism has some major influences on the shape of the force-time profile and the variability of the process. Its influence on tablet properties was however less pronounced. To increase the understanding, this research should be extended with other formulations.
- Throughout this research project, the press and its built-in instrumentation were used as an analytical tool to gain insight in the tableting process in a manufacturing setting. However, the data analysis was not always straight forward and rather time-consuming. The main reason for this is that the instrumentation is more production-centered, with the aim of controlling and managing an established production process. In order to be able to extend the process knowledge, an evaluation of the

implementation of the instrumentation is preferable. For instance, next to the load cells, which are positioned underneath the bottom roller, an additional load cell at the upper punch and a radial die-wall sensor could greatly improve the understanding of the force distribution during compression and unloading. Not only the implementation of this instrumentation, but also the interpretation of the obtained information will be a great challenge in future work.

- Over the last years it became clear that PAT is a valuable and necessary tool in the shift from batch to continuous production. Already some research groups and pharmaceutical companies explored this field and obtained promising results for its applicability in for instance the end-point determination of (continuous) blending experiments, the liquid distribution and moisture content in (continuous) wet granulation processes, the end-point determination of coating experiments etc... In the tableting process, these analytical chemistry tools are already applied in the hopper, chute and feeder to control blend homogeneity and detect segregation, or at the ejection chute to measure content uniformity of the produced tablets. However, the determination of other critical phenomena (e.g. overblending of lubricant) and critical quality attributes (e.g. tensile strength, friability, dissolution rate) still encounters some difficulties. In theory, tablet quality is still mainly assessed offline by performing traditional methods of analysis on tablets collected at the end of production. These methods are often destructive and involve sample pretreatment. As a consequence, the latter becomes the rate-limiting step and annuls the advantages of the fast continuous production process. Consequently, to allow future real-time release, other techniques, either implemented into the tablet press or at the end of the production process, will have to be explored and its applicability investigated.

SUMMARY

Seen in the light of the new movements of Quality-by-Design within the pharmaceutical industry, it appears obvious that there is a need for new knowledge to fund a base for a thorough understanding of the continuous tableting process, a critical unit operation in the continuous manufacturing of solid dosage forms. This thesis aimed to contribute in this large context by the investigation of the tableting process on a high-speed rotary tablet press. The goal was to increase the understanding of the influence of the properties of the starting material and process parameters on dependent process parameters and tablet properties. Since the PAT-initiative stimulates the introduction of new analytical tools to enhance process understanding and product quality, additional analytical chemistry tools, next to the build-in instrumentation, were used. Moreover, due to the large amount of data obtained, Design of Experiments (DoE) and Multivariate Data Analysis (MVA) were administered to perform experiments and analyze data in a structured manner.

In the **Introduction**, an overview is given of the different tableting machines used in research and development and manufacturing. The application of these instrumented machines in both fundamental compaction research as well as in every day production is discussed. Also the use of additional PAT-tools to enhance product and process understanding is addressed. Finally, due to the large amount of data an instrumented tablet press generates, the use of DoE and MVA as valuable tools to conduct experiments and analyze data in a structured manner is highlighted in this chapter.

All tableting experiments described in this thesis were conducted on the ModulTM P (GEA Process Engineering, CourtoyTM, Halle, Belgium). In **Chapter 2**, a general description of the machine design and the set-up as installed at Ghent University is provided. The component units that were subject of research are described in more detail. Finally, the most relevant instrumentation and control mechanisms integrated in the press and the method of data collection is highlighted.

The purpose of the research as described in **Chapter 3** was to investigate the influence of paddle speed on the tensile strength of tablets prepared out of blends of microcrystalline

cellulose and magnesium stearate. Four powder mixtures were prepared, one of them consisting out of pure microcrystalline cellulose, the others out of a mixture of microcrystalline cellulose and magnesium stearate in a concentration of 0.5 % with the difference between the three latter mixtures being the method of blending (low shear 3 minutes; low shear 15 minutes; high shear 5 minutes). After blending the mixtures were compressed into tablets. All parameters of the tableting cycle were kept constant except the speed of the paddles in the forced feeder. The tablets were stored overnight and their weight, hardness, thickness, diameter and friability was determined. The results indicate that the preparation method has an influence on the sensitivity of the mixture to the change of paddle speed. The tensile strength of the tablets made out of pure microcrystalline cellulose did not change with changing paddle speed. The tablets prepared by low shear mixing became softer with increasing paddle speed, albeit to a different extent, depending on the blending time. For the tablets prepared out of the mixture which was blended with the high shear blender, no change in hardness could be observed with changing paddle speed, but was overall low, suggesting that overlubrication of microcrystalline cellulose already occurred during the preceding blending step. Furthermore, analysis of the machine parameters allowed evaluation of the influence of the paddles on the flowability, initial packing and compactability of the powder mixtures. The results elucidated the influence of magnesium stearate but, except at the filling station, the differences in paddle speed did not further contribute to differences in the tableting process (packing, compactability, lubrication). It could be concluded that in the production of tablets with powder mixtures containing magnesium stearate, not only care has to be taken at the blending step prior to tableting, but also at the tableting process itself, as the paddle speed in the feeder can have an important effect on the tensile strength, a critical quality attribute, of the tablets produced.

The effect of the forced feeder was further investigated using two excipients possessing a different flow behavior, microcrystalline cellulose (MCC) and dibasic calcium phosphate dehydrate (DCP). The aim of the study as outlined in **Chapter 4** was to investigate the influence of paddle speeds and fill depth at different tableting speeds on the weight and weight variability of tablets. The two excipients were selected as model powders, based on their different flow behavior. Tablets were manufactured using DoE. During each experiment

also the volume of powder in the forced feeder was measured. Analysis of the DoE revealed that paddle speeds are of minor importance for tablet weight but significantly affect volume of powder inside the feeder in case of powders with excellent flowability (DCP). The opposite effect of paddle speed was observed for fairly flowing powders (MCC). Tableting speed played a role in weight and weight variability, whereas changing fill depth exclusively influenced tablet weight. The DoE approach allowed predicting the optimum combination of process parameters leading to minimum tablet weight variability. Monte Carlo simulations allowed assessing the probability to exceed the acceptable response limits if factor settings were varied around their optimum. This multi-dimensional combination and interaction of input variables leading to response criteria with acceptable probability reflected the design space.

While the compaction rate in most tableting machines is only determined by the tableting speed, the high speed rotary tableting machine used in this research project can adjust and control the dwell time independently from the tableting speed, using an air compensator which allows displacement of the upper (pre-) compression roller. The effect of this machine design on process parameters and tablet properties was investigated in **Chapter 5**. Granules, containing 80 % ibuprofen, were compressed into tablets. The low melting point, poor flow, physico-mechanical properties (particle size distribution, shape, particle surface roughness) and deformation mechanism of ibuprofen in combination with its high dose in tablets all contribute to the problems observed during the compaction of ibuprofen-based formulations. Since ibuprofen is plastically and elastically deforming, the rate of compaction plays an important role in both the final tablet properties and the risk of capping, laminating and sticking to the punches. Tablets were prepared at 250, 500 and 1000 tablets per minute via double compression (pre- and main compression) with or without extended dwell time. Prior to tableting, granule properties were determined. Process parameters and tablet properties were analyzed using Multivariate Data Analysis. Principal Component Analysis (PCA) provided an overview of the main phenomena determining the tableting process and Partial Least Squares Analysis (PLS) unveiled the main variables contributing to the observed differences in the tablet properties. Based on the PCA-analysis, it could be concluded that the tableting speed is a crucial variable in performing tableting experiments. Moreover, the analysis showed that the moving roller set-up influenced to a great extent the tableting

process. Using displacement, both on pre- and main compression, decreased the observed variability in the process and prolonged the dwell time significantly. For main compression displacement, the decrease of the ejection force with increased displacement could also be considered as an important effect. The dimensionless parameter, t/p_{mean} ratio, could be considered a sensitive parameter to describe the shape of the force-time profile within the range of the parameter setting used. Finally, it could be concluded that the tableting speed and the displacement have a larger influence on the compression event (i.e. the other process variables) than the applied (main compression) force. PLS revealed that mainly the tableting speed and the main compression force attributed to the final tablet properties and that the relation between process parameters and tablet properties was not straightforward, as the different variables all contributed simultaneously to the final tablet characteristics. Overall, the analysis provided a summary of the contribution of the moving roller set-up to the tableting process and tablet properties. The research showed that a large amount of parameters influence the compression cycle and it is difficult, if not impossible, to study the contribution of all factors separately.

In **Chapter 6** it was investigated if backscattering Raman, transmission Raman and transmission Near Infrared (NIR) spectroscopy could be used for the prediction of the physical properties of tablets. Granules with different characteristics were produced on the Consigma™-25 continuous powder-to-tablet line by varying a number of granulation parameters (API concentration, liquid feed rate, barrel temperature and screw configuration) according to a full-factorial Design of Experiments. Granules were oven-dried and processed into tablets on a MODUL™ P high speed rotary tablet press. Tableting process parameters were adjusted to obtain tablets with a uniform tablet weight, thickness and diameter for all batches. From all tablets, transmission and backscattering Raman spectra and transmission NIR spectra were collected offline. Tensile strength, friability, disintegration time, apparent density and porosity were determined with traditional analyzing methods. PLS regression was utilized to model and correlate spectral information to tablet properties. Predictive PLS models for disintegration, friability, porosity and tensile strength could not be established. It could be concluded that the utilized PAT-tools are not suitable for the prediction of the physical properties of tablets. PCA was effectively utilized to distinguish between different theophylline concentrations and its hydration level. The

differences between backscattering Raman, transmission Raman and NIR spectroscopy performance in the quantification of theophylline content by means of a PLS model was insignificant. Furthermore, Multiple Linear Regression analysis (MLR) allowed a successful investigation on how the changes in the granulation parameters affected granule properties, tablet properties and dependent tableting process parameters.

In het licht van de nieuwe *Quality-by-Design* beweging in de farmaceutische industrie, is er een duidelijke nood aan een hernieuwde interesse voor het continue tabletteerproces, welke een kritische stap is in de productie van vaste toedieningsvormen. Door het onderzoeken van het tabletteerproces op een industriële machine hoopt het onderzoek verricht in deze thesis hiertoe bij te dragen. Het doel was om een groter inzicht te verwerven in welke eigenschappen van het startmateriaal en procesparameters de afhankelijke procesparameters en de uiteindelijke tableteigenschappen beïnvloeden. Daar het PAT-initiatief van de FDA de implementatie van nieuwe analytische technieken in het verwerven van proces- en productinzicht stimuleert, werden deze, naast de ingebouwde instrumentatie, aangewend in dit onderzoeksproject. Om de grote hoeveelheid aan procesparameters en gegenereerde data op een gestructureerde manier te onderzoeken en analyseren, werden *Design of Experiments* (DoE) en *Multivariate Data Analysis* (MVA) gebruikt.

In **de Introductie** wordt een overzicht gegeven van de verschillende tabletteermachines die gebruikt worden in en enerzijds onderzoek en ontwikkeling en anderzijds in productie. De toepassing van deze machines in zowel het fundamenteel compactie-onderzoek als in dagelijkse productie wordt besproken, net als het gebruik van additionele PAT-technieken. Tot slot wordt kort toegelicht waarom DoE en MVA als waardevolle technieken kunnen beschouwd worden in het uitvoeren van experimenten en het analyseren van data.

Alle tabletteerexperimenten beschreven in deze thesis zijn uitgevoerd op de ModulTM P (GEA Process Engineering, CourtoyTM, Halle, België). In **Hoofdstuk 2** wordt een algemene beschrijving van deze machine gegeven zoals deze aanwezig is aan de Universiteit Gent. De verschillende onderdelen die het onderwerp waren van onderzoek zijn in meer detail beschreven. Verder worden de meest relevante instrumentatie, geïntegreerde controlemechanismen en de methode van datacollectie belicht.

Het doel van het onderzoek beschreven in **Hoofdstuk 3** was om de invloed van de schoepensnelheid op de hardheid van tabletten geproduceerd uit verschillende mengsels van microkristallijn cellulose en magnesiumstearaat na te gaan. Hiervoor werden vier

verschillende poedermengsels gebruikt. Eén daarvan bestond uit enkel microkristallijn cellulose, de anderen uit mengsels van microkristallijn cellulose en magnesiumstearaat in een concentratie van 0.5 %. De mengsels met magnesiumstearaat verschilden verder in de gebruikte mengmethode: gemengd aan lage intensiteit voor 3 minuten; gemengd aan lage intensiteit voor 15 minuten; gemengd aan hoge intensiteit voor 5 minuten. Na mengen werden de mengsels gecompriëerd tot tabletten. Buiten de schoepensnelheid in de vulschoen, werden alle procesparameters tijdens het tableteren constant gehouden. De tabletten werden overnacht bewaard en hun gewicht, hardheid, dikte, diameter en friabiliteit werden bepaald. De resultaten toonden aan dat de bereidingsmethode een invloed had op de gevoeligheid van de mengsels aan de verandering in schoepensnelheid. De hardheid van de tabletten die enkel uit microkristallijn cellulose bestonden veranderde niet door de schoepensnelheid te wijzigen. De tabletten bereid uit de mengsels die met lage intensiteit gemengd werden verminderden in hardheid bij een stijging van de schoepensnelheid, al was de mate waarin deze verandering optrad wel afhankelijk van de mengmethode. Voor de tabletten die geproduceerd werden met het mengsel dat onder hoge intensiteit was gemengd kon er geen verandering in de hardheid door wijziging van de schoepensnelheid vastgesteld worden. Deze was echter globaal lager als die van de andere tabletten, wat erop wijst dat overlubrificatie van het microkristallijn cellulose had plaatsgevonden tijdens de voorgaande mengstap. Verder liet de analyse van de machineparameters toe om de invloed van de schoepensnelheid op de vloeibaarheid, de initiële densificatie en de compactibiliteit van de poeders te evalueren. De resultaten toonden duidelijk de invloed van de aanwezigheid van magnesiumstearaat aan op het vullingsproces. Echter, een invloed op het verdere tableteerproces (densificatie, compactibiliteit, lubricatie) werd niet waargenomen. Er kon geconcludeerd worden dat tijdens de productie van tabletten met mengsels die magnesiumstearaat bevatten niet enkel aandacht moet geschonken worden aan het mengproces voorafgaand aan het tableteren, maar ook aan het tableteerproces zelf, aangezien de schoepen in de vulschoen een belangrijk effect kunnen hebben op de hardheid van de tabletten, welke een kritische kwaliteitseigenschap is van de geproduceerde tabletten.

Het effect van de vulschoen werd verder onderzocht door twee excipiënten met een verschillend vloeigedrag, microkristallijn cellulose (MCC) en dibasisch calcium fosfaat (DCP)

te gebruiken. Het doel van de studie zoals beschreven in **Hoofdstuk 4** was om de invloed van de schoepensnelheid en de vuldiepte bij verschillende tabletteersnelheden op het gewicht en de gewichtsvariatie van tabletten te onderzoeken. De twee excipiënten werden gekozen als model poeders omwille van hun verschillende vloeibaarheid. De tabletten werden geproduceerd via een DoE. Tijdens elk experiment werd ook het volume in de vulschoen bepaald. Analyse van het DoE toonde aan dat de schoepensnelheid van ondergeschikt belang is bij goed vloeiende poeders (DCP), maar dat ze een significant effect hebben op het volume van het poeder binnenin de vulschoen. Het omgekeerde effect kon worden vastgesteld voor het minder goed vloeiende poeder (MCC). Waar de vuldiepte enkel het absolute gewicht beïnvloedde, speelde de tabletteersnelheid zowel een rol in het absolute gewicht als in de gewichtsvariabiliteit. Het DoE maakte het mogelijk om de (optimale) combinatie van procesparameters te voorspellen die zou leiden naar de minimale gewichtsvariabiliteit. Monte Carlo simulaties lieten toe om de probabiliteit van het overschrijden van aanvaardbare responslimieten in te schatten wanneer de instellingen van de factoren rond hun optimale waarden zouden worden gevarieerd. Het *design space* wordt weerspiegeld door deze multi-dimensionele combinatie en interacties van variabelen die leiden tot respons criteria met een aanvaardbare probabiliteit.

Terwijl de compressiesnelheid in de meeste tabletteermachines alleen bepaald wordt door de tabletteersnelheid, kan dat in de machine die in deze thesis gebruikt wordt onafhankelijk van elkaar gecontroleerd worden. Dit gebeurt door gebruik te maken van een compensator gevuld met lucht, die verticale beweging van de bovenste (pre-)compressierol toelaat. Het effect van dit mechanisme op de procesparameters en de tableteigenschappen werd onderzocht in **Hoofdstuk 5**. Granulen, die 80 % ibuprofen bevatten, werden gecompriëerd tot tabletten. Ibuprofen staat bekend om zijn slechte compactie-eigenschappen die mede veroorzaakt worden door het lage smeltpunt, de slechte vloeieigenschappen, de fysico-mechanische eigenschappen (partikelgrootte distributie, vorm, ruwheid van het partikeloppervlak), de deformatie mechanismen en de hoge doses waarin dit actief bestanddeel in tabletten voorkomt. Sinds ibuprofen plastisch en elastisch vervormbaar is, speelt de compressiesnelheid een belangrijke rol in zowel de finale tableteigenschappen als in het risico van “dekselen” (het bovenste gedeelte komt los van de tablet), “lamineren” (de tablet splitst verticaal (axiaal) in verschillende schijven) en kleven aan de stempels. Tabletten

werden gemaakt aan een snelheid van 250, 500 en 1000 tabletten per minuut via dubbele compressie (precompressies en hoofdcompressie) met en zonder verlengde dwell tijd. Alvorens te tableteren werden de granulaateigenschappen bepaald. De procesparameters en de tablet eigenschappen werden geanalyseerd met MVA. *Principal Component Analysis* (PCA) leverde een inzicht in de onderliggende fenomenen die het tabletteerproces bepalen en *Partial Least Squares Analysis* (PLS) lieten toe om de hoofdvariabelen die bijdroegen aan de geobserveerde verschillen in de tableteigenschappen te identificeren. Op basis van de PCA-analyse kon er geconcludeerd worden dat de tabletteersnelheid een cruciale variabele is in het tabletteerproces. Verder toonde de analyse aan dat compressie met bewegende compressierollen ook het tabletteerproces tot op grote hoogte beïnvloedt. Door verplaatsing te gebruiken, zowel tijdens precompressie als hoofdcompressie, verminderde de procesvariatie en verlengde de dwell tijd significant. Voor de hoofdcompressie bleek de daling in ejectiekracht ook een belangrijk effect te zijn bij het gebruik van verplaatsing. Verder kon de dimensie-loze parameter, t/p_{mean} ratio, beschouwd worden als een gevoelige parameter om de vorm van het kracht-tijd profiel te beschrijven binnen de grenzen van de gebruikte parameterinstellingen. Tenslotte kon er geconcludeerd worden dat de tabletteersnelheid en de verplaatsing een grotere invloed hadden op het compressieproces (op de andere procesvariabelen) dan de gebruikte (hoofd)compressiekracht. PLS toonde aan dat voornamelijk de tabletteersnelheid en de kracht op hoofdcompressie bijdroegen tot de finale tableteigenschappen. Bovendien kan er besloten worden dat de relatie tussen de procesparameters en tableteigenschappen niet eenvoudig is, daar de verschillende variabelen allemaal gelijktijdig bijdragen aan de uiteindelijke tablet karakteristieken. Deze analyse verstrekke een overzicht van de invloed van de beweging van de compressierollen op het tabletteerproces en de tableteigenschappen. Dit onderzoek toonde aan dat een grote hoeveelheid parameters het compressieproces beïnvloeden en dat het moeilijk, zo niet onmogelijk is om de bijdrage van al deze factoren afzonderlijk te bestuderen.

In **Hoofdstuk 6** werd er onderzocht of *backscattering* Raman, *transmission* Raman en *transmission Near-Infrared (NIR)* spectroscopie konden gebruikt worden om de fysische eigenschappen van tabletten te voorspellen. Granulen met verschillende karakteristieken werden geproduceerd op de Consigma™-25 continue poeder-tot-tablet productielijn. Een aantal granulatieparameters (de concentratie aan actief bestanddeel, de toevoersnelheid

van vloeistof, de temperatuur van de schroefkamer en de schroefconfiguratie) werd daarbij, aan de hand van een *full-factorial* DoE, gevarieerd. De granulaten werden in de oven gedroogd en getabletteerd op de MODUL™ P. De procesparameters van het tabletteerproces werden aangepast opdat tabletten met een uniform gewicht, dikte en diameter voor alle loten verkregen werden. Van alle tabletten werden transmissie en *backscattering* Raman spectra en transmission NIR spectra *offline* gecollecteerd. De hardheid, friabiliteit, desintegratietijd, schijnbare dichtheid en porositeit werden bepaald volgens de traditionele analysemethoden. Om de spectrale informatie te modelleren en te correleren aan de tableteigenschappen werd PLS regressie gebruikt. Er konden op deze manier geen goede PLS modellen die voorspellingen toelaten voor desintegratie, friabiliteit, porositeit en hardheid geconstrueerd worden. Er kon geconcludeerd worden dat de gebruikte PAT-technieken niet geschikt zijn om de fysische eigenschappen van tabletten te voorspellen. PCA kon wel efficiënt gebruikt worden om de verschillende concentraties en hydratieniveaus van het actief bestanddeel (theofylline) te onderscheiden. De verschillen aangetoond in het PLS model tussen *backscattering* Raman, transmissie Raman en NIR spectroscopie in de kwantificatie van de theofylline concentratie waren niet significant. Tot slot kan gesteld worden dat *Multiple Linear Regression analysis* (MLR) toeliet om succesvol te onderzoeken hoe de verschillen in granulatieparameters de granulatie-eigenschappen, tableteigenschappen en afhankelijke procesparameters beïnvloedden.

CURRICULUM VITAE

PERSONAL INFORMATION

Name: PEETERS Elisabeth R.
Date of birth: February 19th, 1983
Place of birth: Edegem, Belgium
Professional Address: Ghent University
Faculty of Pharmaceutical Sciences
Laboratory of Pharmaceutical Technology
Ottergemsesteenweg 460
9000 Ghent
Phone: +32(0)92648039
Elisabeth.Peeters@Ugent.be

LANGUAGE SKILLS

Dutch (native proficiency)
English (full professional proficiency)
French (basic proficiency)
German (basic proficiency)

EDUCATION

2007 – present: PhD candidate in Pharmaceutical Technology
Laboratory of Pharmaceutical Technology, Ghent University
Scientific promoters: Prof. dr. J.P. Remon, Prof. dr. C. Vervaet
2006 – 2007: Master after Master of Industrial Pharmacy
Inter-university program (UA, UGent, KUL, VUB)
2001 – 2006: Master of Pharmaceutical Sciences
University of Antwerp

RESEARCH EXPERIENCE

- 2007 – present: PhD research: “Investigation of the tableting process in continuous production: Influence of feeding and extended dwell time during compression on dependent process variables and tablet properties.”
Laboratory of Pharmaceutical Technology, Ghent University
Scientific promoters: Prof. dr. J.P. Remon, Prof. dr. C. Vervaet
- Sep 2006 – Jan 2007: Master after Master thesis: “Production, physical characterization and in vitro dissolution profile of ocular minitablets with miconazole nitrate.”
Laboratory of Pharmaceutical Technology and Biopharmacy, University of Antwerp
Promoter: Prof. dr. A. Ludwig
- Feb – Jun 2006: Master thesis: “Production, physical characterization and in vitro dissolution profile of ocular minitablets with miconazole nitrate.”
Laboratory of Pharmaceutical Technology and Biopharmacy, University of Antwerp
Promoter: Prof. dr. A. Ludwig

PROFESSIONAL EXPERIENCE

- 2007 – present Laboratory of Pharmaceutical Technology, Ghent University
Assistant
- Mentoring master students during laboratory internship.
 - Organizing, planning and teaching practical courses “Artsenijbereidkunde” (3rd Bachelor Pharmaceutical Sciences) and “Farmaceutische Technology” (2nd Master Pharmaceutical Sciences)
- 2006 – 2007 Laboratory of Pharmaceutical Technology and Biopharmacy, University of Antwerp
Educational project employee

INTERNATIONAL PUBLICATIONS

- Assessment of the properties of continuously produced tablets using transmission and backscattering Raman spectroscopy and transmission NIR spectroscopy.
E. Peeters, A.F.T. Silva, M. Toivaainen, M. Juuti, J. Van Renterghem, M. Fonteyne, J. Vercruysse, T. De Beer, C. Vervaet, J.P. Remon.
In progress
- Influence of extended dwell time during pre- and main compression on the properties of ibuprofen tablets.
E. Peeters, A.F.T. Silva, M. Fonteyne, T. De Beer, C. Vervaet, J.P. Remon.
In progress
- Effect of the paddle movement in the forced feeder on lubricant sensitivity.
E. Peeters, V. Vanhoorne, C. Vervaet, J.P. Remon.
In progress
- Use of a continuous twin screw granulation and drying system during formulation development and process optimization.
J. Vercruysse, **E. Peeters**, M. Fonteyne, P. Cappuyns, U. Delaet, I. Van Assche, T. De Beer, J.P. Remon, C. Vervaet.
Submitted to European Journal of Pharmaceutics and Biopharmaceutics
- Crystal coating via spray drying to improve powder tabletability.
V. Vanhoorne, **E. Peeters**, B. Van Snick, J.P. Remon, C. Vervaet.
Accepted by European Journal of Pharmaceutics and Biopharmaceutics
- Reduction of tablet weight variability by optimizing paddle speed in the forced feeder of a high-speed rotary tablet press.
E. Peeters, T. De Beer, C. Vervaet, J.P. Remon.
Drug Development and Industrial Pharmacy (DOI: 10.3109/03639045.2014.884121)
- Moisture and drug solid state monitoring during a continuous drying process using empirical and mass balance models.
M. Fonteyne, D. Gildemyn, **E. Peeters**, S. Mortier, J. Vercruysse, K. V Gernaey, C. Vervaet, J.P. Remon, I. Nopens, T. De Beer.

European Journal of Pharmaceutics and Biopharmaceutics (DOI: 10.1016/j.ejpb.2014.02.015)

- Influence of raw material properties upon critical quality attributes of continuously produced granules and tablets.

M. Fonteyne, H. Wickström, **E. Peeters**, J. Vercruyssen, H. Ehlers, B.H. Peters, J.P. Remon, C. Vervaet, J. Ketolainen, N. Sandler, J. Rantanen, K. Naelapää, T. De Beer.

European Journal of Pharmaceutics and Biopharmaceutics (DOI: 10.1016/j.ejpb.2014.02.011)

- Prediction of quality attributes of continuously produced granules using complementary PAT tools.

M. Fonteyne, S. Soares, J. Vercruyssen, **E. Peeters**, A. Burggraeve, C. Vervaet, J.P. Remon, N. Sandler, T. De Beer.

European Journal of Pharmaceutics and Biopharmaceutics, 08/2012; 82(2): 429-436

- Continuous twin screw granulation: Influence of process variables on granule and tablet quality.

J. Vercruyssen, D. Córdoba Díaz, **E. Peeters**, M. Fonteyne, U. Delaet, I. Van Assche, T. De Beer, J.P. Remon, C. Vervaet.

European Journal of Pharmaceutics and Biopharmaceutics, 06/2012; 82(1): 205-211

- Coprocessing via spray drying as a formulation platform to improve the compactability of various drugs.

Y. Gonnissen, E. Verhoeven, **E. Peeters**, J.P. Remon, C. Vervaet.

European Journal of Pharmaceutics and Biopharmaceutics, 06/2008; 69(1): 320-334

ORAL PRESENTATIONS

- Influence of Compression Force and Extended Dwell Time during Pre- and Main Compression on the Properties of Ibuprofen Tablets.

E. Peeters, A.F.T. Silva, M. Fonteyne, T. De Beer, C. Vervaet, J.P. Remon.

Kuopio-Ghent Summerschool in Continuous Manufacturing, Kuopio, Finland, August 27-29, 2014.

- Optimisation of the tableting process through continuous production of tablets with constant porosity.
E. Peeters, C. Vervaet, J.P. Remon.
Advanced Pharmaceutical Technology (Master of Science in Drug Development), Ghent University, December 9, 2014.
- Influence of Compression Force and Extended Dwell Time during Pre- and Main Compression on the Properties of Ibuprofen Tablets (part II).
E. Peeters, T. De Beer, C. Vervaet, J.P. Remon.
VII Annual Symposium of the Pharmaceutical Solid State Research Cluster (PSSRC), Lille, France, July 4-6, 2013.
- Effect of mixing intensity and time in the forced feeder of a high speed rotary tablet press on lubricant sensitivity.
E. Peeters, C. Vervaet, J.P. Remon.
15th Forum of Pharmaceutical Sciences, Belgian Society of Pharmaceutical Sciences, Spa, Belgium, May 12-13, 2011.
- Influence of compression force and extended dwell time during pre- and main compression on the properties of ibuprofen tablets (part I).
E. Peeters, T. De Beer, C. Vervaet, J.P. Remon.
IV Annual PSSRC Symposium, Cambridge, UK, September 19-21, 2010.

POSTER PRESENTATIONS

- Influence of compression force and extended dwell time during pre- and main compression on the properties of ibuprofen tablets.
E. Peeters, M. Fonteyne, T. De Beer, C. Vervaet, J.P. Remon.
9th World Meeting on Pharmaceutics, Biopharmaceutics and Pharmaceutical Technology, Lisbon, Portugal, March 31- April 03, 2014.
- Study on the influence of granulation process parameters on tablet properties using transmission Raman and NIR.
E. Peeters, A.F.T. Silva, M. Toiviainen, M. Juuti, J. Van Renterghem, M. Fonteyne, T. De Beer, C. Vervaet, J.P. Remon.
6th International Granulation Workshop, Sheffield, UK, June 26-28, 2013.

- Reduction of tablet weight variability by optimizing paddle speed in the forced feeder of a high speed rotary tablet press.
E. Peeters, T. De Beer, C. Vervaet, J.P. Remon.
8th World Meeting on Pharmaceutics, Biopharmaceutics and Pharmaceutical Technology, Istanbul, Turkey, March 19-22, 2012.
- Reduction of tablet weight variability by optimizing paddle speed in the forced feeder of a high speed rotary tablet press.
E. Peeters, T. De Beer, C. Vervaet, J.P. Remon.
American Association of Pharmaceutical Scientists (AAPS) Annual meeting and exposition, Washington DC, USA, October 23-27, 2011.
- Influence of compression force and extended dwell time during pre- and main compression on tablet properties.
E. Peeters, T. De Beer, C. Vervaet, J.P. Remon.
AAPS Annual meeting and exposition, New Orleans, USA, November 13-18, 2010.
- Overlubrication of MCC-based formulations in the forced feeder of a tablet press.
E. Peeters, C. Vervaet, J.P. Remon.
AAPS Annual meeting and exposition, New Orleans, USA, November 13-18, 2010.
- Influence of hydroxypropyl- β -cyclodextrine on the properties of bioadhesive miconazole nitrate ocular minitables.
E. Peeters, J. Vandervoort, A. Ludwig, J.P. Remon.
36th Controlled Release Society (CRS) Annual Meeting & Exposition, Copenhagen, Denmark, July 18-22, 2009.

ATTENDED CONFERENCES, COURSES AND WORKSHOPS

Conferences

- EuPAT5, Ghent, Belgium, May 8-10, 2012.
- 7th World Meeting on Pharmaceutics, Biopharmaceutics and Pharmaceutical Technology, Valletta, Malta, March 8-11, 2010.
- Biopharmacy Day, Lunteren, The Netherlands, October 6, 2008.
- 2nd PSSRC Symposium, Ghent, Belgium, August 27, 2008.
- Biopharmacy Day, Louvain, Belgium, May 30, 2008.

Courses

- Multivariate Data Analysis, Prof. T. De Beer, Doctoral Schools, Ghent University, Ghent, Belgium, December-January, 2012-2013.
- Design Of Experiments, Prof. T. De Beer, Doctoral Schools, Ghent University, Ghent, Belgium, October-November, 2012.
- Module 4: Analysis of Variance, Institute for continuing education in Science (ipvw), Ghent University, Ghent, Belgium, December 17-February 16, 2009-2010.
- Module 3, Introductory Statistics. Basics of Statistical Interference, ipvw, Ghent University, Ghent, November 24-December 15, 2009.
- Umetrics; Multivariate Data Analysis Basic Course, Ghent University, Ghent, Belgium, January 06-07, 2009.
- Umetrics; Design of experiments "Pharma Applications", Ghent University, Ghent, Belgium, December 16-17, 2008.
- Statistics: SPSS, Navormingscyclus Onderzoek Associatie Universiteit Gent, Ghent University, Ghent, Belgium, January, 2008.

Workshops

- IWPCPS-12 (twelfth International Workshop on Physical Characterization of Pharmaceutical Solids), Lille, France, June 21-24, 2010.
- Leadership foundation course; Doctoral Schools (transferable skills), Ghent University, Ghent, Belgium, October-November, 2011.
- Project Management; Doctoral Schools (transferable skills), Ghent University, Ghent, Belgium, April-May 2010.
- Het Feedbackgesprek; Basis Assistententraining, Ghent University, Ghent, Belgium, April 07, 2009.
- APV basics: Practical training tableting, Brussels, Belgium, November 4-5, 2008.
- "Hands-on Implementation of Process Analytical Technology (PAT) Systems in Production Processes"; Ghent University, Ghent, Belgium, August 25-26, 2008.
- Workshop No: TTC129 "Granulation & Tableting"; Technology Training Center, Binzen, Germany, March 26-28, 2008.

